

Delta Salinity Constituent Analysis



**Richard A. Denton
Richard Denton & Associates
Oakland, California**

**Prepared for the
State Water Project Contractors Authority
February 2015**

Cover Photo: Looking south at the junction of Middle River and Victoria Canal (upper right of the photo) in the Sacramento-San Joaquin Delta. The bridge in the center of the photo is the Highway 4 crossing. The photo was taken on March 24, 2008. Photo courtesy of the California Department of Water Resources.

Table of Contents

List of Figures

List of Tables

Executive Summary ES-1

1. Introduction	1-1
2. Purpose	2-1
3. Previous Work	3-1
4. Data Description	4-1
4.1 Data Sources	4-1
4.2 Analyte Characteristics	4-2
4.3 Evaluation of Water Analyses	4-3
4.3.1 Relationship between TDS and EC	4-4
4.3.2 Relationship between total anions or cations and electrical conductivity	4-6
4.3.3 Correlation between different water quality constituents	4-6
5. Development of Regression Equations	5-1
6. Variation of Constituent Ratios with TDS	6-1
7. Regression Equations for Delta Boundary Conditions	7-1
7.1 Seawater Dominated Boundary Locations	7-1
7.2 San Joaquin River Dominated Boundary Locations	7-4
7.3 Sacramento River Dominated Boundary Locations	7-6
7.4 Mokelumne and Cosumnes River Boundary Locations	7-7
8. Regression Relationships by Interior Delta Region	8-1
8.1 Suisun Bay and Western Delta	8-6
8.2 Old River – Lower Reach	8-9
8.3 Middle River – Lower Reach	8-15
8.4 SWP Export Facility	8-18
8.5 CVP Export Facility	8-23
8.6 Old and Middle River – Upper Reach	8-26
8.7 San Joaquin River from Vernalis to Jersey Point	8-29
8.8 Sacramento River from Freeport to Rio Vista Bridge	8-33
8.9 Lower Mokelumne and Cosumnes River Region	8-36
8.10 Barker Slough	8-36
8.11 Agricultural Drainage and Drains	8-41
8.12 Summary of Findings	8-42
9. Estimating Seawater Intrusion at Interior Delta Stations	9-1
9.1. Seasonal Variations in Seawater Contributions	9-2
9.2. Determine seawater EC contribution using DSM2 fingerprint data from a historical simulation run	9-3

9.3. Estimate seawater EC from grab sample data if a second constituent concentration is also known (e.g. chloride, calcium or sulfate)	9-4
9.4. Estimate seawater EC at a given location from “known” values of EC at Jersey Point EC	9-7
9.5. Estimate Jersey Point EC and seawater EC from antecedent Delta outflow	9-14
9.6. Estimate seawater EC from typical monthly and water year variations	9-15
9.7. Estimating Contribution from San Joaquin EC	9-21
10. Conclusions	10-1
Acknowledgements	10-2
About the Author	10-2
11. List of References	11-1
12. Glossary	12-1

Appendices

A. Seawater Boundary Condition	A-1
A.1. Variation with Specific Conductance (EC)	A-3
A.2. Variation with Total Dissolved Solids	A-14
A.3. Bromide as a function of Chloride Concentration	A-15
B. San Joaquin River Boundary Condition	B-1
B.1. Variation of Water Quality Constituents with EC	B-3
B.2. Variation of Water Quality Constituents with TDS	B-9
B.3. Bromide as a function of Chloride Concentration	B-9
B.4. Influence of Export Water Quality on Vernalis Water Quality	B-10
C. Sacramento River Boundary Condition	C-1
D. Mokelumne River Boundary Condition	D-1
E. Water Quality Constituent Ratios	E-1
F. Tracking Sources of Delta Water Using DSM2 Fingerprint Data	F-1
G. General Mixing Equations for Three Sources of Water	G-1
H. Checking the Quality of the Grab Sample Data	H-1
I. Summary of Grab Sample Data Used in this Analysis	I-1

List of Figures

Figures follow the chapter or appendix in which they are referenced

- 1-1 Map of the Sacramento-San Joaquin Delta system showing the locations of the key boundary condition stations (large red dots). The locations of other key monitoring stations are shown as smaller green dots.
- 3-1 Conversion equations for chloride concentration as a function of specific conductance for Clifton Court Forebay from Guivetchi (1986).
- 3-2 Chloride concentration as a function of specific conductance when seawater dominates (Mallard Island and Jersey point) and when San Joaquin agricultural return flows dominate (Vernalis). Graph from CUWA (1995).
- 3-3 Sulfate concentration as a function of specific conductance when seawater dominates (Mallard Island and Jersey point) and when San Joaquin agricultural return flows dominate (Vernalis). The seawater equation in this figure was $\text{SO}_4 = 0.041 \text{ EC} + 6$ and the San Joaquin equation was $\text{SO}_4 = 0.18 -6$. Graph from CUWA (1995).
- 3-4 Chloride concentrations at Rock Slough (as 14-day averages) as a function of specific conductance when seawater dominates (Mallard Island and Jersey point) and when San Joaquin agricultural return flows dominate (Vernalis). Graph from CUWA (1995).
- 4-1 Ratio of total dissolved solids to specific conductance (EC) for grab sample data from Suisun Bay at Mallard Island.
- 4-2 Ratio of total dissolved solids to specific conductance (EC) for grab sample data from the San Joaquin River at Vernalis
- 4-3 Ratio of total dissolved solids to specific conductance (EC) for grab sample data from the Sacramento River at Hood
- 5-1 Variation of chloride concentration (Cl) as a function of specific conductance (EC) for grab sample data from Mallard Island and Jersey Point. The data are fitted with a quadratic regression equation over the range $2600 < \text{EC} < 19,000 \mu\text{S}/\text{cm}$.
- 5-2 Variation of chloride concentration (Cl) as a function of specific conductance (EC) for grab sample data from Mallard Island and Jersey Point. Setting the coefficient a to zero would result in significant errors in the estimates of Cl at very high EC.
- 5-3 Variation of chloride concentration (Cl) as a function of specific conductance (EC) for Mallard Island and Jersey Point grab samples over the lower salinity range ($\text{EC} < 1,000 \mu\text{S}/\text{cm}$) generally experienced in the south and central Delta. A different quadratic equation (with zero intercept) is needed to fit the data for $\text{EC} < 260 \mu\text{S}/\text{cm}$.

- 5-4 Variation of chloride concentration (Cl) as a function of specific conductance (EC) for Mallard Island and Jersey Point grab samples over the very low salinity range (EC < 400 $\mu\text{S}/\text{cm}$). A quadratic equation (with zero intercept) is used to fit the data for EC < 260 when the effect of seawater intrusion is very small.
- 5-5 Variation of chloride concentration (Cl) as a function of specific conductance (EC) for Mallard Island and Jersey Point grab samples for EC < 2,000 $\mu\text{S}/\text{cm}$. A separate quadratic equation is needed to fit the data for EC < 260 when the effect of seawater intrusion is very small.
- 8-1 Variation of chloride concentration as a function of specific conductance (EC) for the Headworks of Banks Pumping Plant in the south Delta. The equations for the seawater-dominated relationships (labeled Sea, red line) and agricultural drainage-dominated relationship (labeled SJR Ag, green line) are given in Table 7.1 and 7.7.
- 8-2 Variation of chloride concentration as a function of specific conductance (EC) for the Headworks of Banks Pumping Plant in the south Delta.
- 8-3 Variation of total dissolved solids (TDS) as a function of specific conductance (EC) for the Headworks of Banks Pumping Plant in the south Delta.
- 8-4 Variation of calcium concentration (Ca) as a function of chloride concentration (Cl) for the Headworks of Banks Pumping Plant in the south Delta. This type of graph was used by Suits (2002) to more clearly distinguish between seawater-dominated data and agricultural drainage-dominated data.
- 8-5 Map of western Delta showing the location of key monitoring stations
- 8-6 Variation of chloride concentration as a function of specific conductance (EC) for San Pablo Bay at Pinole Point and San Pablo Point and Suisun Bay at Port Chicago.
- 8-7 Variation of chloride concentration as a function of specific conductance (EC) for Antioch, Collinsville, Emmaton and Blind Point (western end of Jersey Island).
- 8-8 Variation of chloride concentration as a function of specific conductance (EC) for Antioch and Blind Point for EC < 800 $\mu\text{S}/\text{cm}$.
- 8-9 Map of Old River and Middle River showing the location of key monitoring stations. The map shows the area of the south and central Delta that is north and east of the Middle River, Old River and Grant Line temporary barriers.
- 8-10 Variation of chloride concentration as a function of specific conductance (EC) for stations on Old River between Holland Tract and Bacon Island.

- 8-11 Variation of chloride concentration as a function of specific conductance (EC) for Old River at Highway 4 and the northeastern end of Victoria Canal. This latter station best represents the water quality at CCWD's new Victoria Canal intake.
- 8-12 Variation of chloride concentration for CCWD's intake on Old River at Highway 4 as a function of time (January 1997 – December 2001). The chloride data are bounded by the seawater-dominated upper limit and agricultural drainage-dominated lower limit. Seawater intrusion generally occurs during the late summer and fall, except in wetter years.
- 8-13 Variation of calcium concentration at CCWD's intake on Old River at Highway 4 as a function of time (January 1997 – December 2001). The periods when agricultural drainage dominates correspond to higher calcium concentrations.
- 8-14 Variation of chloride concentration at Contra Costa Canal at Pumping Plant No. 1 as a function of time (January 1993 through December 1996).
- 8-15 Variation of chloride concentration at Contra Costa Canal at Pumping Plant No. 1 as a function of time (January 2009 through March 2013).
- 8-16 Variation of chloride concentration as a function of specific conductance at the northern end of Middle River.
- 8-17 Variation of chloride concentration as a function of specific conductance along the middle reach of Middle River.
- 8-18 Variation of chloride concentration as a function of specific conductance at the southern end of Middle River and along Victoria Canal.
- 8-19 Variation of calcium concentration as a function of specific conductance on Middle River at the Mokelumne Aqueduct crossing, at Connection Slough and at the Bacon Island Bridge.
- 8-20 Variation of chloride concentration with time on Middle River at the Mokelumne Aqueduct crossing from January 1981 through December 1986. The seawater-dominated and agricultural drainage-dominated curves indicate when each of those conditions dominate. The corresponding plot of Jersey Point EC illustrates when seawater intrusion would be expected to occur, i.e., when Jersey Point EC is high.
- 8-21 Map of the SWP and CVP export facilities in the south Delta and key monitoring stations.
- 8-22 Variation of chloride concentration as a function of specific conductance at the intake to Clifton Court Forebay.

- 8-23 Variation of sulfate concentration as a function of specific conductance at the intake to Clifton Court Forebay.
- 8-24 Variation of bromide concentration at the intake to Clifton Court Forebay from 2009-2012. Seawater dominates in late 2009, late 2010 and late 2012 but there is no seawater intrusion in 2011. Agricultural drainage dominates February-June 2010 and March-June 2012.
- 8-25 Variation of sulfate concentration as a function of time at the intake of Clifton Court Forebay from 2009-2012. During February-June 2010 and March-June 2012, the sulfate concentrations are large and are consistent with the agricultural drainage dominated regression relationship (SJR Ag line).
- 8-26 Variation of chloride concentration as a function of specific conductance at the intake to the Jones Pumping Plant and the Delta Mendota Canal.
- 8-27 Variation of chloride concentration as a function of specific conductance at the Delta Mendota Canal intake at Byron Road for an earlier period of time (1952-1965).
- 8-28 Chloride concentration as a function of specific conductance at the Delta Mendota Canal intake at Lindeman Road for wet and above normal years only. When conditions are wetter and Delta outflows are higher, the water quality is dominated by agricultural drainage.
- 8-29 The corresponding variation of chloride concentration as a function of specific conductance at the Delta Mendota Canal intake for dry and critical years. Seawater intrusion makes a major contribution to the DMC chloride concentration during these drier years.
- 8-30 Map of Old River and Middle River showing areas upstream and west of the temporary barriers showing key locations, including the SWRCB's agricultural water quality stations.
- 8-31 Variation of chloride concentration as a function of specific conductance at upper Middle River stations, in particular those east of the temporary agricultural barriers.
- 8-32 Variation of chloride concentration as a function of specific conductance on Grant Line Canal at the Tracy Road Bridge.
- 8-33 Corresponding variation of sulfate concentration as a function of specific conductance on Grant Line Canal at the Tracy Road Bridge.
- 8-34 Map of the San Joaquin River from Vernalis to Jersey Point showing the location of key monitoring stations.

- 8-35 Variation of chloride concentration as a function of EC from Vernalis to Brandt Bridge on the San Joaquin River. The data are consistent with agricultural drainage-dominated water.
- 8-36 Variation of chloride concentration as a function of specific conductance from Buckley Cove to Prisoners Point (further north and more seaward) on the San Joaquin River.
- 8-37 Variation of sulfate concentration as a function of specific conductance from at Little Connection Slough at Empire Tract, Buckley Cove and the Highway 4 crossing on the San Joaquin River.
- 8-38 Map of Sacramento River in the northern Delta showing the location of key monitoring stations.
- 8-39 Variation of chloride concentration as a function of specific conductance from the Delta Cross Channel to Rio Vista.
- 8-40 Variation of chloride concentration with time at Rio Vista during the period January 1975 through December 1995. This period includes the severe 1976-1977 drought.
- 8-41 Variation of chloride concentration as a function of specific conductance from the Delta Cross Channel to Rio Vista for EC < 450 $\mu\text{S}/\text{cm}$.
- 8-42 Variation of sulfate concentration as a function of specific conductance from the Delta Cross Channel to Rio Vista.
- 8-43 Map of the Barker Slough region in the vicinity of the North Bay Aqueduct intake (Barker Slough Pumping Plant).
- 8-44 Variation of chloride concentration as a function of EC at the intake in the region of the North Bay Aqueduct intake at Barker Slough.
- 8-45 Variation of sodium concentration as a function of EC at the intake in the region of the North Bay Aqueduct intake at Barker Slough. The data follow a similar, but extrapolated, relationship to the Sacramento River sodium regression equation.
- 8-46 Variation of calcium concentration as a function of specific conductance in the region of the North Bay Aqueduct intake at Barker Slough. A site-specific calcium regression equation was derived because the Sacramento River regression equation does not represent these Barker Slough region data.
- 8-47 Variation of chloride concentration during the period January 2005 through December 2008 in the region near the North Bay Aqueduct intake. During July-December, the area is dominated by freshwater, consistent with the Sacramento River regression equation, but in some winters, drainage from local tributary runoff events significantly increases chloride concentrations.

- 8-48 Variation of chloride concentration as a function of specific conductance at the City of Vallejo's former drinking water intake (1950-1992).
- 8-49 Variation of chloride concentration as a function of specific conductance (EC) for representative agricultural drains in the Central Delta area: Jersey Point Ag drain; Holland Tract Ag pumping plant No. 1; Bacon Island Ag pumping plant; and, a Palm Tract Ag drain.
- 9-1 Monthly-averaged Delta outflows (from DWR's DAYFLOW database) for the period October 2003 through September 2012. The four quarters of each year are color-coded to show the seasonal trends in outflow, and seawater intrusion. Delta outflows greater than 18,000 cfs are sufficient to substantially repel seawater intrusion into the Delta. Only the range of Delta outflows from 0 to 18,000 cfs to better show the variations in Delta outflow during the drier months of the year.
- 9-2 Variation of chloride concentration as a function of specific conductance for grab samples from West Canal near the intake to the Clifton Court Forebay (1990-1994). The purple circles indicate the estimated seawater EC of 358 μ S/cm.
- 9-3 Estimates of specific conductance from seawater from EC and chloride, EC and calcium and EC and sulfate. These estimates are for grab sample from West Canal near the intake to the Clifton Court Forebay (2005-2009). Also plotted is the corresponding seawater EC estimate from Jersey Point EC.
- 9-4 Comparison of Old River at Bacon Island EC with weighted Jersey Point EC (1975-2012 data). The seawater dominated relationship (red line) can be used to estimate the seawater contribution at Bacon Island. The linear regression (green line) is different because it is also influenced by periods when agricultural drainage dominates, e.g., during periods of low Jersey Point EC.
- 9-5 Comparison of estimated Old River at Bacon Island EC due to seawater intrusion with measured EC data (1975-1979).
- 9-6 Comparison of estimated Old River at Bacon Island EC due to seawater intrusion with measured EC data (July 2006 – February 2012).
- 9-7 Comparison of the entrance to Clifton Court Forebay EC with weighted Jersey Point EC (1964-2012 data). The seawater-dominated relationship (red line) can be used to estimate the seawater contribution at Clifton Court.
- 9-8 Comparison of estimated Clifton Court EC due to seawater intrusion with measured EC data (2000 – 2003).
- 9-9 Comparison of Clifton Court grab sample chloride data with calculated seawater- and agricultural drainage-dominated chloride concentrations (2000 – 2003).

- 9-10 Comparison of historical Middle River at Victoria Canal EC data with weighted Jersey Point EC (1999-2012 data). The seawater-dominated relationship (red line) can be used to estimate the seawater contribution at Victoria Canal.
- 9-11 Comparison of estimated Victoria Canal EC due to seawater intrusion with measured continuous EC and grab sample EC data (2006 – 2010).
- 9-12 Comparison of Victoria Canal grab sample chloride data with calculated seawater- and agricultural drainage-dominated chloride concentrations (2006 – 2010).
- 9-13 Variation of the ratio of seawater EC to total EC for Middle River at Victoria Canal with water year type for the month of September. These daily data are from a DSM2 historical fingerprint study (1976-2009).
- 9-14 Variation of the ratio of seawater EC to total EC for Middle River at Victoria Canal with water year type for the month of July. These daily data are from a DSM2 historical fingerprint study (1976-2009).
- 9-15 Variation of the ratio of seawater EC to total EC for the intake to Clifton Court Forebay with water year type for the month of August. These daily data are from a DSM2 historical fingerprint study (1976-2009).
- 9-16 Variation of the ratio of seawater EC to total EC for the intake to Clifton Court Forebay with water year type for the month of March. These daily data are from a DSM2 historical fingerprint study (1976-2009).
- 9-17 Variation of the seawater EC ratio derived from historical September grab sample data from the intake to Clifton Court Forebay for years 2000 through 2013. These are data collected since the 1995 SWRCB Water Quality Control Plan. These data represent the effect of more recent operations with Spring X2 and the biological opinions.
- 9-18 Variation of the seawater EC ratio derived from historical July grab sample data from the intake to Clifton Court Forebay for years 1983-1994. These are data collected before the 1995 SWRCB Water Quality Control Plan. These data represent the effect of Delta operations before Spring X2 and the biological opinions.
- 9-19 Ratio of San Joaquin source EC to total EC for the intake to Clifton Court Forebay as a function of San Joaquin River flow at Vernalis. The data are from a historical DSM2 fingerprint study.
- A-1 Variation of chloride, sodium and sulfate ratios of total dissolved solids with TDS at Mallard Island and Jersey Point. These stations represent the seawater source to the Delta.

- A-2 Variation of sulfate, magnesium, calcium and potassium ratios of total dissolved solids with TDS at Mallard Island and Jersey Point. Sulfate is shown in both Figures A-1 and A-2 to provide a common point of reference over the large range of constituent ratios (0.01 – 0.06).
- A-3 Variation of chloride (Cl) concentration as a function of specific conductance (EC) at Mallard Island and Jersey Point.
- A-4 Variation of chloride concentration as a function of specific conductance (EC) at Mallard Island and Jersey Point for EC < 1,200 $\mu\text{S}/\text{cm}$.
- A-5 Variation of chloride concentration as a function of specific conductance (EC) at Mallard Island and Jersey Point for EC < 350 $\mu\text{S}/\text{cm}$.
- A-6 Variation of bromide (Br) concentration as a function of specific conductance (EC) at Mallard Island and Jersey Point.
- A-7 Variation of bromide concentration as a function of specific conductance (EC) at Mallard Island and Jersey Point for EC < 350 $\mu\text{S}/\text{cm}$.
- A-8 Variation of sodium (Na) concentration as a function of specific conductance (EC) at Mallard Island and Jersey Point.
- A-9 Variation of sodium concentration as a function of specific conductance (EC) at Mallard Island and Jersey Point for EC < 350 $\mu\text{S}/\text{cm}$.
- A-10 Variation of calcium (Ca) concentration as a function of specific conductance (EC) at Mallard Island and Jersey Point.
- A-11 Variation of calcium concentration as a function of specific conductance (EC) at Mallard Island and Jersey Point for EC < 350 $\mu\text{S}/\text{cm}$.
- A-12 Variation of sulfate (SO_4) concentration as a function of specific conductance (EC) at Mallard Island and Jersey Point.
- A-13 Variation of sulfate concentration as a function of specific conductance (EC) at Mallard Island and Jersey Point for EC < 350 $\mu\text{S}/\text{cm}$.
- A-14 Variation of magnesium (Mg) concentration as a function of specific conductance (EC) at Mallard Island and Jersey Point.
- A-15 Variation of magnesium concentration as a function of specific conductance (EC) at Mallard Island and Jersey Point for EC < 350 $\mu\text{S}/\text{cm}$.
- A-16 Variation of potassium (K) concentration as a function of specific conductance (EC) at Mallard Island and Jersey Point.

- A-17 Variation of potassium concentration as a function of specific conductance (EC) at Mallard Island and Jersey Point for EC < 350 $\mu\text{S}/\text{cm}$.
- A-18 Variation of hardness concentration as a function of specific conductance (EC) at Mallard Island and Jersey Point.
- A-19 Variation of hardness concentration as a function of specific conductance (EC) at Mallard Island and Jersey Point for EC < 350 $\mu\text{S}/\text{cm}$.
- A-20 Variation of alkalinity concentration as a function of specific conductance (EC) at Mallard Island and Jersey Point.
- A-21 Variation of alkalinity concentration as a function of specific conductance (EC) at Mallard Island and Jersey Point for EC < 1,100 $\mu\text{S}/\text{cm}$.
- A-22 Variation of total dissolved solids as a function of specific conductance (EC) at Mallard Island and Jersey Point.
- A-23 Variation of total dissolved solids as a function of specific conductance (EC) at Mallard Island and Jersey Point for EC < 350 $\mu\text{S}/\text{cm}$.
- A-24 Variation of chloride concentration as a function of total dissolved solids (TDS) at Mallard Island and Jersey Point.
- A-25 Variation of chloride concentration as a function of TDS at Mallard Island and Jersey Point for TDS < 200 mg/L. The break between seawater dominated and agricultural drainage dominated water occurs at about a TDS of 150 mg/L.
- A-26 Variation of bromide (Br) concentration as a function of chloride (Cl) concentration at Mallard Island and Jersey Point.
- A-27 Variation of bromide concentration as a function of chloride concentration at Mallard Island and Jersey Point for Cl < 60 mg/L.
- B-1 Variation of alkalinity, calcium and sulfate ratios of total dissolved solids with TDS from the San Joaquin River at Vernalis and at Maze. These stations represent the source of San Joaquin Valley inflow to the Delta.
- B-2 Variation of sodium and chloride ratios of total dissolved solids with TDS from the San Joaquin River at Vernalis and at Maze.
- B-3 Variation of chloride concentration with specific conductance (EC) for grab samples from the San Joaquin River at Vernalis and at Maze.

- B-4 Variation of bromide concentration with specific conductance (EC) for grab samples from the San Joaquin River at Vernalis and at Maze.
- B-5 Variation of sodium concentration with specific conductance (EC) for grab samples from the San Joaquin River at Vernalis and at Maze.
- B-6 Variation of calcium concentration with specific conductance (EC) for grab samples from the San Joaquin River at Vernalis and at Maze.
- B-7 Variation of sulfate concentration with specific conductance (EC) for grab samples from the San Joaquin River at Vernalis and at Maze.
- B-8 Variation of magnesium concentration with specific conductance (EC) for grab samples from the San Joaquin River at Vernalis and at Maze.
- B-9 Variation of potassium concentration with specific conductance (EC) for grab samples from the San Joaquin River at Vernalis and at Maze.
- B-10 Variation of hardness concentration with specific conductance (EC) for grab samples from the San Joaquin River at Vernalis and at Maze.
- B-11 Variation of alkalinity concentration with specific conductance (EC) for grab samples from the San Joaquin River at Vernalis and at Maze.
- B-12 Variation of total dissolved solids with specific conductance (EC) for grab samples from the San Joaquin River at Vernalis and at Maze.
- B-13 Variation of chloride concentration with total dissolved solids (TDS) for grab samples from the San Joaquin River at Vernalis and at Maze.
- B-14 Variation of bromide concentration as a function of chloride concentration for grab samples from the San Joaquin River at Vernalis and Maze.
- B-15 Variation of chloride to TDS ratios for seawater, San Joaquin and Sacramento boundary conditions from 1989-1995. During periods of high outflow, the chloride/TDS ratio at Mallard Island decrease significantly to a value representing a mixture of Sacramento and San Joaquin water. During prolonged dry periods, export of saltier Delta water, containing a higher proportion of seawater, causes a subsequent increase in the chloride/TDS ratio at Vernalis. No data are available at Vernalis for 1995.
- B-16 Sacramento Basin 40-30-30 water year indices for 1988 through 1995.
- B-17 Variation of calcium to TDS ratios for seawater, San Joaquin and Sacramento boundary conditions from 1989-1995. During periods of high outflow, the calcium/TDS ratio at Mallard Island increases significantly to a value representing a mixture of Sacramento and San Joaquin water. No data are available at Vernalis for 1995.

- B-18 Variation of chloride concentration as a function of sulfate concentration for grab samples from the San Joaquin River at Vernalis and Maze showing grab sample data collected prior to 1982. The higher chloride concentrations for a given sulfate concentration suggest the water in the San Joaquin River prior to 1982 often had a higher percentage of seawater than after 1982. The regression equation is based on post 1982 data only.
- C-1 Variation of the ratios of chloride and calcium concentration to total dissolved solids (TDS) as a function of TDS for the combined grab samples from the Sacramento River at Hood and Greenes Landing.
- C-2 Variation of the ratio of sulfate concentration to TDS as a function of TDS for the combined grab samples from the Sacramento River at Hood and Greenes Landing.
- C-3 Variation of chloride concentration as a function of specific conductance on the Sacramento River at Hood and Greenes Landing.
- C-4 Variation of bromide concentration as a function of specific conductance on the Sacramento River at Hood and Greenes Landing.
- C-5 Variation of sodium concentration as a function of specific conductance on the Sacramento River at Hood and Greenes Landing.
- C-6 Variation of calcium concentration as a function of specific conductance on the Sacramento River at Hood and Greenes Landing.
- C-7 Variation of sulfate concentration as a function of specific conductance on the Sacramento River at Hood and Greenes Landing.
- C-8 Variation of magnesium concentration as a function of specific conductance on the Sacramento River at Hood and Greenes Landing.
- C-9 Variation of potassium concentration as a function of specific conductance on the Sacramento River at Hood and Greenes Landing.
- C-10 Variation of hardness as a function of specific conductance on the Sacramento River at Hood and Greenes Landing.
- C-11 Variation of alkalinity concentration as a function of specific conductance on the Sacramento River at Hood and Greenes Landing.
- C-12 Variation of total dissolved solids as a function of specific conductance on the Sacramento River at Hood and Greenes Landing.

- C-13 Variation of chloride concentration as a function of total dissolved solids (TDS) on the Sacramento River at Hood and Greenes Landing.
- C-14 Variation of bromide concentration as a function of chloride concentration on the Sacramento River at Hood and Greenes Landing.
- D-1 Map showing key stations on the Mokelumne and Cosumnes River as well as the location of the adjacent Delta Cross Channel.
- D-2 Variation of Mokelumne and Cosumnes chloride concentrations as a function of specific conductance.
- D-3 Variation of Mokelumne and Cosumnes calcium concentrations as a function of specific conductance.
- D-4 Variation of Mokelumne and Cosumnes sulfate concentrations as a function of specific conductance.
- E-1 Ratio of chloride concentration to total dissolved solids as a function of TDS for three different sources of Delta water: seawater intruding through Suisun Bay (represented by grab samples from Mallard Island and Jersey Point), San Joaquin inflow and Sacramento inflow.
- E-2 Ratio of bromide (Br) concentration to total dissolved solids as a function of TDS for three different sources of Delta water: seawater intruding through Suisun Bay (represented by grab samples from Mallard Island and Jersey Point), San Joaquin inflow and Sacramento inflow. The trend is similar to that for chloride concentration.
- E-3 Ratio of sodium (Na) concentration to total dissolved solids as a function of TDS for three different sources of Delta water: seawater intruding through Suisun Bay, San Joaquin inflow and Sacramento inflow. The trend is similar to that for chloride and bromide concentrations.
- E-4 Ratio of calcium (Ca) concentration to total dissolved solids as a function of TDS for three different sources of Delta water: seawater intruding through Suisun Bay, San Joaquin inflow and Sacramento inflow. In this case, the Ca/TDS ratio for seawater is much lower than for San Joaquin River water, i.e., the opposite of the chloride concentration ratios.
- E-5 Ratio of sulfate (SO₄) concentration to total dissolved solids as a function of TDS for three different sources of Delta water: seawater intruding through Suisun Bay, San Joaquin inflow and Sacramento inflow. As was the case for calcium, the SO₄/TDS ratio for seawater is much lower than for San Joaquin River water. However, unlike for calcium, the SO₄/TDS ratio for San Joaquin River water decreases at low TDS rather than increasing.

- E-6 Ratio of magnesium (Mg) concentration to total dissolved solids as a function of TDS for three different sources of Delta water: seawater intruding through Suisun Bay, San Joaquin inflow and Sacramento inflow. The Mg/TDS ratio for seawater increases as TDS decreases. The San Joaquin River water ratio remains relatively constant with TDS and is only slightly larger than the seawater ratio at high TDS.
- E-7 Ratio of potassium (K) concentration to total dissolved solids as a function of TDS for three different sources of Delta water: seawater intruding through Suisun Bay, San Joaquin inflow and Sacramento inflow. The K/TDS ratios for seawater and San Joaquin River water both increase as TDS decreases.
- E-8 Ratio of hardness to total dissolved solids as a function of TDS for three different sources of Delta water: seawater intruding through Suisun Bay, San Joaquin inflow and Sacramento inflow. The hardness ratios for seawater and San Joaquin River water both increase as TDS decreases.
- E-9 Ratio of alkalinity to total dissolved solids as a function of TDS for three different sources of Delta water: seawater intruding through Suisun Bay, San Joaquin inflow and Sacramento inflow.
- E-10 Ratio of specific conductance to total dissolved solids as a function of TDS for three different sources of Delta water: seawater intruding through Suisun Bay, San Joaquin inflow and Sacramento inflow.
- F-1 DSM2 salinity fingerprint data for the San Joaquin River at Jersey Point in the western Delta for the period 1976 through 2002. This period includes the 1976-1977 and 1987-1992 droughts as well as the very wet year 1983.
- F-2 DSM2 salinity fingerprint data for the San Joaquin River at Jersey Point in the western Delta for the period 1980 through 1985. During the wet years 1982 and 1983 there is almost no seawater intrusion at Jersey Point.
- F-3 DSM2 salinity fingerprint data for the Clifton Court Forebay in the southern Delta for the period 1976 through 1996.
- F-4 DSM2 salinity fingerprint data for the Jones Pumping Plant and intake to the Delta Mendota Canal in the southern Delta for the period 1976 through 1996.
- F-5 DSM2 salinity fingerprint data for Middle River at Union Point (near the Highway 4 crossing) in the southern Delta for the period 1976 through 1996.
- F-6 DSM2 salinity fingerprint data for the San Joaquin River at Prisoners Point (on Venice Island) in the central Delta for the period 1985 through 2002.
- F-7 DSM2 salinity fingerprint data for the intake to the North Bay Aqueduct at Barker Slough in the northern Delta for the period 1988 through 2000.

- F-8 Variation in daily EC due to seawater intrusion (DSM2 salinity fingerprint data) for Old River at Bacon Island, Clifton Court Forebay intake, and Middle River at Union Point in the central and south Delta for the period 1984 through 1989.
- F-9 Relationship between EC due to seawater at Clifton Court Forebay intake and total EC at Jersey Point (taking into account an approximate 14 day time lag in response).
- F-10 Comparison of the DSM2 EC at Clifton Court due to seawater intrusion alone and the prediction based on total EC at Jersey Point for the period 1985 through 1993.
- F-11 A more detailed comparison of the DSM2 EC at Clifton Court due to seawater intrusion alone and the prediction based on total EC at Jersey Point for the period 1986 through 1989. The total EC at Clifton Court is also shown to indicate the relative contributions from other sources of salinity.
- G-1 Theoretical relationship between the chloride concentration and total dissolved solids derived from the mixing equations for three sources. The theoretical equations are compared with grab sample data from Mallard Island, Chipps Island, and Jersey Point. Seawater typically dominates at this location but not when Delta outflows are very high (low TDS).
- G-2 Theoretical mixing relationship between chloride concentration and total dissolved solids for $TDS < 400 \text{ mg/L}$ (high Delta outflows). At very high outflows, seawater intrusion is negligible ($a = 0$) and the Mallard Island and Jersey Point data follow the mixing equation for Sacramento and San Joaquin sources only.
- G-3 Theoretical mixing relationship between the chloride/TDS ratio and total TDS for $TDS < 400 \text{ mg/L}$ (higher Delta outflows). At very high outflows (very low TDS), seawater intrusion is negligible ($a = 0$) and even the Mallard Island and Jersey Point data tend to follow the mixing equation for Sacramento and San Joaquin sources only.
- G-4 Comparing the theoretical three-source mixing equations for $b = 0.05$ and $a = 0$ with the fitted quadratic equations for chloride concentration as a function of TDS (for seawater, San Joaquin and Sacramento River boundary conditions).
- G-5 Corresponding three-source mixing equations for the calcium/TDS ratio as a function of TDS. These theoretical curves are compared with data from Mallard Island and Jersey Point.

List of Tables

3-1	Percentages of total dissolved solids for seawater, Sacramento River water, and San Joaquin River water (Hutton 2006)	3-6
4.1	List of National Secondary Drinking Water Maximum Contaminant Levels	4-2
6-1	Categories of constituent ratio variation with total dissolved solids	6-1
7.1	Regression Coefficients for Estimating Water Quality Constituents from Specific Conductance for Seawater-Dominated Locations (EC > 260 $\mu\text{S}/\text{cm}$)	7-2
7.2	Regression Coefficients for Estimating Water Quality Constituents from Specific Conductance for Seawater-Dominated Locations (EC < 260 $\mu\text{S}/\text{cm}$)	7-2
7.3	Regression Coefficients for Estimating Water Quality Constituents from Total Dissolved Solids for Seawater-Dominated Locations (TDS > 150 mg/L)	7-3
7.4	Regression Coefficients for Estimating Water Quality Constituents from Total Dissolved Solids for Seawater-Dominated Locations (TDS < 150 mg/L)	7-3
7.5	Regression Coefficients for Estimating Bromide Concentration from Chloride Concentration for Seawater-Dominated Locations when Cl > 25 mg/L	7-4
7.6	Regression Coefficients for Estimating Bromide Concentration from Chloride Concentration for Seawater-Dominated Locations when Cl < 25 mg/L	7-4
7.7	Regression Coefficients for Estimating Water Quality Constituents from Specific Conductance for Agricultural Drainage-Dominated Locations	7-5
7.8	Regression Coefficients for Estimating Water Quality Constituents from Total Dissolved Solids for Agricultural Drainage-Dominated Locations	7-5
7.9	Regression Coefficients for Estimating Bromide Concentration from Chloride Concentration for Agricultural Drainage-Dominated Locations	7-6
7.10	Regression Coefficients for Estimating Water Quality Constituents from Specific Conductance for Sacramento Inflow (Freshwater)	7-6
7.11	Regression Coefficients for Estimating Water Quality Constituents from Total Dissolved Solids for Sacramento Inflow (Freshwater)	7-7
7.12	Regression Coefficients for Estimating Bromide Concentration from Chloride Concentration to Bromide for Sacramento Inflow (Freshwater)	7-7

9.1	Matrix showing a simplified example of the expected pattern of seawater intrusion in the central Delta as a function of both time of the year (season) and water year type	9-1
A-1	Percentages of total dissolved solids for seawater-dominated grab samples	A-1
B-1	San Joaquin River percentages of TDS from Hutton (2006)	B-1
B-2	Updated San Joaquin River percentages of TDS	B-2
E-1	Constituent Concentrations as a Percentage of Total Dissolved Solids	E-1
H.1	Valences and atomic weights for key water quality constituents	H-2
H.2	Concentration Data and Charge Balance Calculations for a Mallard Island Grab Sample (B0702000) from 4/7/2009 at 9:34 am	H-3
H.3	Calculation of Specific Conductance from Individual Ion Conductances	H-4
H.4	Comparison of measured ion concentrations with estimates from conversion equations	H-5
H.5	Concentration Data and Charge Balance Calculations for a Mallard Island Grab Sample (B0702000) from 1/6/2009 at 10:25 am	H-6

Executive Summary

Salinity in the Sacramento-San Joaquin Delta is generally measured as electrical conductivity (EC) but other constituents such as chloride, bromide, sodium, calcium, sulfate, and total dissolved solids (TDS) are also important for management of water operations in the Delta and regulation of drinking water. Computer simulations of Delta water quality are often reported as electrical conductivity. These simulated EC data often need to be converted to other water quality constituents to assess, e.g., compliance with chloride-based drinking water standards, or potential changes in bromide concentrations due to the Bay Delta Conservation Plan.

Previous regression equations for estimating chloride and TDS from EC are described in detail in Chapter 3. These previous equations only accounted for variations by water year type (wet, above and below normal, dry and critical years) and did not explicitly account for seasonal changes in the relative contributions to water quality from different sources. During the summer and fall, seawater intrusion from San Francisco Bay is likely to dominate, but in the winter and spring, Delta flows are often high and seawater is repelled from the Delta. During those higher runoff periods, agricultural drainage from the San Joaquin River and local discharges dominates. The ratio of chloride to TDS is less for agricultural drainage than for seawater, and the ratios of calcium and sulfate to TDS for agricultural drainage is higher than for seawater. To accurately predict water quality constituent concentrations from measurements or simulations of EC and/or TDS it was necessary to develop more reliable regression equations that account for seasonal changes in the sources of water at a given Delta location.

The California Department of Water Resources (and its predecessors), U.S. Bureau of Reclamation, and other agencies have been systematically collecting detailed grab sample measurements of water quality constituents from the Sacramento-San Joaquin Delta from as early as the 1950s. These grab sample data were used in this report to develop more detailed regression relationships between the key indicators of salinity and water quality in the Delta, i.e., specific conductance (EC) and total dissolved solids (TDS), as well as chloride, bromide, sodium, calcium, sulfate, magnesium, potassium, hardness and alkalinity. These regression equations are discussed in Chapters 7, 8 and 9. The work presented in this report was conducted in support of the Department of Water Resources' Municipal Water Quality Investigations Program.

In the western Delta and San Francisco Bay, the regression equations developed in this report are consistent with that of seawater, and in the northern Delta, the regression equations are consistent with very low salinity river water from the Sacramento and Mokelumne Rivers. Seawater intrusion only makes a contribution in the north Delta during drought situations like 1976-1977.

In the south and central Delta near major drinking water intakes, the relationships between the water quality constituents and EC or TDS depend upon the particular mixture of seawater and agricultural drainage from the San Joaquin River and Delta islands. The contribution from seawater intrusion at locations in the central and south Delta at any given time can be calculated from measured salinities at Jersey Point in the western Delta. The remaining contributions are from local and San Joaquin agricultural return flows and very low salinity water from the Sacramento River and other smaller rivers on the eastside of the Delta. A second relationship for agricultural drainage is used to calculate the chloride, bromide, sodium, calcium, sulfate, etc. contribution from the non-seawater sources.

A simpler, but less accurate, approach for estimating water quality constituents is also presented that predicts the contribution from seawater at different locations as a function of the month of the year and Sacramento Valley unimpaired runoff. Seawater intrusion often dominates during the late summer and fall and is typically negligible during the winter. However, in extreme drought situations, seawater intrusion can dominate all year. On the other hand, during very wet years, seawater intrusion at interior Delta stations can be zero or negligible the whole year.

These approaches for estimating other water quality constituents from historical EC data can also be applied to simulated EC output data from the California Department of Water Resources' Delta Simulation Model (DSM2). DSM2 simulations of Jersey Point EC can be used to estimate the contribution from seawater intrusion at a given Delta location. The DSM2 model can also be used to calculate the individual contributions to EC from different sources separately, as well as the source water volumes (fingerprint data). The DSM2 fingerprint data were used to gain an understanding of how seawater intrusion at a given interior Delta location varies by month and with water year runoff index. However, where there are differences between the simulated and historical EC, the simulated contribution from seawater intrusion and other sources may quite different than for the corresponding field data.

1. Introduction

The Sacramento-San Joaquin River Delta is the source of drinking water for over 25 million Californians. The suitability of Delta water for urban, industrial and agricultural use depends in large part on the salinity of that water, which can be quantified in terms of total dissolved solids (TDS), chloride (Cl), bromide (Br), and sodium (Na) concentration or specific electrical conductance (EC).

Chloride concentration is used to quantify and regulate municipal and industrial water quality in the California State Water Resources Control Board (SWRCB) Bay-Delta Water Quality Control Plan (WQCP). Bromide concentration, in conjunction with organic carbon concentration, is an indicator of the potential for high concentrations of harmful disinfection byproducts to be produced when water is treated for drinking water use. TDS is of interest, e.g., in determining whether recycled water is fresh enough to be stored in groundwater aquifers.

Regression equations between water quality constituents are important where grab sample data are only available for a limited number of constituents, or in the case of computer simulations of Delta water quality, only one constituent (typically EC) is calculated. The current analysis of the relationships between Delta water quality constituents also helps explain the contributions of different sources of Delta inflow to the quality of water in different regions of the Delta. The sources of inflow are seawater from San Francisco Bay intruding into the Delta at Mallard Island, Sacramento River freshwater inflow, San Joaquin River inflows at Vernalis, inflow from east side Delta tributaries, and local discharges within the Delta (Figure 1-1).

Salinity of Delta water is typically measured using an electrical conductivity (EC) meter. However, the relationship between EC and the corresponding chloride, bromide and TDS concentrations varies by location within the Delta. Even at a given location, the contributions of water from different sources depend upon the rainfall-runoff hydrology, the season of the year and other factors such as flow barrier operations. During periods of low Delta outflow (typically in the summer and fall months), seawater often dominates. During periods of high runoff, seawater intrusion will be minimal, even in the western Delta. Salinities may still be high in some locations due to local discharges of agricultural drainage, and agricultural return flows entering the Delta from the San Joaquin Valley.

The contribution of San Joaquin River inflow to the quality of water diverted at the South Delta export pumps is made more complicated by operational factors such as the timing of the Clifton Court gate operations and pumping levels (see Montoya, 2004), installation of temporary barriers in the south Delta, and the magnitude of the inflow at Vernalis. Although high flows on the San Joaquin typically correspond to lower salinities at Vernalis (because of higher dilution), the flushing of salt and other contaminants off agricultural lands in the San Joaquin Valley after the first large storm of the water year can result in high salinities even when San Joaquin flows are high (as occurred in February 2005).

The concentrations of other parameters such as calcium (Ca), sodium (Na), sulfate (SO₄) as well as pesticides and other toxic contaminants will also depend upon the particular mixture of water from various sources: Sacramento River, San Joaquin River, seawater intrusions, the eastside

tributaries to the Delta, and local drainage from Delta islands and cities. The particular mixtures (percentage volumes) of various sources are often referred to as “fingerprints.” Knowing the proportions of water from each source is important, e.g., because the chloride concentration in seawater for a given EC or TDS value is about twice as much as the chloride concentration in agricultural drainage.

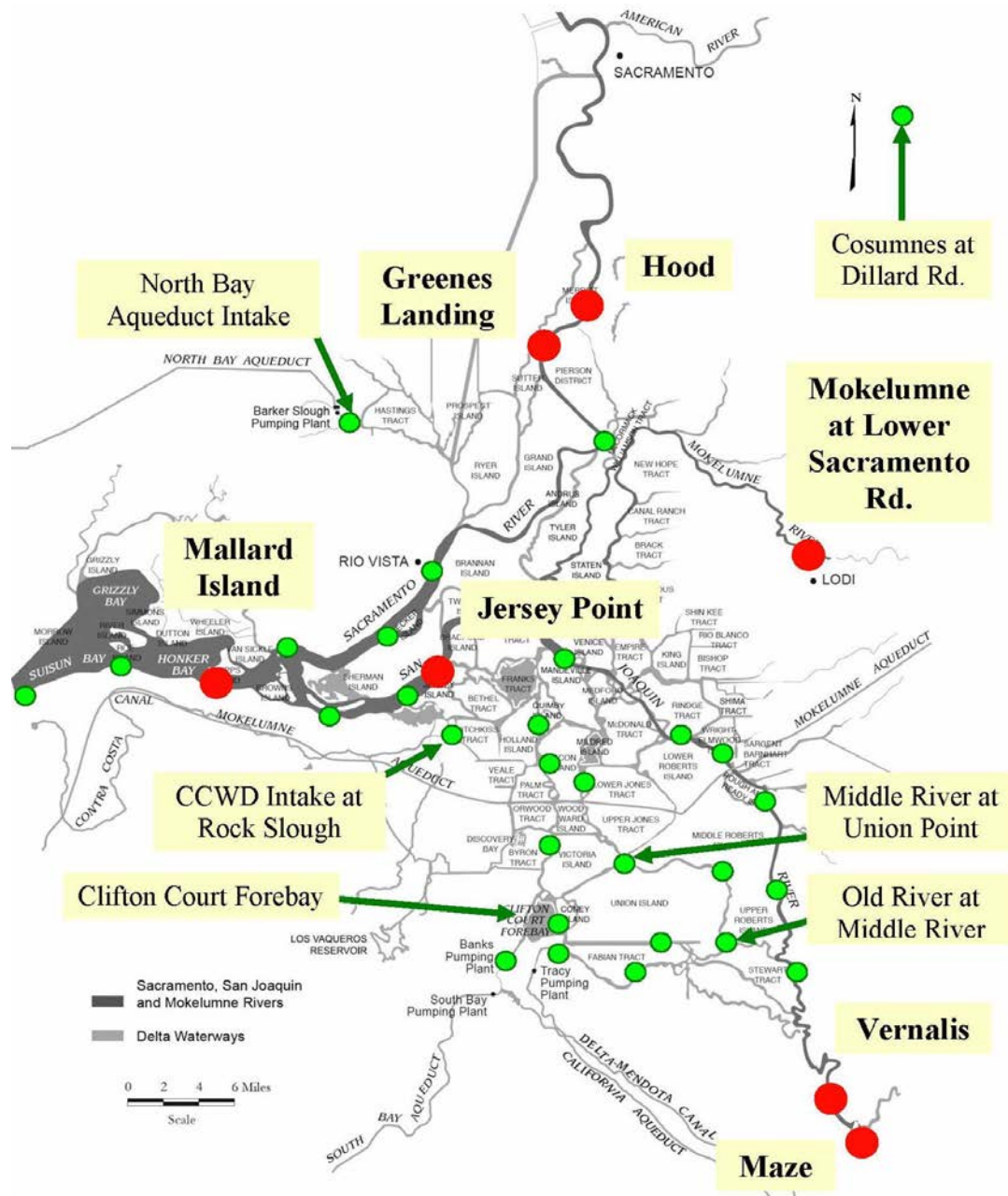


Figure 1-1: Map of the Sacramento-San Joaquin Delta system showing the locations of the key boundary condition stations (large red dots). The locations of other key monitoring stations are shown as smaller green dots.

2. Purpose

The primary purpose for this study was to develop equations for estimating water quality constituents, such as chloride, calcium and sulfate, from EC data obtained from field grab samples or computer simulations for key monitoring stations and locations throughout the Delta and upstream. Regression relationships were also developed between EC and other anion and cation concentrations, such as bromide, sodium, magnesium, potassium, alkalinity and hardness, as well as regression equations for estimating water quality constituents as a function of TDS.

The regression equations developed in this report account for variations in the mixture of water from different sources by location, by water year type and during different seasons of the year. Where applicable, these local regression equations are combined into regional equations representing larger areas of the Delta.

These regression relationships will be able to be used by the State Water Contractors, the California Department of Water Resources (DWR) and other Bay-Delta stakeholders to convert output from water quality computer models, such as DWR's Delta Simulation Model 2 (DSM2), into chloride, bromide, TDS and other anion and cation concentrations. The chloride concentrations at key municipal intakes are of particular importance when analyzing the effect of Bay-Delta projects on the SWRCB's municipal and industrial water quality standards.

The variation of other ions such as calcium, sodium, sulfate, magnesium and potassium with EC (or TDS) will help understand (and confirm) the percentages of water reaching a given location. The south-east Delta can be expected to be dominated by San Joaquin River water and the north Delta above Rio Vista can be expected to be dominated by Sacramento River water. The percentage contributions of chloride, calcium, sulfate, etc. to total dissolved solids in a grab sample at a given location will depend on whether seawater or agricultural drainage is dominating at that particular sample time.

Over the range of salinities typically experienced at urban intakes in the Delta (EC < 1,100 $\mu\text{S}/\text{cm}$ or a chloride concentration of about 250 mg/L), linear regression relationships of the form $Y = bX + c$ can be used with a high degree of correlation. However, in the western Delta and Suisun Bay, the EC can be as large as 20,000 $\mu\text{S}/\text{cm}$ and a quadratic equation of the form $Y = aX^2 + bX + c$ is needed to capture the observed non-linear variation over this much larger range of EC. In these equations, a, b and c are regression fitting coefficients.

3. Previous Work

In 1986, Kamyar Guivetchi (DWR) analyzed the Bay-Delta grab sample data for specific conductance, total dissolved solids and chloride concentration and developed linear regression equations for each pair of parameters, e.g., EC as a function of TDS and vice versa. Guivetchi (1986) categorized the data according to water year type and developed linear regression equations for wet, normal and dry years as well as equations for the full data set (all years) at a number of locations in the Delta. An example of these equations for Clifton Court Forebay is provided in Figure 3-1. Although these equations were very useful, water quality data in some areas such as the south and central Delta receive different sources of water depending upon the season, not just water year type, and a single linear equation, classified solely in terms of water year type, was not able to capture the seasonal variations.

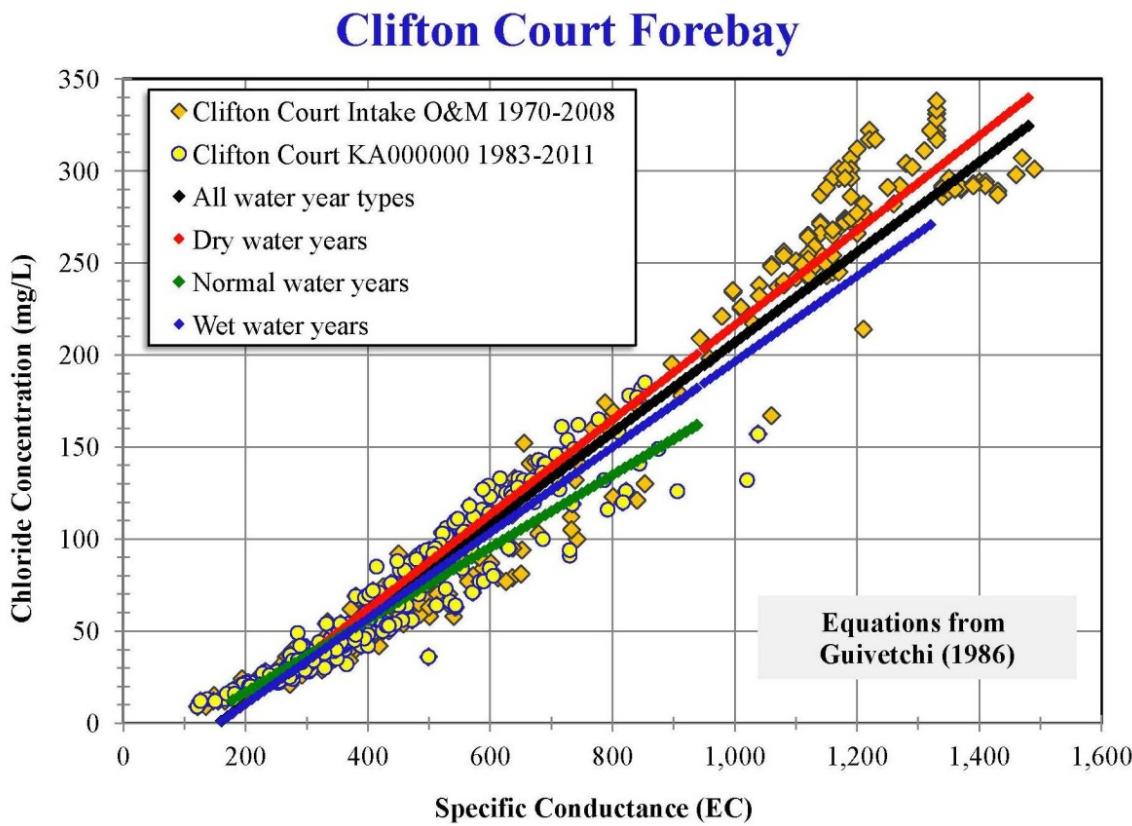
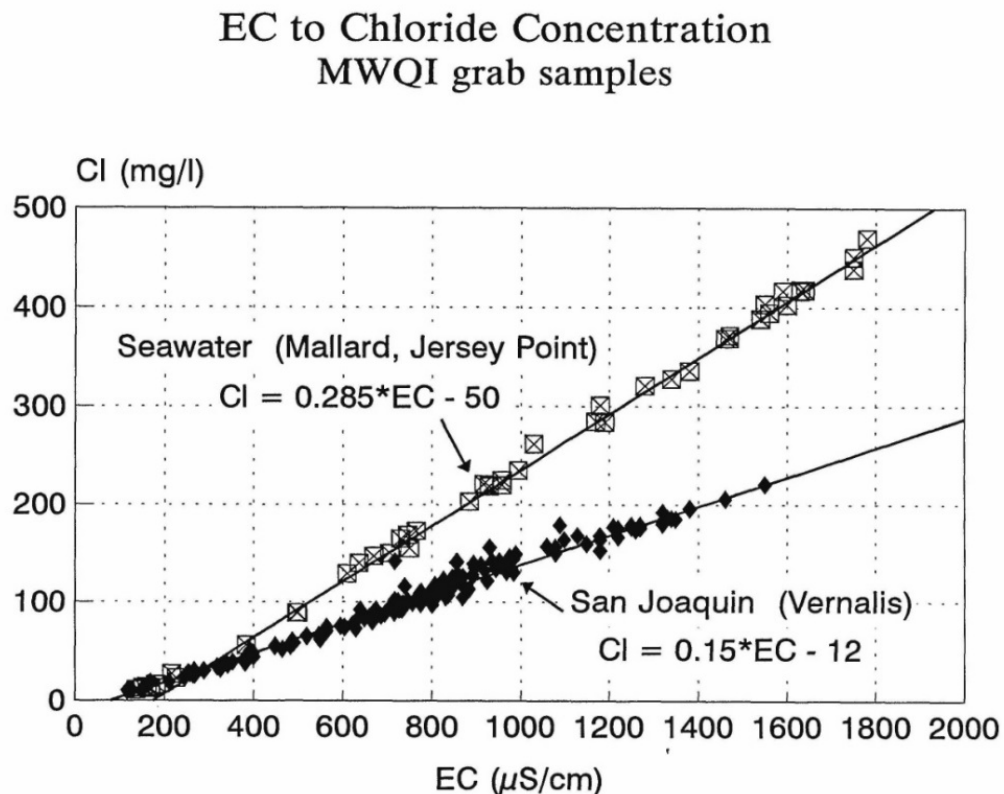


Figure 3-1: Conversion equations for chloride concentration as a function of specific conductance for Clifton Court Forebay from Guivetchi (1986).

In May 1995, the California Urban Water Agencies (CUWA) published a “*Study of Drinking Water Quality in Delta Tributaries*.” Appendix A of that report presented graphs prepared by Contra Costa Water District (CCWD) that plotted MWQI grab sample data for bromide, sulfate, total dissolved solids, and chloride as a function of EC. Those graphs illustrated how the water at CCWD’s Rock Slough intake comes from different sources. Sometimes seawater dominates (e.g., during summer and early fall); at other times agricultural drainage from local sources and the San Joaquin Valley dominates. The bromide, sulfate, TDS and chloride grab sample data

were bounded by the regression relationships for the two primary sources: seawater and agricultural drainage.

Figure 3-2, from CUWA (1995), shows the different relationships between chloride concentration and EC for seawater (represented by the characteristics of seawater-dominated grab samples from Mallard Island and Jersey Point) and agricultural return flows (represented by San Joaquin River water at Vernalis).

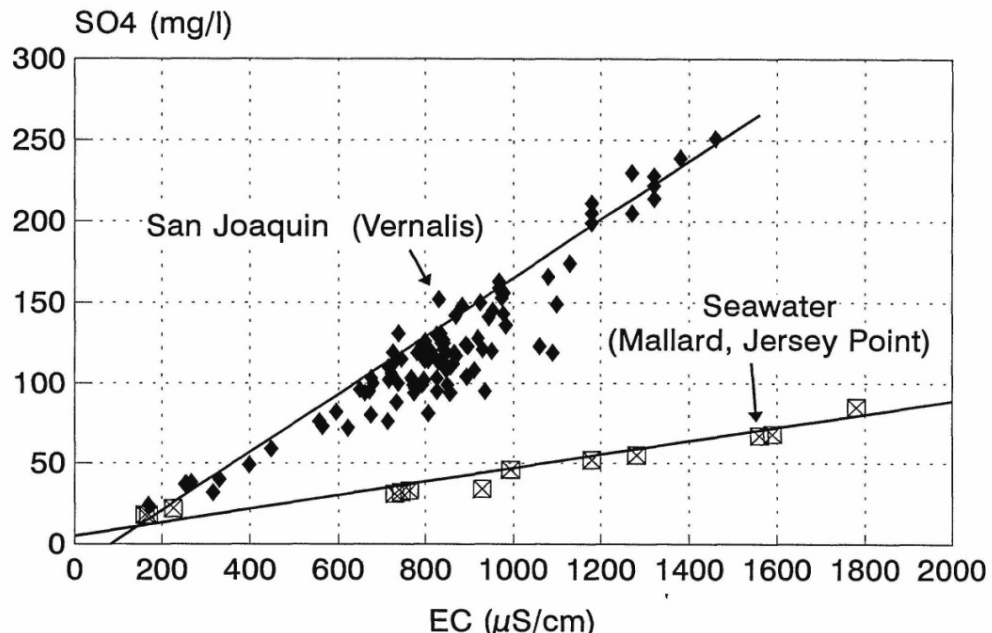


CCWD rad Jan 10, 1994

Figure 3-2: Chloride concentration as a function of specific conductance when seawater dominates (Mallard Island and Jersey point) and when San Joaquin agricultural return flows dominate (Vernalis). Graph from CUWA (1995).

The corresponding plot of sulfate versus EC from the May 1995 report (Figure 3-3) shows a similar bifurcation. However, in this case, the Vernalis sulfate grab sample data represent the upper bound and the seawater-dominated sulfate data the lower bound.

EC to Sulphate Concentration MWQI grab samples



CCWD rad Jan 10, 1994

Figure 3-3: Sulfate concentration as a function of specific conductance when seawater dominates (Mallard Island and Jersey point) and when San Joaquin agricultural return flows dominate (Vernalis). The seawater equation in this figure was $SO_4 = 0.041 EC + 6$ and the San Joaquin equation was $SO_4 = 0.18 - 6$. Graph from CUWA (1995).

As shown in Figure 3-4, the 14-day averaged chloride concentrations at the intake to the Contra Costa Canal vary between a lower agricultural return flow bound and the upper seawater dominated bound (CUWA (1995)). The periods when agricultural return flows dominate appeared to correspond to periods of large outflow from the western Delta from the San Joaquin River. In CUWA (1995), periods of high outflow were classified as QWEST > 4000 cfs, where QWEST is the amount of San Joaquin River flow past Jersey Point, through Dutch Slough and northwards through Threemile Slough. QWEST is generally highly correlated with Delta outflow, i.e., high QWEST corresponds to high Delta outflow. When QWEST and Delta outflows are very low, seawater intrusion dominates.

Rock Slough EC to Chloride Conversion 14-day averages 1968-1990

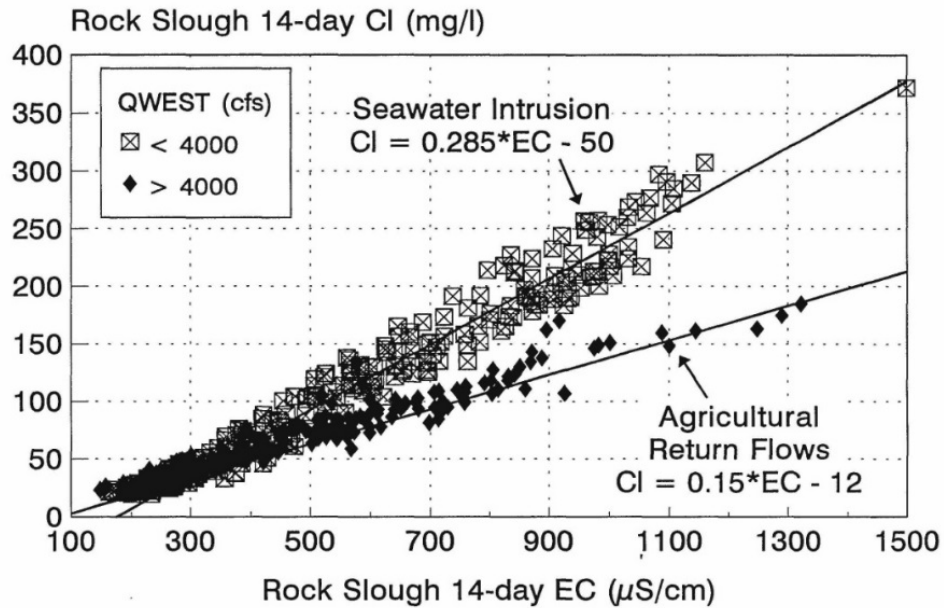


Figure 3-4: Chloride concentrations at Rock Slough (as 14-day averages) as a function of specific conductance when seawater dominates (Mallard Island and Jersey point) and when San Joaquin agricultural return flows dominate (Vernalis). Graph from CUWA (1995).

In December 2000, Marvin Jung and Associates completed a report on Delta island return flow quality for DSM2 and DICU model runs (Jung, 2000). The report was prepared for a CALFED Ad-Hoc Workgroup under contract to DWR's MWQI Program. Jung (2000) looked at correlations between key disinfectant byproduct precursors in drainage water as well as EC, TDS, bromide, calcium, chloride, magnesium, sodium and sulfate. Data from a large number of discharge points were aggregated according to different regions of the Delta.

In 2001, Bob Suits (DWR) developed linear relationships between EC, chloride, and bromide at Delta export locations. Suits focused on calculating the EC value that represented a given chloride or bromide concentration. The relationships developed by Bob Suits were:

Contra Costa Canal

$$\text{EC Old River at Rock Slough} = 89.6 + 3.73 \text{ (Chloride Contra Costa Pumping Plant \#1)} \quad \dots \quad (3.1)$$

$$\text{EC Old River at Rock Slough} = 118.7 + 1040.30 \text{ (Bromide Contra Costa Pumping Plant #1)} \dots (3.2)$$

Los Vaqueros Intake, Clifton Court Forebay, DMC Intake

$$\text{EC} = 160.6 + 3.66 \text{ (Chloride)} \quad \dots \quad (3.3)$$

$$EC = 189.2 + 1020.77 \text{ (Bromide)} \quad \dots \quad (3.4)$$

where EC is in $\mu\text{S}/\text{cm}$, and chloride and bromide concentrations are in mg/L.

These equations can be rearranged to express chloride and bromide concentrations as a function of EC, i.e.,

Contra Costa Canal

$$\text{Chloride}_{\text{Contra Costa Pumping Plant } \#1} = 0.268 \text{ EC}_{\text{Old River at Rock Slough}} - 24 \quad \dots \quad (3.5)$$

$$\text{Bromide}_{\text{Contra Costa Pumping Plant } \#1} = 0.0010 \text{ EC}_{\text{Old River at Rock Slough}} - 0.11 \quad \dots \quad (3.6)$$

Los Vaqueros Intake, Clifton Court Forebay, DMC Intake

$$\text{Chloride} = 0.273 \text{ EC} - 44 \quad \dots \quad (3.7)$$

$$\text{Bromide} = 0.0010 \text{ EC} - 0.19 \quad \dots \quad (3.8)$$

The regression between chloride at Contra Costa Canal Pumping Plant #1 and EC at Old River at Rock Slough was based on an earlier relationship developed by Aaron Miller (DWR) in January, 2001 (Suits, 2001). Suits also determined the following relationship between chloride and bromide concentration at the export pumps.

$$\text{Chloride} = 278.9 (\text{Bromide}) + 7.8 \quad (\text{in mg/L}) \quad \dots \quad (3.9)$$

In 2002, Bob Suits reported on the relationships between Delta water quality constituents as derived from grab sample data. This work was published as Chapter 5 of DWR's 23rd Annual Progress Report on "*Methodology for Flow and Salinity Estimates in the Sacramento-San Joaquin Delta and Suisun Marsh*." Suits grouped various stations within the Delta according to the similarity of their site-specific relationships between calcium and chloride. The ratio of calcium to chloride is lowest in the west Delta, and highest where freshwater dominates (Sacramento River area). Suits noted that the key urban drinking water intakes (SWP Clifton Court, CVP Jones and Contra Costa Canal) represented areas where either seawater or agricultural return flows can dominate, or a combination of both can dominate.

In 2004, Barry Montoya completed a detailed report on "*Factors affecting the composition and salinity of exports from the south Sacramento-San Joaquin Delta*" (Montoya, 2004). Montoya looked at the sources of salt affecting the water quality at the SWP and CVP export sites, in particular the relative amounts of cross-Delta flow from the Sacramento River and inflow from the San Joaquin River. Montoya found that when San Joaquin flow at Vernalis exceeded about 3,400 cfs, the water at the CVP's Delta-Mendota Canal intake was primarily San Joaquin River water. When Vernalis flow exceeded about 7,400 cfs, water diverted into Clifton Court Forebay was also primarily San Joaquin water. Montoya also found that the composition of the inflow to Clifton Court Forebay varied according to the tidal variations. During the ebb phase of the tide, San Joaquin water dominates, whereas during the flood, Sacramento River water dominates

In 2005, Contra Costa Water District, City of Stockton, and Solano County Water Agency prepared a "*Delta Region Drinking Water Quality Management Plan*." The Plan was prepared for the CALFED Bay-Delta Program and published as a Draft Final Report. The Plan included graphs of the chloride concentration versus EC at key urban intakes in the Delta, as well as the

variations of chloride, calcium and sulfate versus EC and bromide versus chloride in the western Delta and at Vernalis (Appendix 2C of the Plan). These graphs were used to demonstrate the influence of different sources of water in the Delta.

In March 2006, Paul Hutton (MWDSC) gave a presentation on “Validation of DSM2 Volumetric Fingerprints Using Grab Sample Mineral Data” at the California and Environmental Modeling Forum Annual Meeting. Hutton (2006) reviewed the typical mineral composition of source waters in the Delta (see Table 3-1) and presented pie charts showing the percentage composition of ions and cations for seawater (using grab samples from Mallard Island) and the San Joaquin River at Vernalis grab sample data.

Table 3-1: Percentages of total dissolved solids for seawater, Sacramento River water, and San Joaquin River water (Hutton 2006).

Mineral	Symbol	Percentage for Seawater	Percentage for Sacramento River water (<i>Greenes Landing</i>)	Percentage for San Joaquin River water (<i>Vernalis</i>)
Chloride	Cl	55	7	21
Sodium	Na	31	11	18
Sulfate	SO ₄	8	9	22
Magnesium	Mg	4	8	4
Calcium	Ca	1	14	8
Potassium	K	1	2	1
Alkalinity (as Bicarbonate)	HCO ₃		44	16
Nitrate	NO ₃		5	10

Hutton (2006) looked at the relationship between chloride and sulfate ions and how the ratio varies from about 7 where seawater dominates down to about 1 where San Joaquin River water dominates. Hutton also presented graphs of various mineral ions as a function of EC, as well as alkalinity, but did not quantify any of these relationships. However, he did show how these relationships with EC varied depending upon the modeled source water contributions from DSM2 model runs.

In April 2012, Shankar Parvathinathan (Montgomery Watson Harza) gave a presentation on “Validation of DSM2 QUAL for Simulation of Various Cations and Anions” at the California and Environmental Modeling Forum Annual Meeting. He ran DSM2 not only with EC boundary conditions, but also with corresponding chloride, bromide, sodium, calcium, sulfate and alkalinity (bicarbonate) boundary conditions. Parvathinathan (2012) concluded the DSM2 model is able to simulate EC and other cations and anions reasonably well, but underestimates EC in South Delta. Where there were discrepancies between field and simulated EC due to incorrect tidal transport, dispersion and errors in estimating the quantity and quality of Delta island diversions and discharges, similar discrepancies occurred with the cations and anions. Simulating historical data for a range of cation and anion boundary conditions may be a way, albeit time

consuming, of directly estimating the cation and anion concentrations at different regions in the Delta.

DWR's "*Methodology for Flow and Salinity Estimates in the Sacramento-San Joaquin Delta and Suisun Marsh*," 33rd Annual Progress Report, June 2012 includes a chapter on "*Estimating Delta-wide Bromide Using DSM2-Simulated EC Fingerprints*" (Liu and Suits, 2012). Liu and Suits compared different approaches to determining bromide at select locations in the Delta, i.e.:

1. Simulate bromide directly with DSM2
2. Convert EC to bromide using regressions based on: (a) grab samples; (b) volumetric fingerprints; and (c) EC-fingerprint-based multiple regressions.

They concluded that Delta-wide regression based on DSM2-calculated EC performs as well as direct bromide simulation using DSM2. They also determined that although site-specific regressions perform best, regional regressions perform nearly as well as site-specific regression. Liu and Suits also presented this material at the April 2012 California Water and Environmental Modeling Forum Annual Meeting.

Although a great deal of work has already been done, the seasonal and water year variations in the site-specific contributions of different sources of water on the conversion relationships are not well understood and have not been quantified. The DSM2 fingerprint data do quantify the volume percentages from each source and the contributions to EC, but a more general approach is needed for field data and for computer simulations when fingerprint data are not available.

The most recent work has only focused on chloride and bromide concentrations as a function of EC. However, other salinity constituents such as sodium, calcium, sulfate, potassium and magnesium are important factors in determining drinking water quality and protecting other beneficial uses of Delta water. The purpose of this study is to develop more accurate estimates of a wider range of water quality constituents and to gain more insight into the influences of seawater intrusion and agricultural drainage in the Delta.

4. Data Description

4.1 Data Sources

Grab sample data from the Sacramento-San Joaquin Delta and the northern parts of San Francisco Bay were used to develop linear relationships for key water quality constituents of concern as a function of EC. The key constituents are: chloride (Cl), bromide (Br), sodium (Na), calcium (Ca), sulfate (SO₄), magnesium (Mg), potassium (K), alkalinity, and hardness. Corresponding relationships for these constituent concentrations with TDS were also developed. The variations with TDS represent the percentage contribution of each constituent to total dissolved solids.

Note that hardness is calculated directly from calcium and magnesium concentrations using standard method SM 2340B, so is not an independent measurement:

$$\text{Hardness, mg equivalent CaCO}_3 / \text{L} = 2.497 [\text{Ca, mg/L}] + 4.118 [\text{Mg, mg/L}] \quad \dots \dots \dots \quad (4.1)$$

The grab sample data were downloaded from DWR's Water Data Library (WDL) website: <http://www.water.ca.gov/waterdatalibrary/>. These data were collected by DWR as part of the Municipal Water Quality Investigations (dating back to 1983), and its predecessor the Interagency Delta Health Monitoring Program (IDHAMP). The earliest data came from DWR's Water Information Management System (1948-1991). DWR and U.S. Bureau of Reclamation grab sample data dating back at least to 1964 are also available from the U.S. Environmental Protection Agency's STORET website. The California Department of Public Works collected water quality data starting in the 1950s and published these data in Bulletin 23 starting in 1935. <http://www.water.ca.gov/waterdatalibrary/docs/historic/bulletins.cfm> Those data were not used in this report. DWR has recently updated the Water Data Library to include pre-1983 grab sample data.

The analyte databases contain some measurement errors and data entry errors. Because the variation of the various analytes with EC or TDS is generally strongly correlated, erroneous data appeared as outliers on the data plots.

DWR has also developed historical fingerprint data using the Delta Simulation Model 2 (DSM2). These data are spatially and temporally compatible with the field grab sample data. These computer simulation data were used to determine how much water is reaching a given monitoring location from the various source of Delta water, and what contribution each source makes to the total EC.

DWR and Reclamation also measure continuous EC data throughout the Delta (available from the CDEC and IEP websites). Continuous EC data from Jersey Point were used to determine when seawater intrusion is important at Clifton Court and various other locations within the Delta. The continuous hourly EC data were also used to check the consistency of the grab sample EC data.

4.2 Analyte Characteristics

The following is a general discussion of the significance of the various water quality constituents drawn from various U.S. EPA drinking water documents and other related documents (including Wikipedia). Table 4-1 lists the national secondary drinking water regulations for four of the water quality constituents analyzed in this report.

Table 4.1: List of National Secondary Drinking Water Maximum Contaminant Levels¹

Contaminant	Secondary Maximum Contaminant Level
Chloride	250 mg/L
Manganese	0.05 mg/L
Sulfate	250 mg/L
Total Dissolved Solids	500 mg/L

There is no federally enforceable standard (i.e., Maximum Contaminant Level) for **chloride** in drinking water. The U.S. Environmental Protection Agency (USEPA) and the California Department of Public Health recommended standard for chloride levels in drinking water is 250 milligrams per liter (mg/L). Drinking water with chloride levels of 250 mg/L, or even lower, may exhibit a salty taste. The State Water Resources Control Board through Water Rights Decision 1641² limits the daily chloride concentration at key municipal and industrial intakes in the Delta to 250 mg/L year round. Decision 1641 also limits the chloride concentration at either the intake to the Contra Costa Canal or the City of Antioch's intake to 150 mg/L for 155-240 days per year depending upon the water year type.

Bromide is important because of its role, along with organic carbon and drinking water disinfectants, in the formation of disinfection byproducts such as bromated, brominated trihalomethanes, and brominated haloacetic acids. These disinfection byproducts are suspected carcinogens and their concentrations are regulated by the USEPA. The bromide ion itself has a low degree of toxicity.

¹ <http://water.epa.gov/drink/contaminants/secondarystandards.cfm>

² http://www.waterboards.ca.gov/waterrights/board_decisions/adopted_orders/decisions/d1600_d_1649/wrd1641_1999dec29.pdf

High levels of salt intake (**sodium** and chloride) may contribute to hypertension in some individuals. Both **calcium** and **magnesium** are essential to human health. Inadequate intake of either nutrient can impair health.

Sulfate in drinking water currently has a secondary maximum contaminant level (SMCL) of 250 mg/L, based on aesthetic effects (i.e., taste and odor). This regulation is not a federally enforceable standard, but is provided as a guideline for states and public water systems. EPA estimates that about 3% of the public drinking water systems in the country may have sulfate levels of 250 mg/L or greater.

Potassium is an essential element and is present in all animal and plant tissues. The primary source of potassium for humans is through foods such as vegetables and fruits. Although concentrations of potassium normally found in drinking water are generally low and do not pose health concerns, the high solubility of potassium chloride and its use in treatment devices such as water softeners can lead to significantly increased exposure. Potassium is very important in the human body. Along with sodium, it regulates the water balance and the acid-base balance in the blood and tissues. Elevations or depletions of potassium can cause health problems and even death. Maintaining consistent levels of potassium in the blood and cells is vital to body function.

Alkalinity in seawater is caused by the dissolution of calcium carbonate to form Ca^{2+} and CO_3^{2-} (carbonate) and absorption of two hydrogen ions by the carbonate ion. There are other ways alkalinity can be generated. However, anaerobic degradation processes, such as denitrification and sulfate reduction, have a much greater impact on oceanic alkalinity. These processes consume hydrogen ions and increase alkalinity. Conversely, aerobic degradation can decrease alkalinity by dissolving organic matter and producing hydrogen ions. Alkalinity in freshwater is determined by the soil and bedrock through which it passes. The main sources are rocks which contain carbonate, bicarbonate, and hydroxide compounds. Alkalinity is important in water treatment and the removal of total organic carbon from drinking water is based on source water alkalinity. High alkalinity can cause excessive calcium scaling on the insides of pipelines and other drinking water infrastructure.

The **hardness** of water is determined from the concentration of the multivalent cations, specifically calcium (Ca^{2+}) and magnesium (Mg^{2+}). These ions enter a water supply by leaching from minerals such as calcite, gypsum and dolomite. Hard drinking water is generally not harmful to human health but can cause problems by causing deposits on industrial and household equipment.

4.3 Evaluation of Water Analyses

The accuracy of the regression relationships between water quality constituents will depend in large part upon the accuracy of the collection, analysis and reporting of the grab sample data³.

³ The accuracy of the regression relationship between chloride and EC and other constituents also depends upon the relative proportions of water from different sources. Attempting to fit a single linear or quadratic equation to grab sample data at, say, Clifton Court, is very inaccurate because sometimes seawater dominates and at other times agricultural drainage dominates.

Two simple checks of the grab sample data are:

- (a) Mass Balances: Check that the sum of the concentrations of the water quality constituents equals the reported value for total dissolved solids (in mg/L).
- (b) Charge Balances: Check that the sum of the cations (positively charged ions) equals the sum of the anions. Note, for an anion/cation balance, everything is converted to an “electrical charge per volume,” expressed in milliequivalents per liter (meq/L). The conversion is based on the relationship between the mass and the charge for each ion species. This is discussed in more detail in Appendix I.

The 1985 USGS water supply paper “Study and Interpretation of the Chemical Characteristics of Natural Water,” Third Edition, by John D. Hem (U.S. Geological Survey Water Supply Paper 2254) contains detailed descriptions of the accuracy of chemical analysis of water samples (see, e.g., Evaluation of the Water Analysis, starting on page 163. Hem (1985) presents a number of additional tests of the accuracy and consistency of water quality data. These methods are presented below.

4.3.1 Relationship between TDS and EC

Hem (1985) suggests that the TDS value in mg/L should generally be from 0.55 to 0.75 times the specific conductance in micromhos per centimeter (for $TDS < 2,000 \text{ mg/L}$). He further states that water in which anions are mostly bicarbonate and chloride will have a factor near the lower end of this range, and waters high in sulfate may reach or even exceed the upper end.

Figures 4-1 through 4-3 show the TDS/EC ratios for grab sample data for Suisun Bay at Mallard Island, the San Joaquin River at Vernalis, and the Sacramento River at Hood. The San Joaquin River TDS/EC ratio is higher than at Mallard Island over the range $600 < TDS < 1,000 \text{ mg/L}$. Both relationships reach a maximum ratio of 0.62 - 0.63 at their highest TDS values. The TDS/EC ratios in the Delta can be as low as 0.50.

TDS to EC Ratio - Suisun Bay

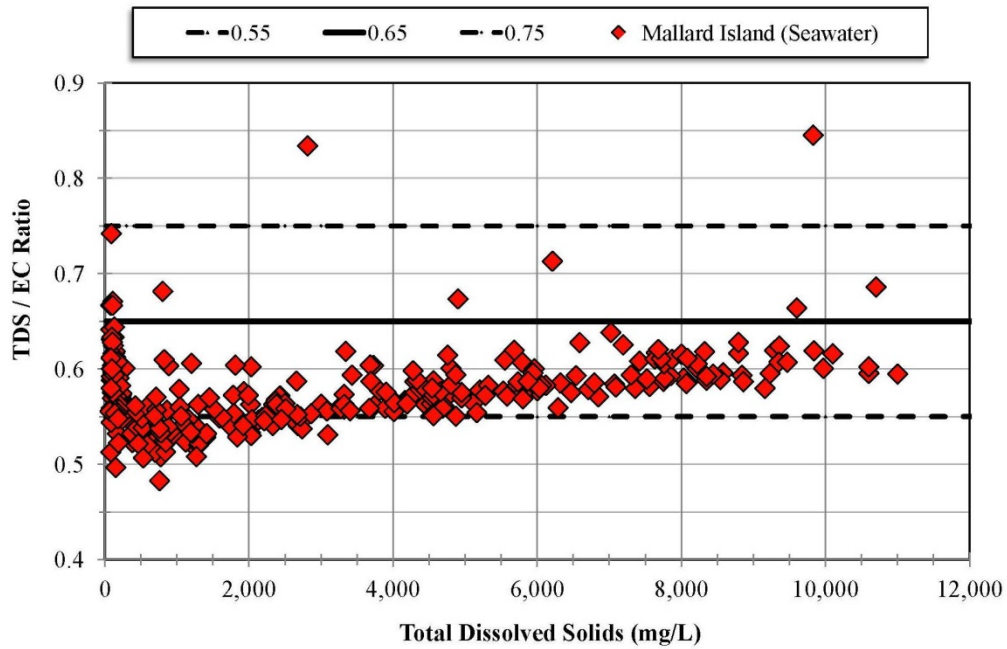


Figure 4-1: Ratio of total dissolved solids to specific conductance (EC) for grab sample data from Suisun Bay at Mallard Island.

TDS to EC Ratio - San Joaquin

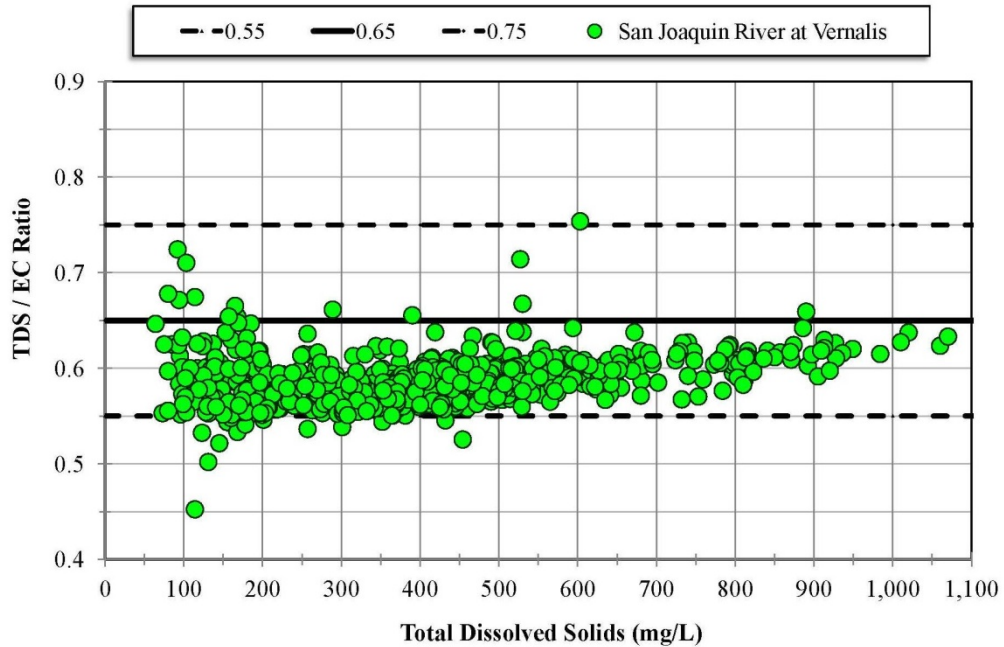


Figure 4-2: Ratio of total dissolved solids to specific conductance (EC) for grab sample data from the San Joaquin River at Vernalis

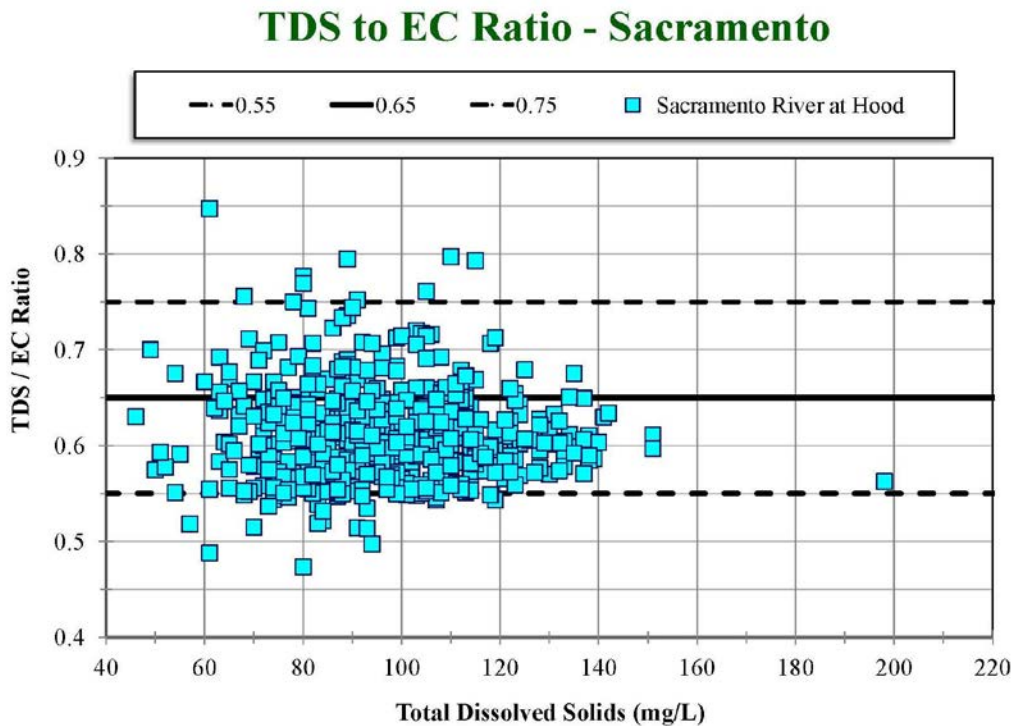


Figure 4-3: Ratio of total dissolved solids to specific conductance (EC) for grab sample data from the Sacramento River at Hood

These techniques were used to check the accuracy and consistency of the grab sample data, especially outliers, but are not definitive enough to fully determine the accuracy of the data.

4.3.2 Relationship between total anions or cations and electrical conductivity

The total of meq/L for either anions or cations multiplied by 100 usually agrees approximately with the conductivity in micro mhos per centimeter. This relationship is not exact, but it is somewhat less variable than the relationship between conductivity and dissolved solids in milligrams per liter. These relationships between EC and TDS break down for high TDS ($> 50,000 \text{ mg/L}$) and very low TDS.

4.3.3 Correlation between different water quality constituents

The individual cations and anions for water from similar sources can be expected to be highly correlated when plotted as a function of EC or TDS. This technique was used in this report to check for errors in reporting and analyzing the grab sample data.

5. Development of Regression Equations

The water quality constituent data typically show relatively high correlations with EC and TDS. They are also highly correlated with respect to each other, e.g., bromide versus chloride and chloride versus sulfate. For interior Delta stations where the range of salinity was relatively low, the relationships are generally linear, i.e.,

where Y is the water quality constituent, X is either EC or TDS, and b and c are the coefficients used to fit the available grab sample data.

At the western Delta and Suisun and San Pablo Bay stations where the range of salinities is very high, due to a high level of seawater intrusion. In those cases, a quadratic equation was found to be more suitable, i.e.,

where there are three coefficients a, b, and c.

The coefficients for these quadratic and linear equations can be obtained using the regression programs in Excel. However, these Excel least-squares quadratic or linear regressions do not agree with the data over the full range of EC and TDS. As shown in Figure 5-1, the quadratic regression fit using Excel (for $EC > 260 \mu\text{S}/\text{cm}$) appears to fit the data well over the maximum range of EC, i.e., up to 19,000 $\mu\text{S}/\text{cm}$. The blue line is the Excel regression with an r-squared of 0.991. In Figure 5-1, grab sample data from Mallard Island in Suisun Bay are used to represent a situation where seawater intrusion generally dominates. The exception is during very high Delta outflows (very low EC), when runoff from the Sacramento and San Joaquin Rivers is high enough to repel seawater intrusion. Because there is a limited amount of grab sample data from Mallard Island for low EC, data from the Jersey Point station are also plotted.

The EC of 260 $\mu\text{S}/\text{cm}$ is used in this report to represent the transition from seawater dominated conditions to conditions when Delta outflows are very high and the water at Mallard Island is a mixture of Sacramento and San Joaquin River water and some local drainage. As will be shown later in this chapter, for $\text{EC} < 260 \mu\text{S}/\text{cm}$, a different regression relationship is needed to represent the variation of water quality constituents with EC.

Mallard Island and Jersey Point Chloride

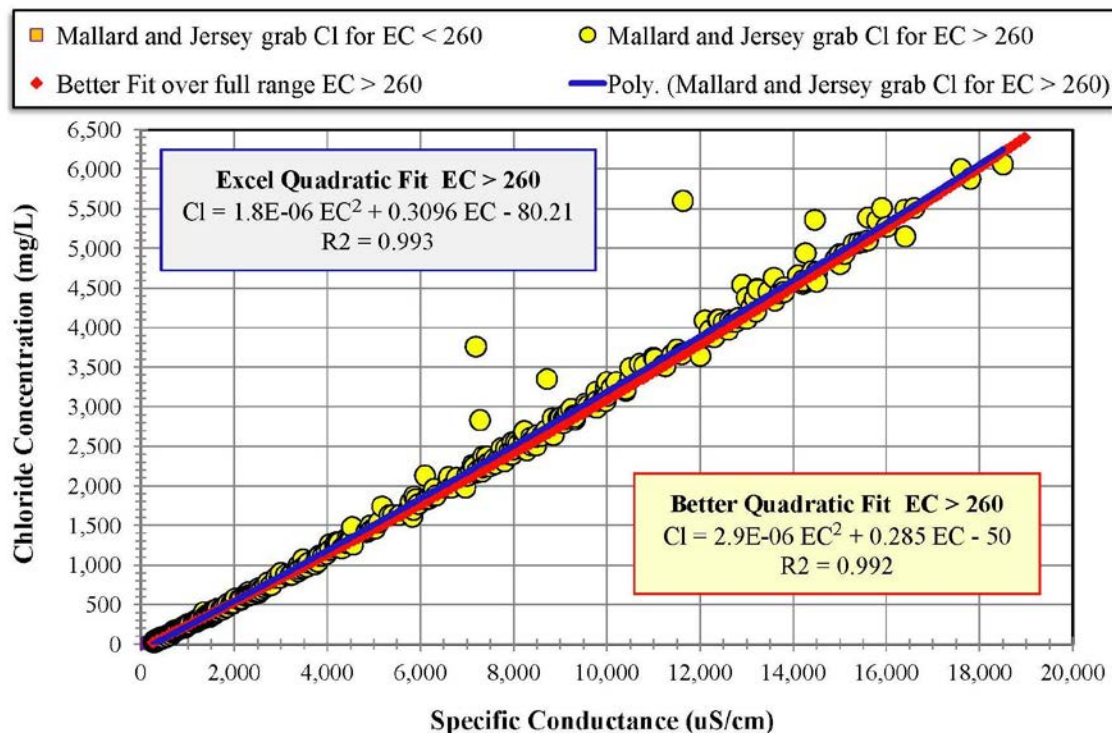


Figure 5-1: Variation of chloride concentration (Cl) as a function of specific conductance (EC) for grab sample data from Mallard Island and Jersey Point. The data are fitted with a quadratic regression equation over the range $2600 < EC < 19,000 \mu\text{S}/\text{cm}$.

Although the coefficient a for this western Delta and Suisun Bay location (Figure 5-1) is small, it cannot be eliminated. Figure 5-2 shows a comparison of the better quadratic regression equation with the Cl estimate if the coefficient a were set to zero. This is the equivalent of extrapolating Denton's linear fit (CUWA, 1995) well beyond $EC = 1,100 \mu\text{S}/\text{cm}$. The Cl estimate error would be very large at high EC without this additional x -squared coefficient.

Mallard Island and Jersey Point Chloride

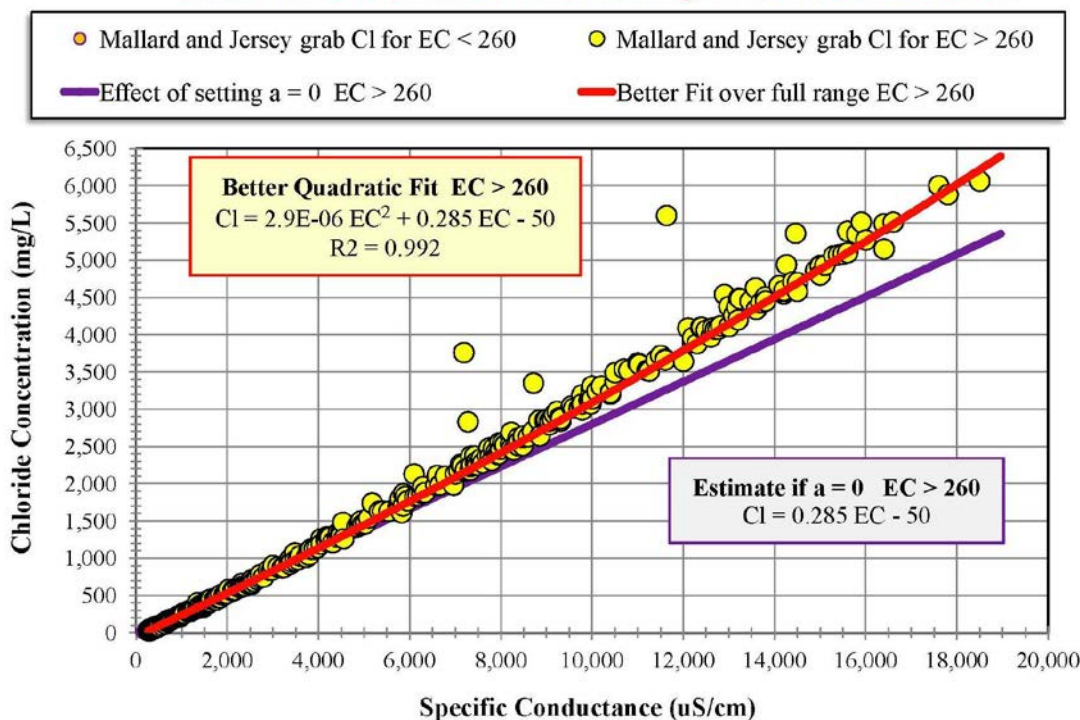


Figure 5-2: Variation of chloride concentration (Cl) as a function of specific conductance (EC) for grab sample data from Mallard Island and Jersey Point. Setting the coefficient a to zero would result in significant errors in the estimates of Cl at very high EC .

The quadratic regression fits using Excel sometimes deviate from the grab sample data when EC is low. As shown Figure 5-3, despite the good r-squared value, the Excel quadratic regression equation (red line) estimates much lower chlorides for $EC < 1,100 \mu\text{S}/\text{cm}$. This is the range of EC values that typically occur at the SWP, CVP and CCWD intakes in the interior Delta.

The better quadratic equation fit (blue dots) was adjusted to better fit the data over the full range of $EC > 260 \mu\text{S}/\text{cm}$ (r-squared 0.989). This quadratic fit is based on an earlier linear fit by Denton (CUWA, 1995) for lower ranges of EC in the interior Delta, $Cl = 0.285 EC - 50$, i.e., where $b = 0.285$ and $c = -50$. The coefficient a for the EC -squared term was then adjusted to also fit the data at high EC .

Mallard Island and Jersey Point Chloride

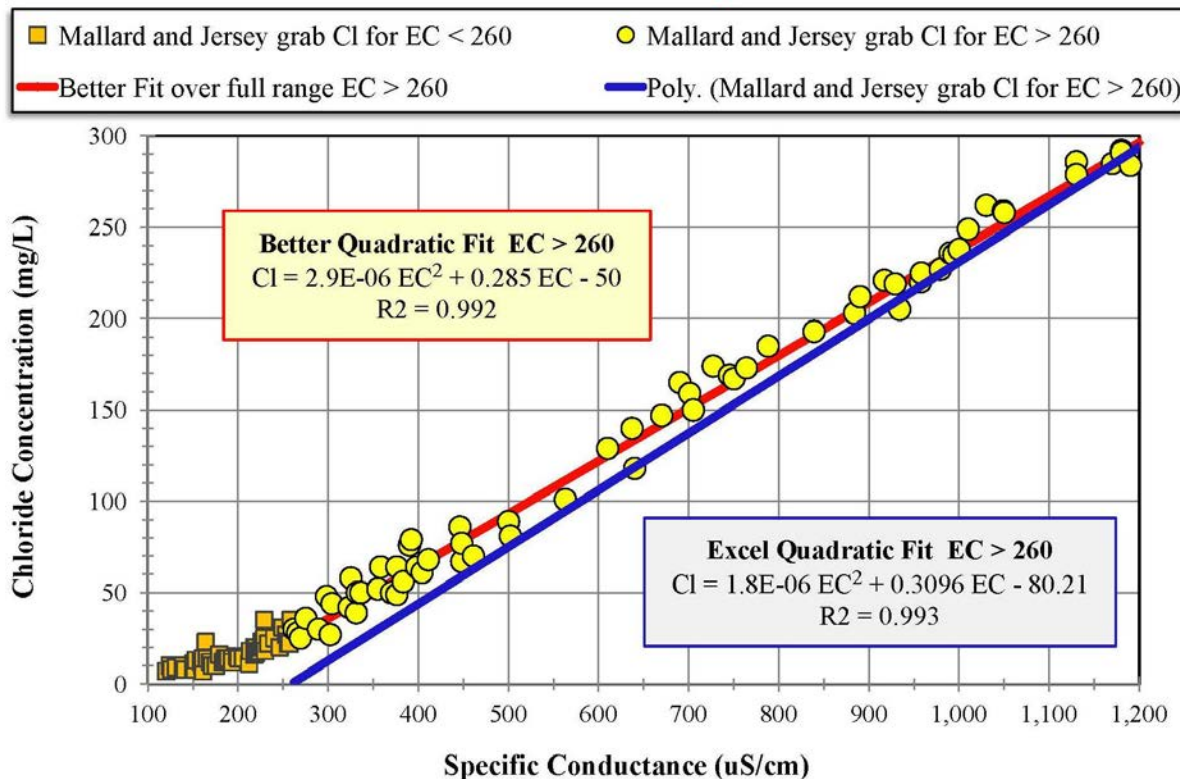


Figure 5-3: Variation of chloride concentration (Cl) as a function of specific conductance (EC) for Mallard Island and Jersey Point grab samples over the lower salinity range ($\text{EC} < 1,000 \mu\text{S}/\text{cm}$) generally experienced in the south and central Delta. A different quadratic equation (with zero intercept) is needed to fit the data for $\text{EC} < 260 \mu\text{S}/\text{cm}$.

The values of r-squared shown in Figure 5-3 are for the full range of the Mallard Island and Jersey Point grab sample data, i.e., $260 < \text{EC} < 19,000 \mu\text{S}/\text{cm}$. However, over the range applicable to central and south Delta stations ($260 < \text{EC} < 1,000 \mu\text{S}/\text{cm}$), the r-squared values for the Excel quadratic fit and the better quadratic fit are 0.931 and 0.989, respectively. In other words, the Excel fit for all $\text{EC} > 260 \mu\text{S}/\text{cm}$ would give poor estimates of chloride concentration over the range of EC of most interest to urban agencies diverting drinking water from the Delta.

The grab sample data for Mallard Island and Jersey Island when seawater intrusion is very small (very high Delta outflows) were also fitted using a quadratic equation. Under these conditions ($\text{EC} < 260 \mu\text{S}/\text{cm}$), the water is a mixture of Sacramento River water and agricultural drainage. The EC of distilled water ($\text{Cl} = 0 \text{ mg/L}$) is about $0.5\text{-}3.0 \mu\text{S}/\text{cm}$, so the intercept c for this quadratic equation is effectively zero. For these very low values of EC , the grab sample data were fitted with a quadratic equation with a zero intercept using Excel.

Figure 5-4 shows in more detail the agreement of the regression equation (Excel) for EC < 260 $\mu\text{S}/\text{cm}$ and the grab sample data. The r-squared value for this regression equation (green line) is 0.693.

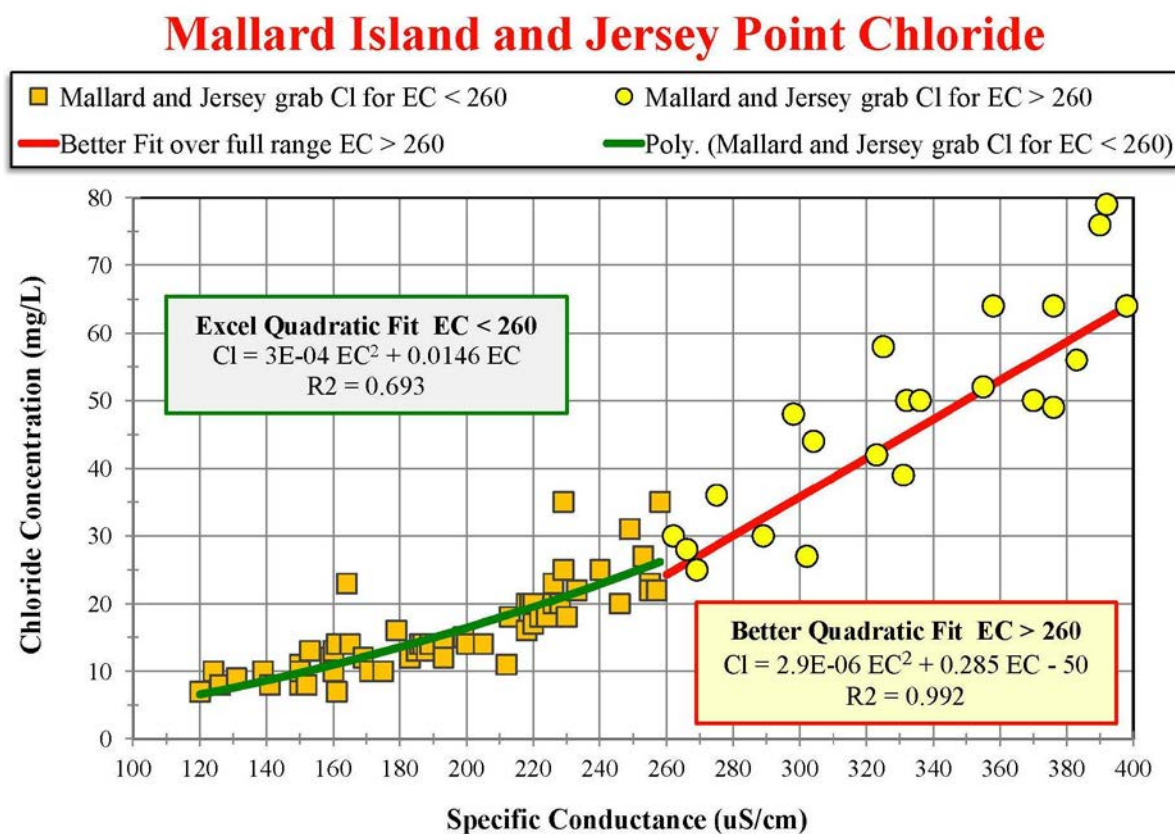


Figure 5-4: Variation of chloride concentration (Cl) as a function of specific conductance (EC) for Mallard Island and Jersey Point grab samples over the very low salinity range (EC < 400 $\mu\text{S}/\text{cm}$). A quadratic equation (with zero intercept) is used to fit the data for EC < 260 when the effect of seawater intrusion is very small.

This approach for deriving regression equations for chloride as a function of EC was also used for the other water quality constituents as a function of EC and TDS. In the western Delta and Suisun Bay, seawater generally dominates but when EC < 260 $\mu\text{S}/\text{cm}$ a different regression equation is needed, representing a mixture of Sacramento River water and agricultural drainage. EC = 260 $\mu\text{S}/\text{cm}$ represents the approximate break point in the relationship between chloride and EC below which the effects of seawater intrusion are greatly diminished.

Figure 5-5 shows the variation in calcium concentration with EC for Mallard Island and Jersey Point grab sample data for EC < 2,000 $\mu\text{S}/\text{cm}$. In this case, the Excel quadratic equation showed good agreement for low EC values ($260 < \text{EC} < 2,000 \mu\text{S}/\text{cm}$) and no adjustment to the regression fit was necessary. As was the case for chloride concentration at this location (Figure 5-4, as separate regression equation is needed for EC < 260 $\mu\text{S}/\text{cm}$.

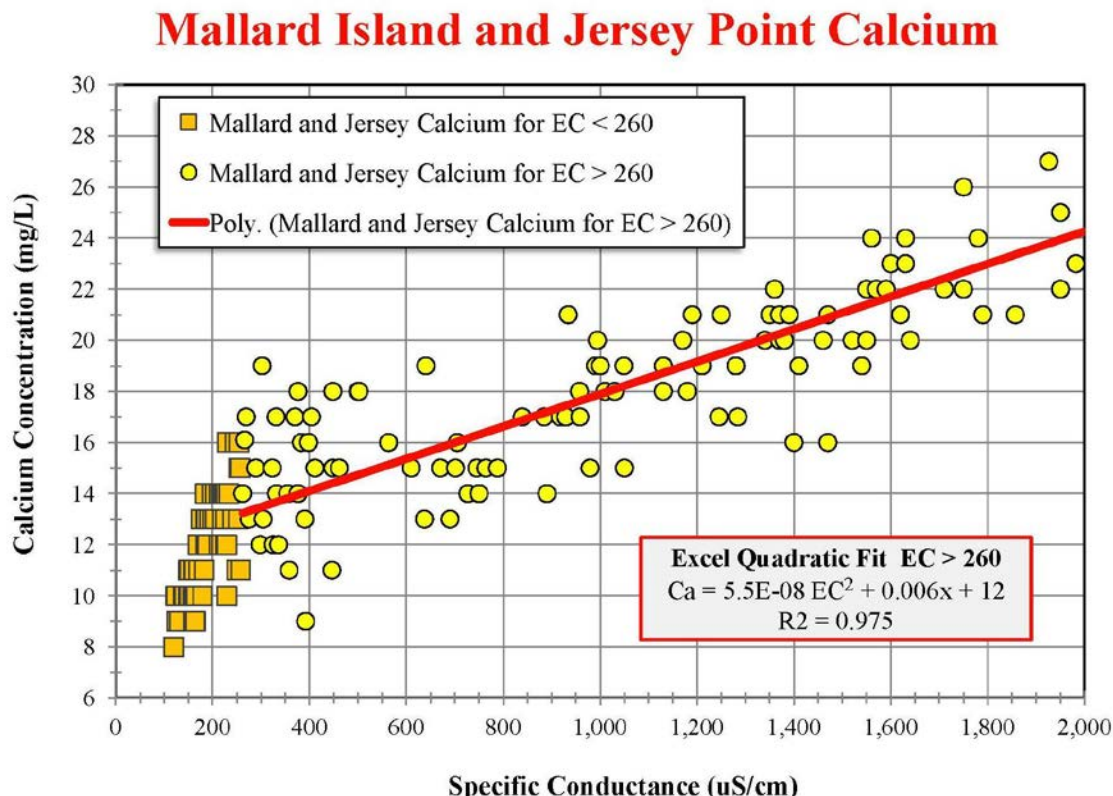


Figure 5-5: Variation of chloride concentration (Cl^-) as a function of specific conductance (EC) for Mallard Island and Jersey Point grab samples for $EC < 2,000 \mu S/cm$. A separate quadratic equation is needed to fit the data for $EC < 260$ when the effect of seawater intrusion is very small.

For interior Delta stations, the contribution from seawater intrusion is smaller and the contribution from agricultural drainage is often large. In the interior Delta, the data were generally bounded by a quadratic equation representing times when seawater intrusion dominated and a quadratic regression equation representing times when agricultural drainage dominated. Because EC is typically $< 1,100 \mu S/cm$ in the interior Delta the regression equations were essentially linear.

The graphs in this chapter are intended to illustrate the approach used to derive regression equations for water quality constituents as a function of EC or TDS. Regression equations were developed for all of the water quality constituents (Cl, Br, Na, Ca, SO₄, Mg, K, alkalinity and hardness) as functions of both EC and TDS, as well as equations for bromide as a function of chloride concentration.

6. Variation of Constituent Ratios with TDS

Plotting salinity constituent ratios with TDS (e.g. chloride to TDS ratio) as a function of TDS is a useful way to illustrate how source water composition influences the relationship between constituents. The variations of the different ratios as a function of TDS can be categorized into four groups (See Table 6-1).

As discussed in more detail in Appendix E, the ratios of chloride, bromide and sodium show similar patterns as a function of TDS (and EC). The ratios with TDS increase with increasing TDS, eventually tending to a higher value than the agricultural drainage value at high TDS (Figures E-1, E-4 and E-5, respectively). At low TDS, all the curves tend to a low ratio, corresponding to Sacramento-dominated water.

The ratio of sulfate to TDS (Figure E-7) is different in that agricultural drainage data trends to a high ratio (0.28) at high TDS whereas the seawater-dominated water trends to a low ratio (0.07). The sulfate ratios for seawater and agricultural drainage dominated water both trend toward a low value at low TDS.

The variations of calcium, magnesium, hardness and alkalinity are all similar (Figures E-6, E-8, E-10 and E-11). They differ from the chloride group in that the ratios with TDS decrease rather than increase with increasing TDS. The high TDS asymptote for seawater-dominated locations is lower than for agricultural drainage-dominated locations.

The ratio of potassium to TDS is different than the other three categories in that both agricultural drainage and seawater-dominated data tend to a low ratio, but unlike calcium and magnesium, the seawater asymptote is higher than the agricultural-dominated asymptote (Figure E-9).

Table 6-1: Categories of constituent ratio variation with total dissolved solids

Category	Constituent	Variation at Low TDS	Variation at High TDS	See Figures
1A	Cl, Br and Na	Ratio increases with increasing TDS.	High ratio asymptotes. Seawater ratio higher than agricultural drainage ratio.	E-1, E-4 and E-5
1B	SO ₄	Ratio increases with increasing TDS.	Seawater ratio lower than agricultural drainage ratio. Seawater ratio decreases slightly with increasing TDS.	E-7
2A	Ca, Mg, Hardness and Alkalinity	Ratio decreases with increasing TDS.	Low ratio asymptotes. Seawater ratio lower than agricultural drainage ratio.	E-6, E-8, E-10 and E-11
2B	K	Ratio decreases with increasing TDS.	Low ratio asymptotes. Seawater ratio higher than agricultural drainage ratio.	E-9

The estimate of calcium from TDS, for example, at a given Delta location will depend on the mixture of different sources of water at that location at that particular time. When seawater dominates (which typically corresponds to periods of high TDS), the Ca/TDS ratio will be close to that of seawater. However, during periods of high outflow, the Ca/TDS ratio will be closer to that for freshwater sources such as the Sacramento River.

7. Regression Equations for Delta Boundary Conditions

These regression coefficients provided in this section represent the range of water quality constituent data for locations characteristic of seawater, agricultural drainage, and fresh upstream tributary conditions. In the case of chloride concentrations at medium to high EC, the seawater case is the upper limit and the agricultural drainage case is the lower limit. For calcium and sulfate the two limits are reversed.

The following tables assume a quadratic relationship between salinity constituents of the following form:

$$Y = a X^2 + b X + c$$

where Y is the unknown constituent concentration to be estimated, X is the known constituent concentration, and a, b, and c are regression constants.

These seawater, agricultural drainage and freshwater source regression equations can be used to estimate the total concentrations of the water quality constituents from known values of EC or TDS once the percentages of seawater and other sources are known at a given location. The methods for estimating the percentage of seawater are discussed in detail in Chapter 9.

7.1 Seawater Dominated Boundary Locations

The western Delta and Suisun Bay are the areas closest to San Francisco Bay and the Pacific Ocean where seawater intrusion dominates. The variations of each constituent with EC and TDS at Mallard Island¹ and Jersey Point (Figure 1-1) during periods of low or medium Delta outflow are representative of the expected variations at other interior Delta stations when seawater dominates. Tables 7.1 through 7.6 present the regression coefficients for estimating various salinity constituent concentrations when seawater dominates. Graphs showing the relationships between these constituents are presented in Appendix A.

The regression equation for chloride concentration as a function of sulfate concentration is included in Tables 7.5 and 7.6 because plotting Cl as a function of SO₄ is a good way of identifying whether a given measurement was taken during a period when seawater intrusion dominated or when seawater intrusion was not significant and agricultural drainage dominated. It is also possible that the water at that time was a mixture of both sources of salinity. The seawater-dominated equation for Cl as a function of SO₄ represents the expected upper range of data at interior Delta stations. The corresponding agricultural drainage equation in section 7.2 represents the expected lower range of the grab sample data.

¹ The Mallard Island monitoring station is sometimes referred to as RSAC075 or D10. It is very close to Chipps Island.

Table 7.1: Regression Coefficients for Estimating Water Quality Constituents from Specific Conductance for Seawater-Dominated Locations (EC > 260 $\mu\text{S}/\text{cm}$)

X	Y	a	b	c	r-squared
EC	TDS	4.5E-06	0.53	14	0.991
	Cl	2.9.E-06	0.285	-50	0.992
	Br	1.0E-08	0.001	-0.18	0.996
	Na	1.6.E-06	0.156	-18	0.990
	Ca	5.5.E-08	0.006	12	0.975
	SO4	4.5.E-07	0.0375	6.0	0.930
	Mg	2.0E-07	0.019	4.5	0.980
	K	9.0E-08	0.0054	0.61	0.974
	Hardness	1.5.E-06	0.0863	50	0.977
	Alkalinity	0	0.0014	63	0.392

Table 7.2: Regression Coefficients for Estimating Water Quality Constituents from Specific Conductance for Seawater-Dominated Locations (EC < 260 $\mu\text{S}/\text{cm}$)

X	Y	a	b	c	r-squared
EC	TDS	-2.0E-04	0.646	0.0	0.930
	Cl	3.0.E-04	0.0146	0.0	0.693
	Br	1.3.E-06	-3.0E-05	0.0	0.492
	Na	1.2.E-04	0.0519	0.0	0.853
	Ca	1.4.E-04	0.0899	0.0	0.587
	SO4	-4.0.E-05	0.078	0.0	0.415
	Mg	-1.3.E-05	0.0391	0.0	0.758
	K	0.0	0.0079	0.0	0.098
	Hardness	3.7E-04	0.380	0.0	0.730
	Alkalinity	-6.0E-04	0.390	0.0	0.569

Table 7.3: Regression Coefficients for Estimating Water Quality Constituents from Total Dissolved Solids for Seawater-Dominated Locations (TDS > 150 mg/L)

X	Y	a	b	c	r-squared
TDS	EC	-1.9E-05	1.85	-20	
	Cl	2.8E-07	0.55	-56	0.997
	Br	4.0E-09	0.0019	-0.20	0.932
	Na	1.0E-06	0.292	-22	0.994
	Ca	5.5E-08	0.011	12	0.940
	SO4	4.6E-07	0.071	7	0.980
	Mg	2.0E-07	0.0351	3.7	0.986
	K	2.0E-08	0.0112	0.33	0.980
	Hardness	1.1E-06	0.170	47	0.987
	Alkalinity	0.0	0.0023	63	0.396

Table 7.4: Regression Coefficients for Estimating Water Quality Constituents from Total Dissolved Solids for Seawater-Dominated Locations (TDS < 150 mg/L)

X	Y	a	b	c	r-squared
TDS	EC	8.0E-05	1.6578	0.0	0.9115
	Cl	1.0E-03	0.013	0.0	0.641
	Br	3.6E-06	-4.5E-05	0.0	0.516
	Na	4.0E-04	0.0772	0.0	0.807
	Ca	-3.9E-04	0.151	0.0	0.570
	SO4	-5.0E-05	0.1235	0.0	0.448
	Mg	-4.0E-05	0.0643	0.0	0.711
	K	0.0	0.0132	0.0	0.127
	Hardness	-1.0E-03	0.627	0.0	0.711
	Alkalinity	-1.4E-03	0.640	0.0	0.509

Table 7.5: Regression Coefficients for Estimating Bromide Concentration from Chloride Concentration for Seawater-Dominated Locations when Cl > 25 mg/L.

X	Y	a	b	c	r-squared
Cl	Br	1.0E-07	0.0035	-0.0154	0.971

Table 7.6: Regression Coefficients for Estimating Bromide Concentration from Chloride Concentration for Seawater-Dominated Locations when Cl < 25 mg/L.

X	Y	a	b	c	r-squared
Cl	Br	0.0	0.0027	0.0	0.463

7.2 San Joaquin River Dominated Boundary Locations

The point where the San Joaquin River flows into the Delta is dominated by agricultural runoff (Figure 1-1). The water quality at Vernalis², and Maze which is about 4.9 miles upstream, is influenced by agricultural drainage mixed with relatively freshwater from the Stanislaus, Tuolumne and Merced Rivers on the east side of the San Joaquin Valley. The water quality is also affected by the quality of water exported to the Valley from the south Delta diversion points. During prolonged drought periods, the salinity of the exported water is affected by seawater intrusion. This export water from the Delta is applied to irrigated land and some of it eventually shows up in the return flows at Vernalis.

Tables 7.7 through 7.9 present the regression coefficients for the quadratic or linear relationships between various salinity constituents. Graphs showing the relationships between these constituents at the San Joaquin inflow boundary condition are presented in Appendix B.

² The Vernalis monitoring station is sometimes referred to as RSAN112 or C10.

Table 7.7: Regression Coefficients for Estimating Water Quality Constituents from Specific Conductance for Agricultural Drainage-Dominated Locations

X	Y	a	b	c	r-squared
EC	TDS	3.5E-05	0.56	7.0	0.994
	Cl	1.7E-05	0.13	-8.0	0.982
	Br	7.0E-08	0.0004	-0.035	0.894
	Na	1.3E-05	0.109	-3.1	0.984
	Ca	1.0E-06	0.045	2.8	0.960
	SO4	3.5E-05	0.11	-1.2	0.948
	Mg	6.0E-07	0.026	-0.1	0.955
	K	0	0.0029	0.8	0.630
	Hardness	-3.0E-06	0.224	4.3	0.974
	Alkalinity	-3.0E-05	0.15	13.5	0.910

Table 7.8: Regression Coefficients for Estimating Water Quality Constituents from Total Dissolved Solids for Agricultural Drainage-Dominated Locations

X	Y	a	b	c	r-squared
TDS	EC	-2.0E-04	1.82	-10	0.995
	Cl	2.0E-05	0.240	-10	0.976
	Br	1.0E-07	0.00075	-0.035	0.905
	Na	0.0	0.2085	-6.1	0.977
	Ca	-3.0E-06	0.076	3.1	0.958
	SO4	5.5E-05	0.22	-4.0	0.941
	Mg	0.0	0.0437	0.12	0.972
	K	0.0	0.005	0.7	0.608
	Hardness	-1.0E-05	0.377	7.2	0.976
	Alkalinity	-1.0E-04	0.26	12	0.904

Table 7.9: Regression Coefficients for Estimating Bromide Concentration from Chloride Concentration for Agricultural Drainage-Dominated Locations

X	Y	a	b	c	r-squared
Cl	Br	0.0	0.0032	-0.0064	0.942

7.3 Sacramento River Dominated Boundary Locations

Data from the Sacramento River at Hood³ and Greenes Landing represent the Sacramento River boundary location (Figure 1-1). The salinities at these locations are very low and reflect relatively fresh water from the Sacramento, Feather and American Rivers. These regression equations only apply for the range EC < 260 $\mu\text{S}/\text{cm}$ and TDS < 160 mg/L. Because some of the regression equations are quadratic equations, they could give spurious results for salinities higher than this range. Tables 7.10 through 7.12 present the regression coefficients for estimating various salinity constituent concentrations. Graphs showing the relationships between these constituents at the Sacramento River boundary condition are presented in Appendix C.

Table 7.10: Regression Coefficients for Estimating Water Quality Constituents from Specific Conductance for Sacramento Inflow (Freshwater)

X	Y	a	b	c	r-squared
EC	TDS	-5.0E-05	0.61	0.0	0.818
	Cl	1.4.E-04	0.0161	0.0	0.789
	Br	9.0.E-09	0.0001	0.0	0.069
	Na	1.2.E-04	0.0415	0.0	0.868
	Ca	-1.0.E-04	0.0941	0.0	0.736
	SO4	1.5.E-04	0.0237	0.0	0.676
	Mg	1.0.E-05	0.0394	0.0	0.872
	K	0.0	0.0082	0.0	0.262
	Hardness	-2.7.E-04	0.398	0.0	0.854
	Alkalinity	-3.5.E-04	0.45	0.0	0.895

³ The Hood monitoring station is also referred to as RSAC142 or C3A. The Greenes Landing station is also referred to as RSAC139 or C3.

Table 7.11: Regression Coefficients for Estimating Water Quality Constituents from Total Dissolved Solids for Sacramento Inflow (Freshwater)

X	Y	a	b	C	r-squared
TDS	EC	2.0.E-04	1.62	0.0	0.863
	Cl	4.0E-04	0.024	0.0	0.645
	Br	0.0	0.00016	0.0	0.085
	Na	3.4.E-04	0.066	0.0	0.776
	Ca	0.0	0.120	0.0	0.620
	SO4	4.8.E-04	0.0316	0.0	0.682
	Mg	4.0.E-05	0.0629	0.0	0.770
	K	0.0	0.0136	0.0	0.354
	Hardness	-6.0.E-04	0.639	0.0	0.771
	Alkalinity	0.0	0.623	0.0	0.712

Table 7.12: Regression Coefficients for Estimating Bromide Concentration from Chloride Concentration to Bromide for Sacramento Inflow (Freshwater)

X	Y	a	b	c	r-squared
Cl	Br	0.0	0.0023	0.0	0.077

7.4 Mokelumne and Cosumnes River Boundary Locations

As shown in Appendix D, the variations of chloride, calcium and sulfate with EC at these locations closely follow the relationships for Sacramento River water. Tables 7-10, 7-11 and 7-12 can be used to estimate salinity constituents for the Mokelumne and Cosumnes Rivers. In the case of calcium and sulfate, the data suggest some small additional influence of agricultural drainage. Specific Mokelumne and Cosumnes relationships could be developed if more accuracy is needed.

8. Regression Relationships by Interior Delta Region

The objective of this chapter is to analyze the relationships between the water quality constituents at key locations in the interior Delta. The regression equations for the seawater-dominated, agricultural drainage-dominated and freshwater-dominated boundary stations developed in Appendices A, B and C, respectively, and tabulated in Chapter 7, represent the expected range of variation of water quality constituent data (for a given EC or TDS) at interior Delta stations.

The interior Delta grab sample data will be much more scattered, e.g. when plotted as chloride concentration versus EC, because the water quality is the result of more than one source, and the contributions from the different water sources vary by season and by water year type. There have also been long-term changes in the contributions of seawater intrusion, agricultural drainage and Sacramento River inflows because of changes in the operational rules for the Delta (e.g., changes in the Bay-Delta water quality control plans and new facilities) and removal or relocation of agricultural drains and changes in the amount of agricultural drainage reaching the San Joaquin River from the westside of the San Joaquin Valley (e.g., the Grassland Bypass Project).

For example, Figure 8-1 shows chloride grab sample data from the State Water Project's Banks Pumping Plant plotted as a function of specific conductance. The data are bounded by the seawater-dominated regression equation (Table 7.1) and the agricultural drainage-dominated equation (Table 7.7). The former (shown as a red line) is the upper limit, and the latter (shown as a green line) is the lower limit of the range of chloride concentrations for a given EC.

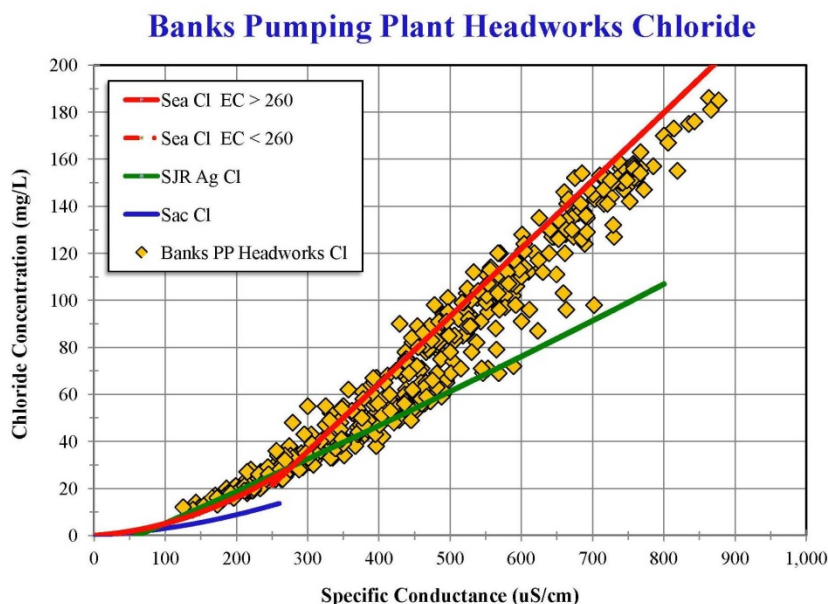


Figure 8-1: Variation of chloride concentration as a function of specific conductance (EC) for the Headworks of Banks Pumping Plant in the south Delta. The equations for the seawater-dominated relationships (labeled Sea, red line) and agricultural drainage-dominated relationship (labeled SJR Ag, green line) are given in Table 7.1 and 7.7.

The Sacramento River regression equation (Table 7.10) is also plotted in Figure 8-1 for comparison purposes. While water from the Sacramento River does reach Banks Pumping Plant, the Sacramento River source does not make a significant contribution to the salinity at this location. During periods of low EC and Banks Pumping Plant the grab sample data are consistent with the agricultural drainage-dominated regression equation (Table 7.7).

Figure 8-2 shows the corresponding variation in bromide concentration at Banks Pumping Plant Headworks. These two plots are similar although the concentrations of bromide are much lower ($\text{Br} < 0.64 \text{ mg/L}$) than the chloride concentrations which were as high as 186 mg/L.

The highest chloride and bromide concentrations in this example correspond to seawater intrusion events. There are also many data points corresponding to periods when agricultural drainage dominated and seawater intrusion was negligible (typically periods of high Delta outflow). Plotting the grab sample data in these ways does separate the data according to which water source is dominating, and also illustrate how neither the seawater-dominated regression equation or the agricultural drainage-dominated equation alone is sufficient to accurately estimate a water quality constituent concentration at given interior Delta location.

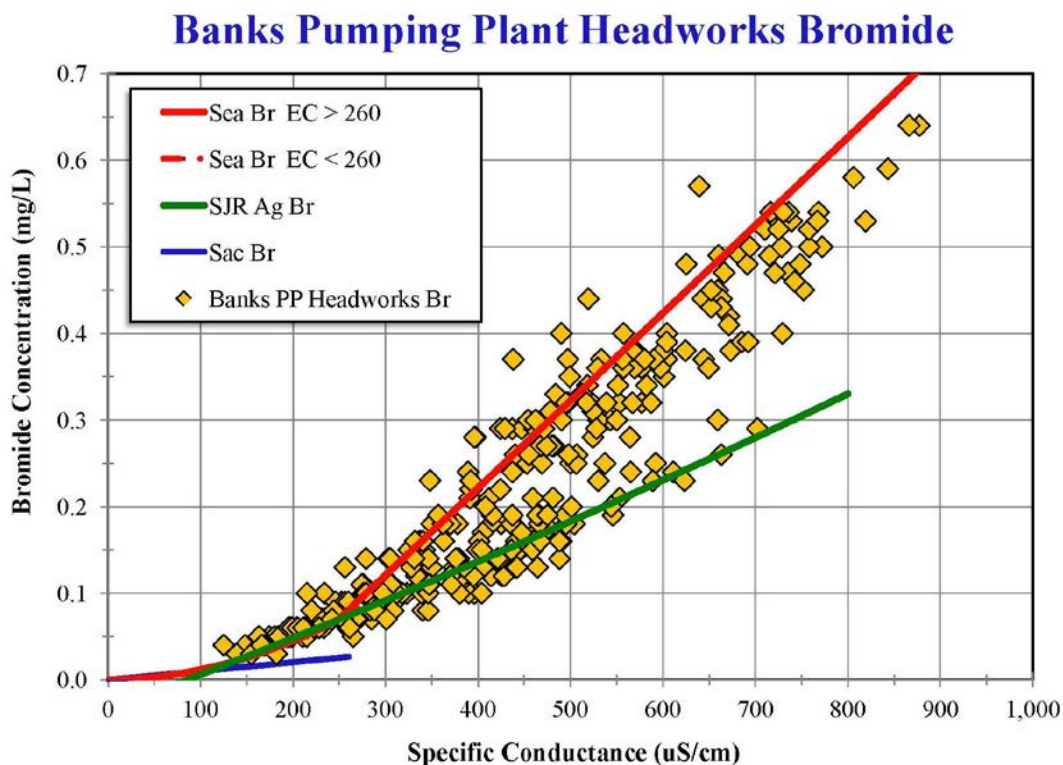


Figure 8-2: Variation of chloride concentration as a function of specific conductance (EC) for the Headworks of Banks Pumping Plant in the south Delta.

Plotting the Banks Pumping Plant data instead as TDS as a function of EC (Figure 8-3) almost collapses the data onto a single line with only a small separation between the regression equations for seawater-dominated and agricultural drainage-dominated events. This makes it

easier to estimate TDS from EC, but does not illustrate whether the percentage contributions from different sources of water vary at this particular location.

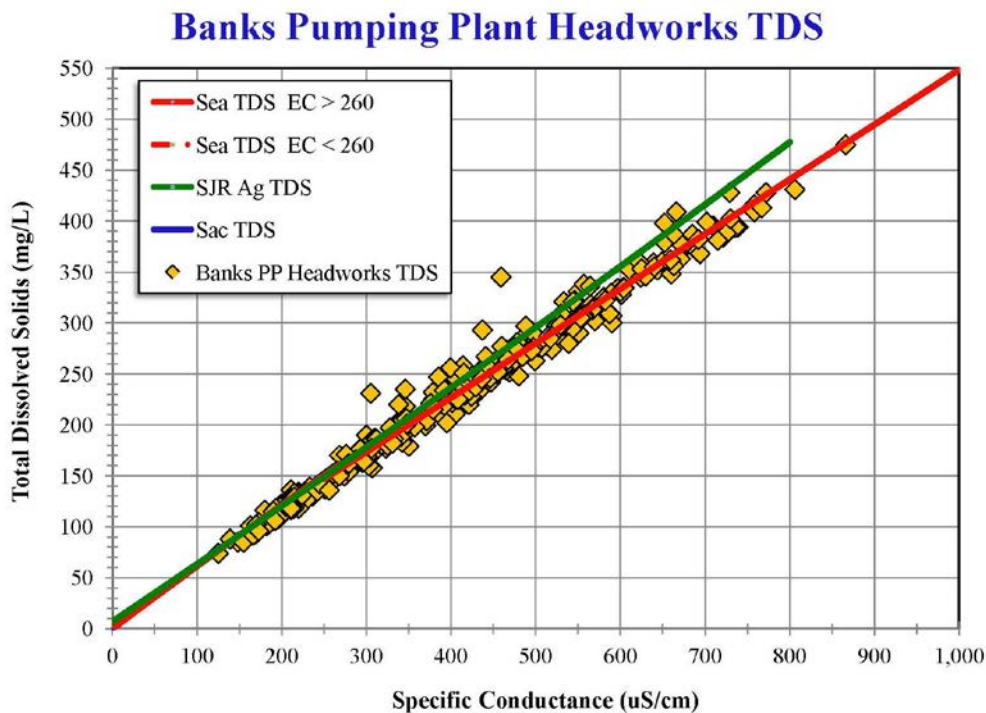


Figure 8-3: Variation of total dissolved solids (TDS) as a function of specific conductance (EC) for the Headworks of Banks Pumping Plant in the south Delta.

Suits (2002) recognized that data collected during periods when seawater intrusion dominates can be distinguished from data collected when agricultural drainage dominates by plotting calcium concentration as a function of chloride concentration. Chloride represents 55% of the TDS in seawater-dominated samples whereas calcium represents only 1% whereas calcium represents only about 1% of seawater and 8% of agricultural drainage in the San Joaquin River at Vernalis (Table 3.1).

Plotting calcium as a function of chloride increases the separation between seawater-dominated and agricultural drainage-dominated data (Figure 8-4). It also shows that, when EC is very small ($EC < 260 \mu\text{S}/\text{cm}$ corresponding to $\text{Cl} < 25 \text{ mg/L}$), the grab sample data follow the agricultural drainage regression equation with no significant contribution from seawater intrusion.

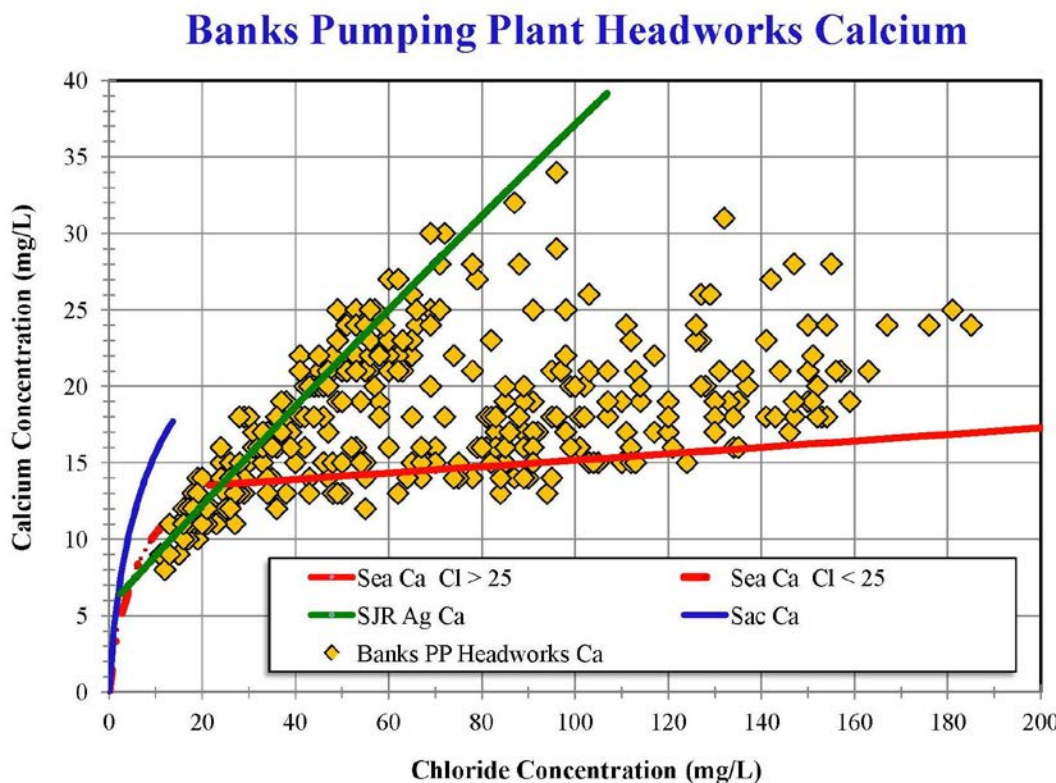


Figure 8-4: Variation of calcium concentration (Ca) as a function of chloride concentration (Cl) for the Headworks of Banks Pumping Plant in the south Delta. This type of graph was used by Suits (2002) to more clearly distinguish between seawater-dominated data and agricultural drainage-dominated data.

The seawater-dominated, agricultural drainage dominated and Sacramento River inflow curves in Figure 8-5 were produced by plotting the estimated Ca as a function of estimated Cl using the regression equations in Chapter 7 (Tables 7.1, 7.2, 7.7 and 7.10).

Agricultural drainage contains a high percentage of sulfate (22% of TDS) but the percentage of sulfate in seawater-dominated areas is only 8% (Table 3.1). Plotting sulfate concentration as a function of EC or chloride can also be used to illustrate whether the sources of water are varying at a given Delta location.

In regions of the Delta where the percentage contributions to salinity from various sources in the Delta are variable, such as Banks Pumping Plant, it will not be possible to use a single regression equation to estimate an unknown water quality constituent concentration, e.g., the bromide concentrations in Figure 8-2. In this chapter, the grab sample data from different regions of the Delta will first be plotted as chloride or bromide concentration as a function of EC to determine whether the percentages of source water contributions are variable. It is important to know or estimate chloride concentrations at locations where the SWRCB's municipal and industrial chloride standards apply. Sometimes only EC measurements are available, or the output from a computer simulation is only in EC or TDS and accurate methods of estimating chloride concentration are needed. Bromide concentrations are also important for determining the

production of disinfection byproducts when Delta water is treated to meet drinking water standards. However, the other water quality constituents analyzed in this report are also important, such as alkalinity and hardness which can adversely impact human health and water distribution infrastructure.

Where applicable, the grab sample data will also be plotted as a times series and compared with the corresponding estimates for seawater-dominated and agricultural drainage-dominated water. This will indicate during which times of the year and under which other situations either seawater intrusion or agricultural drainage dominates. If there is a reliable seasonal pattern of variation, this can be used to determine the relative contributions from each source to a particular water quality constituent concentration.

In this chapter, the stations are separated into the following categories:

1. Suisun Bay and Western Delta;
2. Old River – Lower Reach;
3. Middle River – Lower Reach;
4. State Water Project Export Facility;
5. Central Valley Project Export Facility;
6. Old and Middle River – Upper Reach (i.e., southeast of the temporary agricultural barriers);
7. San Joaquin River from Vernalis to Jersey Point;
8. Sacramento River from Freeport to Rio Vista;
9. Mokelumne and Cosumnes Rivers;
10. Barker Slough (i.e., region around the North Bay Aqueduct intake); and,
11. Agricultural discharge stations.

The contribution from seawater intrusion decreases the further a given location is from the ocean. Similarly, locations close to where the San Joaquin River flows into the Delta, and far from Suisun Bay and the ocean, can be expected to be dominated by agricultural drainage. In the southwest regions of the Delta where the State Water Project, Central Valley Project and CCWD have drinking water intakes, the water concentrations will sometimes be consistent with the seawater-dominated regression equations and sometimes consistent with the agricultural dominated regression equations, or somewhere in between.

Because the boundary regression equations (Chapter 7) bound the range of variation at a given locations, and the data are often scattered between these two bounds, the coefficient of determination, or r squared values are very small. R-squared values are not useful in these cases.

8.1 Suisun Bay and Western Delta

Grab sample data for Mallard Island and Jersey Point were used to develop the regression equations for seawater-dominated areas of the Delta (Figure 8-5). These relationships also apply for other northern San Francisco Bay and western Delta stations. Figure 8-6 shows chloride grab data sample data from the WIMS data base for San Pablo Bay at Pinole Point and San Pablo Point and Suisun Bay at Port Chicago.

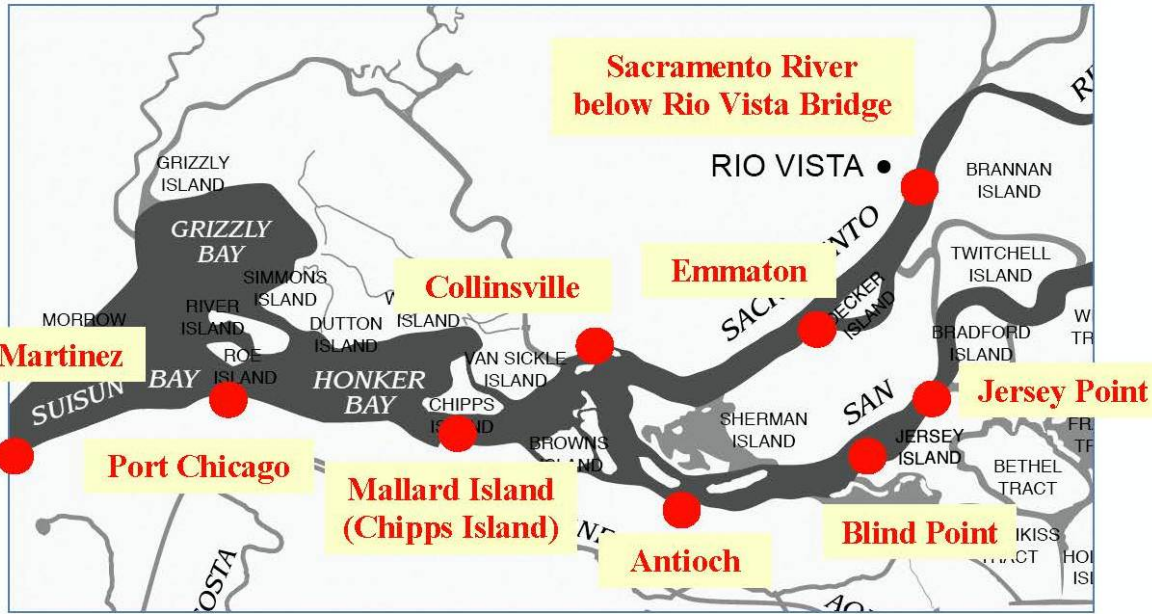


Figure 8-5: Map of western Delta showing the location of key monitoring stations

North San Francisco Bay

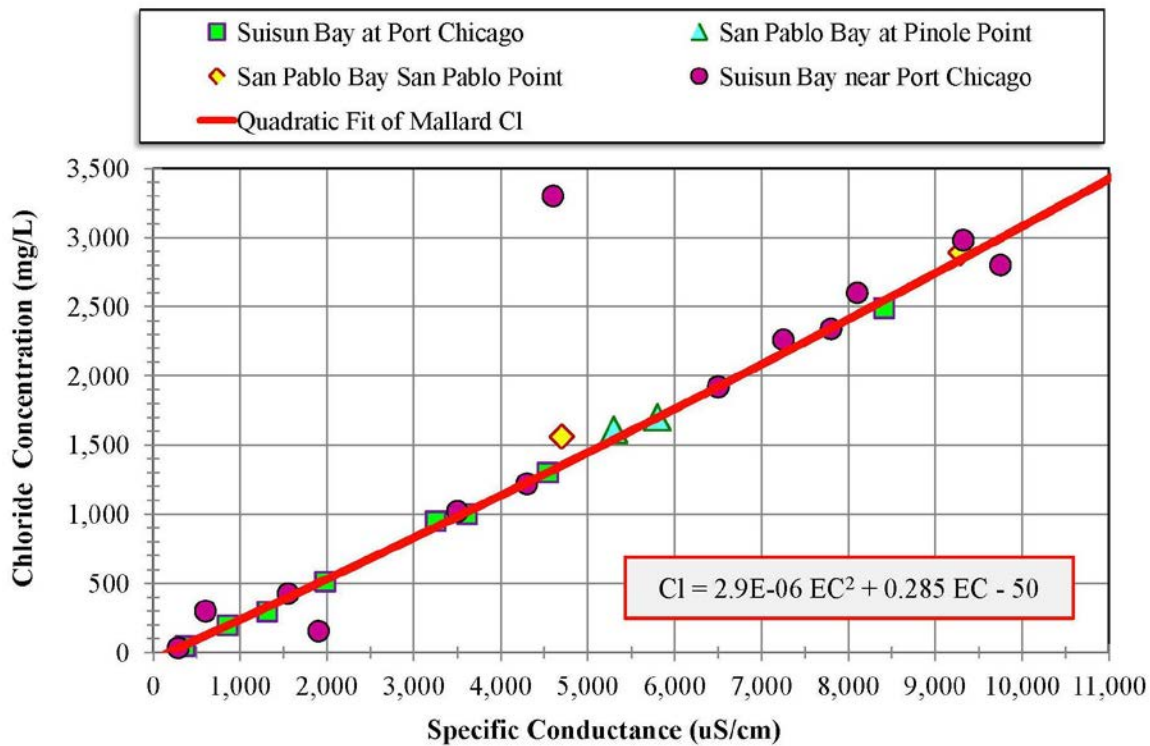


Figure 8-6: Variation of chloride concentration as a function of specific conductance (EC) for San Pablo Bay at Pinole Point and San Pablo Point and Suisun Bay at Port Chicago.

Figure 8-7 shows chloride concentrations for San Joaquin River at Antioch and Blind Point and the Sacramento River at Collinsville and Emmaton. These data are consistent with the seawater boundary condition relationship derived from the Mallard Island and Jersey Point data. There are only limited calcium and sulfate data for these stations so it is not possible to show the corresponding comparisons with the calcium and sulfate relationships.

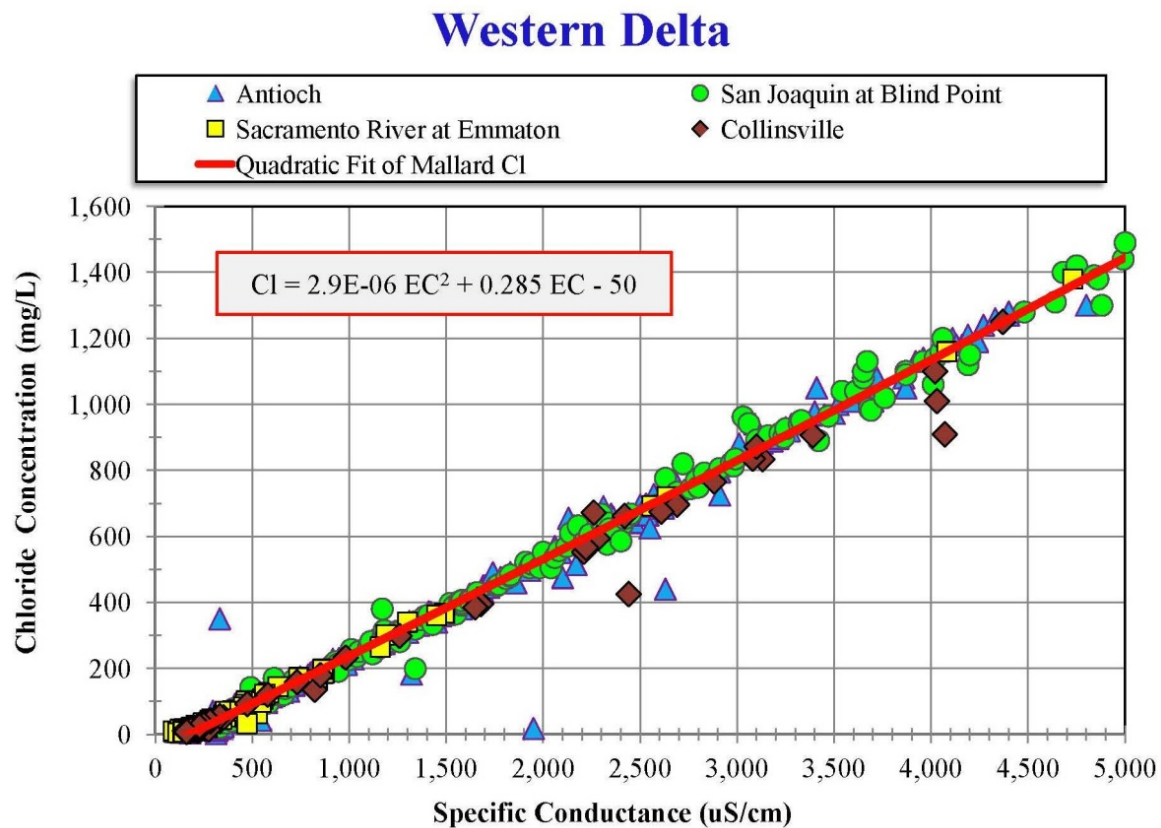


Figure 8-7: Variation of chloride concentration as a function of specific conductance (EC) for Antioch, Collinsville, Emmaton and Blind Point (western end of Jersey Island).

Figure 8-8 shows the chloride concentrations for the western Delta at Antioch, Collinsville, Emmaton and Blind Point for $EC < 800 \mu\text{S}/\text{cm}$. These chloride data also consistent with the seawater boundary condition equation for high Delta outflows ($EC < 260 \mu\text{S}/\text{cm}$) when a mixture of Sacramento and San Joaquin water dominates.

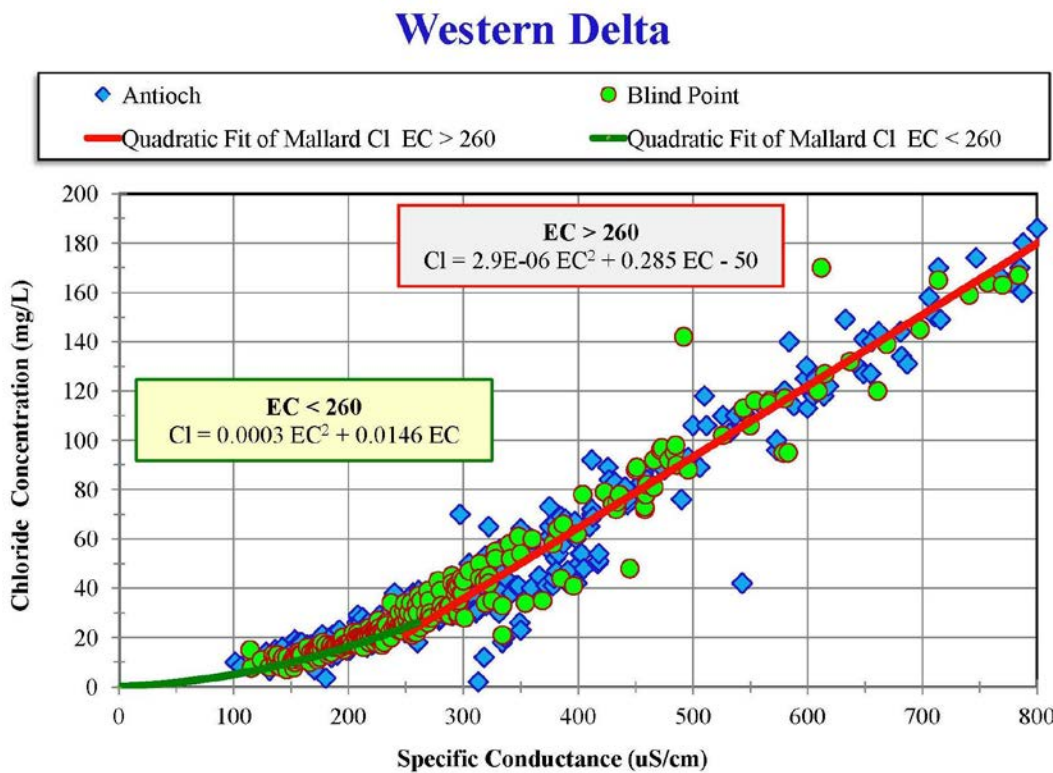


Figure 8-8: Variation of chloride concentration as a function of specific conductance (EC) for Antioch and Blind Point for $EC < 800 \mu\text{S}/\text{cm}$.

8.2 Old River – Lower Reach

The lower reach of Old River is directly affected by seawater intrusion entering via Franks Tract in the north (Figure 8-9). This reach will have different characteristics than the upper reach of Old River which is much further from Suisun Bay, closer to the San Joaquin River inflow at Vernalis, and at times, on the upstream (eastern) side of the temporary barriers. Key stations in this reach are Holland Tract, Bacon Island, Rock Slough, and two of Contra Costa Water District's drinking water intakes at the Contra Costa Canal at Pumping Plant No. 1 and Old River at Highway 4 (Figure 8-9).

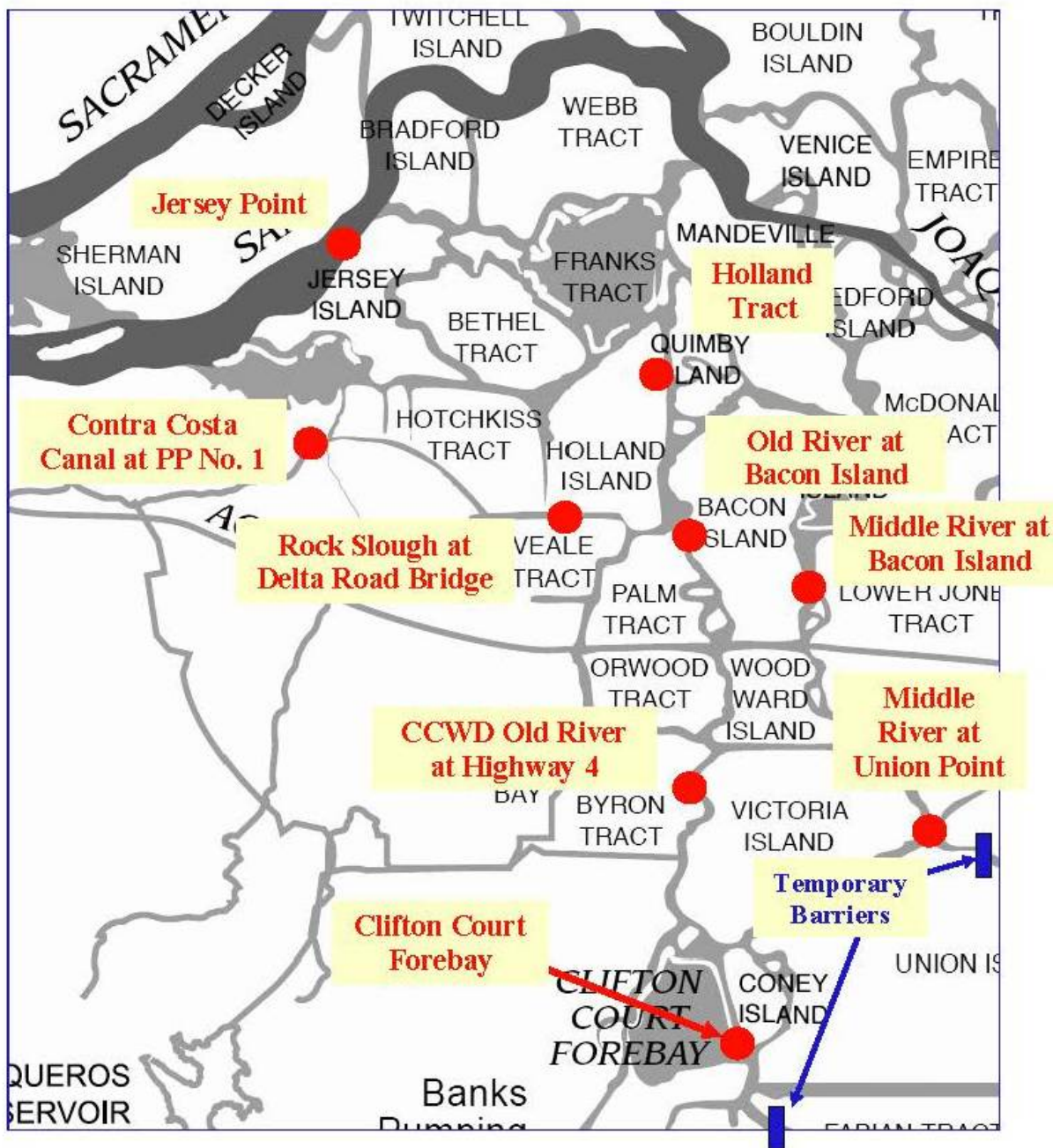


Figure 8-9: Map of Old River and Middle River showing the location of key monitoring stations. The map shows the area of the south and central Delta that is north and east of the Middle River, Old River and Grant Line temporary barriers.

As shown in Figures 8-10 and 8-11, the variation in water quality at stations along this reach of Old River is also influenced by seawater intrusion. Both Old River at Highway 4 and CCWD's intake on Victoria Canal have periods when seawater is not present but agricultural drainage increases EC values up into the 400-550 $\mu\text{S}/\text{cm}$ range.

Old River Stations

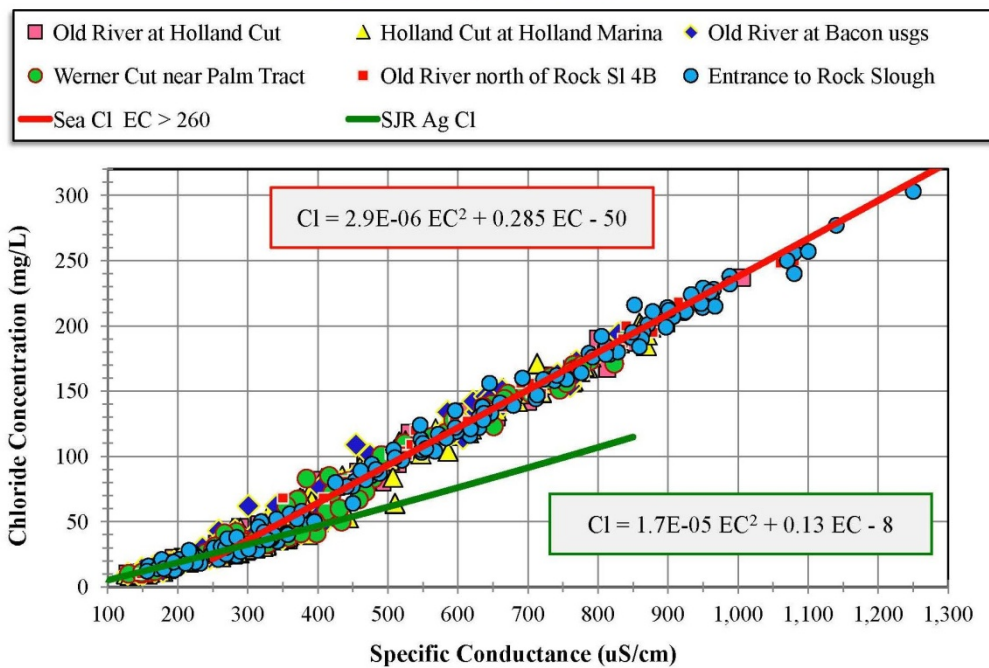


Figure 8-10: Variation of chloride concentration as a function of specific conductance (EC) for stations on Old River between Holland Tract and Bacon Island.

Old River at Highway 4 and Victoria Canal

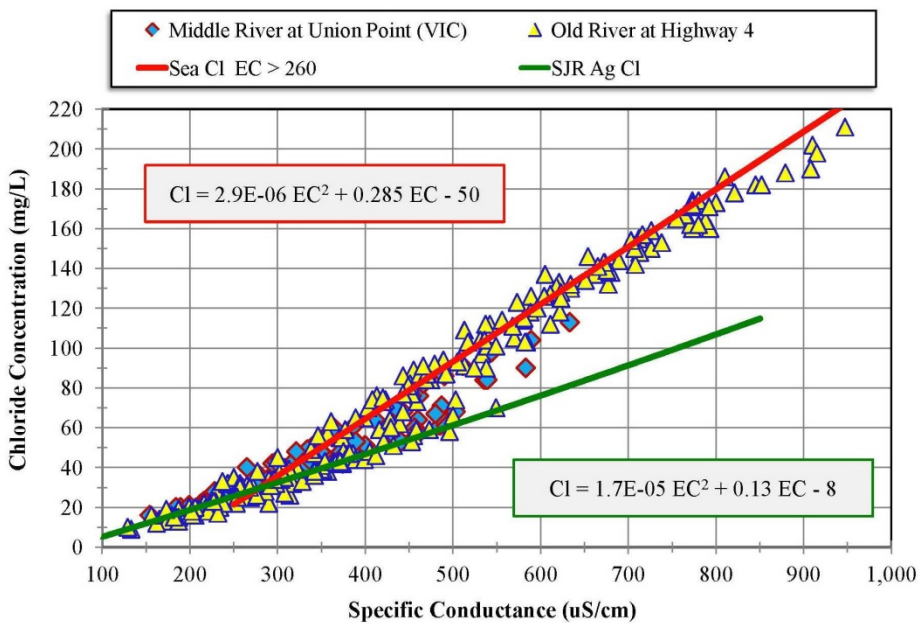


Figure 8-11: Variation of chloride concentration as a function of specific conductance (EC) for Old River at Highway 4 and the northeastern end of Victoria Canal. This latter station best represents the water quality at CCWD's new Victoria Canal intake.

Figure 8-12 shows the variation in chloride concentration at CCWD's intake on Old River at Highway 4 as a function of time (January 1997 – December 2001). The chloride variation is bounded by the upper seawater limit and the lower agricultural drainage limit. For this example, seawater dominates during August-December in 1997, 1999 and 2000. Water Year 1998 was wetter than those three years, so the peak chloride concentration in the August-December period was much lower with much less seawater intrusion.

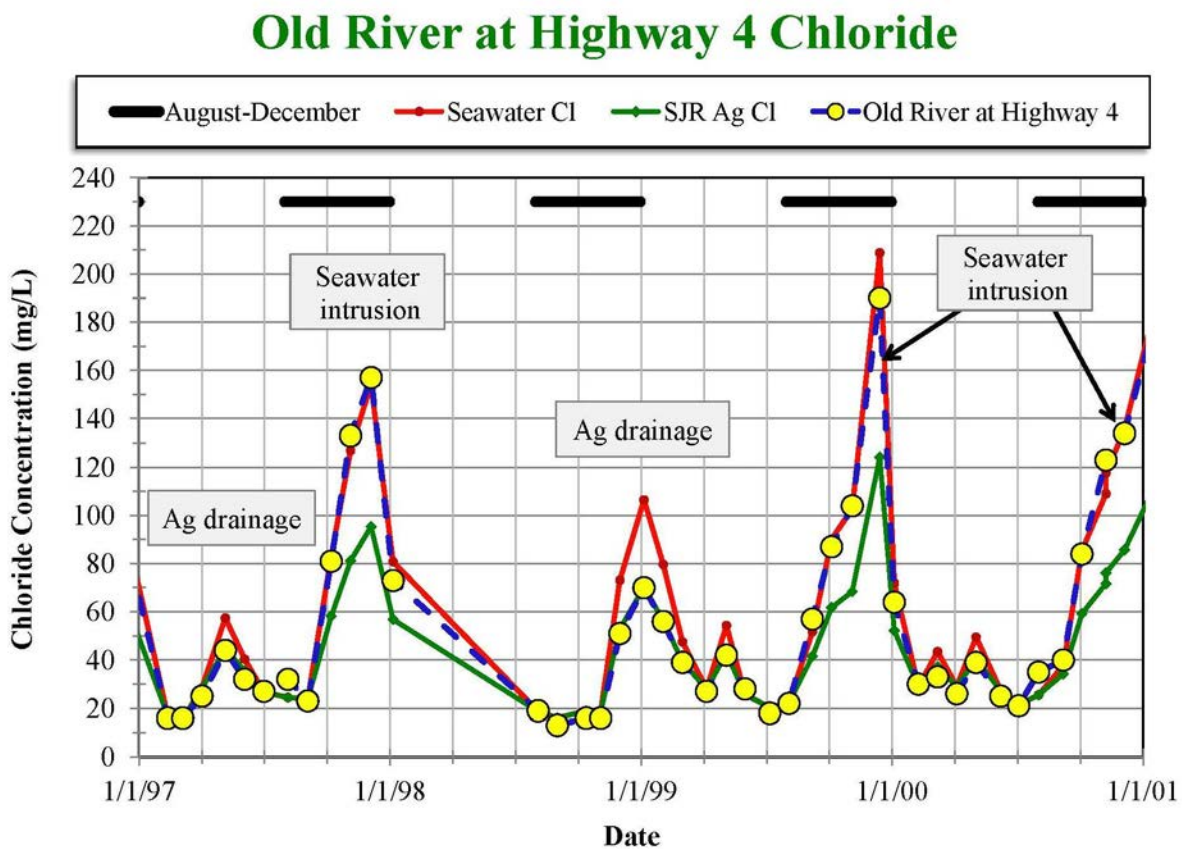


Figure 8-12: Variation of chloride concentration for CCWD's intake on Old River at Highway 4 as a function of time (January 1997 – December 2001). The chloride data are bounded by the seawater-dominated upper limit and agricultural drainage-dominated lower limit. Seawater intrusion generally occurs during the late summer and fall, except in wetter years.

Figure 8-13 shows the corresponding variation in calcium concentration at Old River at Highway 4 for January 1997 – December 2001. The calcium data are bounded by the upper agricultural drainage-dominated limit and the lower seawater-dominated limit. For this example, seawater dominates during August-December in 1997, 1999 and 2000. Water Year 1998 was wetter than those three years, so the peak calcium concentration in the August-December period was much lower with much less seawater intrusion. Plotting calcium or sulfate concentration as a function of time is a good way of highlighting when agricultural drainage is dominating. Agricultural drainage contains high proportions of calcium and sulfate, and the percentage of chloride in agricultural drainage is about half the percentage in seawater (Figure E.1).

Old River at Highway 4 Sulfate

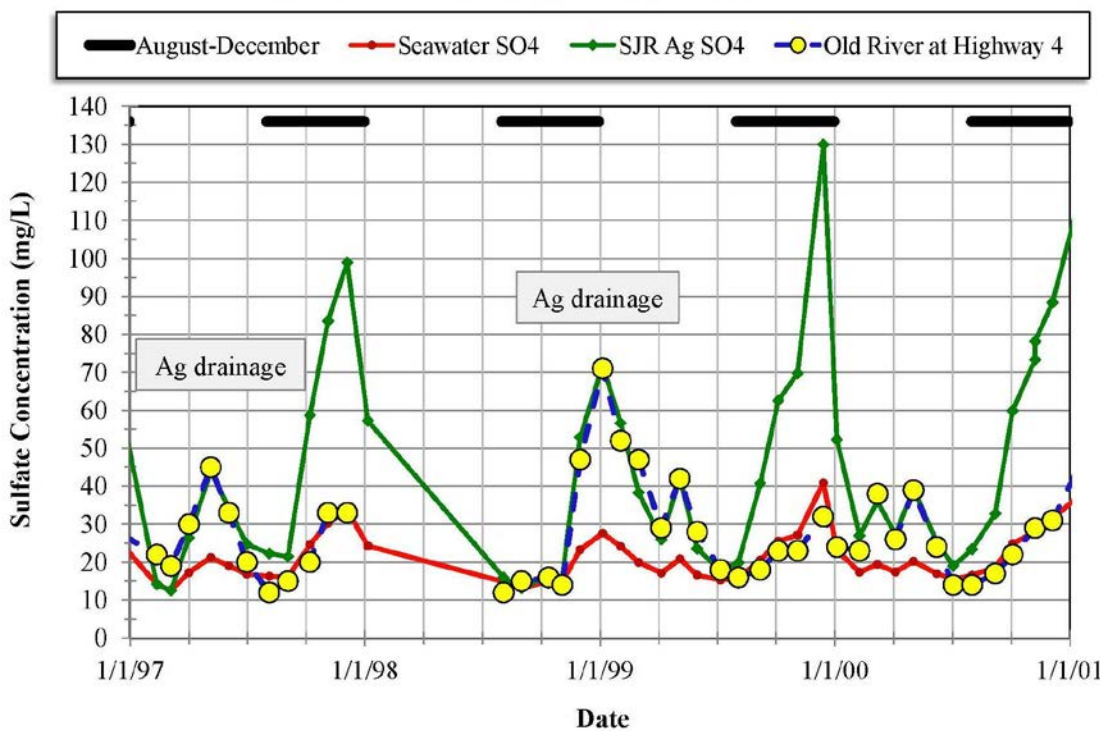


Figure 8-13: Variation of calcium concentration at CCWD's intake on Old River at Highway 4 as a function of time (January 1997 – December 2001). The periods when agricultural drainage dominates correspond to higher calcium concentrations.

The Contra Costa Canal intake at Pumping Plant #1 off Rock Slough was Contra Costa Water District's primary water supply intake until 1998 when the Los Vaqueros Project was completed. This location is also a key compliance point for the SWRCB's municipal and industrial water quality standards. These standards are based on chloride concentrations so it is important to understand the sources of chlorides at this location. Agricultural drainage into Rock Slough and seepage into the earth-lined canal sometimes resulted in increased chloride concentrations at times when seawater intrusion effects were small (periods of high Delta outflow).

CCWD addressed this issue by relocating an agricultural discharge point on Veale Tract from Rock Slough in the north to No-Name Slough at the southern end of Veale Tract. This project was completed in 2006. This has reduced the amount of agricultural drainage at Pumping Plant #1.

Figures 8-14 and 8-15 show the variation of chloride concentration at Pumping Plant #1 for an earlier period of time (1993-1996) and a more recent period (2009-2013). The periods of seawater intrusion are similar, but local agricultural drainage effects were greater during 1993-1996. In March 1993 and March 1996, agricultural drainage increased the chloride concentrations to 110 mg/L. The more recent period (2009-2013) was much drier except for a wet year in 2011. The concentrations when agricultural drainage effects might have been expected were much less (about 50 mg/L).

Contra Costa Canal at Pumping Plant #1

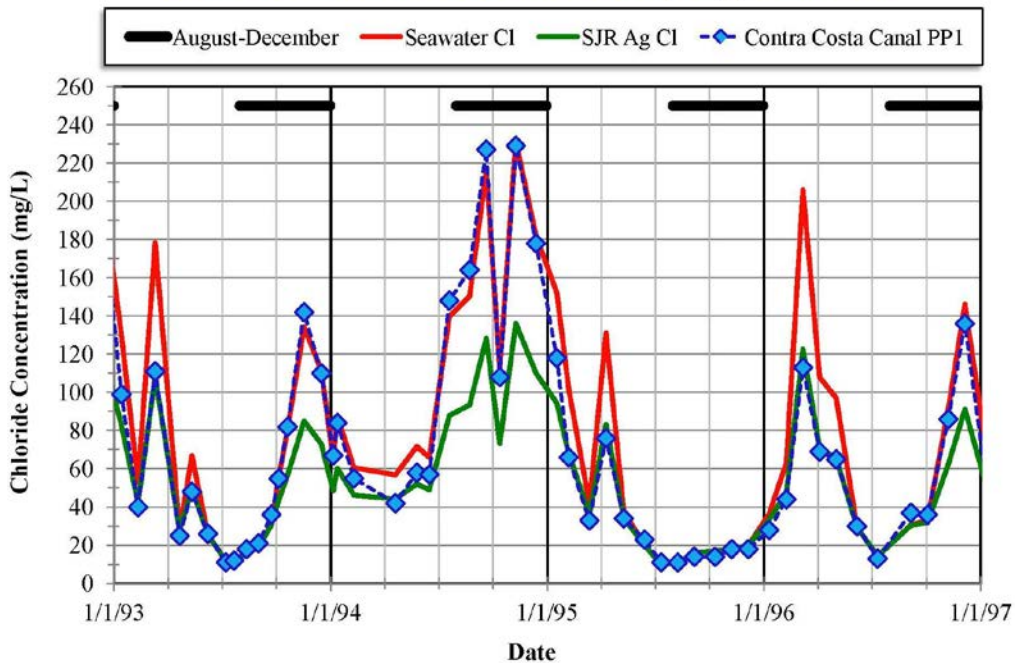


Figure 8-14: Variation of chloride concentration at Contra Costa Canal at Pumping Plant No. 1 as a function of time (January 1993 through December 1996).

Contra Costa Canal at Pumping Plant #1

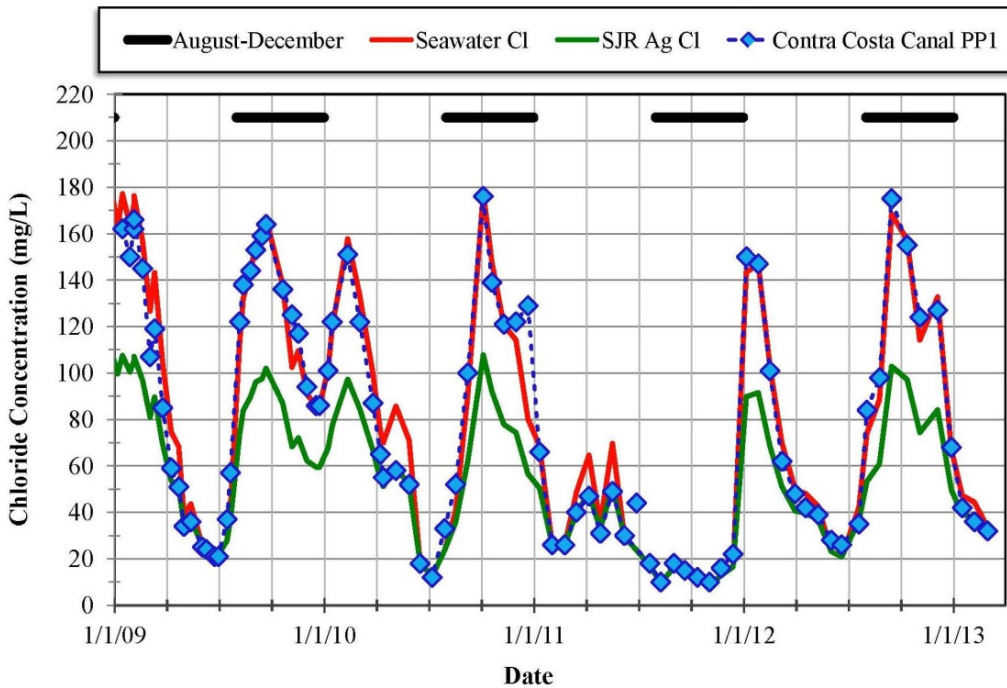


Figure 8-15: Variation of chloride concentration at Contra Costa Canal at Pumping Plant No. 1 as a function of time (January 2009 through March 2013).

8.3 Middle River – Lower Reach

The Middle River reach is the primary route for Sacramento River water drawn south toward the Banks and Jones pumping plants (Figure 8-9). Key stations along this route for which there are adequate grab sample data are: Middle River at Bacon Island Bridge, Middle River at Victoria Canal, Middle River at Woodward Canal, Middle River at Union Point, Middle River at Borden Highway, and North Canal near Old River (the latter is located at the south western end of Victoria Canal).

Figures 8-16, 8-17, and 8-18 show the chloride concentrations as a function of EC for the northern most stations (closest to the source of seawater), middle reach and southern most stations, respectively. Note that the data from Middle River at the Mokelumne Aqueduct crossing include the 1976-1977 drought. During this period, chloride concentrations in this section of Middle River increased to a maximum of almost 220 mg/L and seawater dominated (Figure 8-18).

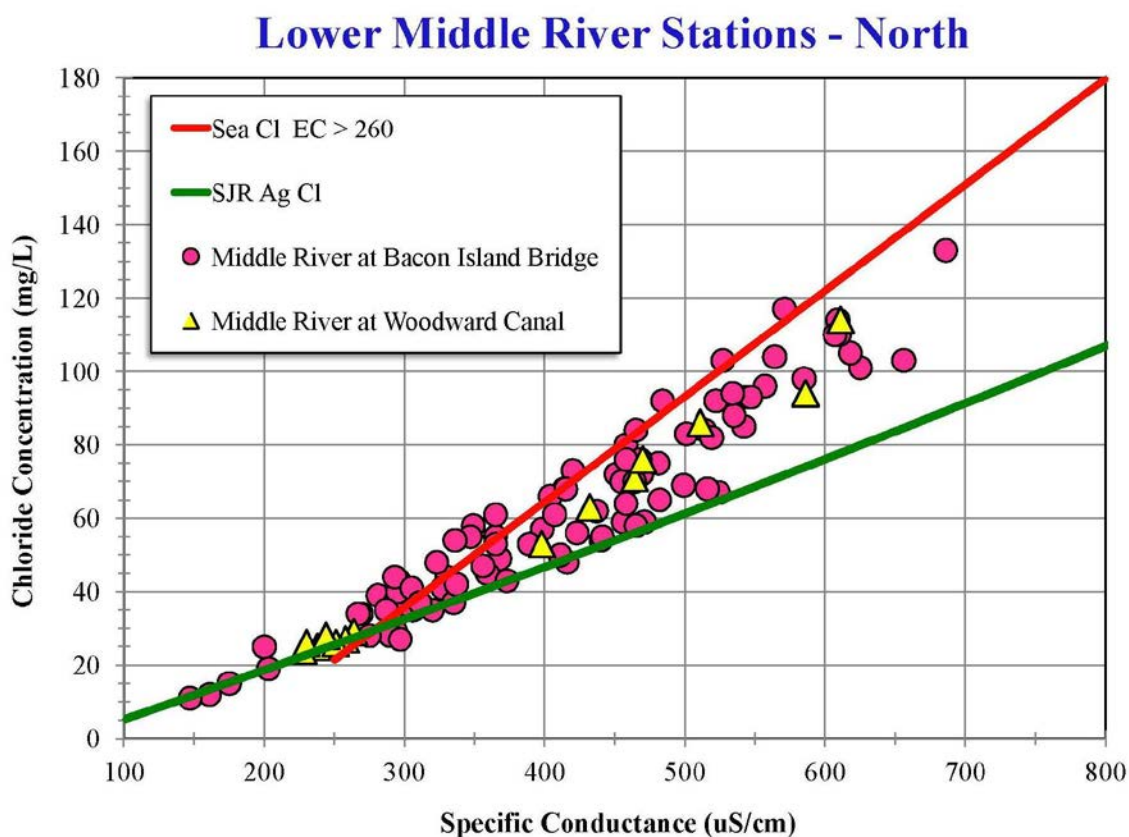


Figure 8-16: Variation of chloride concentration as a function of specific conductance at the northern end of Middle River.

Lower Middle River Stations - Middle

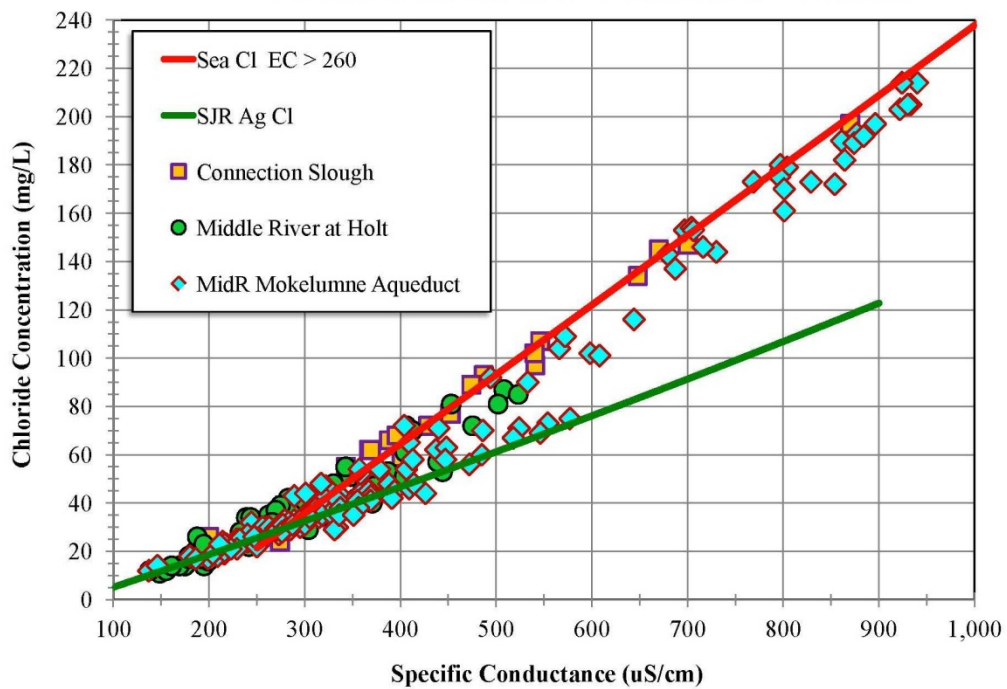


Figure 8-17: Variation of chloride concentration as a function of specific conductance along the middle reach of Middle River.

Lower Middle River Stations - South

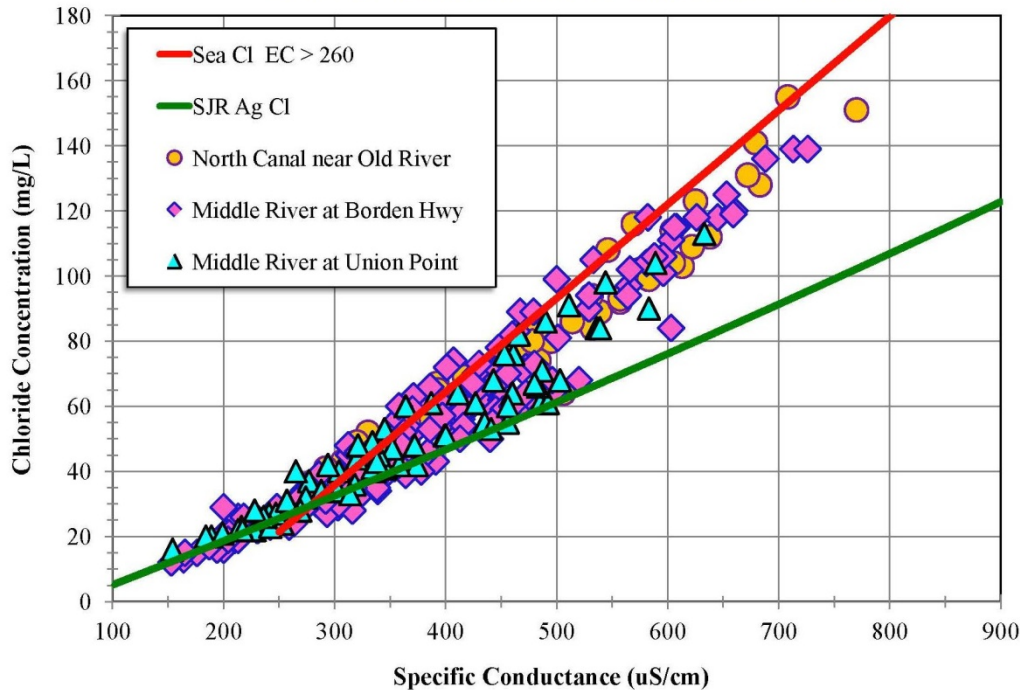


Figure 8-18: Variation of chloride concentration as a function of specific conductance at the southern end of Middle River and along Victoria Canal.

Calcium data from Middle River at the Bacon Island Bridge, Connection Slough and Middle River at the Mokelumne Aqueduct are plotted as a function of EC in Figure 8-19.

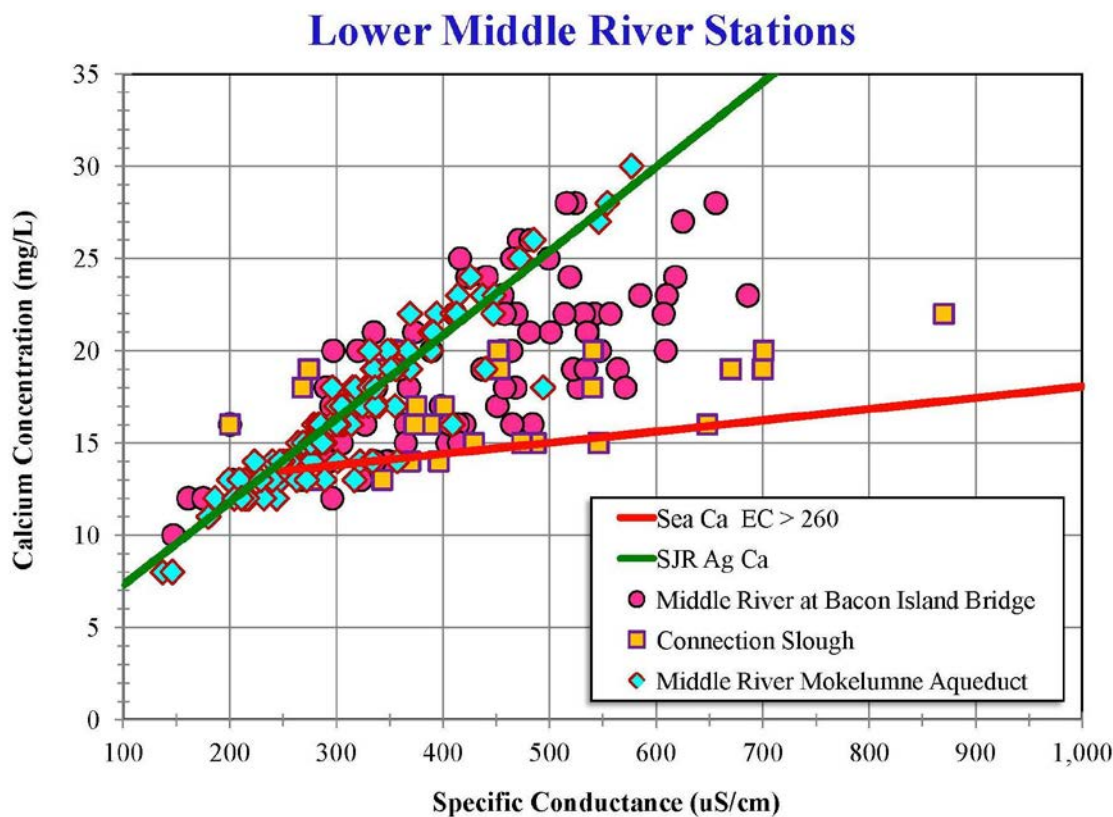


Figure 8-19: Variation of calcium concentration as a function of specific conductance on Middle River at the Mokelumne Aqueduct crossing, at Connection Slough and at the Bacon Island Bridge.

The Connection Slough station is located at the Mandeville Island Bridge, just west of Middle River near the northwestern end of Mildred Island. The small amount of available data is for the periods June 1959 through October 1959, and July 1989 through January 1992. 1959 was a below normal year and 1989, 1990, 1991 and 1992 were dry, critical, critical and critical years, respectively. The Connection Slough calcium data show characteristics of seawater-dominated conditions, consistent with the 1989-1992 dry period. The Middle River at the Mokelumne Aqueduct calcium data were collected from 1979 to 1986 which was primarily wet so these calcium data show the characteristics of agricultural drainage-dominated conditions.

Figure 8-20 shows the variation of chloride concentration (Cl) with time from January 1981 through December 1986. These six years were dry, wet, wet, wet, dry and wet, respectively. The variation in EC at Jersey Point is also plotted to indicate the periods when seawater intrusion might be expected to influence the salinity at Middle River at the Mokelumne Aqueduct crossing. These periods do indeed correspond to the periods when the relationship between chloride and EC is consistent with the seawater-dominated regression equation, i.e., July-October 1981 and July 1985-January 1986.

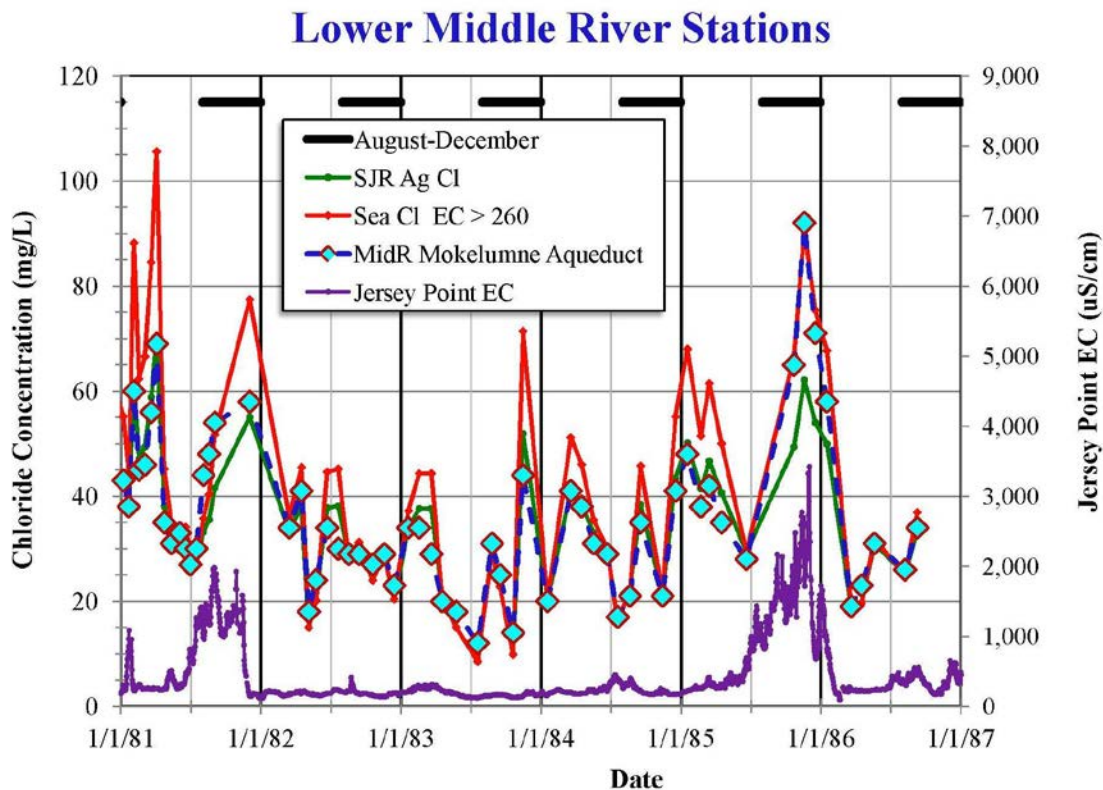


Figure 8-20: Variation of chloride concentration with time on Middle River at the Mokelumne Aqueduct crossing from January 1981 through December 1986. The seawater-dominated and agricultural drainage-dominated curves indicate when each of those conditions dominate. The corresponding plot of Jersey Point EC illustrates when seawater intrusion would be expected to occur, i.e., when Jersey Point EC is high.

8.4 SWP Export Facility

The water quality at the State Water Project export facility are represented by grab sample data collected at the headworks for Banks Pumping Plant and at the intake to the Clifton Court Forebay (Figure 8-21).

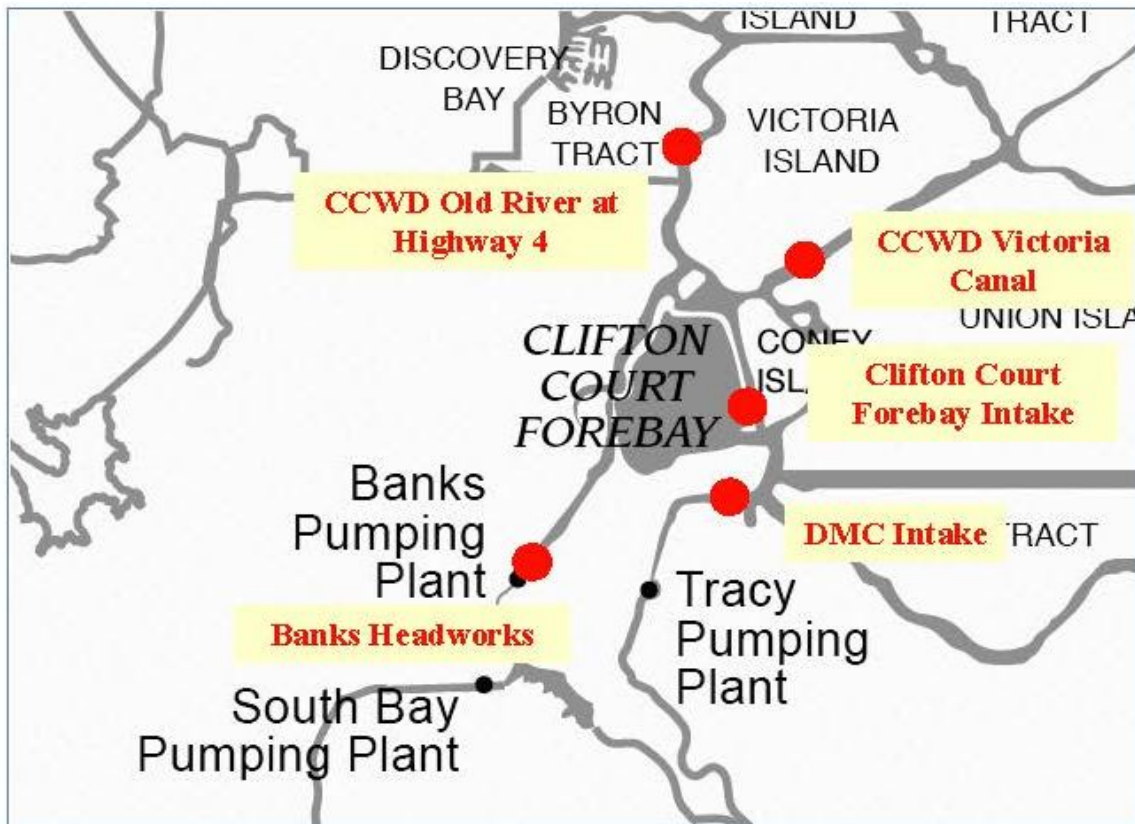


Figure 8-21: Map of the SWP and CVP export facilities in the south Delta and key monitoring stations.

Figure 8-1 showed the variation of chloride concentration as a function of EC at the headworks of the Banks Pumping Plant (downstream of Clifton Court Forebay). Figure 8-22 shows the corresponding variation of chloride concentration at the intake to the Clifton Court Forebay off West Canal.

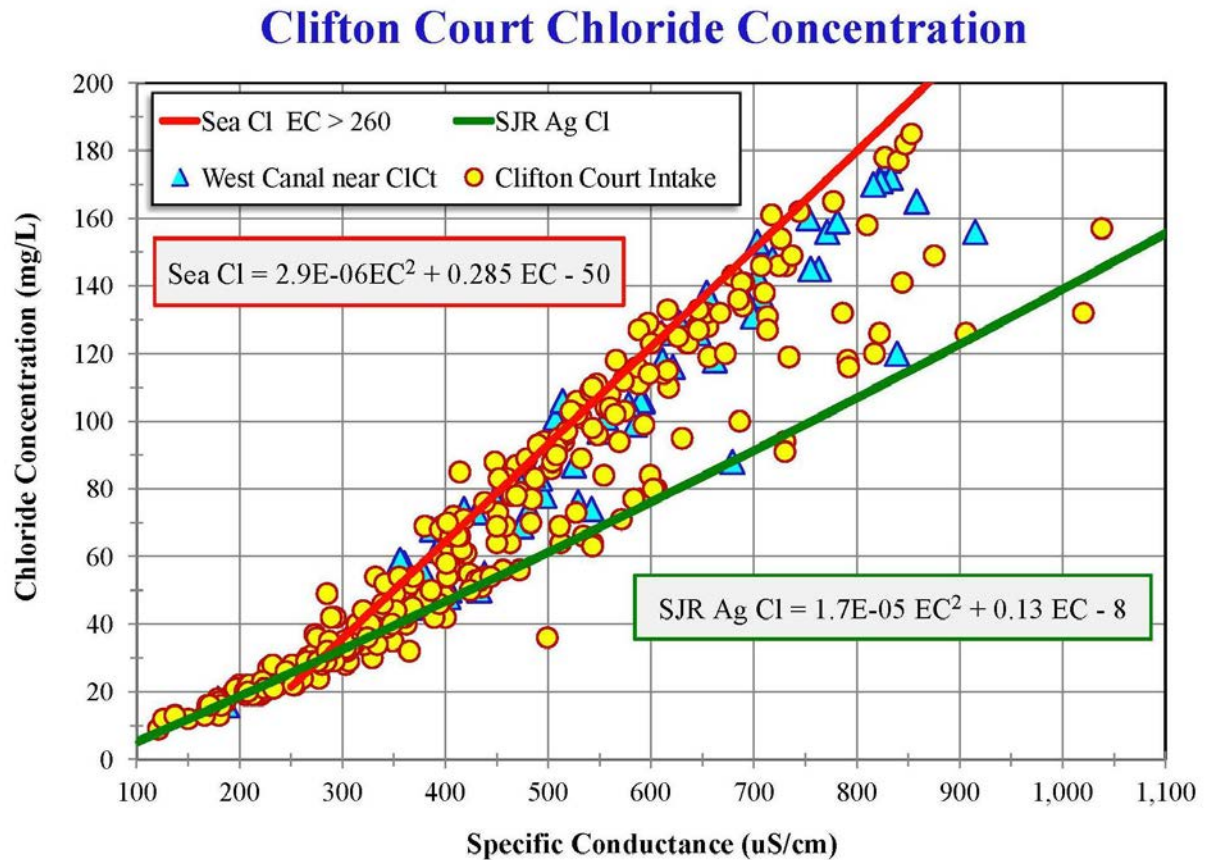


Figure 8-22: Variation of chloride concentration as a function of specific conductance at the intake to Clifton Court Forebay.

The corresponding plot of sulfate concentration at the intake to Clifton Court Forebay (Figure 8-23) shows there are times when agricultural drainage dominates in this region.

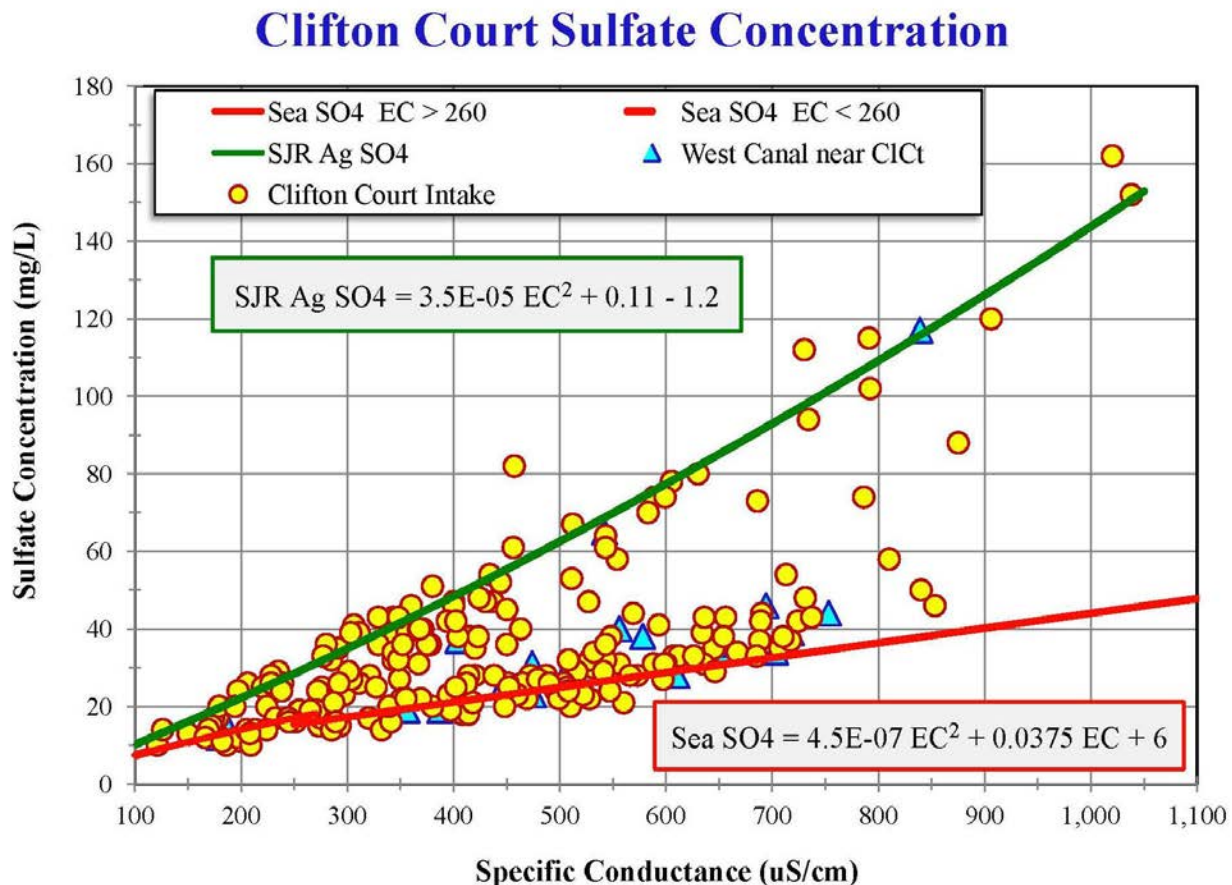


Figure 8-23: Variation of sulfate concentration as a function of specific conductance at the intake to Clifton Court Forebay.

Figure 8-24 shows the variation of the bromide concentration as a function of time at the intake to Clifton Court Forebay for the period January 2009 through December 2012. 2011 was a wet year so bromide concentrations were low most of the year. For the other dry and below normal years, seawater dominated July through December. In 2010 and 2012, the situation then transitioned to a period when agricultural drainage dominated (February-June). The highest bromide concentrations were due to seawater intrusion, but the bromide concentration was as high as 0.35 mg/L in March 2012 when agricultural drainage dominated.

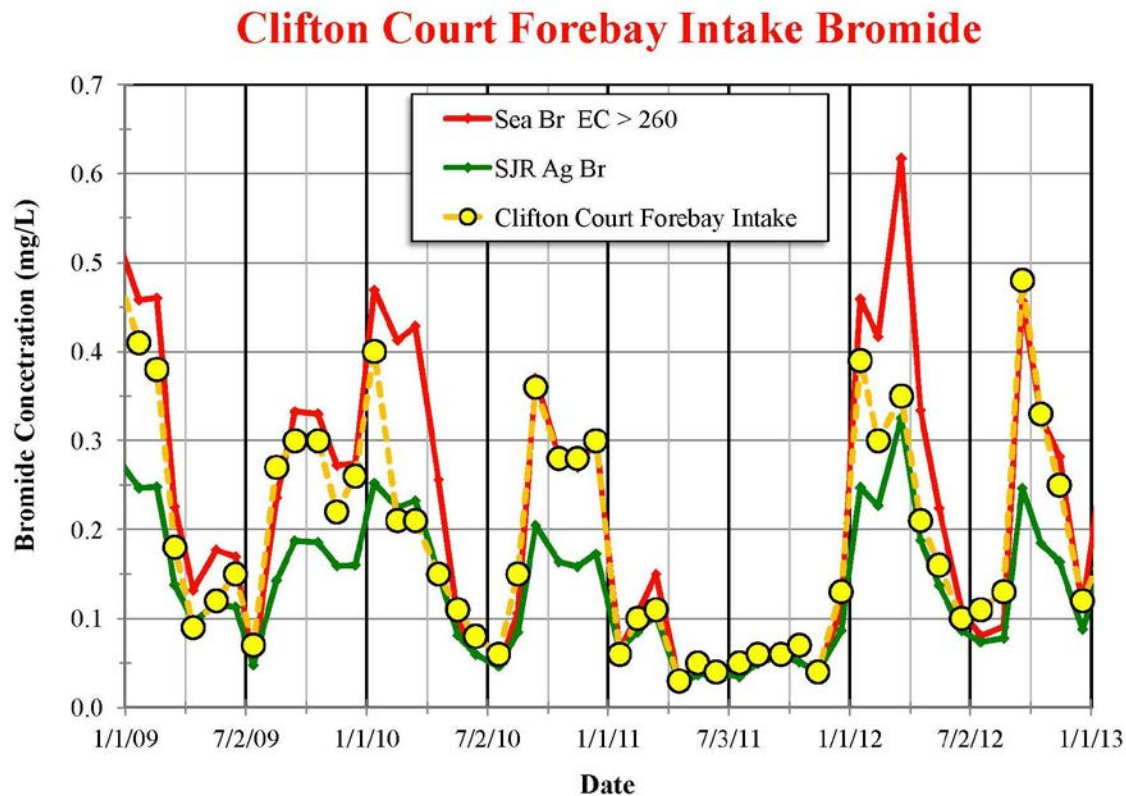


Figure 8-24: Variation of bromide concentration at the intake to Clifton Court Forebay from 2009-2012. Seawater dominates in late 2009, late 2010 and late 2012 but there is no seawater intrusion in 2011. Agricultural drainage dominates February-June 2010 and March-June 2012.

The occurrence of agricultural drainage events during 2009-2012 can be seen more clearly by plotting a time series of sulfate or calcium. Figure 8-25 shows the corresponding variation in sulfate concentration at the intake to Clifton Court Forebay. The sulfate concentrations are large and are consistent with the agricultural drainage-dominated regression relationship during February-June 2010 and March-June 2012.

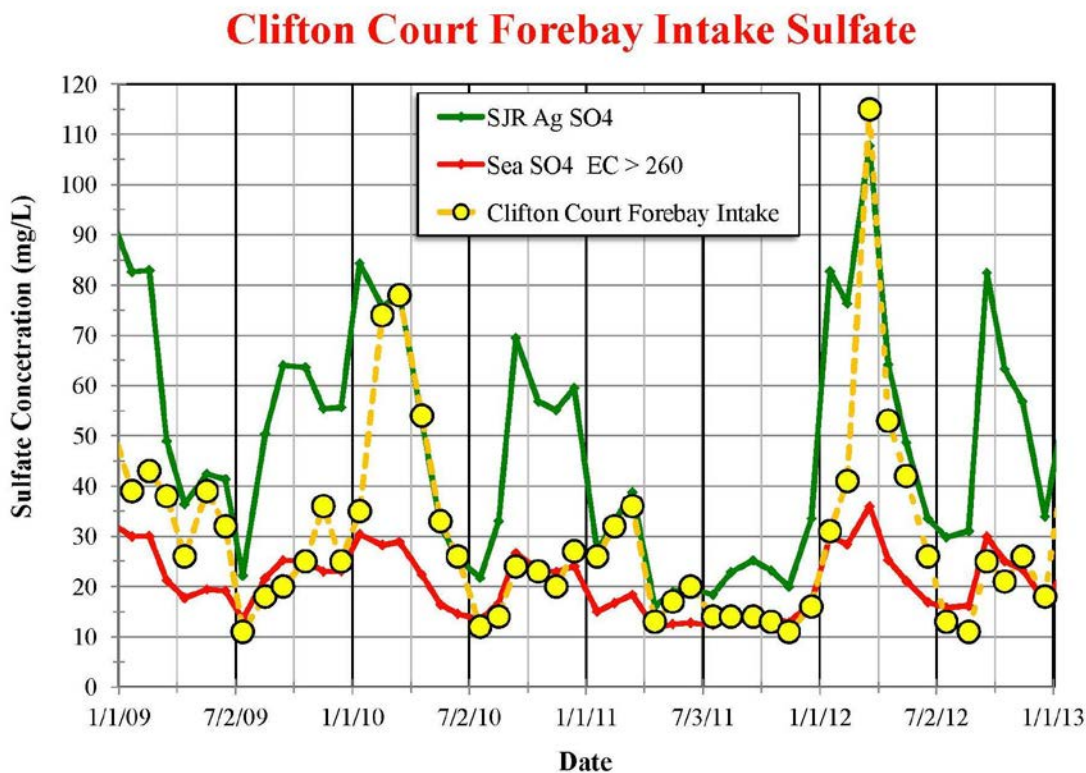


Figure 8-25: Variation of sulfate concentration as a function of time at the intake of Clifton Court Forebay from 2009-2012. During February-June 2010 and March-June 2012, the sulfate concentrations are large and are consistent with the agricultural drainage dominated regression relationship (SJR Ag line).

8.5 CVP Export Facility

The relative contributions of seawater and agricultural drainage at the Central Valley Project's intake to the Delta Mendota Canal (DMC) at Jones Pumping Plant is represented by grab samples from the DMC intake at Lindeman Road (1983-1999) and earlier data from the DMC intake at Byron Road (1952-1965). There is also some grab sample data from Old River upstream of the DMC intake. The region represented by these locations is shown in Figure 8-21.

Figures 8-26 and 8-27 show the variations of chloride concentration as a function of EC at the intake to the Delta Mendota Canal for different periods of time, 1983-1999 and 1952-1965, respectively.

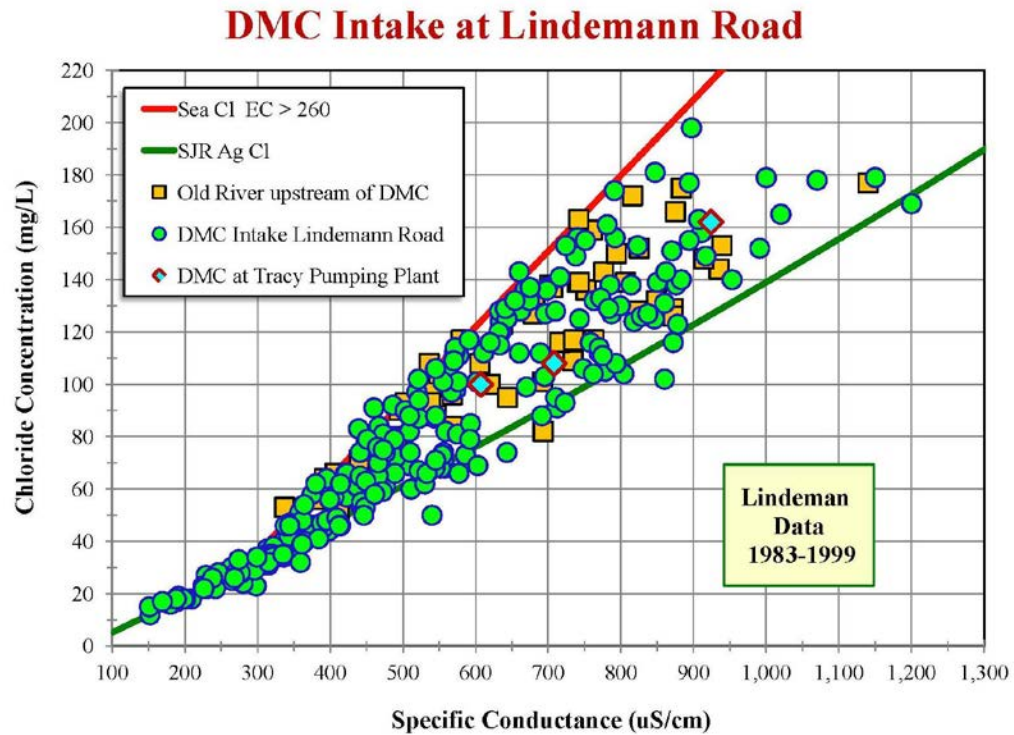


Figure 8-26: Variation of chloride concentration as a function of specific conductance at the intake to the Jones Pumping Plant and the Delta Mendota Canal.

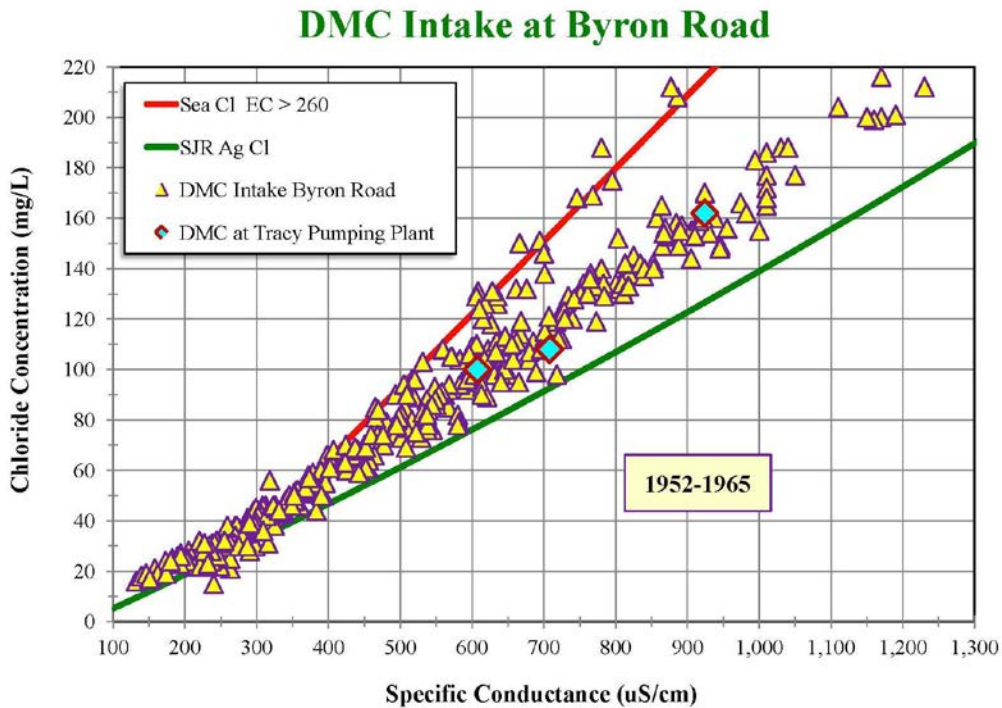


Figure 8-27: Variation of chloride concentration as a function of specific conductance at the Delta Mendota Canal intake at Byron Road for an earlier period of time (1952-1965).

Figures 8-28 and 8-29 show the corresponding variations in chloride concentration for wet and above normal years and dry and critical years, respectively at Lindeman Road. There were no below normal years during this sampling period. During these wet and above normal years, seawater intrusion is low and agricultural drainage tends to dominate. During the dry and critical years both sources of water play a role (depending on the month of the year).

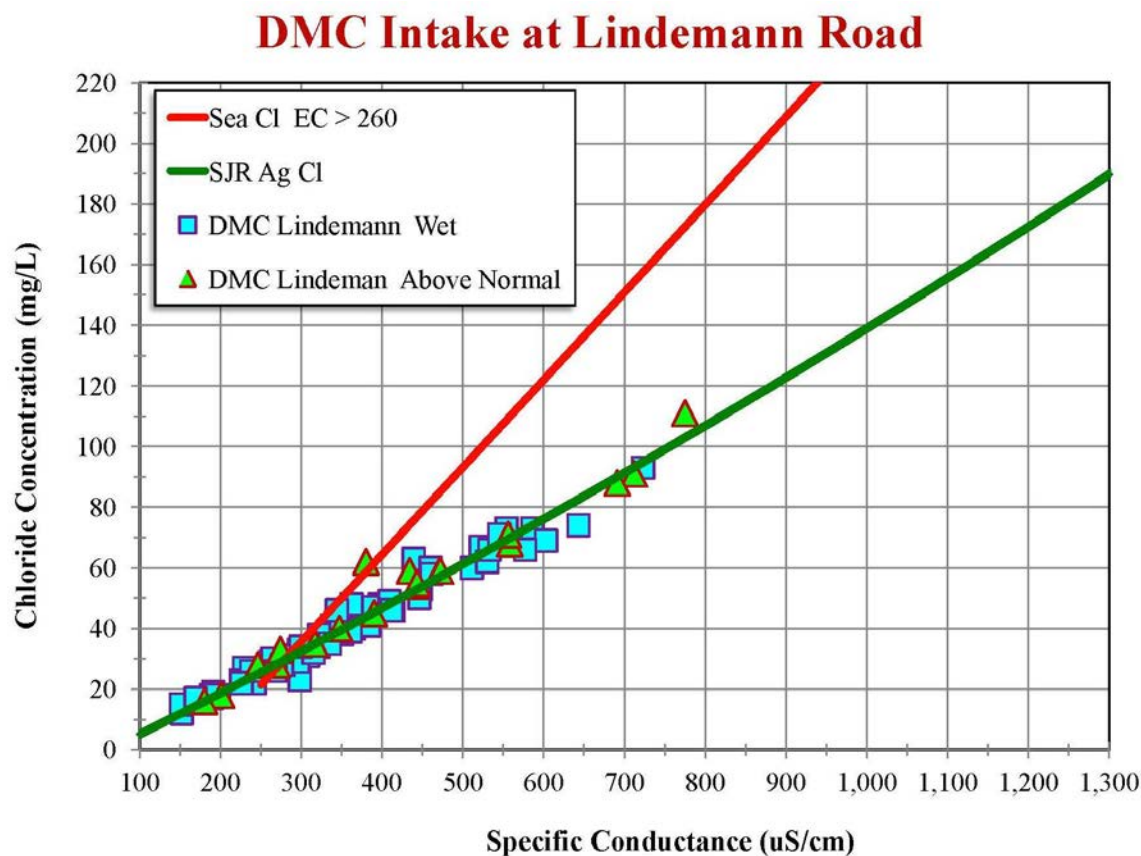


Figure 8-28: Chloride concentration as a function of specific conductance at the Delta Mendota Canal intake at Lindeman Road for wet and above normal years only. When conditions are wetter and Delta outflows are higher, the water quality is dominated by agricultural drainage.

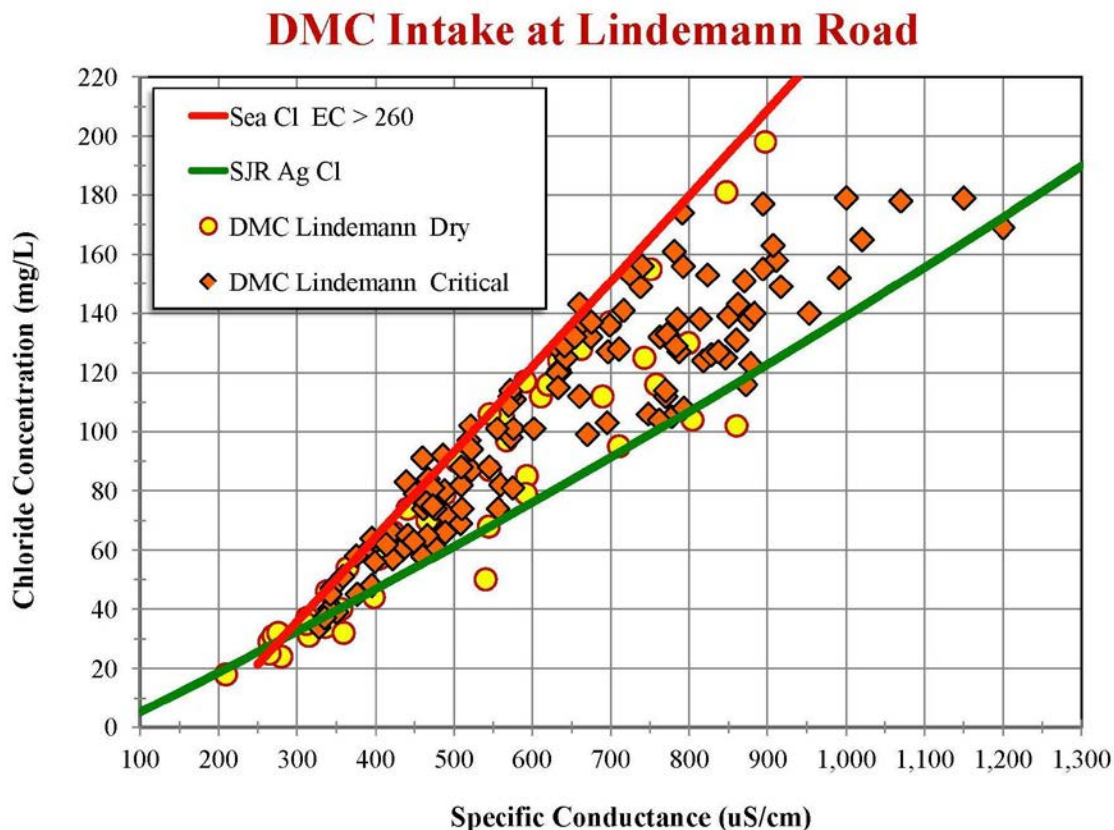


Figure 8-29: The corresponding variation of chloride concentration as a function of specific conductance at the Delta Mendota Canal intake for dry and critical years. Seawater intrusion makes a major contribution to the DMC chloride concentration during these drier years.

8.6 Old and Middle River – Upper Reach

This region is in the vicinity of the SWRCB agricultural salinity standard locations (Figure 8-30). During certain times of the year, in some years, the stations in this region are east of temporary rock barriers and are more directly influenced by local drainage.

Figure 8-31 shows the variation of chloride concentration as a function of EC at the upper Middle River stations. The Grant Line at Tracy Road Bridge data for the period 1989-1994 represents a drought period when seawater intrusion effects might be expected. However, agricultural drainage dominates.



Figure 8-30: Map of Old River and Middle River showing areas upstream and west of the temporary barriers showing key locations, including the SWRCB's agricultural water quality stations.

Middle River and Grant Line Stations

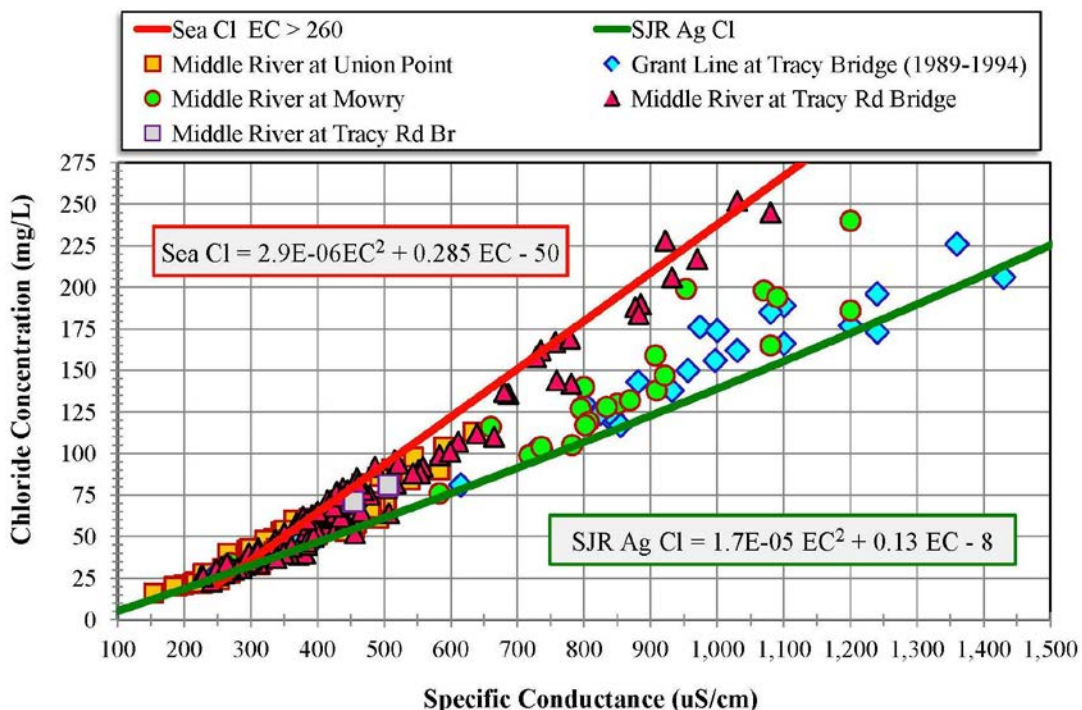


Figure 8-31: Variation of chloride concentration as a function of specific conductance at upper Middle River stations, in particular those east of the temporary agricultural barriers.

Figure 8-32 shows the variation of chloride concentration as a function of specific conductance on Grant Line Canal at the Tracy Road Bridge for a much earlier period 1954-1973. The data appear to be strongly correlated, representing a relatively constant mix of seawater and agricultural drainage. The corresponding sulfate concentration data are also relatively well correlated (Figure 8-33).

The reason why these data do not show a wider range of variation needs to be investigated in more detail. It may be due to local discharges of agricultural drainage from lands that had been irrigated with Delta water with higher salinities. This might explain why the data have higher concentrations than water from the San Joaquin River at Vernalis.

These Grant Line Canal data were collected during the period 1954-1973 (WIMS data base) and may not be representative of current day conditions in that part of the Delta.

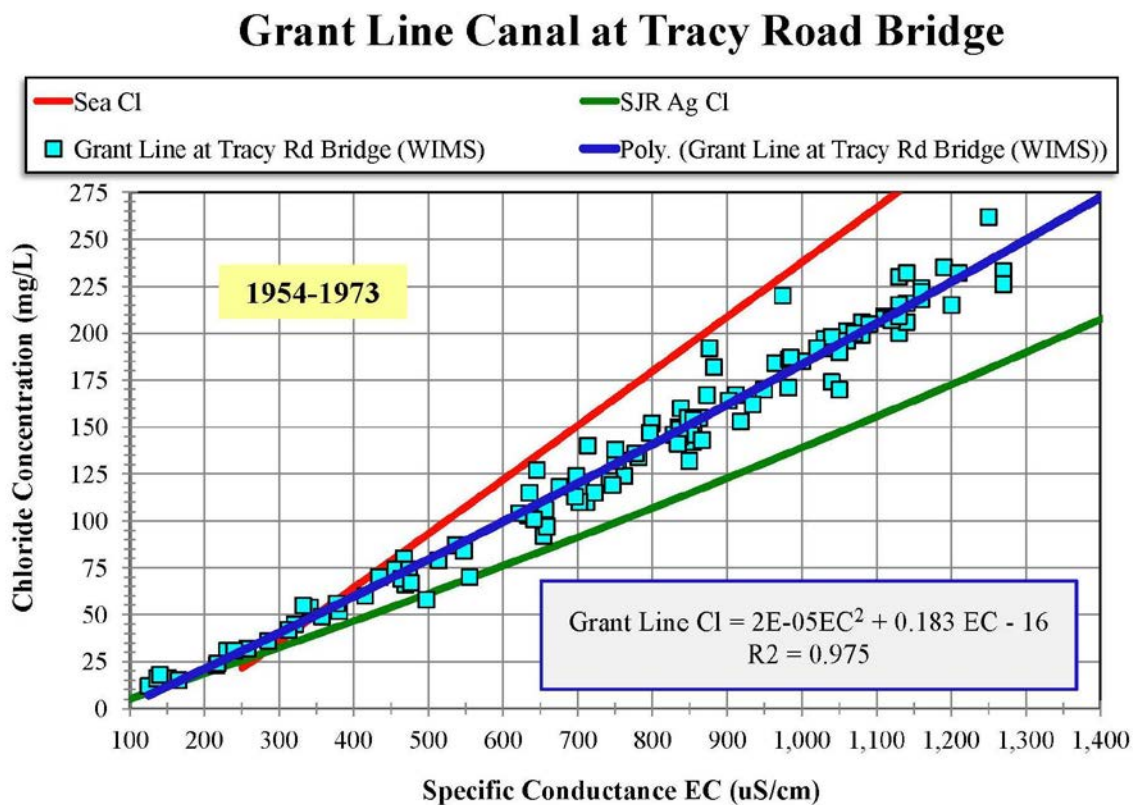


Figure 8-32: Variation of chloride concentration as a function of specific conductance on Grant Line Canal at the Tracy Road Bridge.

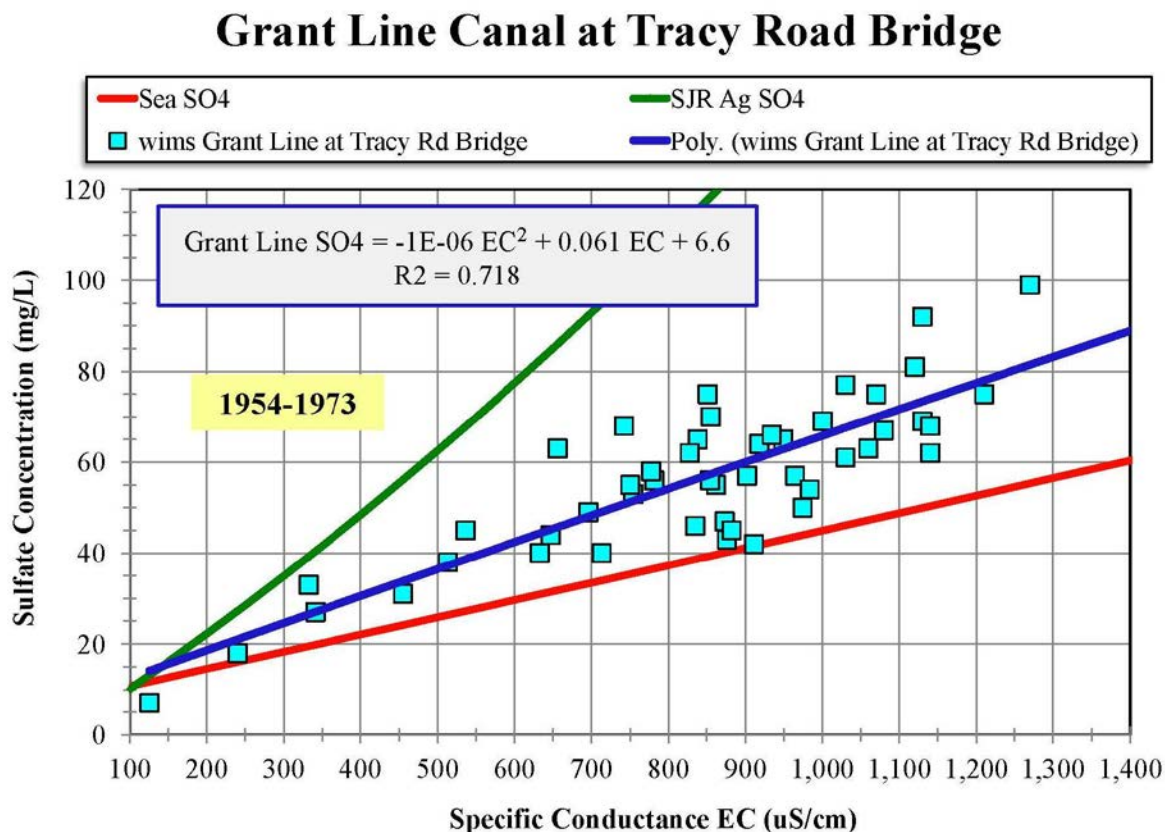


Figure 8-33: Corresponding variation of sulfate concentration as a function of specific conductance on Grant Line Canal at the Tracy Road Bridge.

8.7 San Joaquin River from Vernalis to Jersey Point

The reach of the San Joaquin River from Vernalis to Jersey Point represents the transition from agricultural drainage dominated stations (Vernalis, Mossdale Bridge and Brandt Bridge) to seawater-dominated stations (Jersey Point and, often, Prisoners Point) (Figure 8-34). The periods when seawater dominates at intermediate stations rather than agricultural drainage will depend though on whether there has been a period of low Delta outflow.

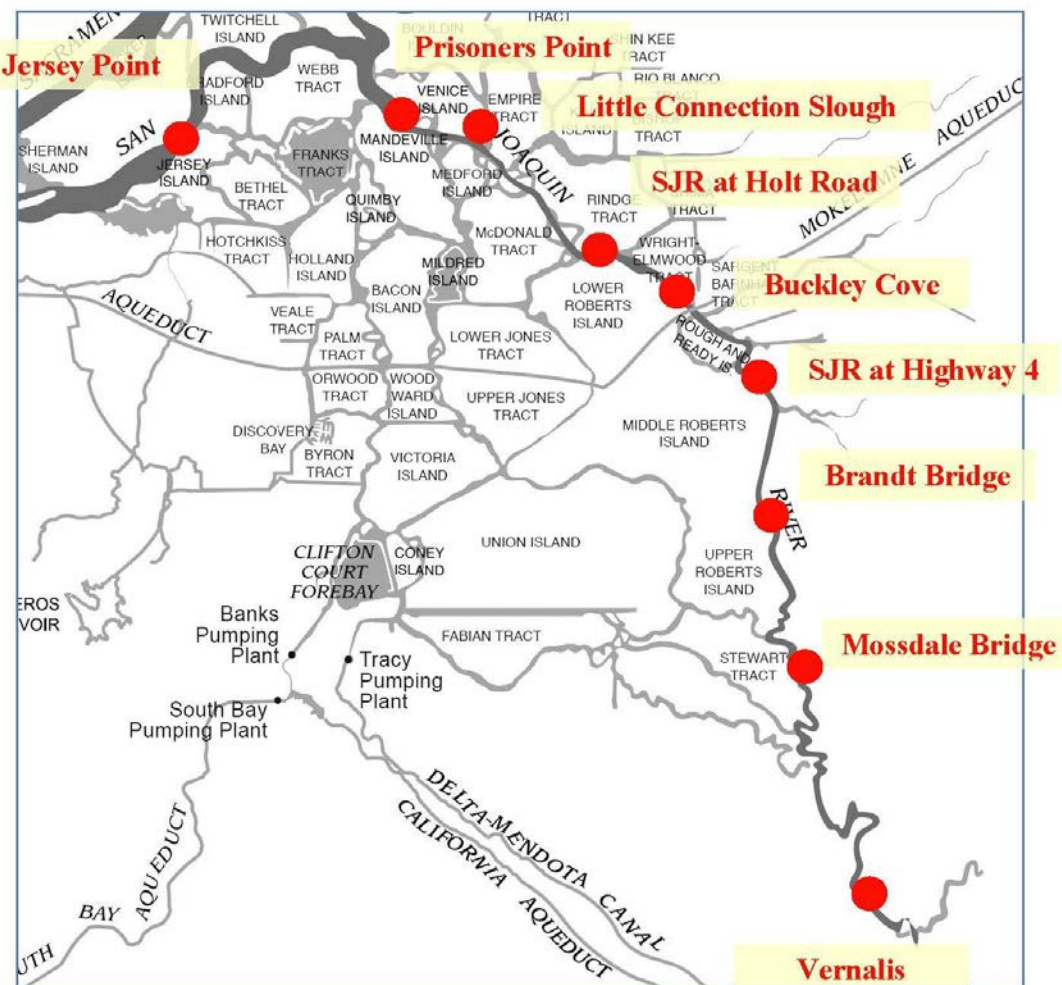


Figure 8-34: Map of the San Joaquin River from Vernalis to Jersey Point showing the location of key monitoring stations.

Figures 8-35 and 8-36 show the chloride concentrations as a function of EC for the southern part of this reach of the San Joaquin River (Vernalis to Brandt Bridge) and the northern section (Buckley Cove to Prisoners Point), respectively. The southernmost stations follow the agricultural drainage regression equation except for Prisoners Point. The Buckley Cove chloride data suggest the water consists primarily of agricultural drainage with a small contribution from seawater intrusion.

San Joaquin River -- Vernalis to Brandt Bridge

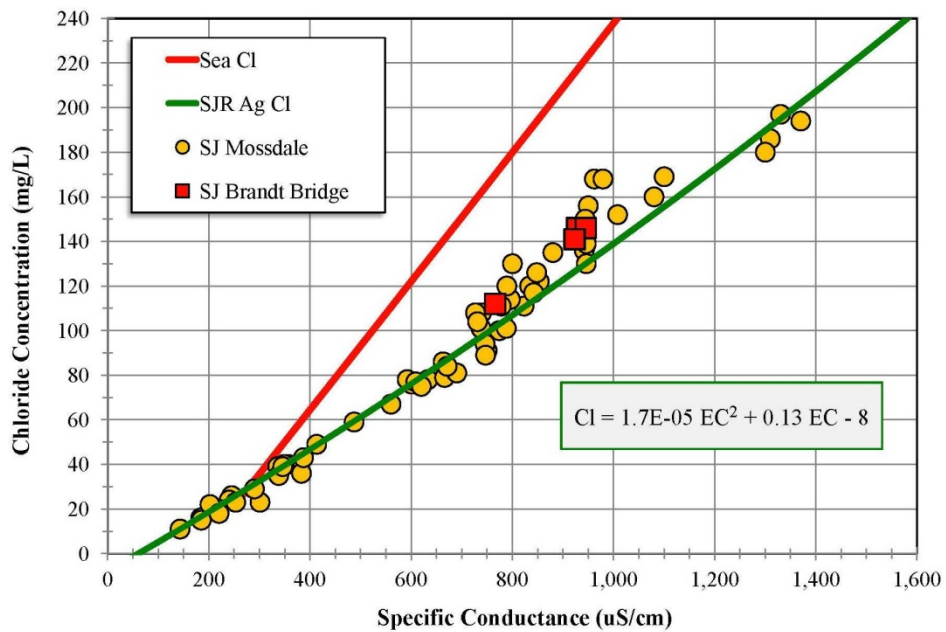


Figure 8-35: Variation of chloride concentration as a function of EC from Vernalis to Brandt Bridge on the San Joaquin River. The data are consistent with agricultural drainage-dominated water.

San Joaquin River -- Highway 4 to Prisoners Pt.

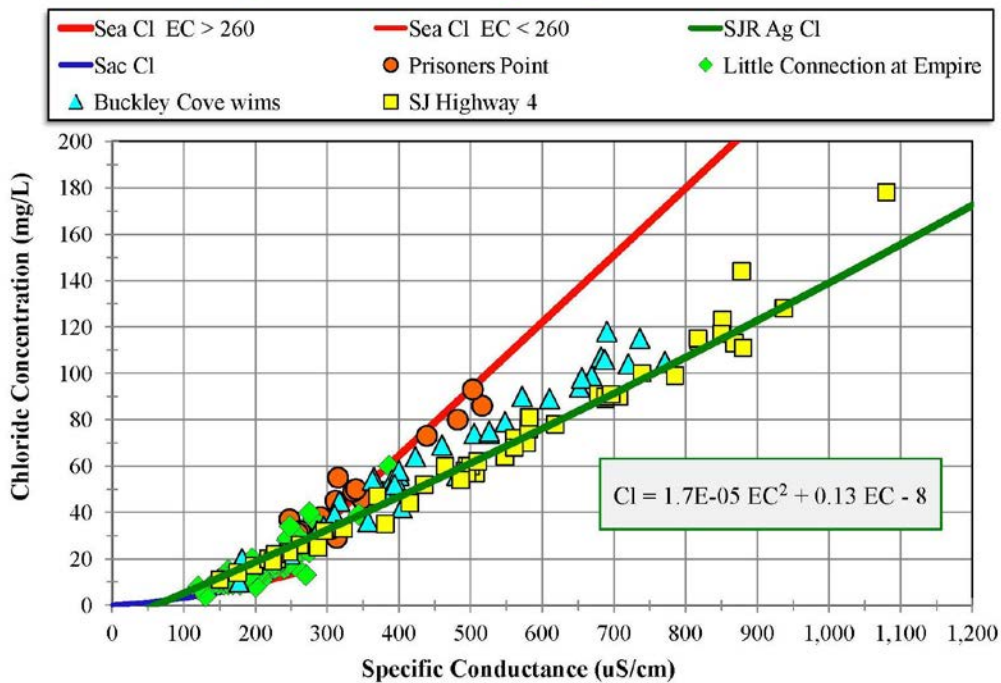


Figure 8-36: Variation of chloride concentration as a function of specific conductance from Buckley Cove to Prisoners Point (further north and more seaward) on the San Joaquin River.

Only chloride, bromide and field EC data were available for Prisoners Point so there is no information regarding the variation of calcium or sulfate at this location. This would be an interesting station to investigate in more detail because it is located similar distances away from the three key sources of water for the Delta. At times of high Sacramento River inflow, Prisoners Point water may consist primarily of Sacramento River water. During periods of very low Delta outflow, seawater intrusion might be expected to reach Prisoners Point. During periods of high San Joaquin flow and high discharges from local agriculture, agricultural drainage may dominate.

The measurement station in Little Connection Slough at Empire Tract is closest to Prisoner Point (Figure 8-34). To further investigate the relative influences of the different water sources in this northern reach, the variation of sulfate concentration is plotted as a function of EC (Figure 8-37). The sulfate data for the San Joaquin River at Highway 4 are agricultural drainage dominated but the Buckley Cove data again suggest a mixture of agricultural drainage and seawater.

The Little Connection Slough data in Figure 8-37 are close to the seawater dominated regression equation, but the maximum EC is only 344 $\mu\text{S}/\text{cm}$. Note that the seawater dominated regression curve and the Sacramento River curve are very similar at low EC ($\text{EC} < 260 \mu\text{S}/\text{cm}$) so it is not possible to distinguish the two effects.

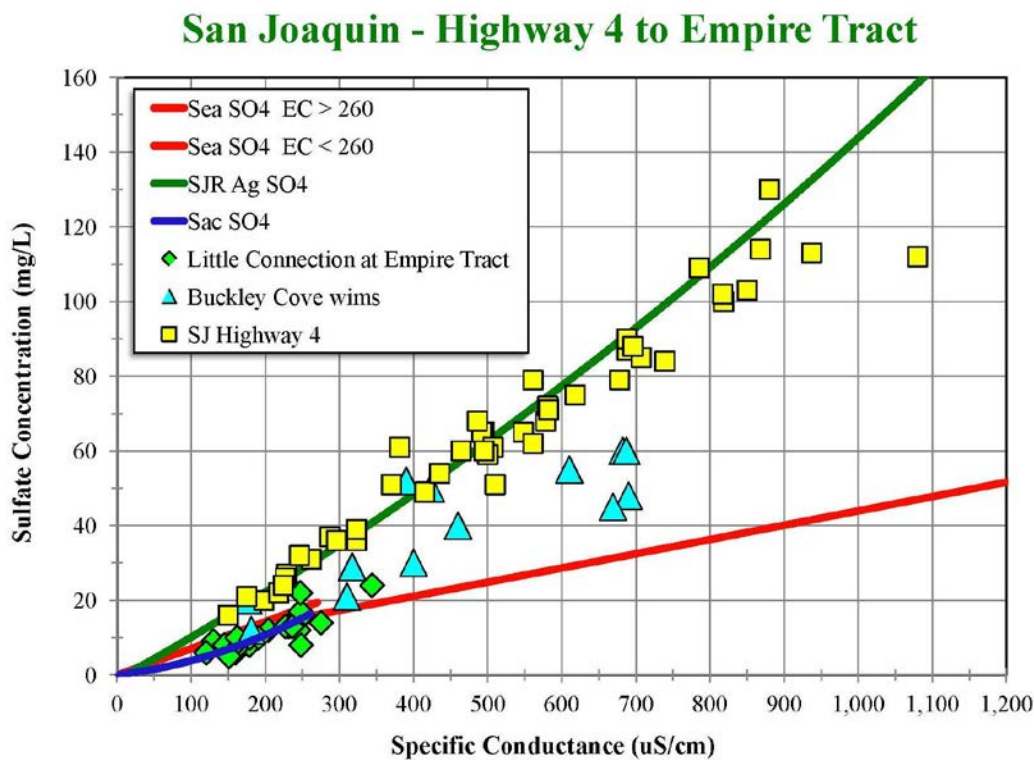


Figure 8-37: Variation of sulfate concentration as a function of specific conductance from at Little Connection Slough at Empire Tract, Buckley Cove and the Highway 4 crossing on the San Joaquin River.

8.8 Sacramento River from Freeport to Rio Vista Bridge

The section of the Sacramento River from Freeport (south of Sacramento) to Rio Vista represents Sacramento-dominated water (Figure 8-38). Seawater intrusion only reaches Rio Vista under extreme drought (low Delta outflow) situations, such as the 1976-1977 drought. In this case, seawater intrusion can be defined as causing salinities to increase above that predicted by the Sacramento River linear regression equations (Table 7.10, 7.11 and 7.12), e.g., Cl > 25 mg/L.

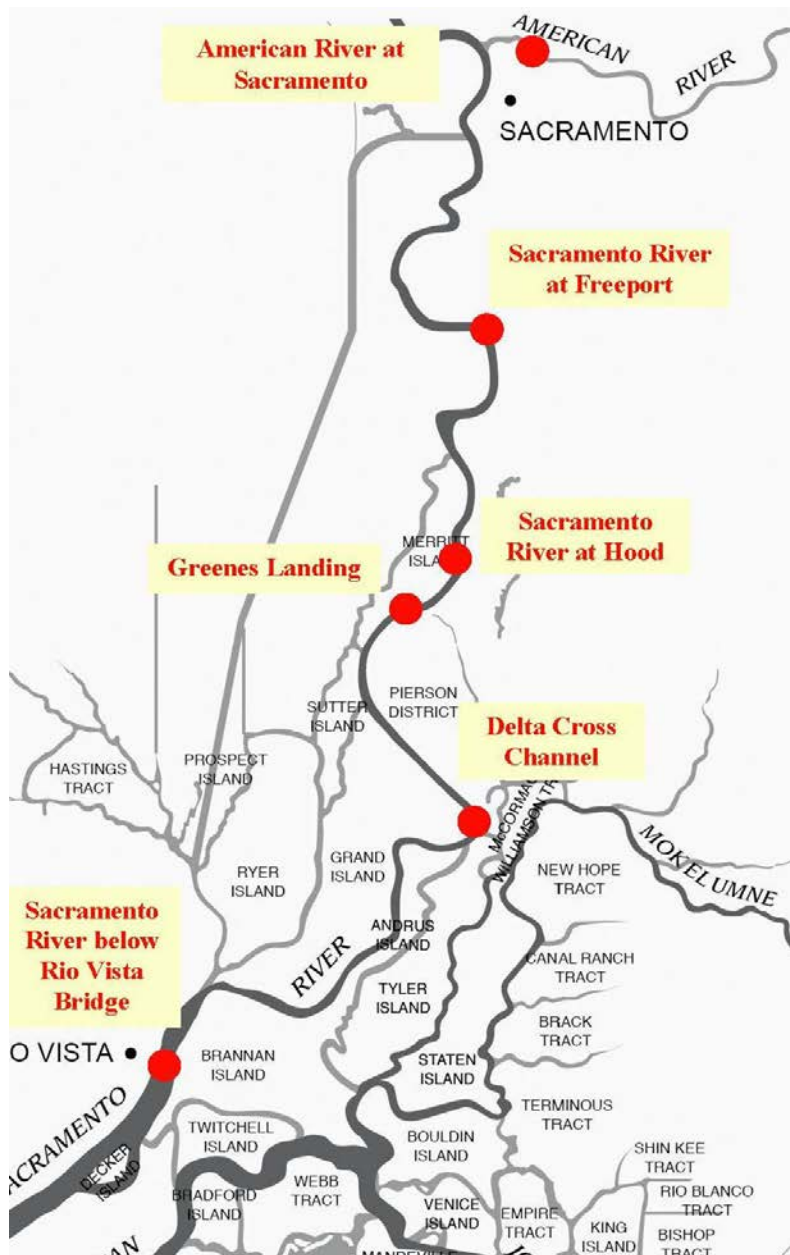


Figure 8-38: Map of Sacramento River in the northern Delta showing the location of key monitoring stations.

When Delta outflows are low during drought periods, salinities increase even in the northern Delta ($EC > 250 \mu\text{S}/\text{cm}$) and seawater rather than Sacramento River water dominates (Figure 8-39).

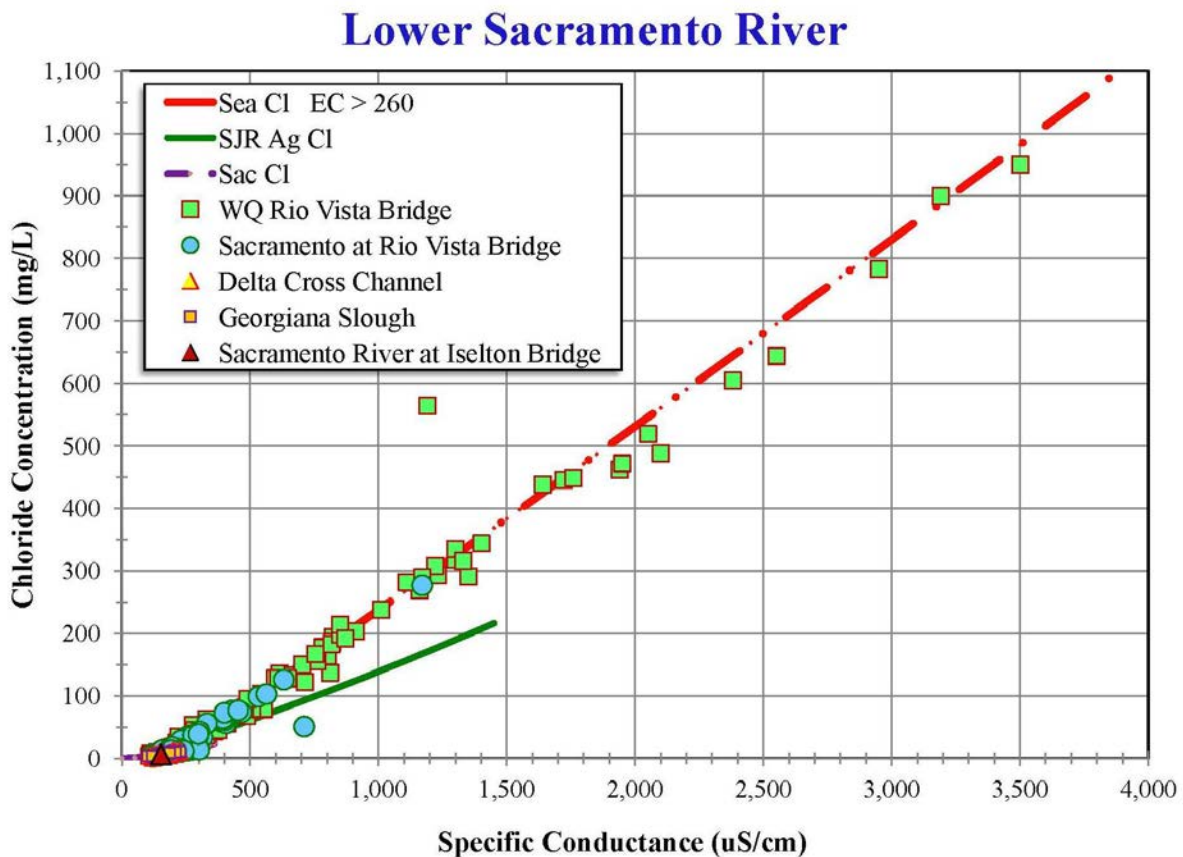


Figure 8-39: Variation of chloride concentration as a function of specific conductance from the Delta Cross Channel to Rio Vista.

The agricultural-drainage dominated regression equation for chloride as a function of EC is also plotted in Figure 8-39 to check whether local sources of agricultural drainage might also influence water quality in this region. It is not expected that San Joaquin River water would ever reach the north Delta, but local drainage in the south and central Delta does have the same characteristics as San Joaquin River water at Vernalis. As will also be shown in more detail later (Figure 8-41), the grab samples do not follow this agricultural drainage-dominated regression equation.

The variation of chloride concentrations with time for grab samples along the lower Sacramento River are shown in Figure 8-40). During the 1977 drought year, the chloride concentrations were extremely high (950 mg/L). Normally, when the salinities are very low and the chloride concentration as a function of EC regression equation is the same as for the Sacramento River at Hood and Greenes Landing (Figure 8-41).

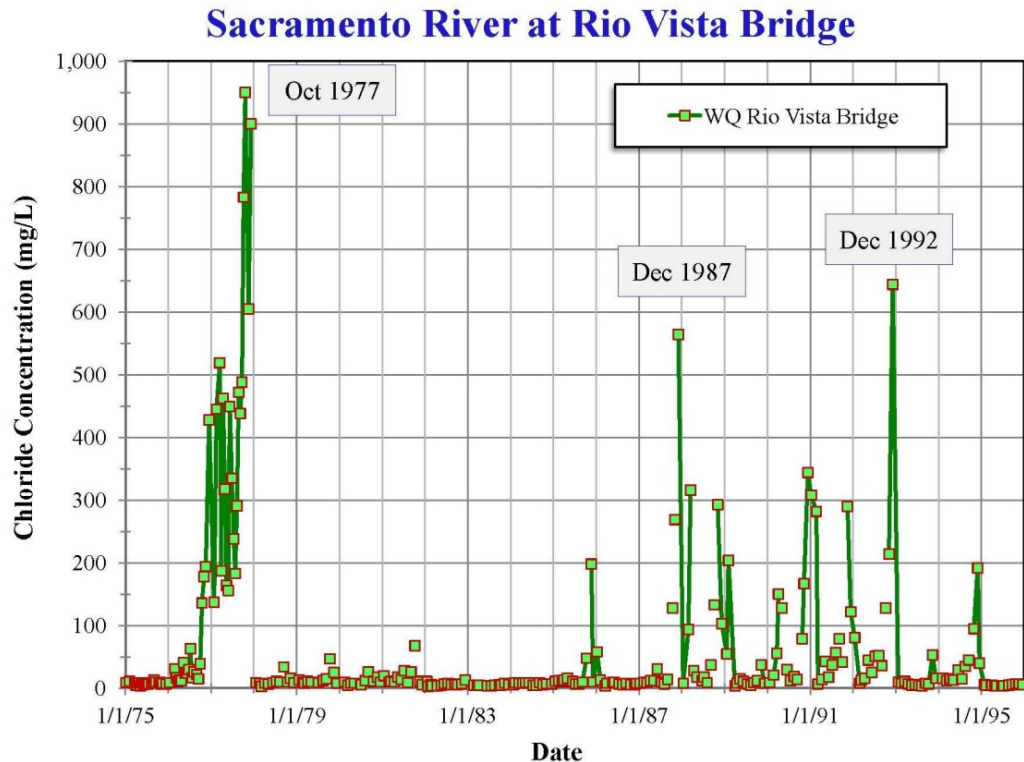


Figure 8-40: Variation of chloride concentration with time at Rio Vista during the period January 1975 through December 1995. This period includes the severe 1976-1977 drought.

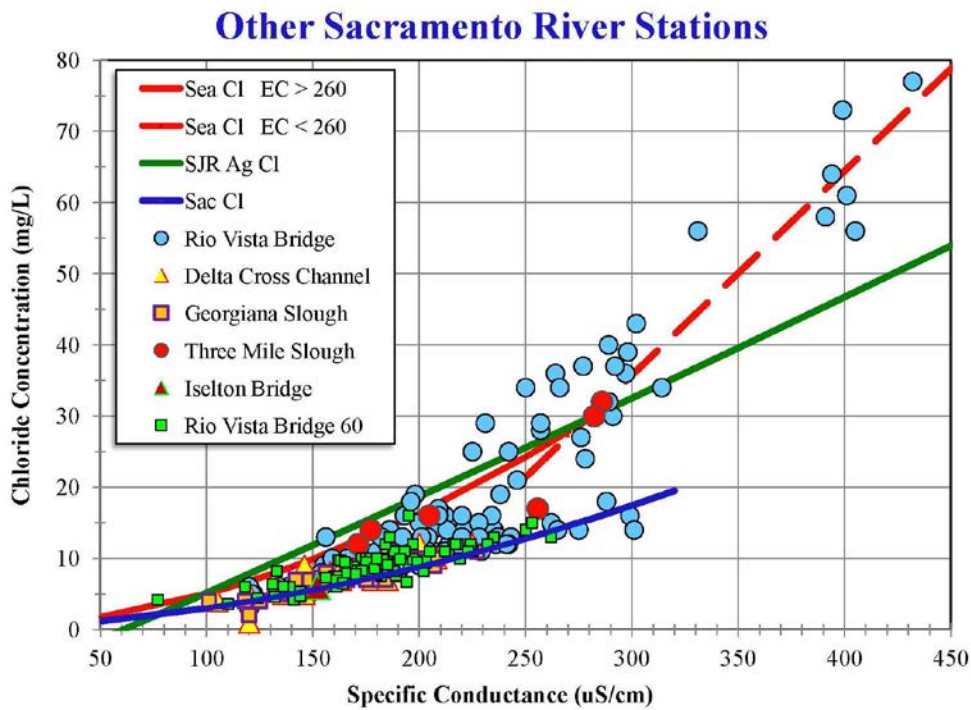


Figure 8-41: Variation of chloride concentration as a function of specific conductance from the Delta Cross Channel to Rio Vista for EC < 450 $\mu\text{S}/\text{cm}$.

The variation of sulfate concentration at Rio Vista and other lower Sacramento River stations follows a similar pattern with sulfates flowing the Sacramento River regression relationship at low EC but following the seawater-dominated relationship for large EC, in this case, $EC > 400 \mu\text{S}/\text{cm}$ (Figure 8-42).

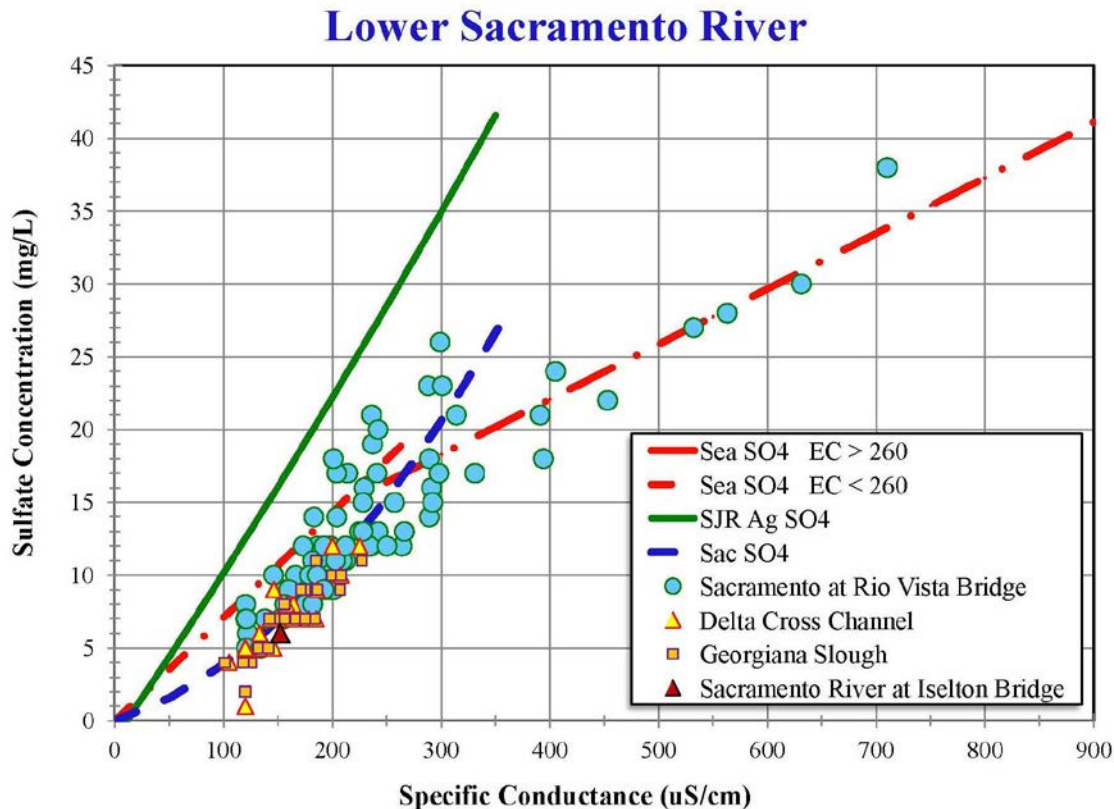


Figure 8-42: Variation of sulfate concentration as a function of specific conductance from the Delta Cross Channel to Rio Vista.

8.9 Lower Mokelumne and Cosumnes River Region

The available grab sample data for the Cosumnes River and Mokelumne River were presented in Appendix D. The water quality constituent regression equations in the upper reaches of the Cosumnes and Mokelumne are consistent with those for the Sacramento River inflow to the Delta.

8.10 Barker Slough

The Barker Slough area is the location of the intake to the North Bay Aqueduct (Figure 8-43). The City of Vallejo also operated a drinking water intake in the region at the confluence of Cache Slough and Ulatis Creek, but this Vallejo Pump Station has not been operated since 1992.



Figure 8-43: Map of the Barker Slough region in the vicinity of the North Bay Aqueduct intake (Barker Slough Pumping Plant).

The variation of chloride concentration as a function of EC at the intake in the region of the North Bay Aqueduct intake at Barker Slough is shown in Figure 8-44. A quadratic regression equation was developed for the North Bay Aqueduct at Barker Slough Pumping Plant grab sample data. The Sacramento River regression equation for chloride as a function of EC is only applicable for EC < 300 $\mu\text{S}/\text{cm}$ however, the Barker Slough region data appear to be consistent with an extrapolation of that regression relationship to an EC of 700 $\mu\text{S}/\text{cm}$. Figure 8-45 shows the corresponding variation in sodium concentration:

$$\text{Cl} = 1.1\text{E-}04 \text{ EC}^2 + 0.036 \text{ EC} \quad r\text{-squared} = 0.818$$

The corresponding regression equation for the sodium data at the NBA Barker Slough Pumping Plant intake is:

$$\text{Na} = 6\text{E-}05 \text{ EC}^2 + 0.0656 \text{ EC} \quad r\text{-squared} = 0.909$$

Using the Sacramento River chloride and sodium regression equations (only applicable for EC < 300 $\mu\text{S}/\text{cm}$) would generally underestimate the Cl and Na concentrations.

Barker Slough Region

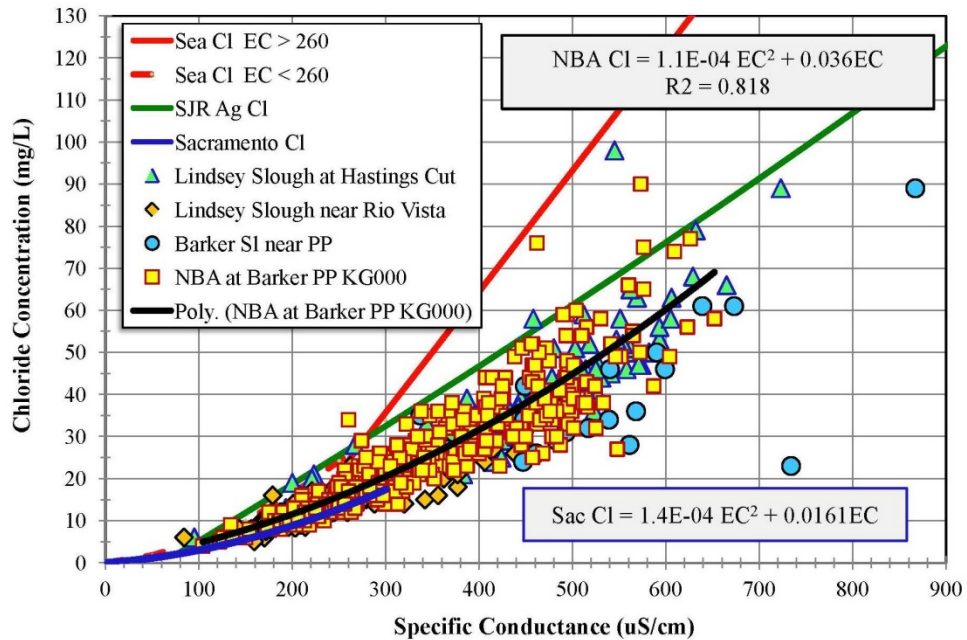


Figure 8-44: Variation of chloride concentration as a function of EC at the intake in the region of the North Bay Aqueduct intake at Barker Slough.

Barker Slough Region

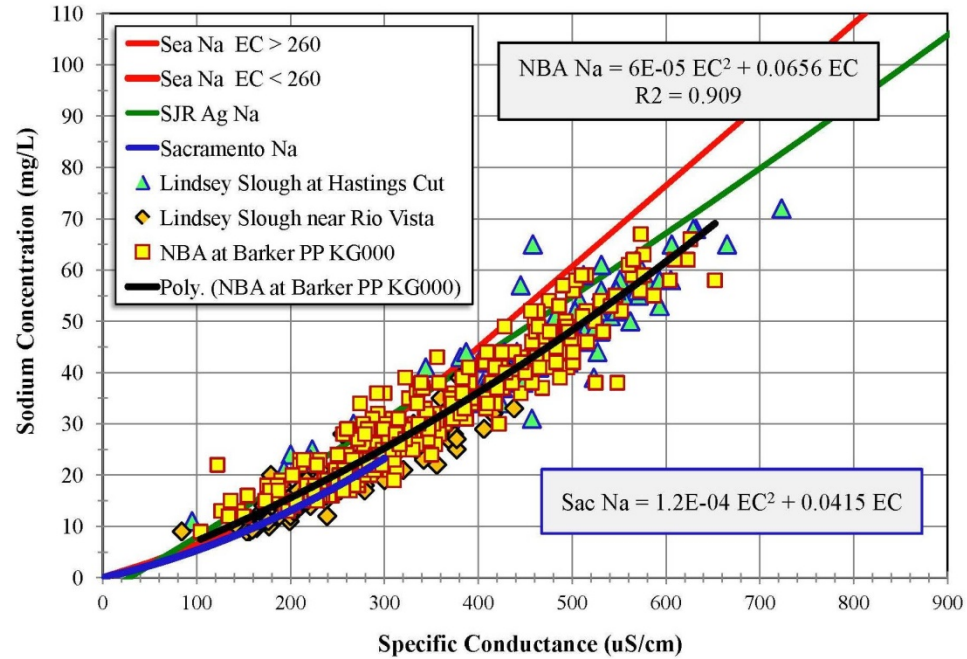


Figure 8-45: Variation of sodium concentration as a function of EC at the intake in the region of the North Bay Aqueduct intake at Barker Slough. The data follow a similar, but extrapolated, relationship to the Sacramento River sodium regression equation.

Figure 8-46 shows the variation of sodium concentration as a function of EC at the intake in the region of the North Bay Aqueduct intake at Barker Slough. The regression equation for the calcium data at the North Bay Aqueduct Barker Slough intake is:

$$Ca = -4E-04 EC^2 + 0.0646 EC \quad r\text{-squared} = 0.786$$

Using the Sacramento River sodium regression equation (applicable for EC < 300 $\mu\text{S}/\text{cm}$) would overestimate the sodium concentration in most months.

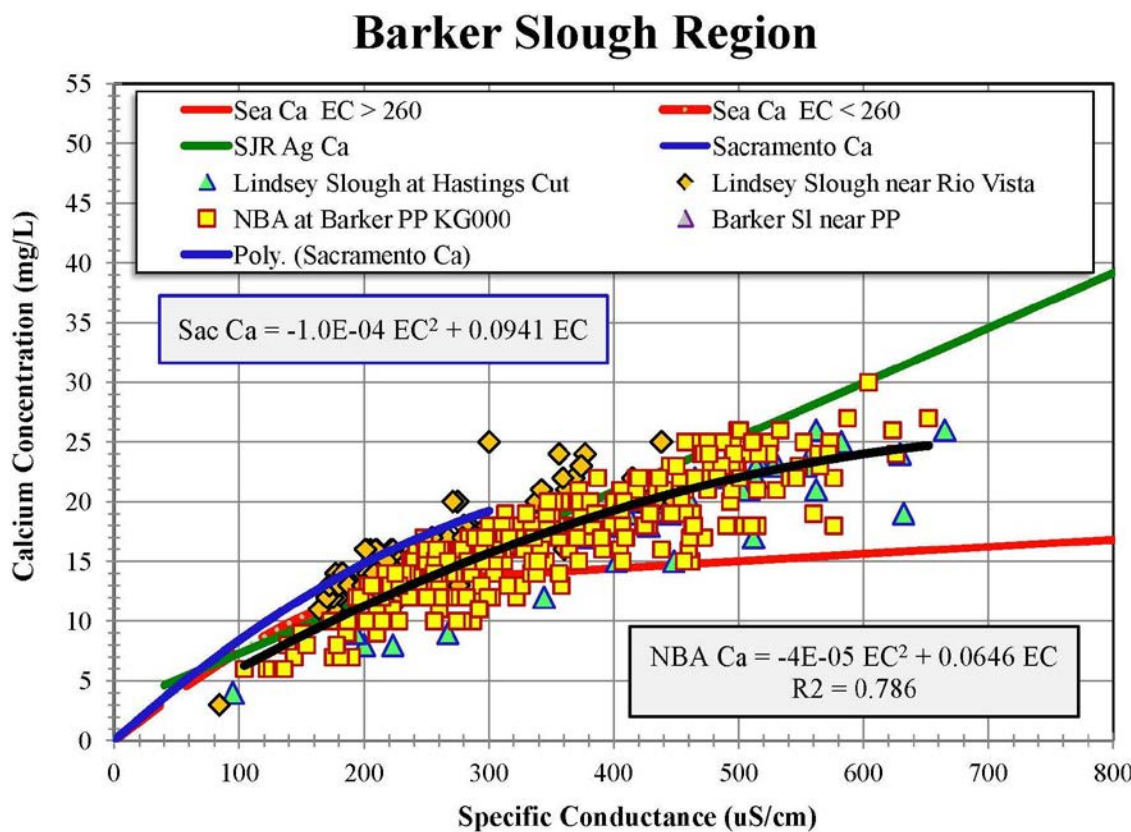


Figure 8-46: Variation of calcium concentration as a function of specific conductance in the region of the North Bay Aqueduct intake at Barker Slough. A site-specific calcium regression equation was derived because the Sacramento River regression equation does not represent these Barker Slough region data.

Some of the scatter in Figures 8-44, 8-45 and 4-46 is due to seasonal effects. The sodium concentration grab sample data are plotted as a function of time in Figure 8-47 for the period January 2005 through December 2008. During July-December, the water near the North Bay Aqueduct intake is dominated by freshwater and the grab sample data regression equation for chloride as a function of EC to chloride is consistent with the Sacramento River regression equation (over its applicable range). However, in some winters, local tributary runoff events mean that agricultural drainage significantly increases chloride concentrations and the regression relationship is closer to that for San Joaquin River water and local Delta drainage. The watershed soils in this area are sodic marine soils which typically have disproportionately high

concentration of sodium. During the winter runoff periods, the grab sample data have similar characteristics to agricultural drainage in the south and central data (and San Joaquin inflow at Vernalis). However, San Joaquin inflow will have no influence on water quality in the Barker Slough region.

The quadratic regression equation derived from the NBA at Barker Slough Pumping Plant grab samples provides a reasonable estimate of the sodium concentrations over the full range of seasonal variations. The r-squared for this regression equation (Na versus EC in Figure 8-45) was 0.909.

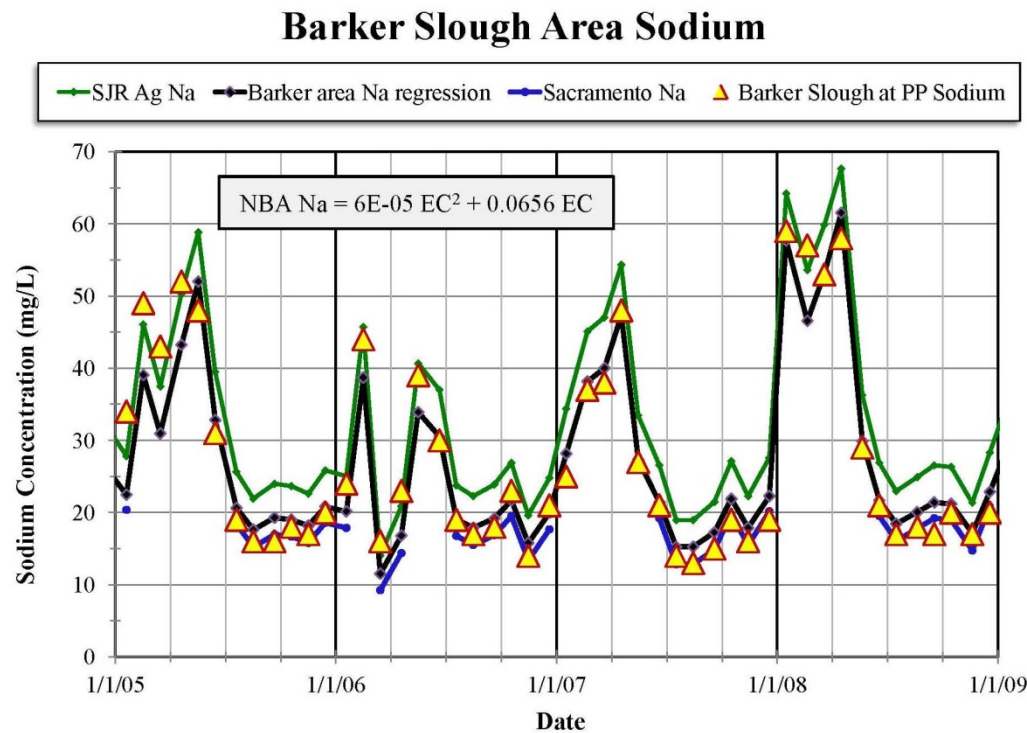


Figure 8-47: Variation of chloride concentration during the period January 2005 through December 2008 in the region near the North Bay Aqueduct intake. During July-December, the area is dominated by freshwater, consistent with the Sacramento River regression equation, but in some winters, drainage from local tributary runoff events significantly increases chloride concentrations.

The City of Vallejo also operated a drinking water intake in the region at the confluence of Cache Slough and Ulatis Creek up until 1992. Grab sample data from the City of Vallejo's former drinking water intake (1950 through 1992) cover a much larger range of salinities (up an EC of 1,050 $\mu\text{S}/\text{cm}$). Figures 8-47 show the variation of chloride with EC at this location. A quadratic regression equation for chloride concentration was derived from the Vallejo intake data:

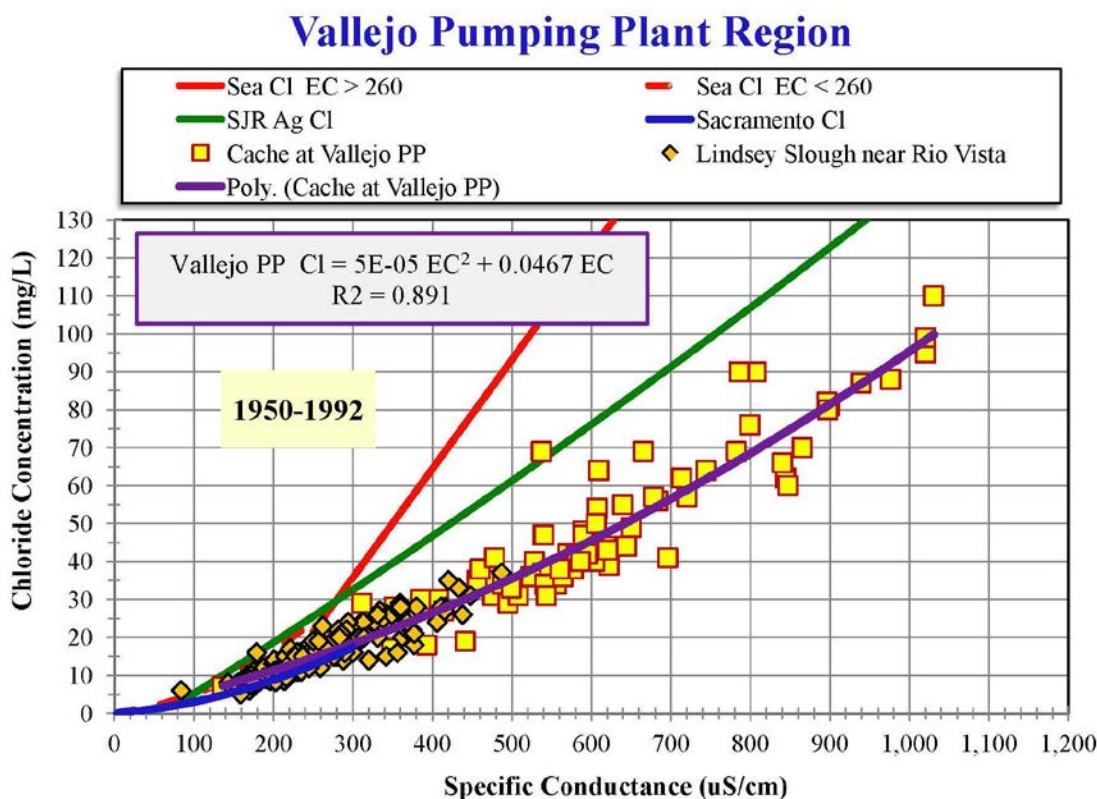


Figure 8-48: Variation of chloride concentration as a function of specific conductance at the City of Vallejo's former drinking water intake (1950-1992).

The regression fit for the Vallejo Pumping Plant chloride data over this larger range of EC is:

$$\text{Cl} = 5\text{E-}05 \text{EC}^2 + 0.0467 \text{EC} \quad r\text{-squared} = 0.891$$

Additional analysis could be done to compare time series of the earlier grab sample data from the City of Vallejo intake with the Barker Slough intake to the North Bay Aqueduct. The times series will likely be similar in the summer and fall period when salinities are low, but the increases in salinity due to the winter runoff may be different.

8.11 Agricultural Drainage and Drains

Grab sample data from a large number of agricultural drains in the Delta and in the San Joaquin Valley are also available on DWR's Water Data Library database. Data from a few of these discharges from agricultural drains were analyzed to see whether these data were in fact consistent with the agricultural drainage-dominated regression equation derived from Vernalis and Maze data (Appendix B). These grab samples tended to either follow the agricultural drainage-dominated relationships or, because they are more concentrated, have an even greater percentage of calcium and sulfate and less chloride. However, the water quality in drainage water is also influenced by the quality of applied irrigation water. For example, the agricultural drainage from Jersey Island has characteristics of a mixture of seawater and agricultural return flows.

Figure 8-49 shows chloride concentration grab samples from representative agricultural drains in the Central Delta area: Jersey Point Ag drain; Holland Tract Ag pumping plant No. 1; Bacon Island Ag pumping plant; and, a Palm Tract Ag drain. The chloride to EC relationship depends upon whether the applied irrigation water contained significant amounts of seawater or not.

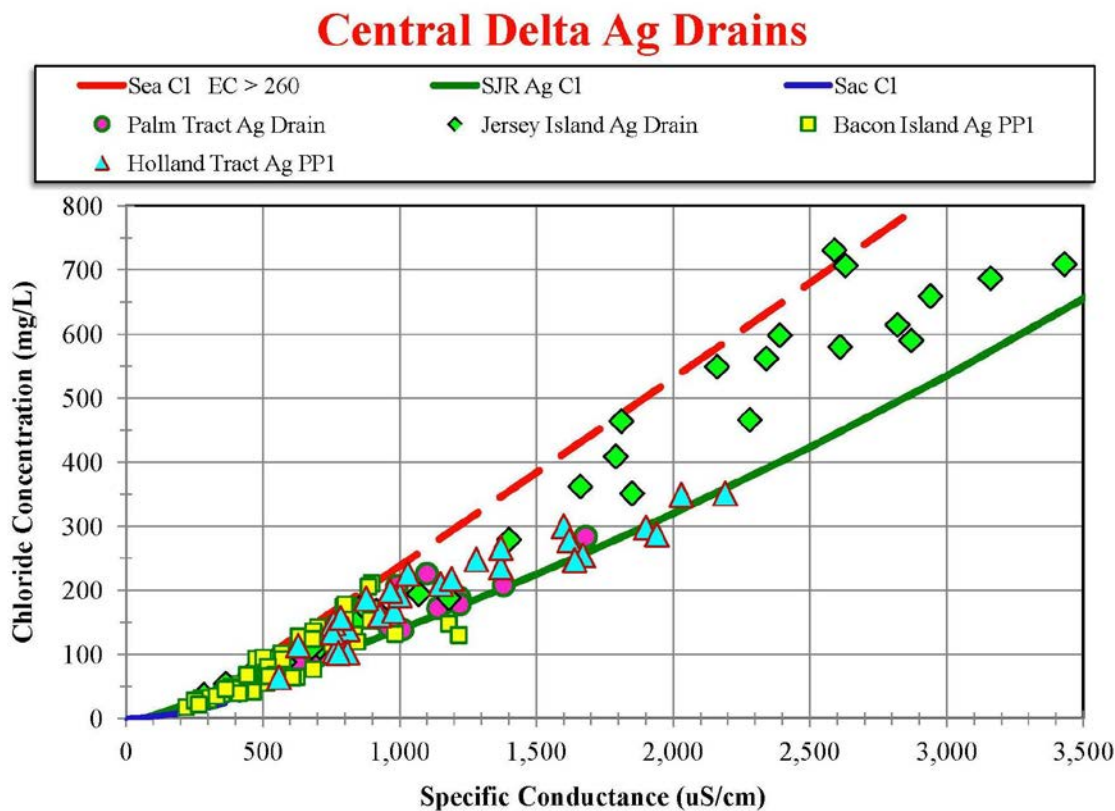


Figure 8-49: Variation of chloride concentration as a function of specific conductance (EC) for representative agricultural drains in the Central Delta area: Jersey Point Ag drain; Holland Tract Ag pumping plant No. 1; Bacon Island Ag pumping plant; and, a Palm Tract Ag drain.

8.12 Summary of Findings

The review of the regional relationships for water quality constituents as a function of EC in this chapter, suggest that it is generally not possible to describe these relationships by a single local or regional regression equation. The one exception is the relationship between TDS and EC (Figure 8-3) where the seawater-dominated and agricultural drainage-dominated regression equations are very close.

Stations in the western Delta and Suisun Bay are generally dominated by seawater intrusion, except under high outflow conditions (corresponding to $EC < 260 \mu\text{S}/\text{cm}$) when the regression relationships in the western Delta more closely represent agricultural drainage-dominated conditions.

Stations in the San Joaquin River from Vernalis to Brandt Bridge generally follow the agricultural drainage-dominated relationships (Tables 7.7, 7.8 and 7.9). However, as discussed in Appendix B, the water quality at Vernalis and Maze is sometimes shows a contribution from water containing seawater that was exported out of the south Delta to San Joaquin Valley for irrigation and subsequently returned to the Delta via the San Joaquin River.

Locations on the Sacramento and Mokelumne Rivers in the north and northeast of the Delta generally follow the Sacramento River regression equations (Tables 7.10, 7.11 and 7.12) but during very low Delta outflow events, or emergency situations such as the 1972 Andrus Island levee failure, seawater intrusion can reach well into the north Delta beyond Rio Vista.

The relationships between the water quality constituents throughout most of the Delta vary by water year type and by month. Seawater intrusion can influence water quality well into the interior Delta, although as shown in Figure F-8, the contribution from seawater intrusion decrease with increasing distance from Suisun Bay and the ocean.

It is also important to account for long-term changes in these relationships due to long-term changes in operations of physical barriers and diversion facilities. There are also short term changes due to the installation of barriers to protect interior Delta water quality during severe droughts.

The plots versus EC (or TDS) can sometimes be misleading if grab sample data is only available for a short period of time that is either very dry (i.e., seawater dominates) or predominantly wet such that the grab sample data indicates that agricultural drainage dominates. However, that location most likely is influenced by both seawater intrusion and agricultural drainage at different times of the year and different water year types.

The plots of water quality constituents versus EC (or TDS) in this chapter do indicate that the range of variations lie within the bounds depicted by the seawater boundary conditions (Mallard Island and Jersey Point) and the agricultural drainage boundary (Vernalis and Maze on the San Joaquin River). Plotting sulfate and calcium as a function of EC (or TDS) or time helps identify when agricultural drainage dominates. This is not always obvious from plots of chloride or bromide versus EC or TDS.

The key to estimating water quality constituent concentrations from EC and TDS is to first estimate the contribution of seawater to the observed EC value at a given location. The corresponding value of the water quality constituent (chloride, calcium, sulfate, magnesium, etc.) due to seawater can then be estimated using the seawater-dominated regression relationships. The remaining constituent concentration can then be calculated from the remaining amount of EC using the agricultural drainage-dominated regression relationship.

Methods for estimating the contribution from seawater intrusion at interior Delta locations are discussed in the next chapter.

9. Estimating Seawater Intrusion at Interior Delta Stations

The primary sources of salinity in the interior Delta are seawater intrusion and agricultural drainage. Freshwater from the Sacramento River and east side streams also contributes but the salinity concentrations are very small. Seawater intrusion tends to dominate during the late summer and fall, except in the wettest years. During other periods, outflows are typically higher and seawater intrusion is generally not significant. During those periods, agricultural drainage from the San Joaquin Valley and local drainage tend to be the major contributor to EC and TDS.

A qualitative example of this seasonal and water year variation for a location in the central Delta is shown in Table 9.1. Because the magnitude of the seawater intrusion also depends on the distance of a given location from the ocean, a location in the western Delta will be dominated by seawater intrusion most of the time, except for wetter months of wetter years. Similarly, a station in the southeast of the Delta will only experience seawater intrusion during the drier months of drier years.

Table 9.1: Matrix showing a simplified example of the expected pattern of seawater intrusion in the central Delta as a function of both time of the year (season) and water year type.

Water Year Type	January-March	April-June	July-September	October-December
Wet	Ag	Ag	Ag	Ag
Above Normal	Ag	Ag	Ag	Seawater
Below Normal	Ag	Ag	Seawater	Seawater
Dry	Ag	Ag	Seawater	Seawater
Critical	Seawater	Seawater	Seawater	Seawater
Season	Winter	Spring	Summer	Fall

To estimate a given water quality constituent such as chloride, calcium or sulfate concentration from a known value of EC or TDS it is, therefore, necessary to estimate the percentage of EC resulting from seawater intrusion. The chloride, calcium, and other salinity constituent concentrations resulting from seawater intrusion can then be calculated using the corresponding seawater boundary condition equation. The remaining concentration can be calculated using the rest of the total EC and the corresponding equation representing both local Delta agricultural drainage and San Joaquin River inflow at Vernalis.

There are a number of different methods for estimating the contribution from seawater and the remaining contribution from the other sources:

- (a) **Determine seawater EC contribution using DSM2 fingerprint data from a historical simulation run.** If a DSM2 fingerprint simulation is available, the calculated contribution from seawater (Martinez) at a given location can be used.

- (b) **Estimate seawater EC from grab sample data if a second constituent concentration is also known (e.g. chloride, calcium or sulfate).** If the values for a pair of constituents are known and there is significant bifurcation between the seawater and agricultural drainage dominated relationships, the seawater contribution to EC can be calculated and used to estimate the unknown concentrations of other constituents.
- (c) **Estimate seawater EC at a given location from “known” values of EC at Jersey Point EC.** High values of Jersey Point EC correspond to periods of low Delta outflow and high seawater intrusion. Seawater intruding to Jersey Point will continue mixing into the interior Delta. The effect of seawater intrusion decreases the further a given location is from the ocean and, in the interior Delta, will occur a week or two later. The SWP and CVP project operators use the field measurements of EC at Jersey Point to estimate the salinity at Rock Slough off Old River about fourteen days later. This was also a component of CCWD’s salinity-outflow model for computing Rock Slough chloride concentrations (Denton, 1993; Denton and Sullivan, 1993).
- (d) **Estimate seawater EC from antecedent Delta outflow.** If Jersey Point EC data are not available, they can be estimated from a time series of “known” Delta outflows using, e.g., CCWD’s salinity-outflow model.
- (e) **Estimate seawater EC from typical monthly and water year variations.** The simpler of these approaches is to acknowledge that, in general, seawater intrusion occurs primarily during the summer and fall. The percentage contribution of seawater to total EC can be expressed as a function of both month of the year and water year index. In the driest years there will be seawater intrusion for more months. In very wet years, seawater intrusion can be minimal all year.

Each of the methods is discussed in more detail below, after a more general discussion of the variations in seawater intrusion in the Delta.

9.1: Seasonal Variations in Seawater Contributions

Outflows from the Sacramento-San Joaquin Delta are typically lowest during July through October. However, as shown in Figure 9-1, the individual months with the lowest outflow can vary. In wet years such as 2011, Delta outflows can remain relatively high during the summer and early fall. These variations in the timing of periods of lowest Delta outflow make it difficult to simply categorize the magnitude of seawater intrusion by just season or just water year type.

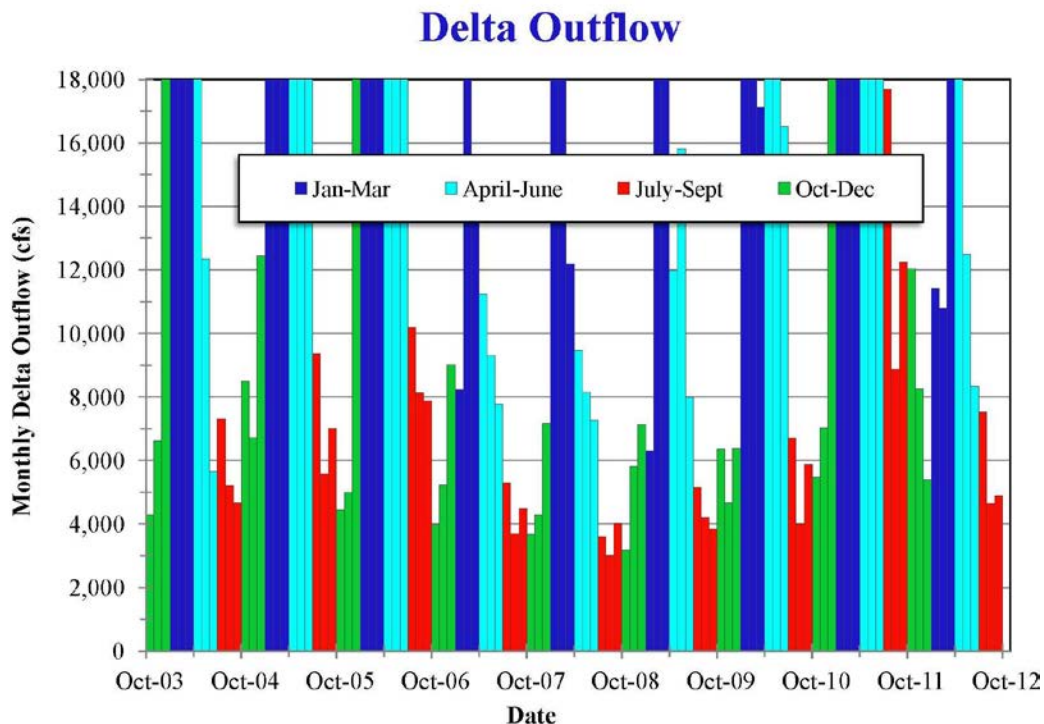


Figure 9-1: Monthly-averaged Delta outflows (from DWR's DAYFLOW database) for the period October 2003 through September 2012. The four quarters of each year are color-coded to show the seasonal trends in outflow, and seawater intrusion. Delta outflows greater than 18,000 cfs are sufficient to substantially repel seawater intrusion into the Delta. Only the range of Delta outflows from 0 to 18,000 cfs to better show the variations in Delta outflow during the drier months of the year.

9.2: Determine seawater EC contribution using DSM2 fingerprint data from a historical simulation run.

As discussed in more detail in Appendix F, DWR's DSM2 model can be used to track the separate contributions to salinity from five different sources: seawater, San Joaquin River, local agricultural drainage, Sacramento River and the eastside tributaries to the Delta. The results are expressed as both EC from each source and the volumetric contribution from each source.

The source-specific EC data can be used to estimate the percentage of total EC contributed by the seawater boundary. This EC is converted using the seawater-dominated regression equation; the remaining EC is converted using the agricultural drainage-dominated regression equation.

Because the seawater boundary condition salinity is very high, the percentage volume from seawater is generally very small, even when the resulting contribution to EC is significant. In Using source EC fingerprint data rather than the volumetric fingerprint data makes it easier to illustrate when seawater dominates and when it doesn't.

9.3: Estimate seawater EC from grab sample data if a second constituent concentration is also known (e.g. chloride, calcium or sulfate).

The water quality at interior Delta locations is a mixture of seawater, inflows from the San Joaquin Valley that contain agricultural drainage, local agricultural and municipal discharges, and fresher water from the Sacramento River and east side streams. Figure 9-2, which plots chloride concentration as a function of specific conductance, illustrates this point by showing that grab sample data lie between the linear regression equation that applies when seawater dominates ($\text{Cl} = 0.285 \text{ EC} - 50$) and the linear regression equation that applies when agricultural drainage dominates ($\text{Cl} = 0.15 \text{ EC} - 12$).

Note that for western Delta stations where the specific conductance can be as high as 20,000 $\mu\text{S}/\text{cm}$ or more, the relationship between chloride concentration and EC is best represented by a quadratic equation (see Tables 7-1 *et seq.* in Chapter 7). However, in the south and central Delta where EC is typically only 1,500 $\mu\text{S}/\text{cm}$ or less, a simple linear relationship is sufficient.

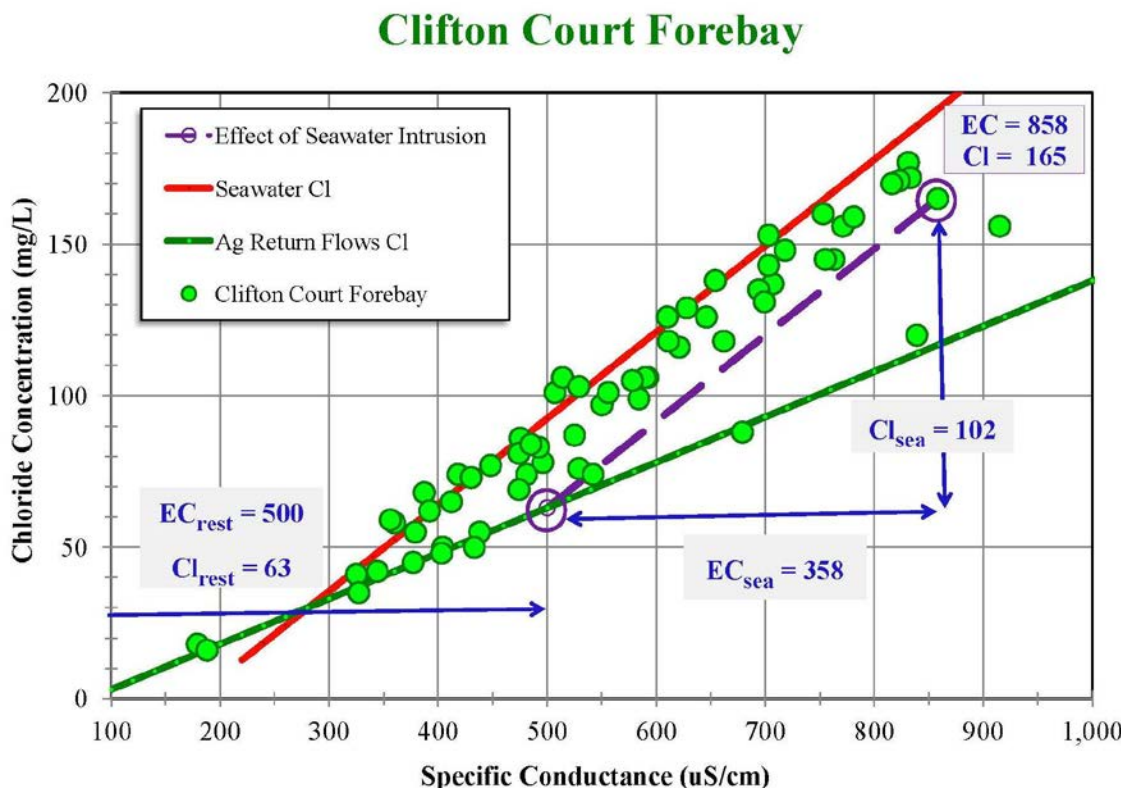


Figure 9-2: Variation of chloride concentration as a function of specific conductance for grab samples from West Canal near the intake to the Clifton Court Forebay (1990-1994). The purple circles indicate the estimated seawater EC of $358 \mu\text{S}/\text{cm}$.

Consider the grab sample taken from West Canal near the intake to the Clifton Court Forebay on December 19, 1991. The specific conductance and chloride concentration of this sample was $858 \mu\text{S}/\text{cm}$ and 165 mg/L , respectively. The upper (seawater) chloride limit for that EC value is 195 mg/L and the lower (agricultural drainage) limit is 117 mg/L . Note that the

corresponding EC in West Canal from the DSM2 Fingerprint data was 643 $\mu\text{S}/\text{cm}$, and the contribution to EC from the seawater boundary condition (Martinez) was 309 $\mu\text{S}/\text{cm}$, i.e., 48% of the total EC. Only 15% of the EC was from the Sacramento River and eastside streams. San Joaquin and local drainage contributed to 37% of the total EC.

The total EC and total Cl for the grab sample of December 19, 1991 can be expressed as

$$\text{Total EC} = (\text{Sac} + \text{ESS}) \text{ EC} + (\text{SJR} + \text{AgR}) \text{ EC} + \text{Sea EC}$$

$$\text{Total Cl} = (\text{Sac} + \text{ESS}) \text{ Cl} + (\text{SJR} + \text{AgR}) \text{ Cl} + \text{Sea Cl}$$

where: AgR = local agricultural drainage

ESS = eastside streams contribution

Sac = Sacramento River contribution

Sea = seawater intrusion contribution

SJR = San Joaquin River contribution (Vernalis)

On a plot of chloride concentration versus EC (Figure 9-2), the values of EC and chloride from every source except seawater are represented by a point on the regression equation for agricultural drainage ($\text{Cl}_2 = 0.15 \text{ EC}_2 - 12$) where it intersects with a line of slope 0.285 passing through the grab sample value.

For this example, the grab sample value is given by the equation:

$$\text{Cl}_2 = 0.285 \text{ EC}_2 + K$$

where K is an unknown. For this example, $\text{EC}_2 = 858 \mu\text{S}/\text{cm}$ and $\text{Cl}_2 = 165 \text{ mg/L}$.

The unknown values of EC_1 and Cl_1 where the two lines intercept are given by the two equations:

$$\text{Cl}_1 = 0.285 \text{ EC}_1 + K \quad \text{and} \quad \text{Cl}_1 = 0.15 \text{ EC}_1 - 12$$

In other words,

$$\text{EC}_1 = (-\text{Cl}_1 + 0.285 \text{ EC}_1 - 12) / (0.285 - 0.15)$$

For this example, $\text{EC}_1 = 500 \mu\text{S}/\text{cm}$ and $\text{Cl}_1 = 63 \text{ mg/L}$.

This means that the seawater contribution to total EC for the grab sample is 358/858 or 42%. As discussed above, the corresponding percentage from the DSM2 Fingerprint data was 48%. This method for estimating the seawater contribution to total EC can be used if both EC and Cl are measured, or otherwise known, but other water quality constituents such as calcium and sulfate are unknown and need to be determined. If only EC is known, e.g., from a continuous field measurement or as output from a DSM2 run, another method is needed (as discussed in the next section).

Estimating seawater EC from known chloride and EC values is possible because of the relatively large separation between the seawater and agricultural drainage boundary condition curves. For

other water quality constituents, such as sodium or total dissolved solids, the bifurcation is much smaller and the estimates of seawater EC will be much less accurate.

The calculated percentage of EC due to seawater can be used to estimate other water quality constituents such as bromide, sodium, calcium, sulfate, etc.

The linear regression equations for calcium as a function of EC (for interior Delta stations where $EC < 1,500 \mu\text{S}/\text{cm}$) are:

$$\text{Ca} = 0.0045 \text{ EC} + 12.6 \quad \text{Seawater}$$

$$\text{Ca} = 0.045 \text{ EC} + 2.8 \quad \text{Ag Drainage}$$

As discussed above, linear regression equations are used to simplify the explanation of the mathematical method for solving for the seawater contribution to EC. These linear regression equations give the same results as the quadratic regression equations presented in Chapter 7 for the range of EC values typically measured in the interior Delta ($EC < 1,500 \mu\text{S}/\text{cm}$.)

The concentration of calcium concentration from the December 19, 1991 grab sample at Clifton Court was 28 mg/L. Using just the measured EC and Ca values from that day, the estimated seawater EC is 331 $\mu\text{S}/\text{cm}$ (compared to 358 $\mu\text{S}/\text{cm}$ from the measured EC and Cl data). For the case where only EC and Cl were known, but not Ca, the estimated value for calcium would be 27 mg/L.

No sulfate grab sample concentration was reported at this location for December 19, 1991. However, the estimate of SO_4 concentration based on the known EC and Cl values would be 77 mg/L.

Figure 9-3 shows estimates of the seawater contribution at Clifton Court Forebay utilizing grab sample data for the period July 2005 through June 2009. The data points represent estimates computed from three different pairs of grab sample data: EC and chloride, EC and calcium, and EC and sulfate. The estimates using chloride and calcium are somewhat similar but the estimate using sulfate is higher.

Also shown in Figure 9-3 is the estimated seawater contribution based on continuous EC measurements at Jersey Point. This method is discussed in more detail in the next section and also in Appendix F. The relationship between total Clifton Court EC and weighted Jersey Point EC, derived from historical daily EC data (DWR CDEC) is represented by the equation:

$$\text{Clifton Court EC} = 0.24 * \text{Weighted Jersey Point EC} + 200.$$

The derivation of this equation is discussed in the next section (see Figure 9-7). The corresponding estimate of just the seawater contribution in Figure 9-3 is

$$\text{Clifton Court Seawater EC} = 0.24 * \text{Weighted Jersey Point EC} - 50,$$

where the value of -50 was chosen to represent seawater EC going to zero during the winter and spring.

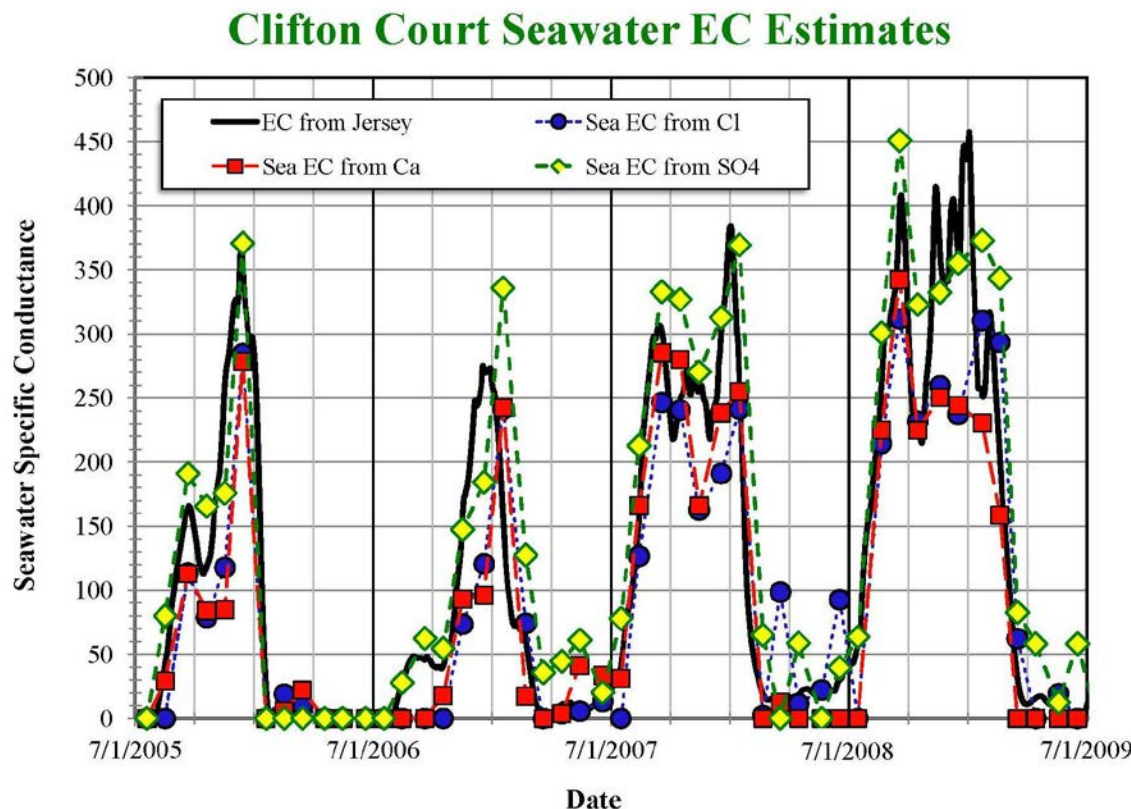


Figure 9-3: Estimates of specific conductance from EC and chloride, EC and calcium and EC and sulfate. These estimates are for grab sample from West Canal near the intake to the Clifton Court Forebay (2005-2009). Also plotted is the corresponding seawater EC estimate from Jersey Point EC.

The various estimates are different but they do serve to indicate that typically during the winter and spring, the agricultural drainage-dominated regression equation can be used (i.e., no seawater intrusion) and typically during July-December, seawater intrusion dominates and the seawater-dominated regression equation can be used.

9.4 Estimate seawater EC at a given location from “known” values of EC at Jersey Point EC

The contribution of seawater to the total EC (or TDS) at a given central or south Delta station is highly correlated with the salinity at Jersey Point. The interior Delta responses to changes in Jersey Point EC occur 10-20 days later depending upon the channel distance from Jersey Point.

This delayed response is taken into account using a “weighted” Jersey Point EC, where:

$$\text{Weighted Jersey Point EC}(t) = c_1 * \text{Average Jersey EC (t-6 through t)} + c_2 * \text{Average Jersey EC (t-13 through t-7)} + c_3 * \text{Average Jersey EC (t-20 through t-14)} + c_4 * \text{Average Jersey EC (t-27 through t-21)}$$

where t represents the current day and $t-n$ represents the conditions n days earlier.

For daily EC data measured on Old River at Bacon Island, the weighting coefficients $c_1 = 0.0$, $c_2 = 0.5$, $c_3 = 0.4$ and $c_4 = 0.1$ were used to represent the time delay between salinity changes at Jersey Point and Bacon Island. It might be possible to further refine these time delay weighting coefficients to better collapse the EC data into a single relationship, but as shown in Figure 9-4, these weightings reduce the data scatter. The EC relationship for Bacon Island when seawater dominates is then obtained by fitting the weighted EC data,

i.e., Old River at Bacon Island EC = 0.41 Weighted Jersey Point EC + 120

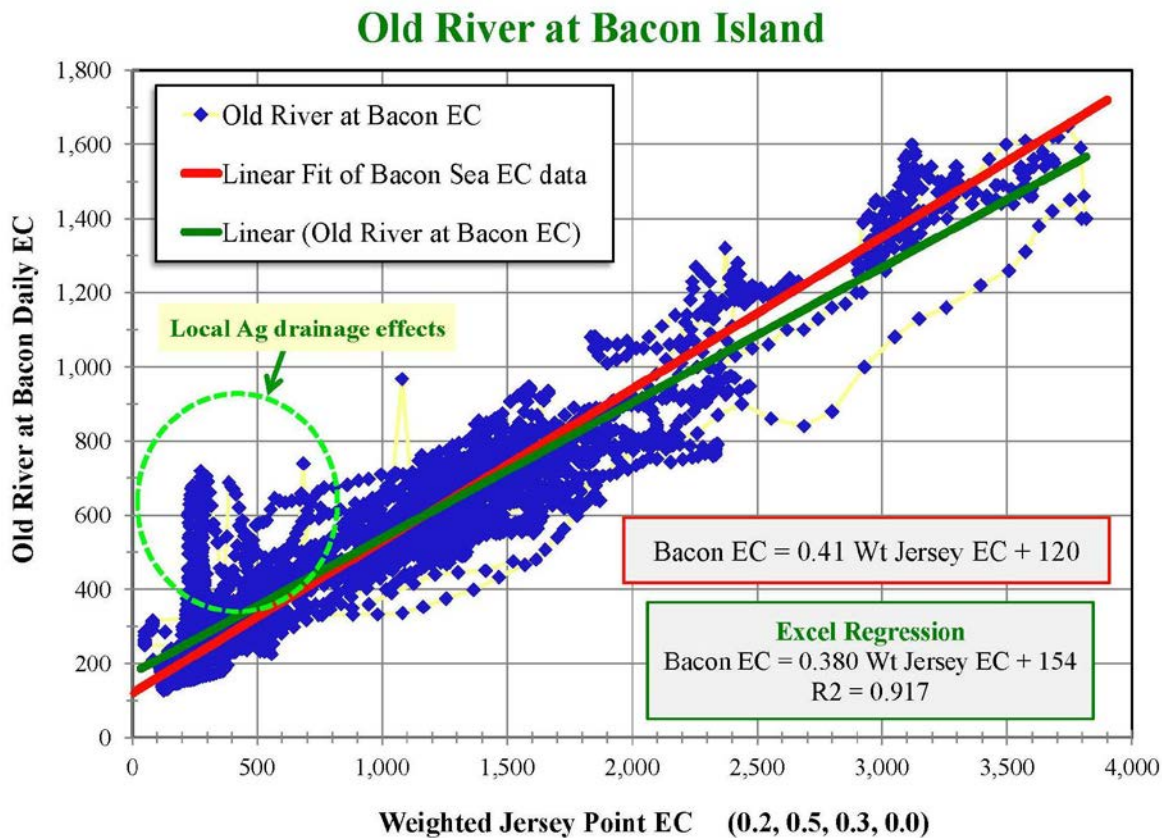


Figure 9-4: Comparison of Old River at Bacon Island EC with weighted Jersey Point EC (1975-2012 data). The seawater dominated relationship (red line) can be used to estimate the seawater contribution at Bacon Island. The linear regression (green line) is different because it is also influenced by periods when agricultural drainage dominates, e.g., during periods of low Jersey Point EC.

The prediction of seawater intrusion at Bacon Island EC from Jersey Point EC depicted in Figure 9-4 does not go to zero when Jersey EC is at its lowest (about 200 $\mu\text{S}/\text{cm}$) because the Bacon Island EC includes some local drainage effects. The corresponding equation for seawater intrusion for Old River at Bacon Island is

Old River at Bacon Island **seawater** EC = 0.41 Weighted Jersey Point EC

Figures 9-5 and 9-6 show the predicted Old River at Bacon EC from historical Jersey Point EC for the periods January 1975 through December 1979, and July 2006 through February 2012, respectively. These predictions show agreement with measured data when seawater dominates. During other periods such as January-June 2008 and February-June 2010, Delta outflows were high and seawater intrusion was very low. Actual Old River at Bacon Island EC was much higher because of the contributions from local drainage and San Joaquin inflow.

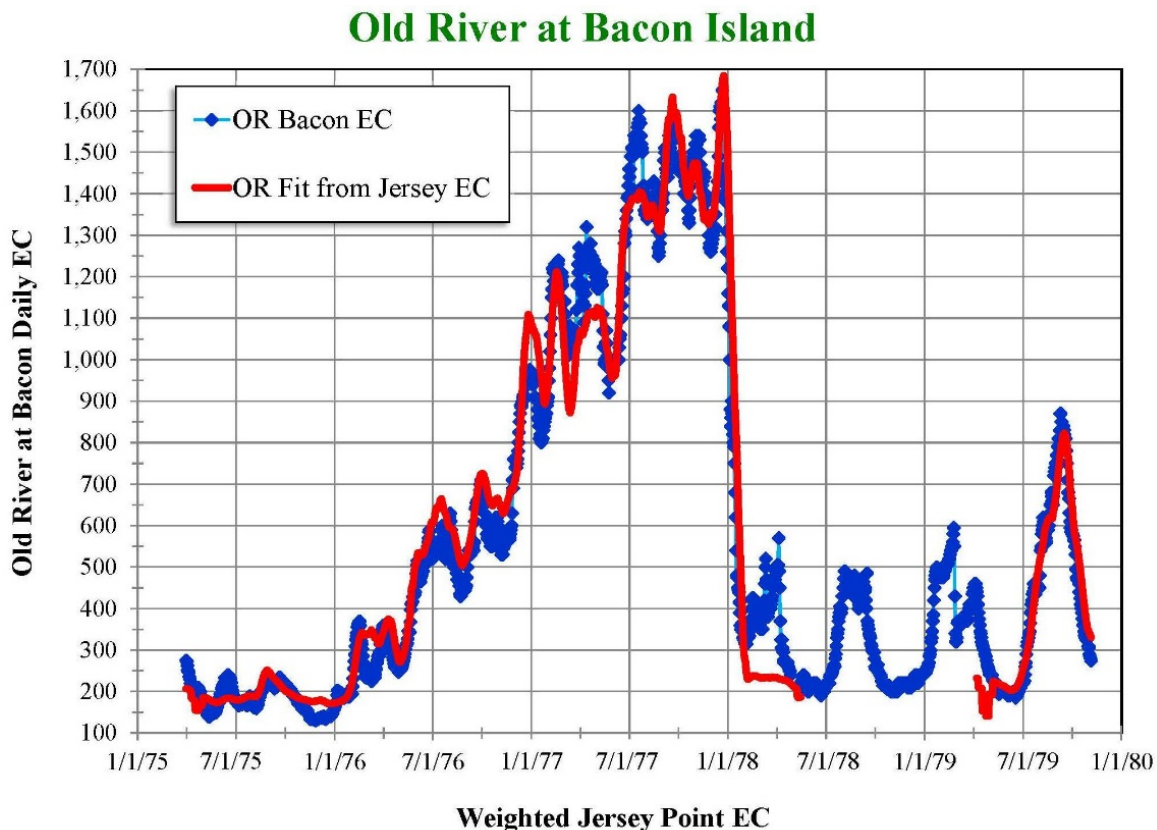


Figure 9-5: Comparison of estimated Old River at Bacon Island EC due to seawater intrusion with measured EC data (1975-1979).

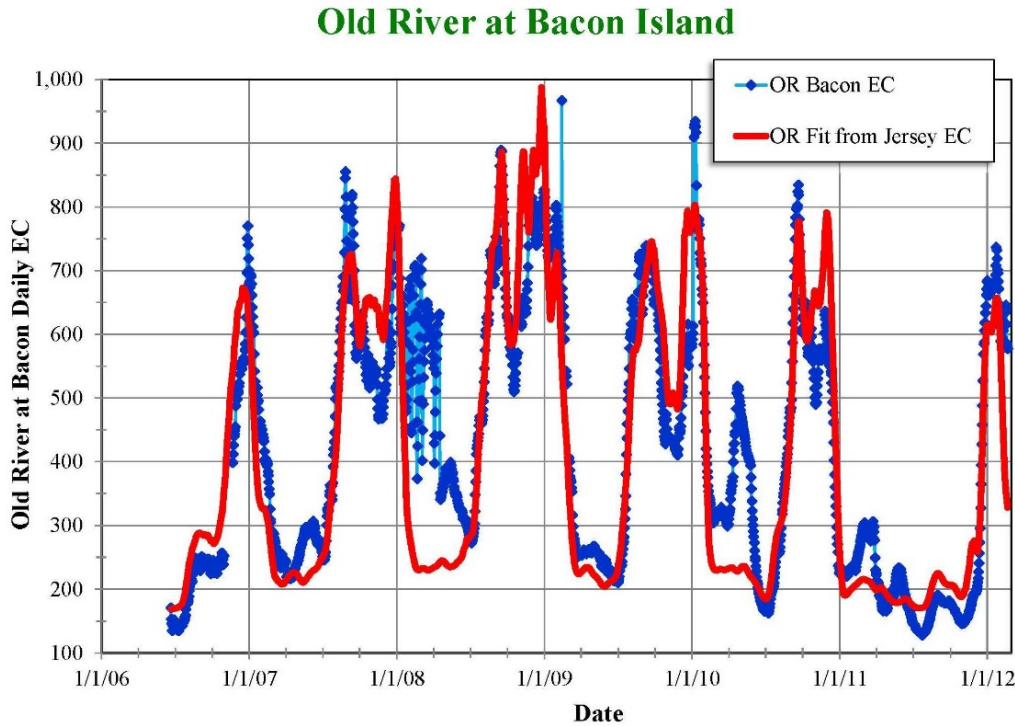


Figure 9-6: Comparison of estimated Old River at Bacon Island EC due to seawater intrusion with measured EC data (July 2006 – February 2012).

Similar analyses can be carried out at other interior Delta stations such as Clifton Court (Figure 9-7 and 9-8). The predictions based on Jersey Point EC become less accurate as the distance from Jersey Point to the particular interior Delta location increases.

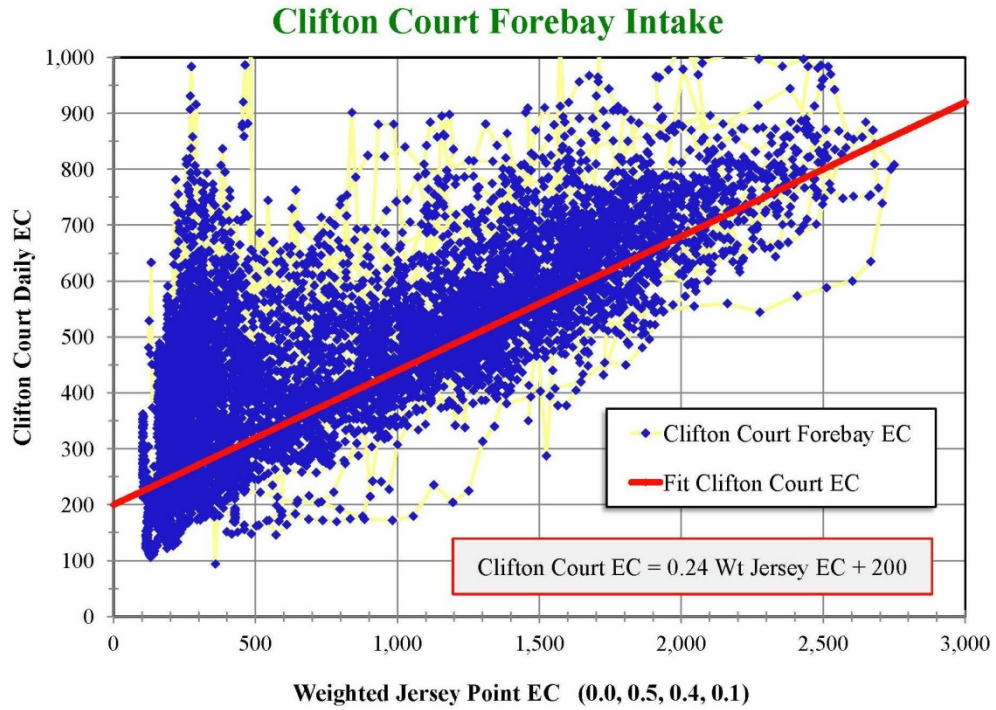


Figure 9-7: Comparison of the entrance to Clifton Court Forebay EC with weighted Jersey Point EC (1964-2012 data). The seawater-dominated relationship (red line) can be used to estimate the seawater contribution at Clifton Court.

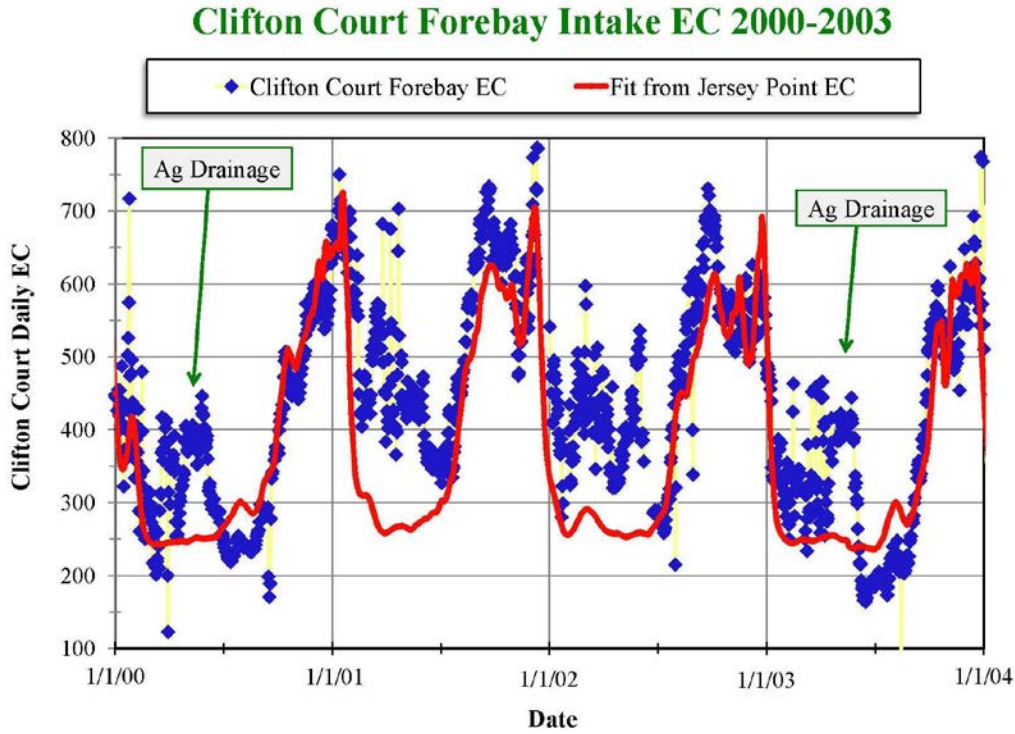


Figure 9-8: Comparison of estimated Clifton Court EC due to seawater intrusion with measured EC data (2000 – 2003).

Figure 9-9 shows the corresponding grab sample chloride concentrations at Clifton Court for the same period shown in Figure 9-8. These chloride data are compared with the regression equation estimates from grab sample EC when seawater dominates and when agricultural drainage dominates. As is apparent from Figure 9-8, seawater intrusion tends to dominate from August through December and agricultural drainage tends to dominate February through June.

The transition from seawater-dominated to agricultural drainage-dominated occurs over one or two months, typically starting in January. The transition from agricultural drainage-dominated back to seawater-dominated is generally very quick and starts from a point where salinities are very low.

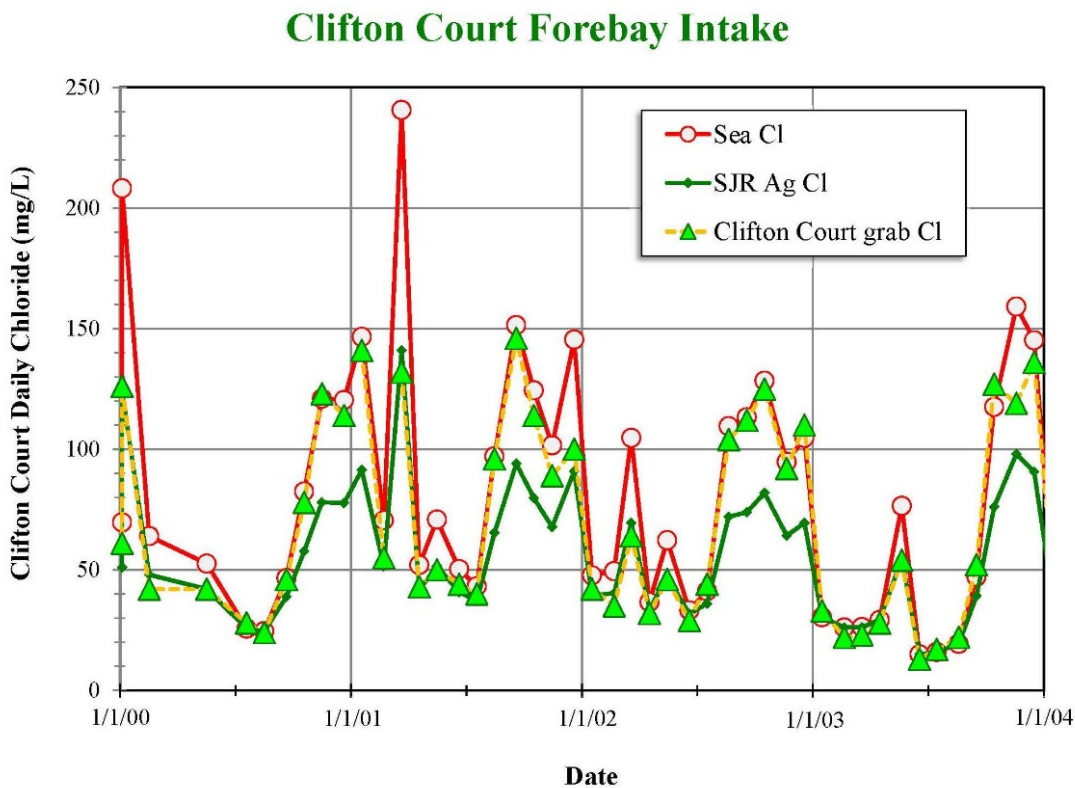


Figure 9-9: Comparison of Clifton Court grab sample chloride data with calculated seawater- and agricultural drainage-dominated chloride concentrations (2000 – 2003).

Predictions of when seawater intrusion dominates on Middle River at Victoria Canal using Jersey Point EC are less accurate, because of the extra distance from the ocean, but still useful. Figure 9-10 shows the agreement between daily Middle River at Victoria Canal EC and the corresponding daily EC data at Jersey Point (with a suitable weighting function).

The resulting predictions for the variation in Middle River EC as a function of time for the period January 2006 through December 2010 is shown in Figure 9-11. Because this location is much closer to the San Joaquin River at Vernalis, and is in an irrigated agriculture area, agricultural drainage makes a large contribution to the measured EC values.

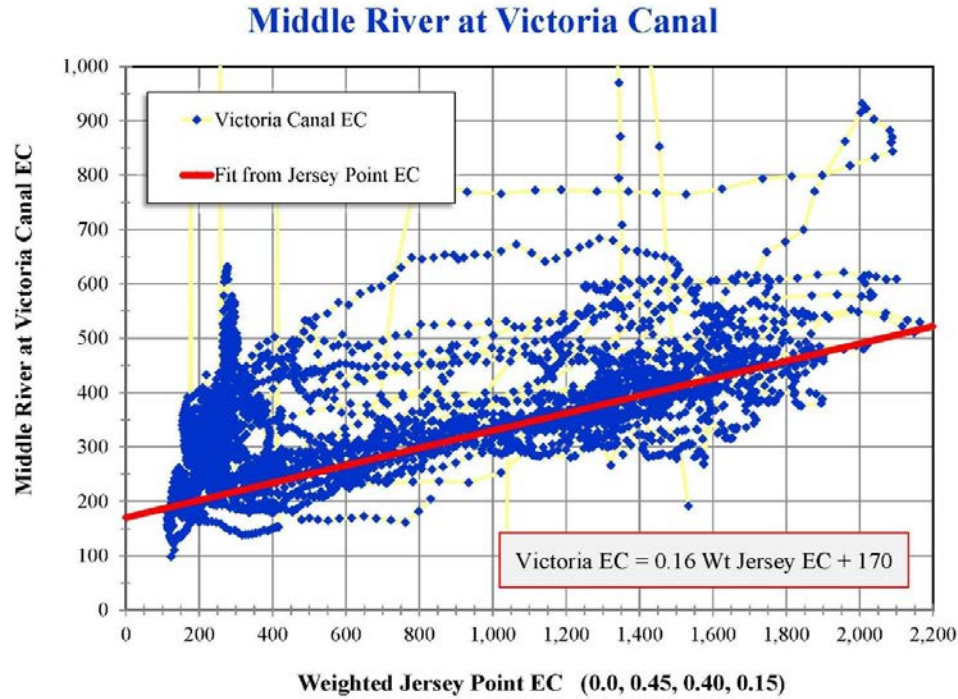


Figure 9-10: Comparison of historical Middle River at Victoria Canal EC data with weighted Jersey Point EC (1999-2012 data). The seawater-dominated relationship (red line) can be used to estimate the seawater contribution at Victoria Canal.

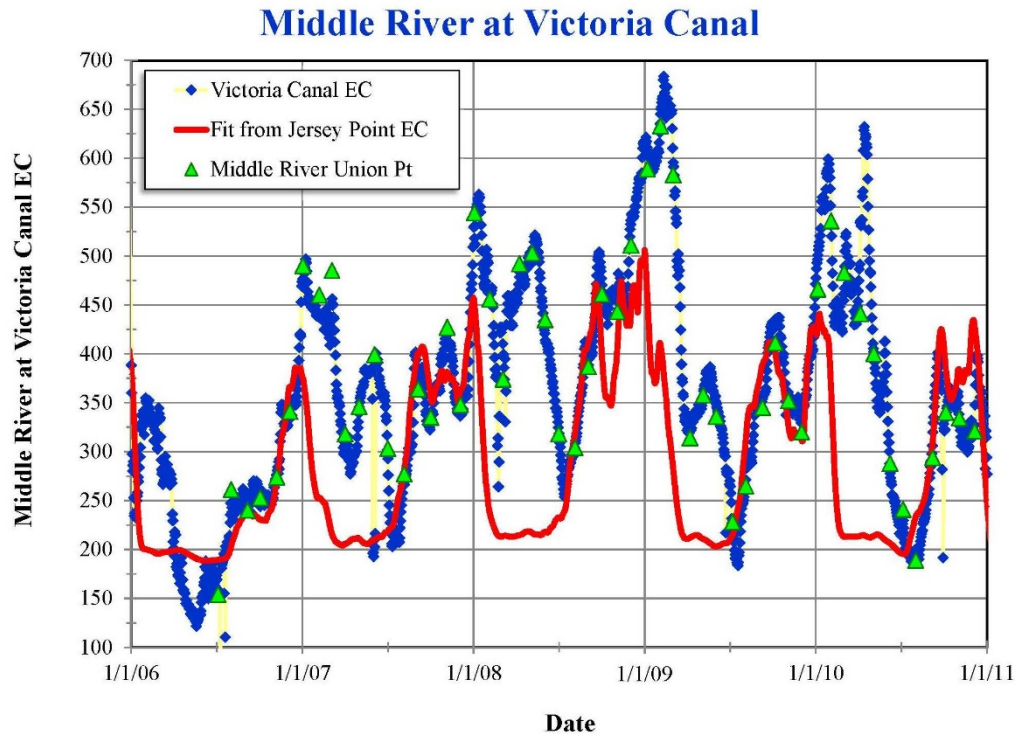


Figure 9-11: Comparison of estimated Victoria Canal EC due to seawater intrusion with measured continuous EC and grab sample EC data (2006 – 2010).

Figure 9-12, shows the corresponding chloride concentration grab sample data for the same period of time (January 2006 through December 2010). During July-December seawater dominates. During March-June, agricultural drainage tends to dominate. The transition period when the chloride data lie between the two regression equations occurs during January and February.

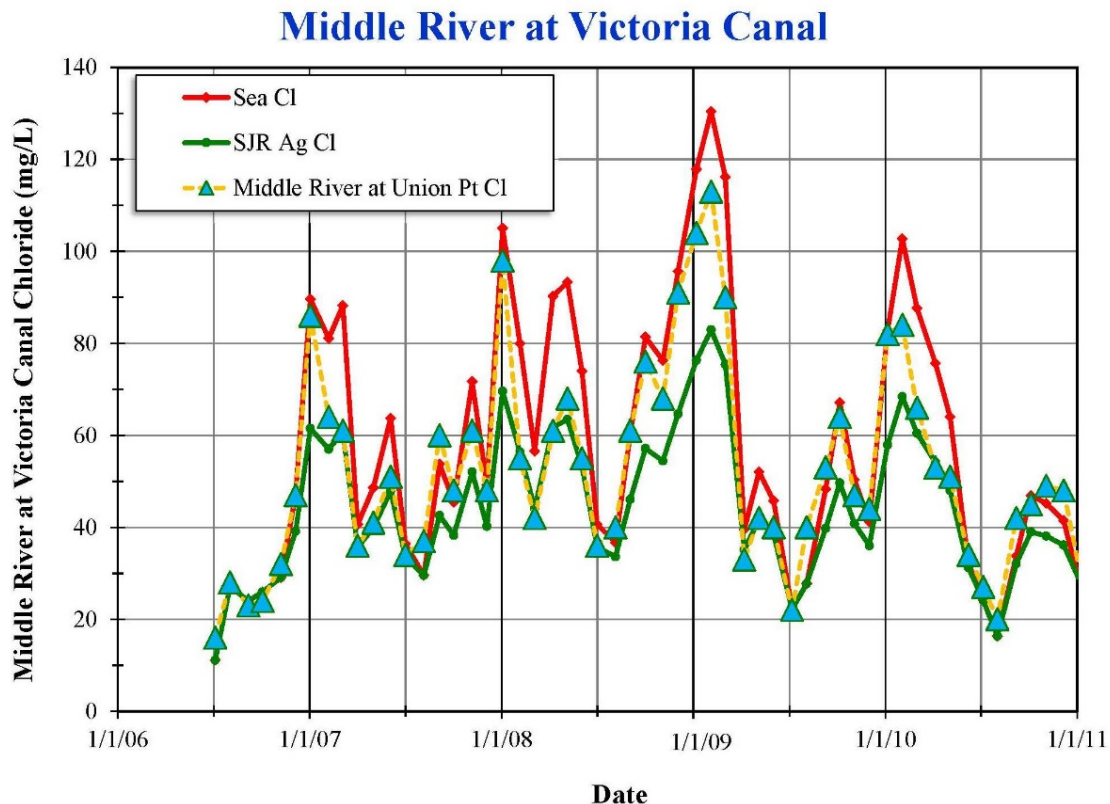


Figure 9-12: Comparison of Victoria Canal grab sample chloride data with calculated seawater- and agricultural drainage-dominated chloride concentrations (2006 – 2010).

When the task is to predict chloride, calcium, sulfate or other water quality constituents from simulated DSM2 EC data, the corresponding Jersey Point EC will also be available. As shown in Appendix F, the relationship between the DSM2 EC at a given location and weighted DSM2 Jersey Point EC may be different than the corresponding equation derived from field measurements.

9.5 Estimate Jersey Point EC and seawater EC from antecedent Delta outflow

In cases where Jersey Point EC data are missing or not available, they can be estimated using a salinity-outflow model such as CCWD's G-Model (Denton, 1993; Denton and Sullivan, 1993). If there are only a few missing data, they can be estimated by correlating with EC data from a nearby station such as Blind Point or Mallard Island (Chippis Island).

9.6: Estimate seawater EC from typical monthly and water year variations.

As discussed above, the seawater contribution to EC at a given interior Delta location can be estimated using known EC data at Jersey Point. However, this approach is relatively complicated. A simpler method is to estimate the contribution from seawater based on the typical contribution by month and water year type. Seawater intrusion into the interior Delta is typically significant during July through December and is minimal after periods of higher outflow (typically January through June). However, during dry or critical water years, the period of seawater intrusion can be longer. Similarly, during very wet years, such as 1983, seawater intrusion can be minimal all year.

Estimating seawater EC based on typical contribution by month and water year type assumes that intra- and inter-annual variability in upstream hydrology is the dominant factor in determining the relative contribution of seawater intrusion and agricultural drainage in the interior Delta. While upstream hydrologic variability has played a dominant role in historically observed contributions, other factors have contributed as well. For example, changes in upstream and Delta water project operations (due to changing regulatory environments and changing export water demands) have affected the pattern of seawater intrusion. Similarly, topographic and bathymetric changes (such as permanent Delta island flooding and ship channel dredging) have affected the pattern of seawater intrusion. Temporary barriers have been installed during drought periods to protect water quality in the central and south Delta. Actions to reduce agricultural drainage impacts (e.g. the San Joaquin Valley westside drainage project and CCWD's Veale Tract project) have reduced the contributions of drainage at interior Delta locations. Given these changes over time, a simple look up table for the seawater EC ratio as a function of month and water year index will not always be applicable over the entire period when grab sample data are available, i.e., 1950 through 2014.

A simple method for estimating the contribution to EC from seawater was developed that is analogous to how the SWRCB Spring X2 standards were set. In that case, the number of days that X2 was achieved at Port Chicago and Mallard Slough historically was determined for each month, February through June. The numbers of days were then plotted as a sliding scale function of the Sacramento 40-30-30 water year index and fitted with a logistic function¹.

For this method, the ratio of seawater EC to total EC was plotted as a different function of the Sacramento Valley 40-30-30 index for each month and fitted to a logistic function. The data follow the expected trend of minimal seawater intrusion when it is a very wet year (i.e., seawater EC / total EC = 0) and relatively large contribution from seawater intrusion in critically dry years (i.e., seawater EC / total EC = 0.8 or higher).

The data are not perfectly correlated. A given water year may have most of the storms in, say February and March, and another water year (with a similar 40-30-30 index) may have most of the storms in, say, December and January. The logistic fit represents the typical trend. Knowing

¹ The logistic functions or S-curves for the Spring X2 standards asymptote to zero days if the water year index became very low (critical years) and asymptote to the maximum of 28-31 days per month if the water year index became very large (wet years). For more information on logistic functions see, e.g., http://en.wikipedia.org/wiki/Logistic_function.

the official or estimated 40-30-30 index, the typical percentage of seawater can be determined for an EC or TDS on a given date (i.e., month) and used to calculate the corresponding chloride, calcium, sulfate concentration, etc.

DSM2 fingerprint data from a historical simulation run (e.g., 1976-2010) was also be used to “inform” the calibration of the logistic curves for the seawater EC ratio versus Sacramento 40-30-30 water year index. Figure 9-13 shows the ratio of the seawater contribution to the total EC as a function of Sacramento Valley 40-30-30 Water Year Index from a DSM2 historical fingerprint study. The data for September for Middle River at Victoria Canal show how the contribution from seawater decreases in the Water Year Index increases. The full data set is for 1976 through 2009. The data trend for the more recent period, 1996-2009, is similar to the earlier data trend, in this example.

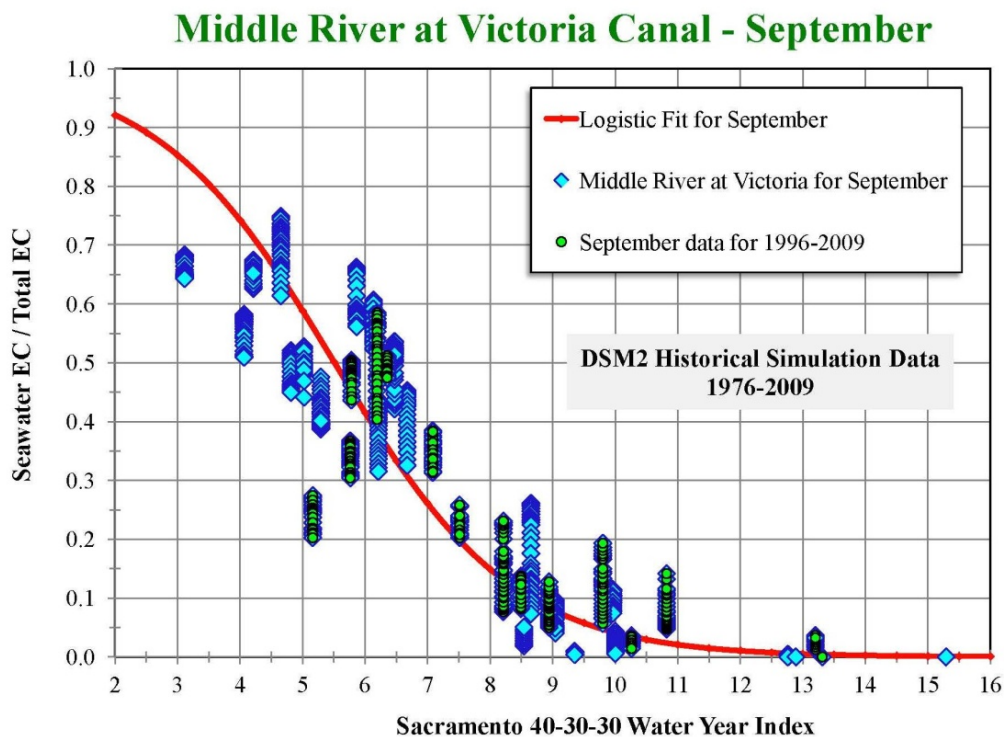


Figure 9-13: Variation of the ratio of seawater EC to total EC for Middle River at Victoria Canal with water year type for the month of September. These daily data are from a DSM2 historical fingerprint study (1976-2009).

The logistic equation used for these examples takes the form

$$\text{Seawater EC Ratio} = 1.0 - 1.0 / (1 + B * \text{EXP}(-C*(X - M)))$$

where X is the Sacramento 40-30-30 Water Year Index, and B, C and M are calibration coefficients. For the logistic curve in Figure 9-15, B = 0.5, C = 0.7 and M = 6.5.

Figure 9-14 shows the corresponding Middle River fingerprint data for the month of July. The amount of seawater intrusion is typically less in July than in September. In this case, the seawater contribution for the period since the SWRCB 1995 Water Quality Control Plan (1996-

2009) appears to have decreased relative to the earlier period (1976-2009). The logistic equation coefficients for Figure 9-14 are $B = 0.5$, $C = 1.0$ and $M = 5.5$.

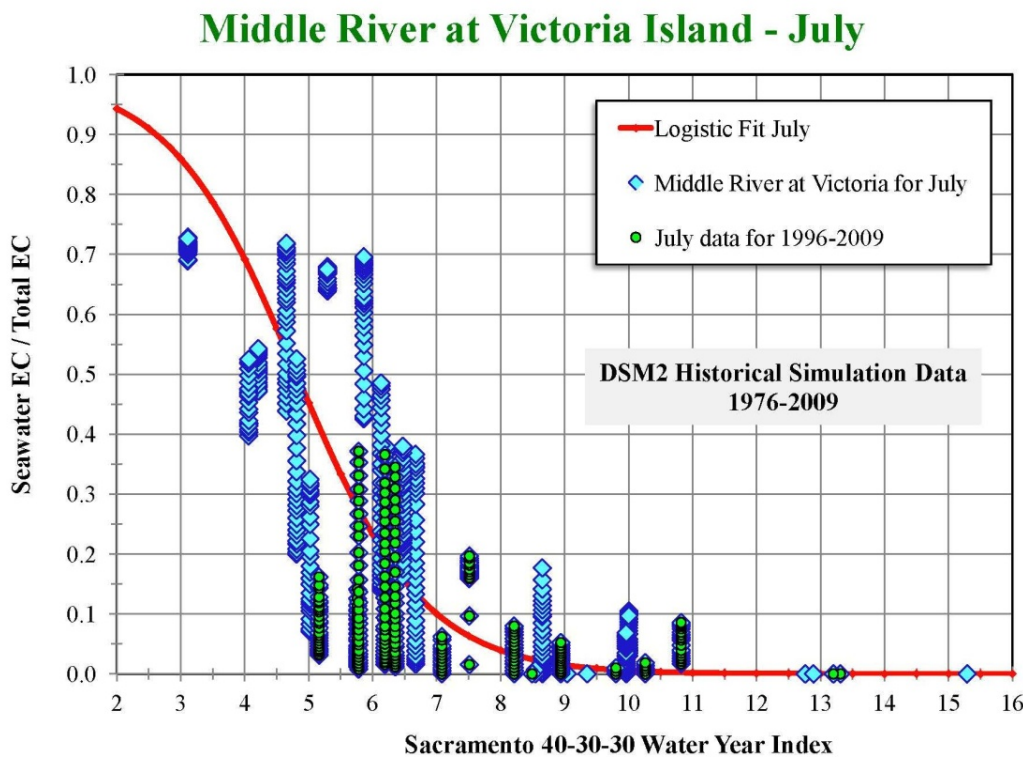


Figure 9-14: Variation of the ratio of seawater EC to total EC for Middle River at Victoria Canal with water year type for the month of July. These daily data are from a DSM2 historical fingerprint study (1976-2009).

Note that the seawater ratio generally remains less than 1.0 even when salinities are relatively high due to seawater intrusion. For example, the maximum chloride concentrations for grab samples from Clifton Court are usually less than 200 mg/L ($EC \approx 870 \mu\text{S}/\text{cm}$). The point of intersection of the EC to chloride regression equations for seawater and agricultural drainage is 282 $\mu\text{S}/\text{cm}$, i.e., there is a background contribution to EC from local and San Joaquin agricultural drainage of about 282 $\mu\text{S}/\text{cm}$. The seawater EC to total EC ratio when chlorides would be considered high (200 mg/L) and seawater intrusion would be significant is still only 0.68.

These fingerprint data can only be used to quantify the logistic equation coefficients in cases where the agreement between DSM2 modeling data and historical data is good.

Figure 9-15 shows fingerprint data for the intake to Clifton Court Forebay from a DSM2 historical simulation for the month of August. In this case, the data are monthly averages rather than daily values. The seawater EC ratios for three different historical periods are plotted. Even though the operating rules for SWRCB standards governing Bay-Delta operations changed during this time (1975-2010), especially as a result of SWRCB Bay-Delta Water Quality Control Plan (May 1995) and corresponding Water Rights Decision 1641 (March 2000), there do not seem to be obvious differences in the variations with water year type between the three periods

in this historical simulation. This warrants further investigation because changes in Delta outflows since Decision 1641 would be expected to change the amount of seawater intrusion into the Delta in August. The historical changes in Delta salinity are analyzed in detail in Contra Costa Water District (2010). The logistic equation coefficients for Figure 9-15 are $B = 0.5$, $C = 0.7$ and $M = 7.5$.

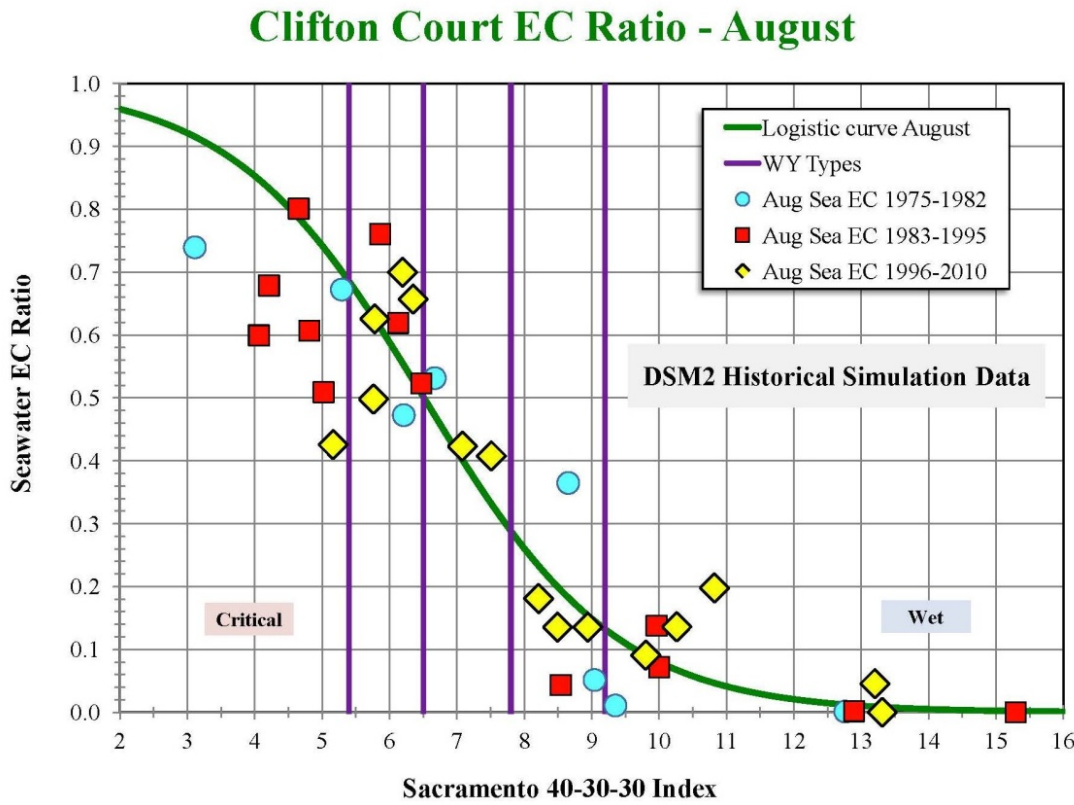


Figure 9-15: Variation of the ratio of seawater EC to total EC for the intake to Clifton Court Forebay with water year type for the month of August. These daily data are from a DSM2 historical fingerprint study (1976-2009).

Figure 9-16 shows the corresponding fingerprint data for Clifton Court Forebay for the month of March. Seawater intrusion is much less than for August. Seawater intrusion is essentially zero for all water year types except critical years. There is again no clear difference between the seawater EC ratios for the three different historical periods plotted. The logistic equation coefficients for Figure 9-16 are $B = 0.5$, $C = 1.8$ and $M = 4.5$.

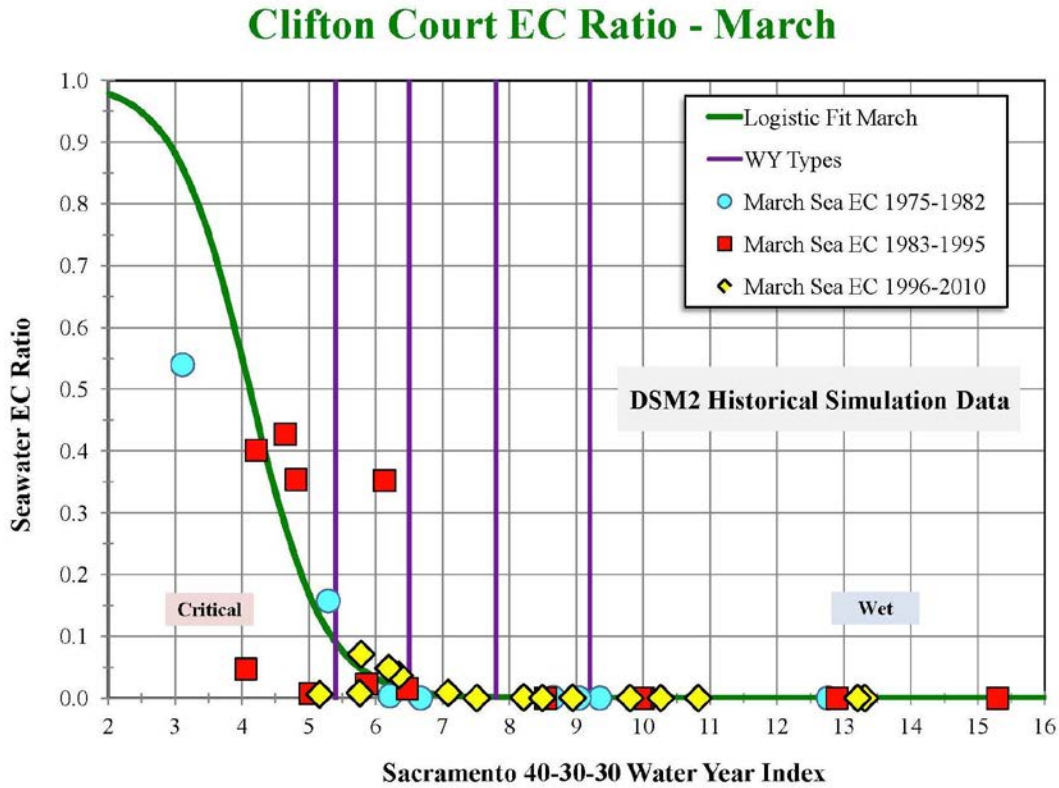


Figure 9-16: Variation of the ratio of seawater EC to total EC for the intake to Clifton Court Forebay with water year type for the month of March. These daily data are from a DSM2 historical fingerprint study (1976-2009).

Figure 9-17 shows the variation of seawater EC ratios from historical grab sample data from the intake to Clifton Court Forebay in September. These ratios were derived from pairs of grab sample data, i.e., EC and chloride, EC and calcium, and EC and sulfate. All three estimates are plotted. Because changes in the Delta operating rules over time may affect the amount of seawater intrusion into the Delta, only grab sample data collected since the 1995 Water Quality Control Plan are plotted in Figure 9-17. There were no data for the period 1996-1999 in this particular data set. The logistic equation coefficients for Figure 9-17 are $B = 0.5$, $C = 1.0$ and $M = 7.5$.

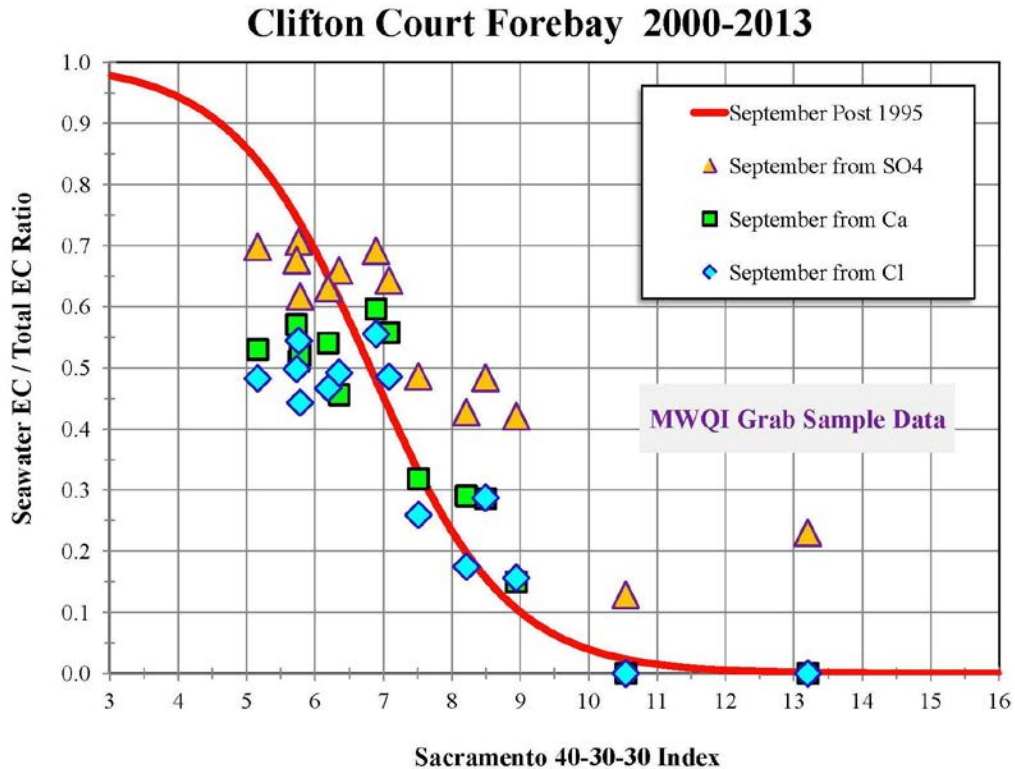


Figure 9-17: Variation of the seawater EC ratio derived from historical September grab sample data from the intake to Clifton Court Forebay for years 2000 through 2013. These are data collected since the 1995 SWRCB Water Quality Control Plan. These data represent the effect of more recent operations with Spring X2 and the biological opinions.

Figure 9-18 shows the variation of seawater EC ratios from historical grab sample data from the intake to Clifton Court Forebay for the month of July. As was the case with Figure 9-17, these ratios were derived from pairs of grab sample data, i.e., EC and chloride, EC and calcium, and EC and sulfate. Only grab sample data collected since the 1995 Water Quality Control Plan are plotted, i.e., 2000-2013. The logistic equation coefficients for Figure 9-18 are $B = 0.5$, $C = 0.7$ and $M = 5.5$.

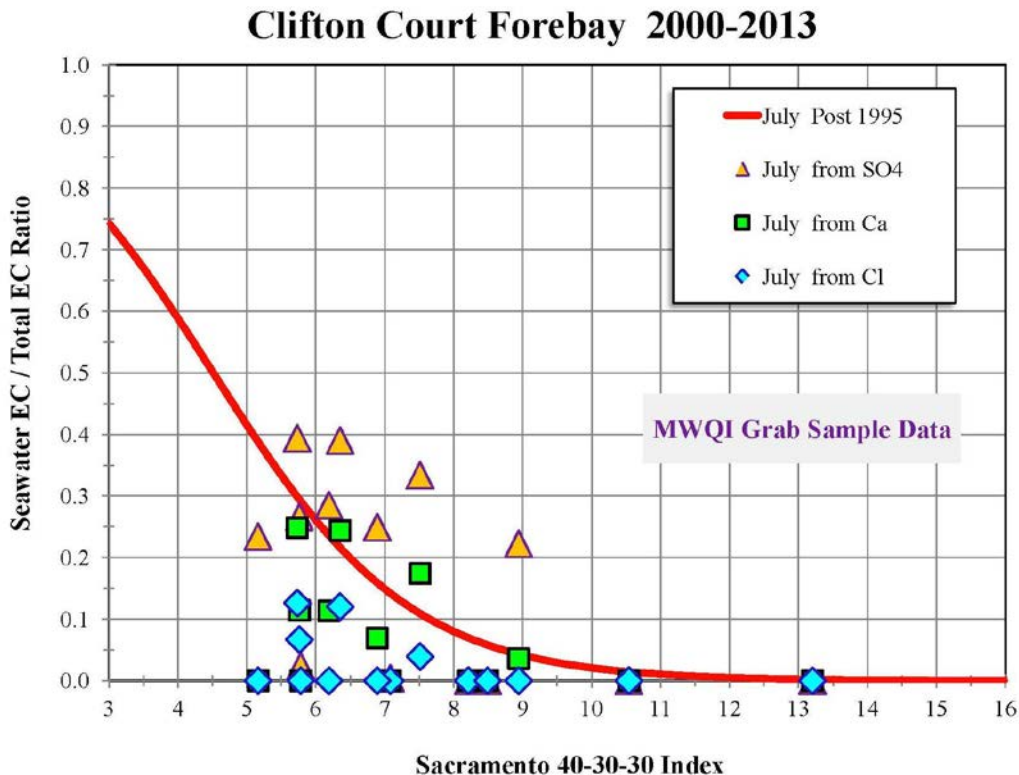


Figure 9-18: Variation of the seawater EC ratio derived from historical July grab sample data from the intake to Clifton Court Forebay for years 1983-1994. These are data collected before the 1995 SWRCB Water Quality Control Plan. These data represent the effect of Delta operations before Spring X2 and the biological opinions.

Seawater intrusion is less in July than in September. The estimates based on sulfate are also much higher than for calcium and chloride. A lookup table relating the seawater EC ratio to month and water year index will not be very accurate during transition months such as June-July and January-February. However, even approximate estimates of the contribution of seawater to total specific conductance will be useful when estimating the water quality constituent concentrations from EC (or TDS).

9.7: Estimating Contribution from San Joaquin EC

Montoya (2004) observed that when San Joaquin flow at Vernalis was above 7,400 cfs, the water at Clifton Court Forebay was mostly from the San Joaquin River. Similarly, the water at the Jones Pumping Plant at the intake to the DMC was almost all San Joaquin River water when Vernalis flow exceeded 3,400 cfs. This is consistent with the fact that seawater intrusion is very small during wet periods (when the runoff from the Sacramento and San Joaquin Rivers are typically both high).

Figure 9-19 shows DSM2 fingerprint EC data for the intake to Clifton Court Forebay for a historical simulation. The ratio of San Joaquin source water EC as ratio of total EC is plotted as a function of San Joaquin inflow at Vernalis. The data show some scatter but the predominant

trend is that the percentage of San Joaquin River water increases as Vernalis flow increases eventually increasing to 100%. The outlier data points that show lower ratios even at high Vernalis flows correspond to days when the DSM2 model predicts zero seawater intrusion, no Sacramento and eastside source water, but a large contribution from local drainage.

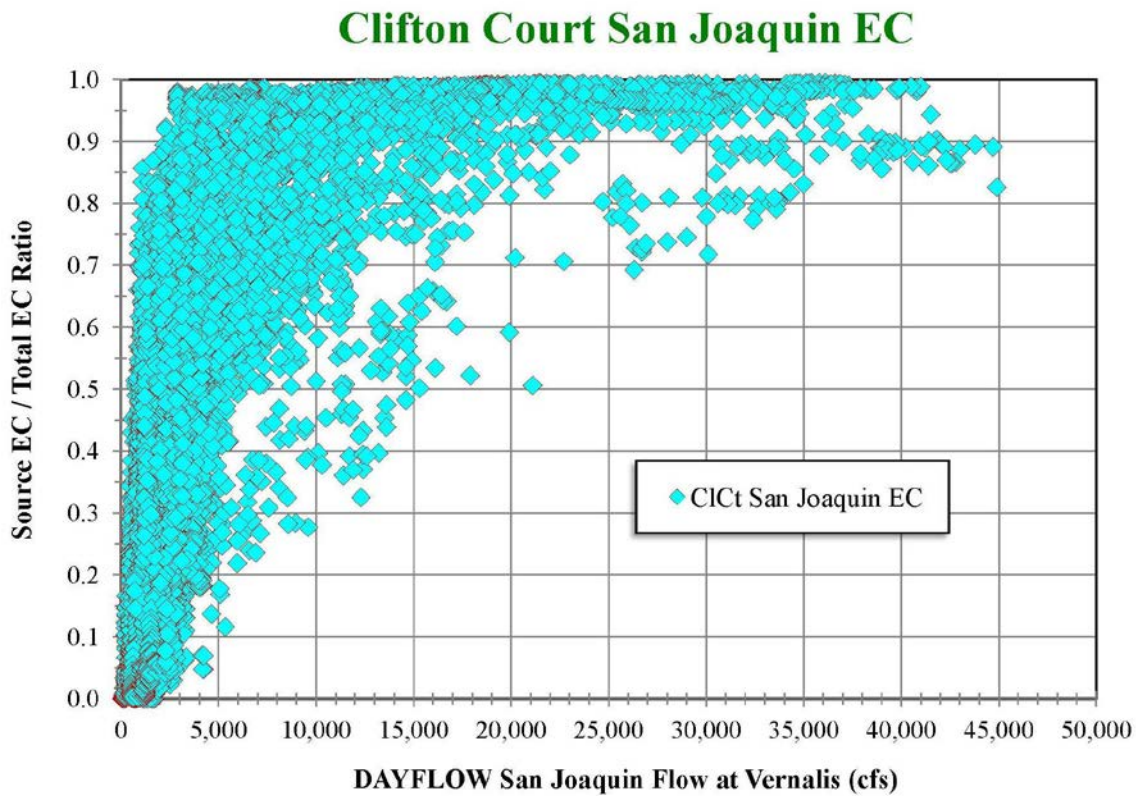


Figure 9-19: Ratio of San Joaquin source EC to total EC for the intake to Clifton Court Forebay as a function of San Joaquin River flow at Vernalis. The data are from a historical DSM2 fingerprint study.

The relationship between Vernalis flow and the amount of San Joaquin source water at Clifton Court and other central and south Delta stations only provides information about one source of agricultural drainage (San Joaquin River) but not the amount of local drainage. It is not possible to estimate the additional contribution from seawater intrusion from the information in Figure 9-19.

10. Conclusions

Grab sample water quality data collected from the Sacramento-San Joaquin Delta by the California Department of Water Resources, the U.S. Bureau of Reclamation, and other agencies since the 1950s provide valuable information regarding the effect of different sources of water on Delta water quality. These grab sample data were used to develop relationships between the key indicators of salinity, i.e., specific conductance (EC) and total dissolved solids (TDS), and other water quality constituents such as chloride, bromide, sodium, calcium, sulfate, hardness and alkalinity.

In the western Delta and San Francisco Bay, the regression equations are consistent with that of seawater-dominated water. In the northern Delta, inflows from the Sacramento and Mokelumne Rivers play a significant role in determining water quality and seawater intrusion only makes a contribution during major drought situations like 1976-1977. In the south and central Delta near major drinking water intakes, the regression equations depend upon the particular mixture of seawater and agricultural drainage from the San Joaquin River and Delta islands. Seawater intrusion generally shows a seasonal dependence with periods of low flow, high seawater intrusion, in the late summer and fall. However, in wet years, Delta outflows can be high throughout the year (e.g., 1983). In some critical years, Delta outflows can remain low during the winter months.

It is not always correct to assume a seawater-dominated equation applies during August through December and an agricultural drainage-dominated regression applies for the rest of the year. If there has been high Delta outflow for the past few months, the influence of seawater intrusion will be small. High Delta outflows typically occurs in December through March, but in drier years Delta outflows will be low even in winter and seawater intrusion can dominate in all months of the year.

A direct method for computing the contribution of seawater in the interior Delta is to estimate the EC (or TDS) due to seawater intrusion from the salinity at Jersey Point in the western Delta. These Jersey Point data are typically available from continuous field measurements of EC. Where there are gaps, the Jersey Point EC can be estimated from DAYFLOW Delta outflow estimates using a salinity-outflow relationship like CCWD's G-Model (Denton, 1993).

Once the contribution by seawater intrusion to total EC is determined, the seawater component of EC can be used to estimate the seawater component of a given water quality constituent using the applicable seawater-dominated regression equation and the remaining water quality constituent can be estimated from the remaining EC using the agricultural drainage-dominated regression equations.

When estimating water quality constituent concentrations from output from a Delta simulation model run, in the form of, say, EC, the simulation model output for Jersey EC can be used to estimate seawater EC at a given location. If fingerprint simulation data, e.g., from DWR's DSM2 model, are available that quantify the volumes of water from individual sources, those volumetric data can be used to separately compute the contributions from seawater and agricultural drainage.

The accuracy of estimates based on water quality simulation model output will of course depend on the ability of the model to accurately represent the advection and dispersion of seawater from the ocean through Suisun Bay to the central and south Delta. An indication of the accuracy of a water quality simulation model can be gained by comparing the relationship between field seawater EC from historical Jersey Point field EC data, and estimates of seawater EC based on simulation model output. The ability of the water quality model to simulate local sources of agricultural drainage will also affect the subsequent estimates of other constituents such as chloride, calcium, sulfate, etc.

In cases where both EC (or TDS) and chloride concentration grab sample data are available, those data can be used to back-calculate the percentage of EC from seawater. The corresponding calcium, sulfate and other constituent concentrations can then be estimated from this estimate of seawater EC. However, this method is not as general as using Jersey Point EC.

Acknowledgements

This work was funded through a contract with the State Water Project Contractors Authority. The author wishes to thank Elaine Archibald and Paul Hutton, as well as the members of the Municipal Water Quality Investigation technical advisory committee for their detailed reviews of the draft of this report.

About the Author

Richard Denton is a water resources consultant who has worked on issues related to San Francisco Bay and Delta since 1982. He was previously Water Resources Manager for Contra Costa Water District, Concord, California (1989–2006). From 1982-1989, he was on the Civil Engineering faculty of the University of California at Berkeley. Richard provided key input to the environmental and water rights permitting for CCWD's Los Vaqueros Project and the development of the 1994 Bay-Delta Accord. In 1995, he received the first annual Hugo B. Fischer Award from the California Water and Environmental Modeling Forum in recognition of his development and innovative application of a salinity-outflow model for the Sacramento-San Joaquin Delta. In 2010, he received a Career Achievement Award from the Modeling Forum. Dr. Denton received a Ph.D. in Civil Engineering from the University of Canterbury, Christchurch, New Zealand, in 1978. He is a Registered Civil Engineer in the State of California.

11. List of References

California Urban Water Agencies (1995), *Study of Drinking Water Quality in Delta Tributaries*. Report prepared by Brown and Caldwell, Archibald & Wallberg Consultants, Marvin Jung & Associates, and McGuire Environmental Consultants, Inc., May 1995

http://www.calwater.ca.gov/Admin_Record/D-036862.pdf	Executive Summary
http://www.calwater.ca.gov/Admin_Record/D-036738.pdf	Bromide v EC
http://www.calwater.ca.gov/Admin_Record/D-036739.pdf	Sulfate v EC
http://www.calwater.ca.gov/Admin_Record/D-036740.pdf	TDS v EC
http://www.calwater.ca.gov/Admin_Record/D-036741.pdf	Cl v EC
http://www.calwater.ca.gov/Admin_Record/D-036742.pdf	14-day Cl v EC at Rock Slough

Contra Costa Water District (2010), *Historical Fresh Water and Salinity Conditions in the Western Sacramento-San Joaquin Delta and Suisun Bay – A summary of historical reviews, reports, analyses and measurements*. Technical Memorandum WR10-001, Water Resources Department, CCWD, February 2010.

<http://www.ccwater.com/salinity/HistoricalSalinityReport-2010Feb.pdf>

Contra Costa Water District, City of Stockton, and Solano County Water Agency (2005), CALFED Draft Final Report, *Delta Region Drinking Water Quality Management Plan*. Prepared by Montgomery Watson Harza. June 2005.

<http://www.ccwater.com/files/DeltaRegion.pdf>

Denton, Richard A. (1993), *Accounting for Antecedent Conditions in Seawater Intrusion Modeling - Applications for the San Francisco Bay-Delta*. Hydraulic Engineering 93, Volume 1, pp. 448-453, Proceedings of ASCE National Conference on Hydraulic Engineering, San Francisco, July 1993.

Denton, Richard and Greg Sullivan (1993), *Antecedent flow-salinity relations: Application to Delta planning models*. Contra Costa Water District report, December 1993.

http://www.waterboards.ca.gov/waterrights/water_issues/programs/bay_delta/deltaflow/docs/exhibits/ccwd/spprt_docs/ccwd_denton_sullivan_1993.pdf

Guivetchi, Kamyar (1986), DWR Interoffice Memo, *Salinity unit conversion equations*

<http://www.water.ca.gov/suisun/facts/salin/index.cfm>

Hem, John D. (1985), *Study and interpretation of the chemical characteristics of natural water*: U.S. Geological Survey Water-Supply Paper 2254, 264 p.

<http://pubs.usgs.gov/wsp/wsp2254/html/pdf.html>

Hutton, Paul (2006), *Validation of DSM2 Volumetric Fingerprints Using Grab Sample Mineral Data*, Power Point presentation at CWEMF Annual Meeting, March 2006

<http://www.cwemf.org/Asilomar/PaulHuttonPresentation.pdf>

Jung, Marvin (2000), *Revision of Representative Delta Island Return Flow Quality for DSM2 and DICU Model Runs*. Prepared for the CALFED Ad-Hoc Workgroup To Simulate Historical Water Quality Conditions in the Delta by Marvin Jung and Associates, Inc. Consultant's Report to the Department of Water Resources Municipal Water Quality Investigations Program (MWQI-CR#3), December 2000

http://baydeltaoffice.water.ca.gov/modeling/deltamodeling/models/dicu/DICU_Dec2000.pdf

Kratzer, Charles and Leslie Grober (1991), *San Joaquin River salinity: 1991 projections compared to 1977*. California Agriculture 45(6):24-27, November-December 1991.

<http://californiaagriculture.ucanr.edu/landingpage.cfm?article=ca.v045n06p24&fulltext=yes>

Liu, Siqing and Bob Suits (2012), *Chapter 5: Estimating Delta-wide Bromide Using DSM2-Simulated EC Fingerprints*, in DWR's "Methodology for Flow and Salinity Estimates in the Sacramento-San Joaquin Delta and Suisun Marsh," 33rd Annual Progress Report, June 2012

http://baydeltaoffice.water.ca.gov/modeling/deltamodeling/AR2012/Chapter%205_2012_Web.pdf

Montoya, Barry (2004), DWR Report, *Factors affecting the composition and salinity of exports from the south Sacramento-San Joaquin Delta*.

http://www.water.ca.gov/pubs/waterquality/swp_o_m/swp_o_m/factors_affecting_the_composition_salinity_of_exports_from_the_sacramento-san_joaquin_delta/factors_affecting_the_composition_and_salinity_of_exports_from_delta_2004.pdf

Parvathinathan, Shankar (2012), *Validation of DSM2 QUAL for Simulation of Various Cations and Anions*. Montgomery Watson Harza Americas. Power Point presentation at CWEMF Annual Meeting, April 2012.

http://www.cwemf.org/AMPresentations/2012/DSM2_QUALValidation.pdf

Suits, Bob (2001), DWR Office Memo, *Relationships between EC, chloride, and bromide at Delta export locations*.

http://baydeltaoffice.water.ca.gov/modeling/deltamodeling/models/misc/EC_chloride_bromide_05_29_01.pdf

Suits, Bob (2002), *Chapter 5, Relationships between Delta Water Quality Constituents as derived from Grab Samples*. In DWR's "Methodology for Flow and Salinity Estimates in the Sacramento-San Joaquin Delta and Suisun Marsh." 23rd Annual Progress Report, June 2002.

<http://modeling.water.ca.gov/delta/reports/annrpt/2002/2002Ch5.pdf>

12. Glossary

Br	Bromide
Ca	Calcium
CALFED	A consortium of California and Federal agencies focusing on interrelated water problems in San Francisco Bay and the Sacramento-San Joaquin Delta.
Cl	Chloride
CCWD	Contra Costa Water District
DICU	Delta Island Consumptive Use
DSM2	Delta Simulation Model developed by DWR
DWR	California Department of Water Resources
EC	Specific conductance (electrical conductivity normalized to 25 degrees Centigrade)
EPA	United State Environmental Protection Agency
IDHAMP	Interagency Delta Health Monitoring Program
IEP	Interagency Ecological Program
K	Potassium
Mg	Magnesium
Mn	Manganese
MWQI	Municipal Water Quality Investigation
Na	Sodium
P	Phosphorus
SO4	Sulfate
STORET	STOrage and RETrieval Data Warehouse maintained by U.S. EPA.
SWRCB	California State Water Resources Control Board
TDS	Total Dissolved Solids
USGS	United States Geological Survey
WDL	DWR's Water Data Library
WIMS	Water Information Management System (earlier database maintained by DWR's Information Systems and Services Office)
WQCP	Bay-Delta Water Quality Control Plan

Appendix A**Seawater Boundary Condition**

Seawater from the Pacific Ocean enters San Francisco Bay through the Golden Gate Bridge. The extent to which the seawater intrudes into the Bay and Delta depends in large part upon the net outflow of freshwater from the Delta. When Delta outflows are very low, seawater contributes to the salinity at monitoring stations as far inland as the south Delta.

Regression equations for seawater intrusion were developed from grab samples taken at Mallard Island and Jersey Point. Some data were available further seaward at Martinez, and in San Pablo Bay, but Mallard Island and Jersey Point represented the largest data sets.

Hutton (2006) analyzed grab sample data from Mallard Island and found the following typical distribution of water quality constituents (Table A-1).

Table A-1: Percentages of total dissolved solids for seawater-dominated grab samples

Ion	Symbol	Valence	Percentage of TDS (at high TDS)*
Chloride	Cl	1-	55
Sodium	Na	1+	31
Sulfate	SO ₄	2-	8
Magnesium	Mg	2+	4
Calcium	Ca	2+	1
Potassium	K	1+	1

* High TDS refers to periods at Mallard Island when Delta outflows are low and seawater intrusion dominates. Alternatively, when Delta outflows are high, the salinities at Mallard Island will be very low and the grab samples will have the characteristics of Sacramento River water. High TDS corresponds to TDS > 3,000 mg/L.

As shown in Figures A-1 and A-2, the percentages of TDS are not constant but vary with TDS. Typically, salinity at Mallard Island is highest during periods of low Delta outflow which corresponds to periods when seawater intrusion dominates. During high runoff periods, freshwater from the Sacramento River, San Joaquin River and Delta eastside streams dominates over seawater so the chloride and sodium ratios are much smaller.

Mallard Island and Jersey Point

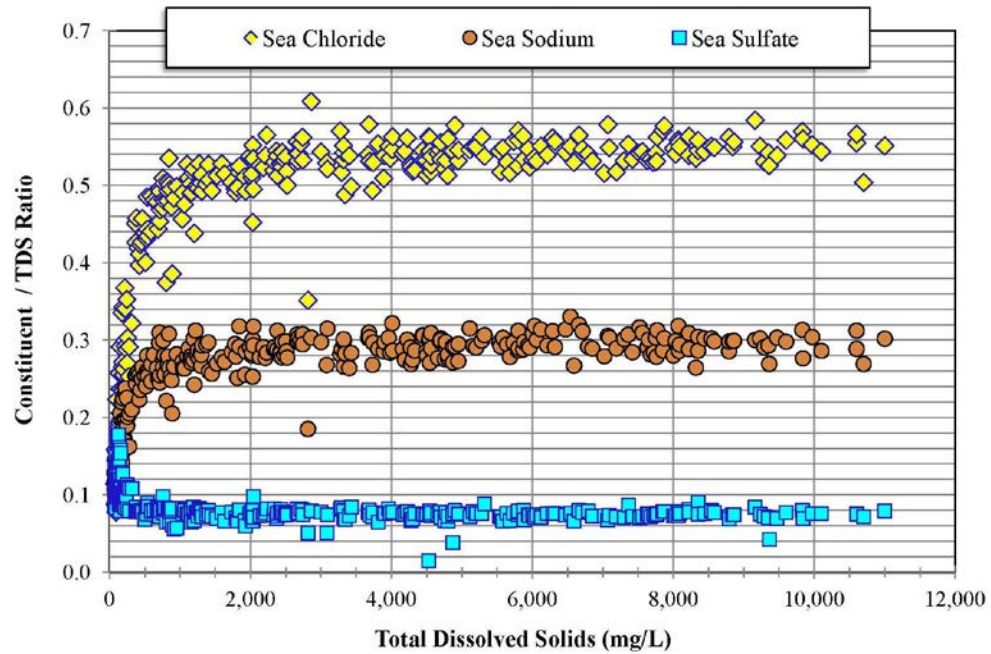


Figure A-1: Variation of chloride, sodium and sulfate ratios of total dissolved solids with TDS at Mallard Island and Jersey Point. These stations represent the seawater source to the Delta.

Mallard Island and Jersey Point

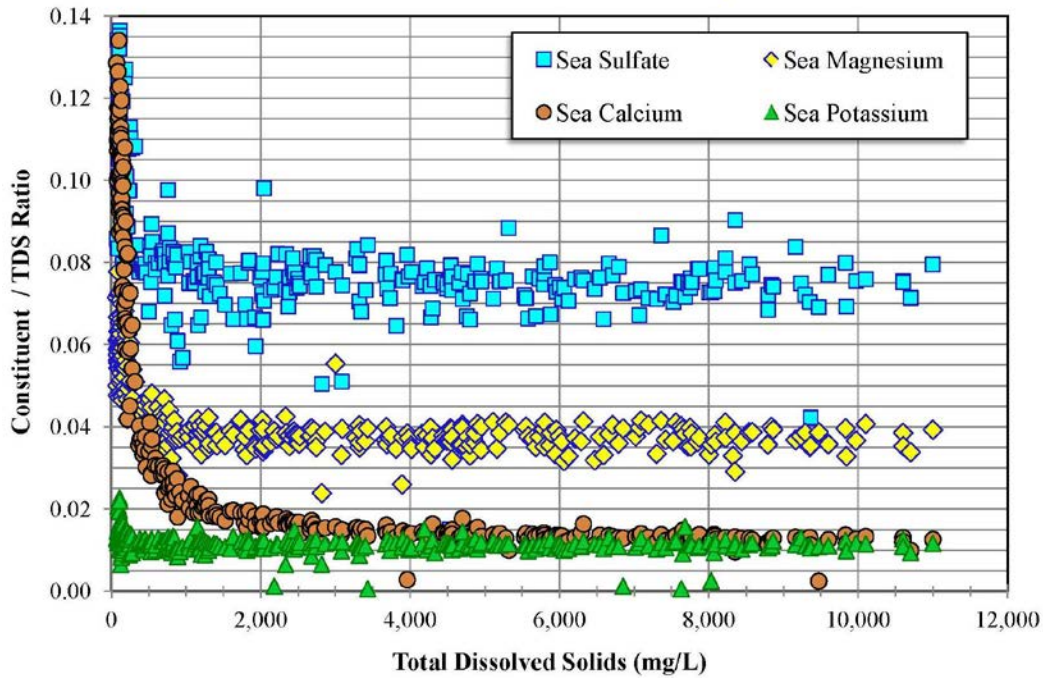


Figure A-2: Variation of sulfate, magnesium, calcium and potassium ratios of total dissolved solids with TDS at Mallard Island and Jersey Point. Sulfate is shown in both Figures A-1 and A-2 to provide a common point of reference over the large range of constituent ratios (0.01 – 0.06).

Because the constituent ratios vary with increasing TDS over this large range of TDS, a simple linear regression is not sufficient to represent the relationship between TDS (or EC) and the individual water quality constituents.

A.1 Variation with Specific Conductance (EC)

Figures A-3, A-4 and A-5 show the variation of chloride concentration with EC at Mallard Island and Jersey Point. Jersey Point data are also plotted because there are insufficient Mallard Island data to fully define the variation with EC and TDS over the lower TDS range of the data.

Subsequent figures, Figures A-6 through A-23 show the corresponding variations of bromide, calcium, sulfate, magnesium, potassium, hardness, alkalinity and total dissolved solids with EC. In each case, the first figure shows Mallard Island and Jersey Point grab sample data (from DWR's Water Data Library¹) for the specific conductance range 260 $\mu\text{S}/\text{cm}$ up to the maximum (about 19,000 $\mu\text{S}/\text{cm}$). In the case of chloride data, additional data from Chipps Island (station D10) were available up to almost 22,000 $\mu\text{S}/\text{cm}$. The second figure for each constituent shows the variation over the lower range of EC to illustrate the variation when Delta outflows are very high and a blend of Sacramento and San Joaquin water dominates. The EC value of 260 $\mu\text{S}/\text{cm}$ is the approximate breakpoint between seawater dominated conditions and Sacramento River dominated conditions.

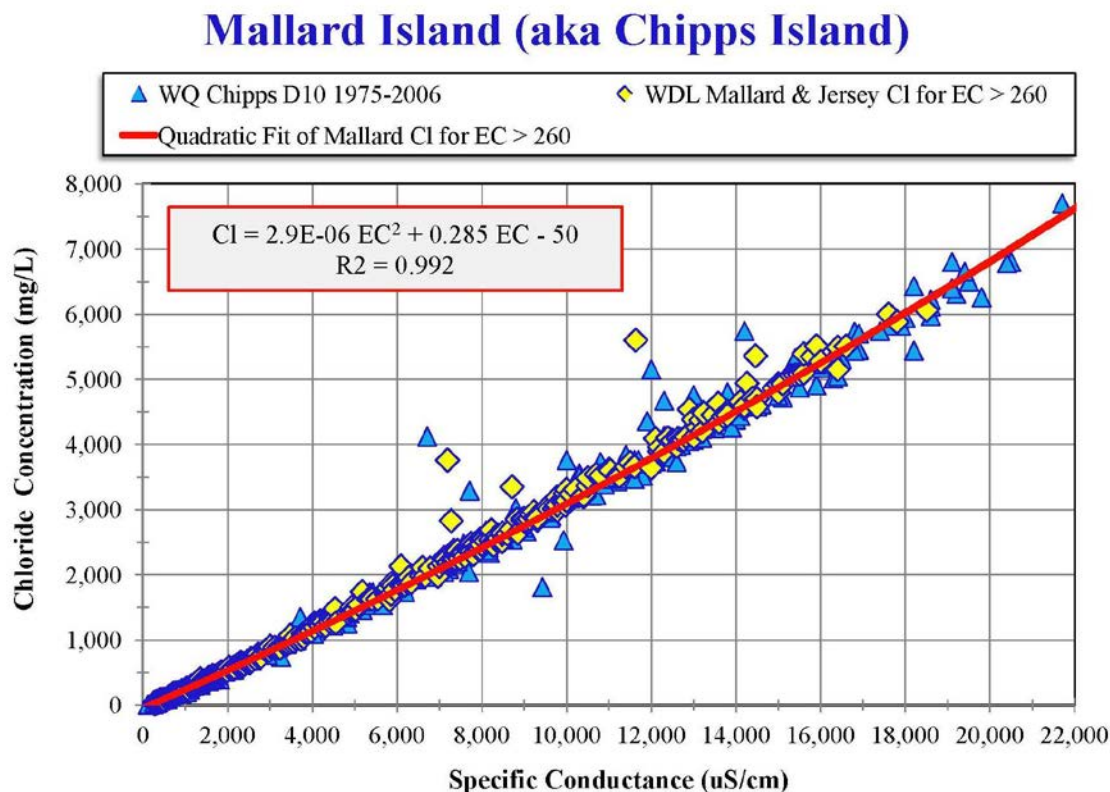


Figure A-3: Variation of chloride (Cl) concentration as a function of specific conductance (EC) at Mallard Island and Jersey Point.

¹ <http://www.water.ca.gov/waterdatalibrary/>

Mallard Island (aka Chipps Island)

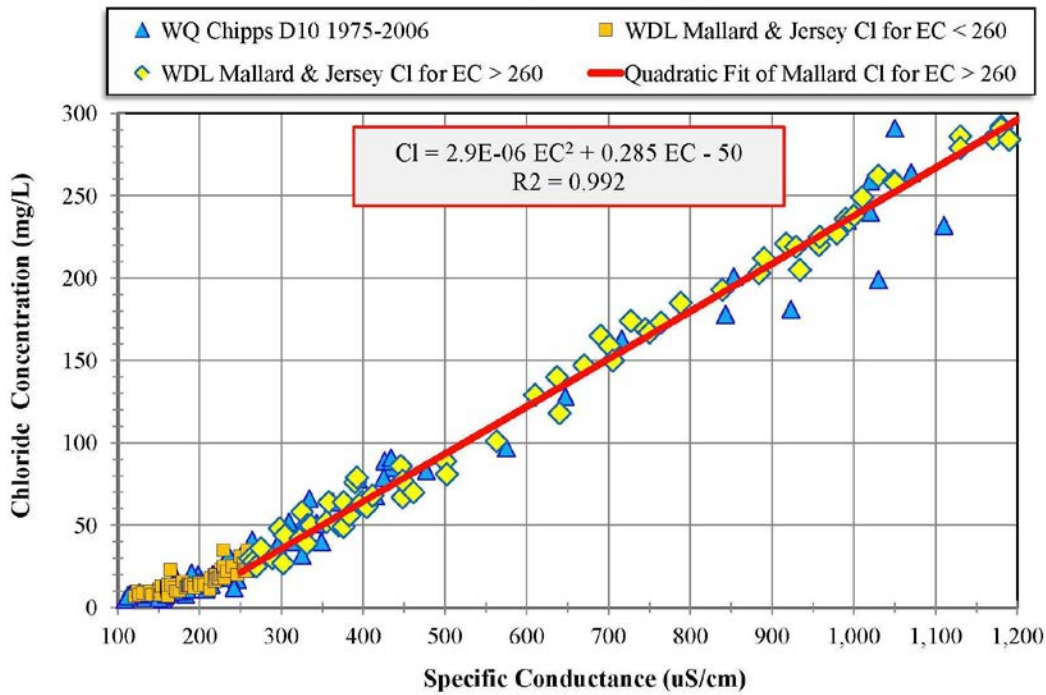


Figure A-4: Variation of chloride concentration as a function of specific conductance (EC) at Mallard Island and Jersey Point for EC < 1,200 $\mu\text{S}/\text{cm}$.

Mallard Island (aka Chipps Island)

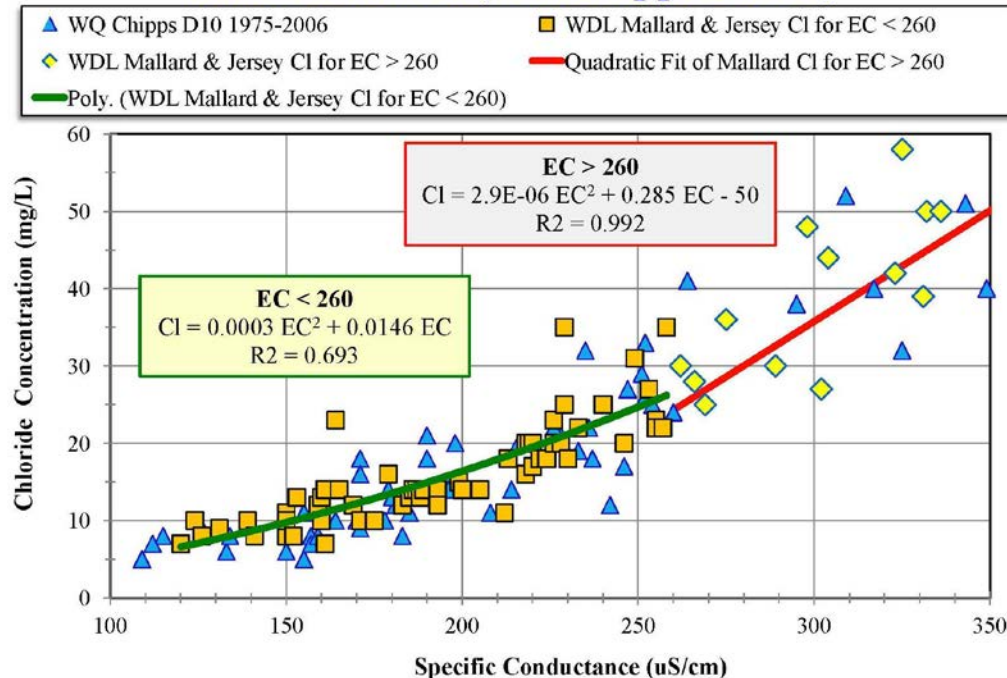


Figure A-5: Variation of chloride concentration as a function of specific conductance (EC) at Mallard Island and Jersey Point for EC < 350 $\mu\text{S}/\text{cm}$.

Mallard Island (aka Chipps Island)

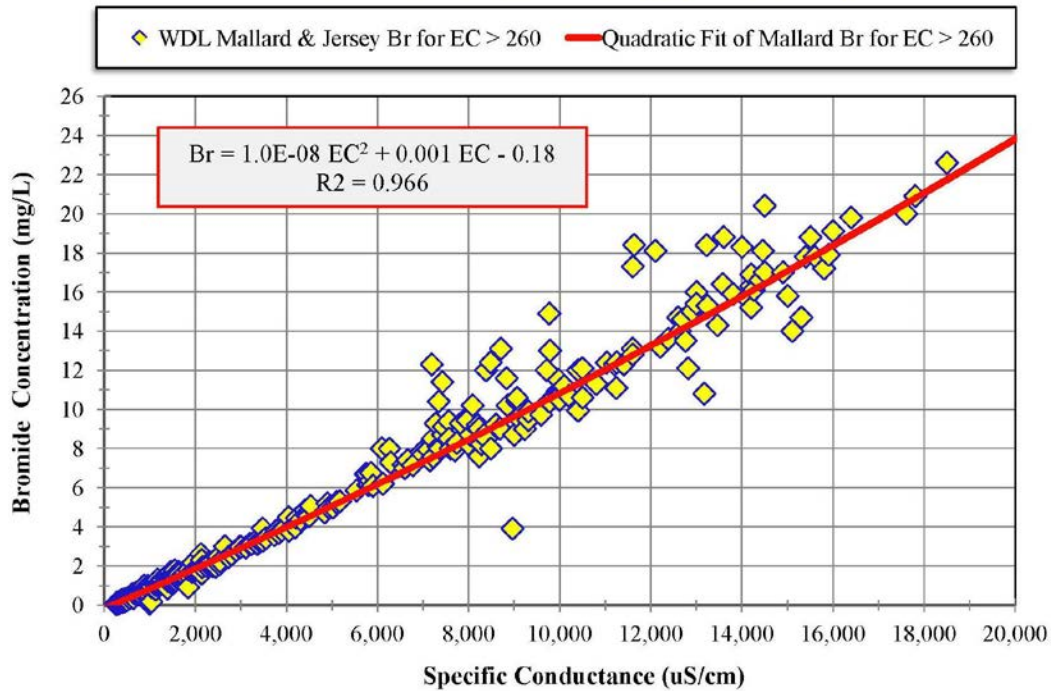


Figure A-6: Variation of bromide (Br) concentration as a function of specific conductance (EC) at Mallard Island and Jersey Point.

Mallard Island (aka Chipps Island)

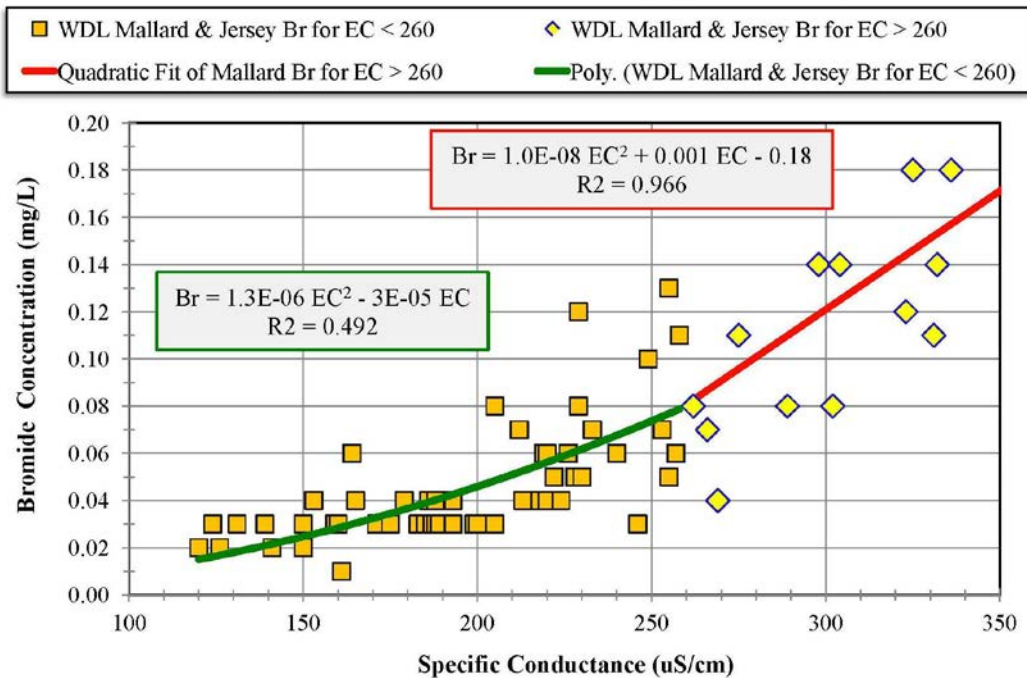


Figure A-7: Variation of bromide concentration as a function of specific conductance (EC) at Mallard Island and Jersey Point for EC < 350 μ S/cm.

Mallard Island (aka Chipps Island)

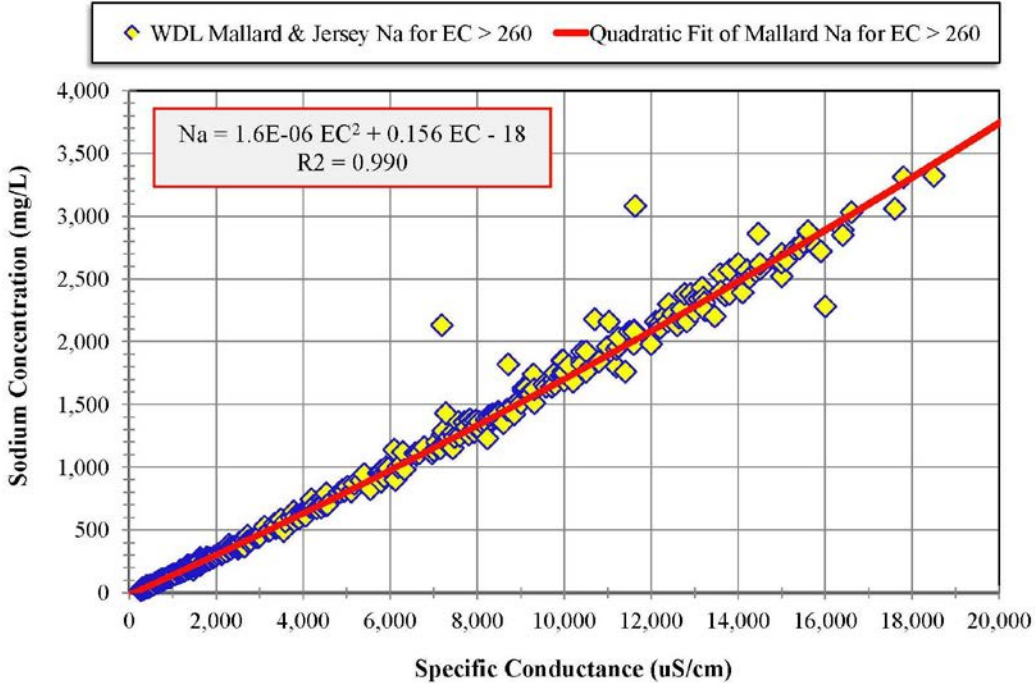


Figure A-8: Variation of sodium (Na) concentration as a function of specific conductance (EC) at Mallard Island and Jersey Point.

Mallard Island (aka Chipps Island)

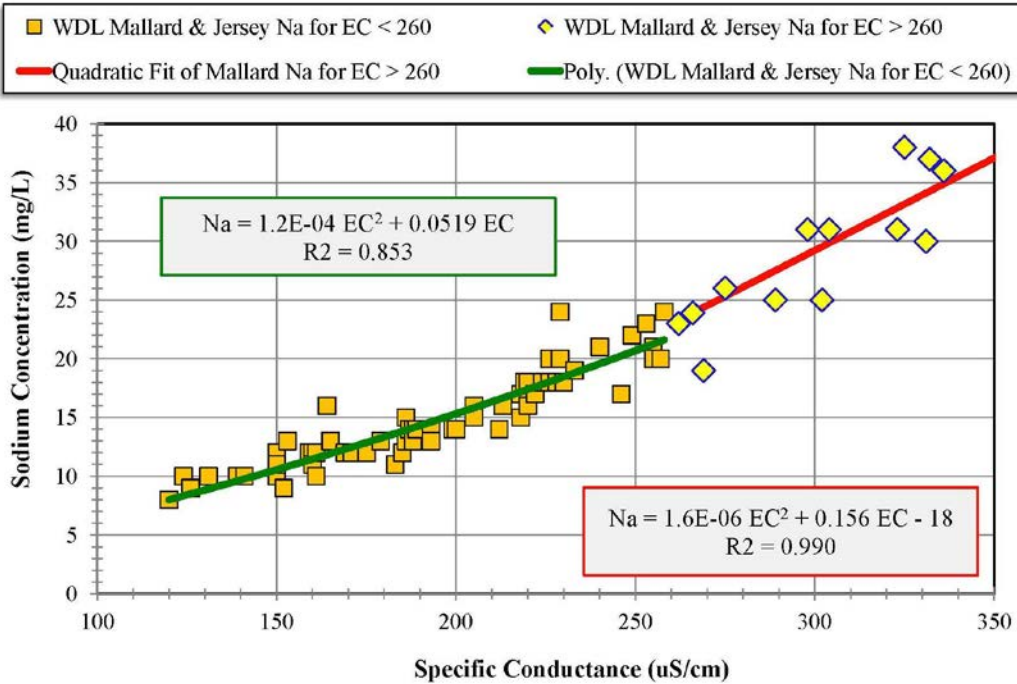


Figure A-9: Variation of sodium concentration as a function of specific conductance (EC) at Mallard Island and Jersey Point for EC < 350 μS/cm.

Mallard Island (aka Chipps Island)

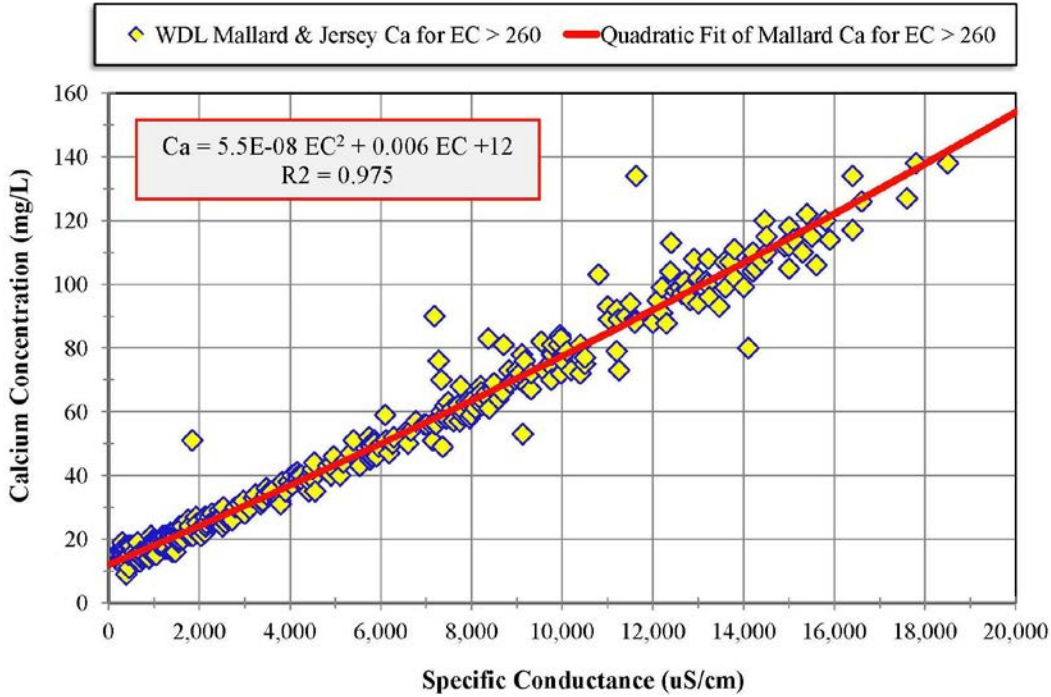


Figure A-10: Variation of calcium (Ca) concentration as a function of specific conductance (EC) at Mallard Island and Jersey Point.

Mallard Island (aka Chipps Island)

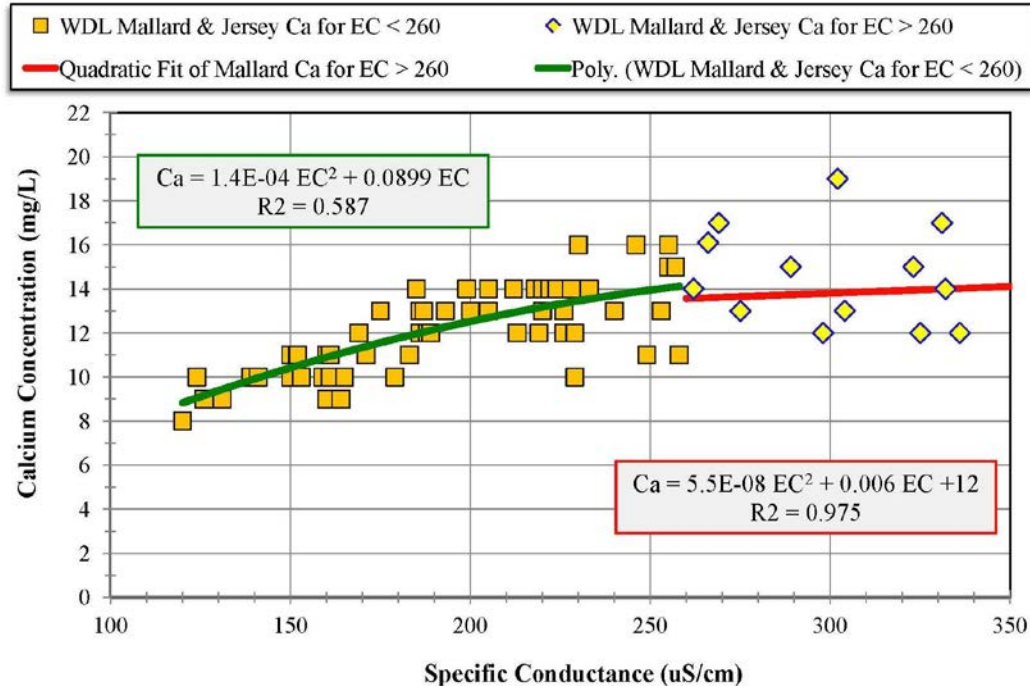


Figure A-11: Variation of calcium concentration as a function of specific conductance (EC) at Mallard Island and Jersey Point for EC < 350 μ S/cm.

Mallard Island (aka Chipps Island)

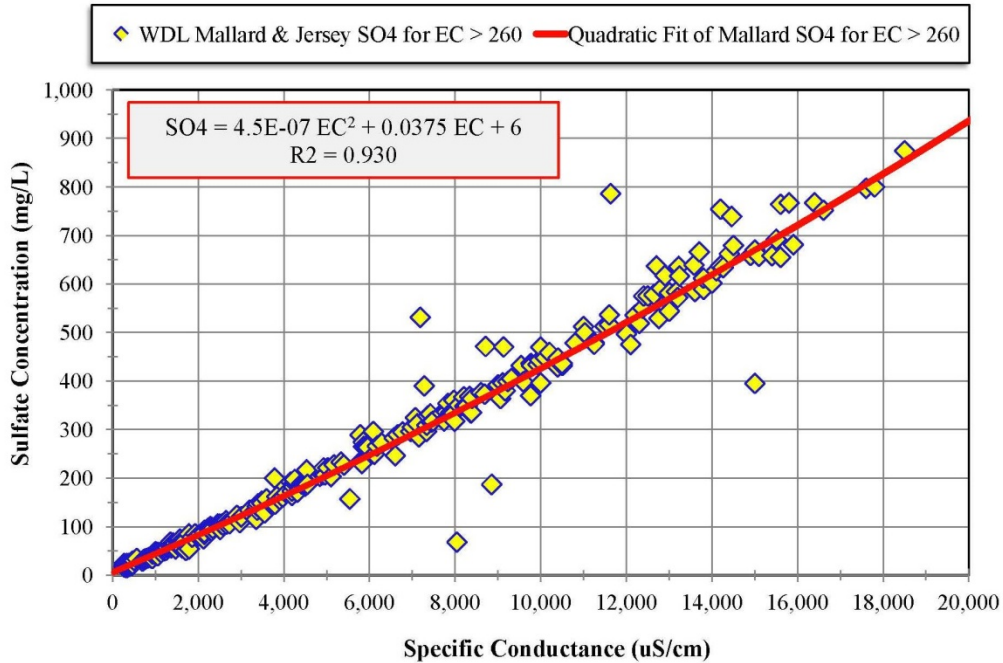


Figure A-12: Variation of sulfate (SO_4) concentration as a function of specific conductance (EC) at Mallard Island and Jersey Point.

Mallard Island (aka Chipps Island)

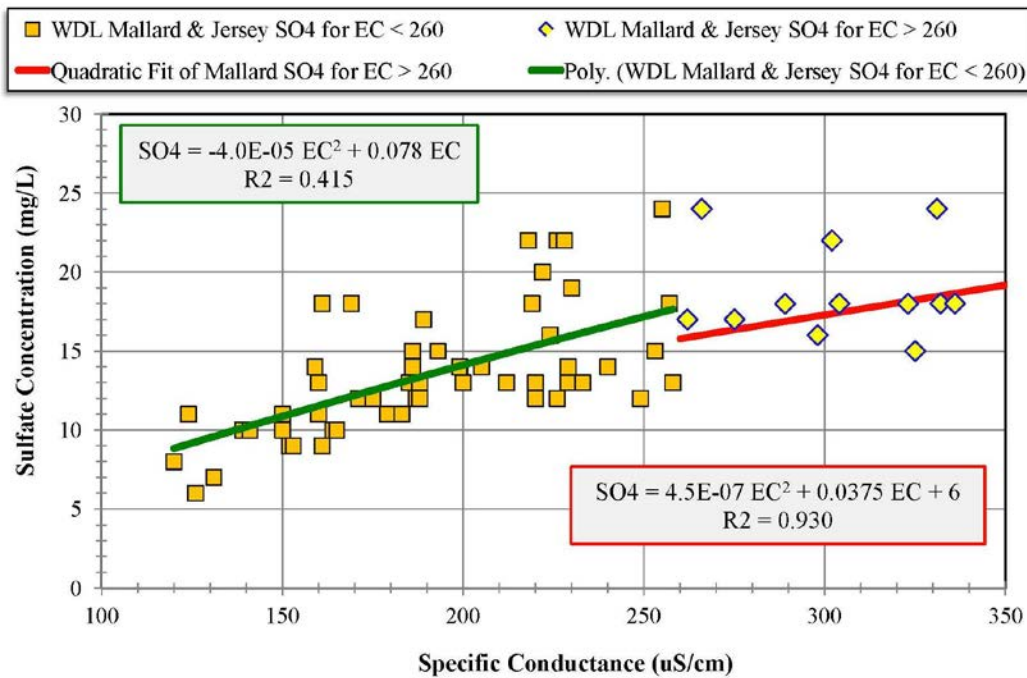


Figure A-13: Variation of sulfate concentration as a function of specific conductance (EC) at Mallard Island and Jersey Point for EC < 350 $\mu S/cm$.

Mallard Island (aka Chipps Island)

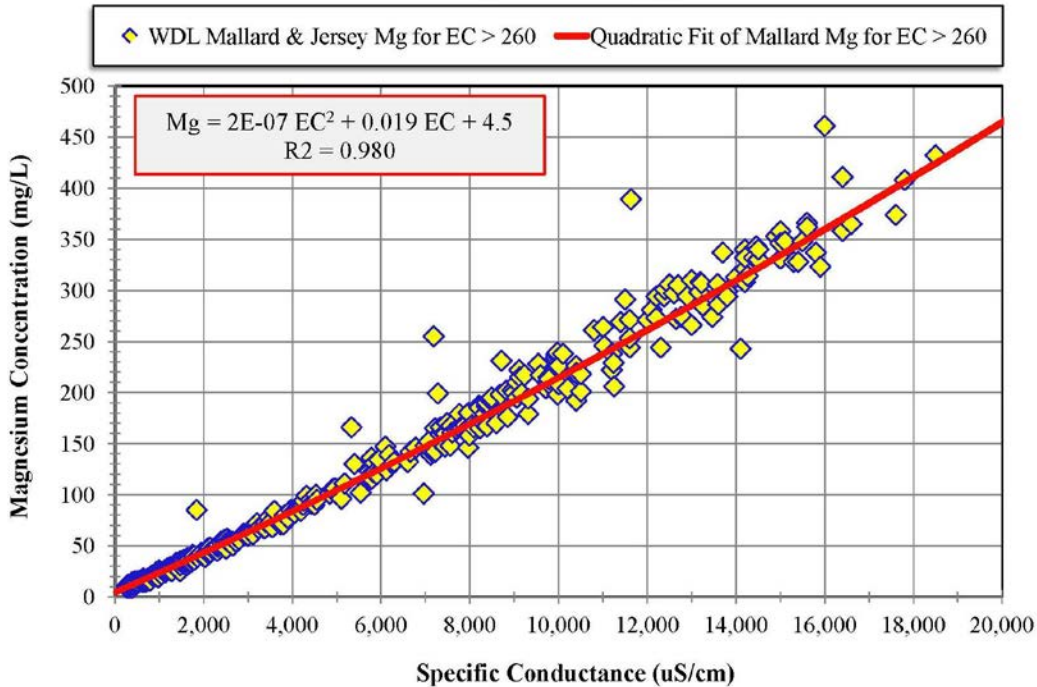


Figure A-14: Variation of magnesium (Mg) concentration as a function of specific conductance (EC) at Mallard Island and Jersey Point.

Mallard Island (aka Chipps Island)

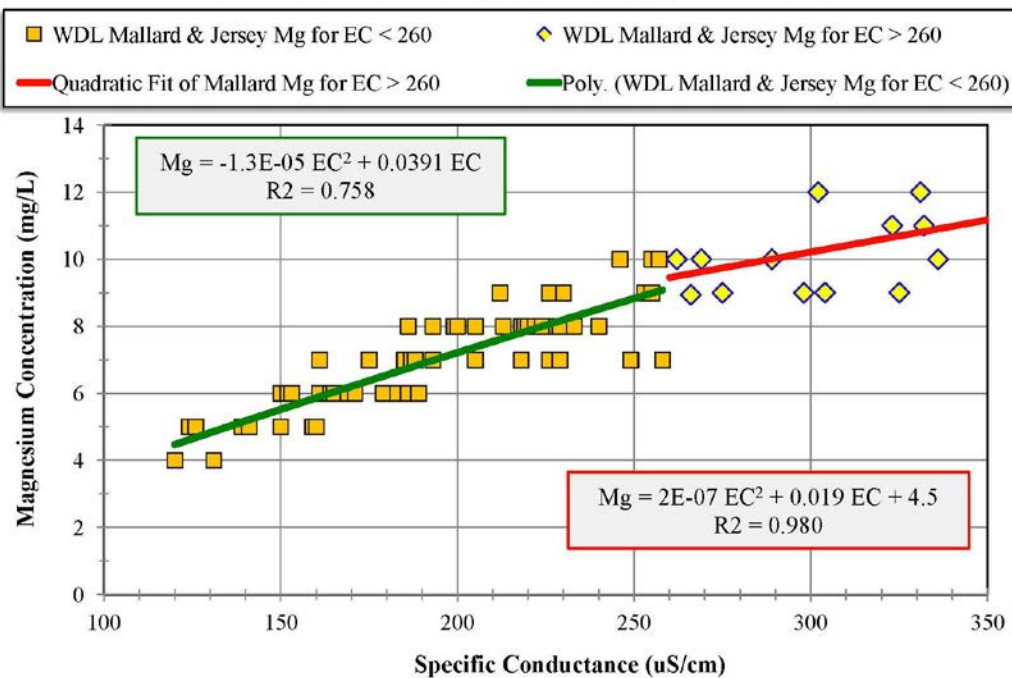


Figure A-15: Variation of magnesium concentration as a function of specific conductance (EC) at Mallard Island and Jersey Point for EC < 350 $\mu\text{S}/\text{cm}$.

Mallard Island (aka Chipps Island)

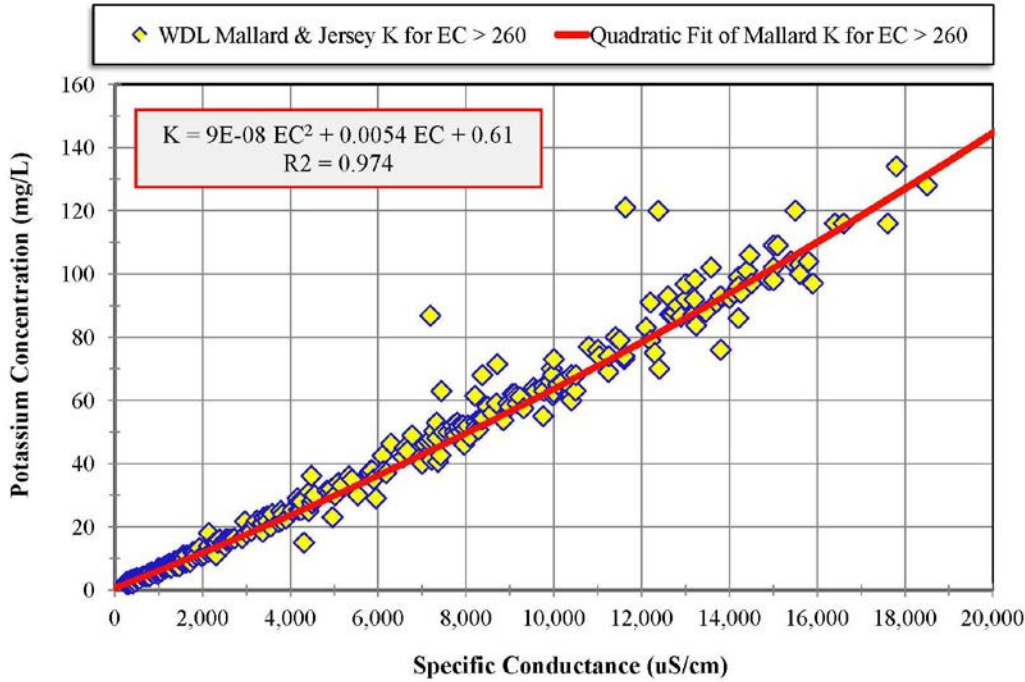


Figure A-16: Variation of potassium (K) concentration as a function of specific conductance (EC) at Mallard Island and Jersey Point.

Mallard Island (aka Chipps Island)

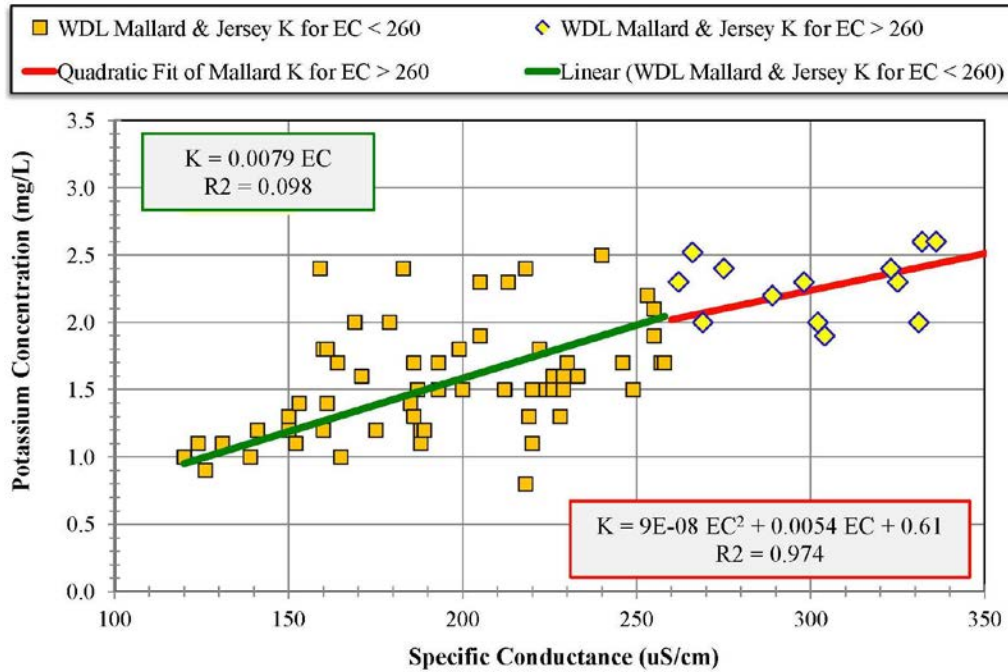


Figure A-17: Variation of potassium concentration as a function of specific conductance (EC) at Mallard Island and Jersey Point for $EC < 350 \mu\text{S}/\text{cm}$.

Mallard Island (aka Chipps Island)

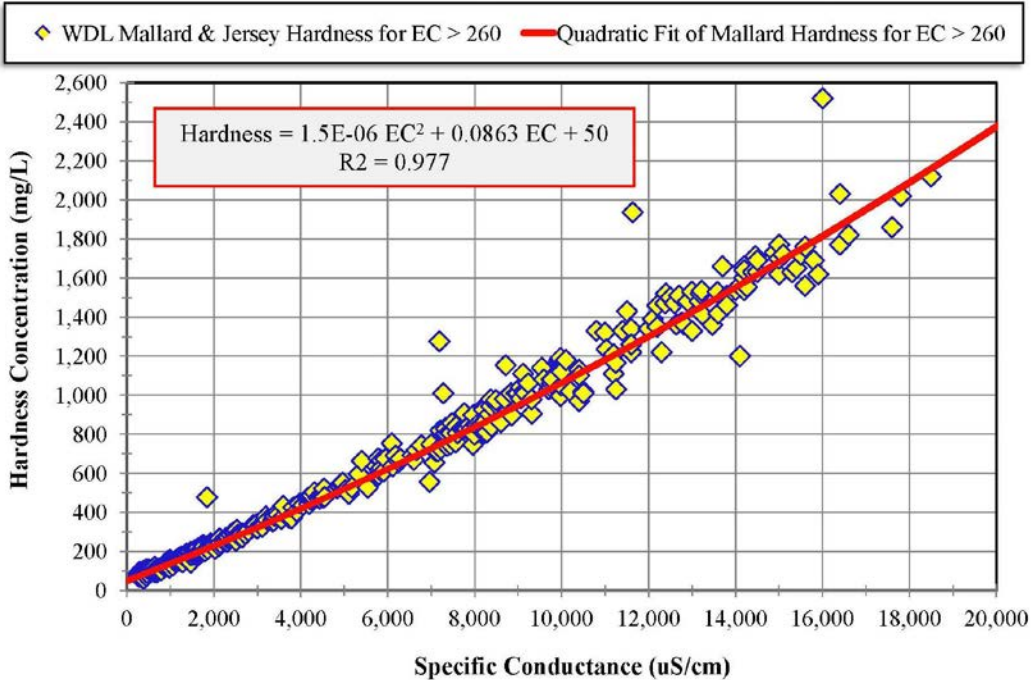


Figure A-18: Variation of hardness concentration as a function of specific conductance (EC) at Mallard Island and Jersey Point.

Mallard Island (aka Chipps Island)

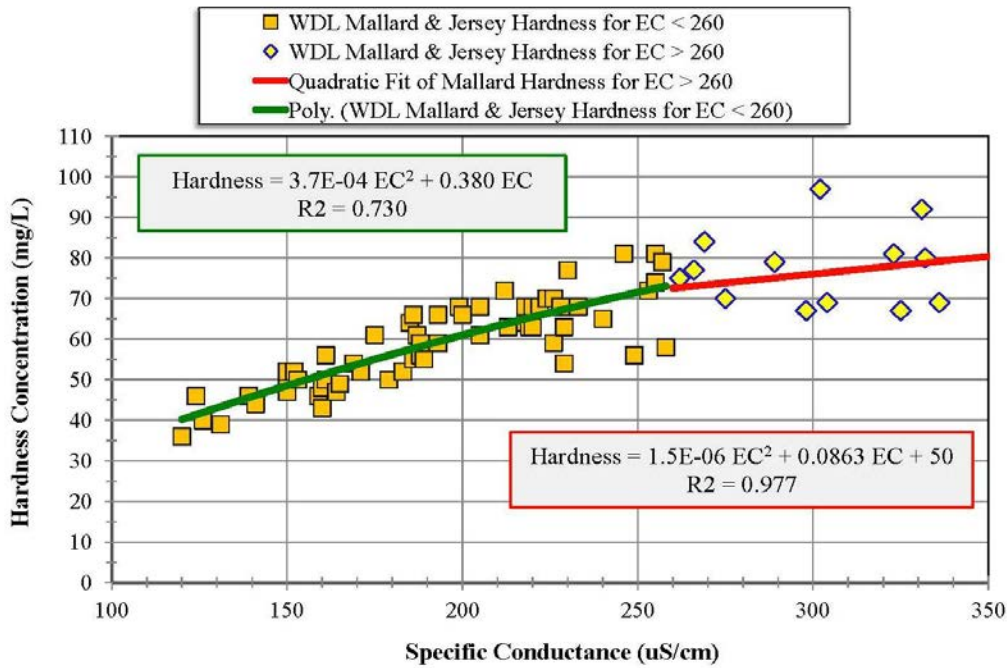


Figure A-19: Variation of hardness concentration as a function of specific conductance (EC) at Mallard Island and Jersey Point for EC < 350 μ S/cm.

Mallard Island (aka Chipps Island)

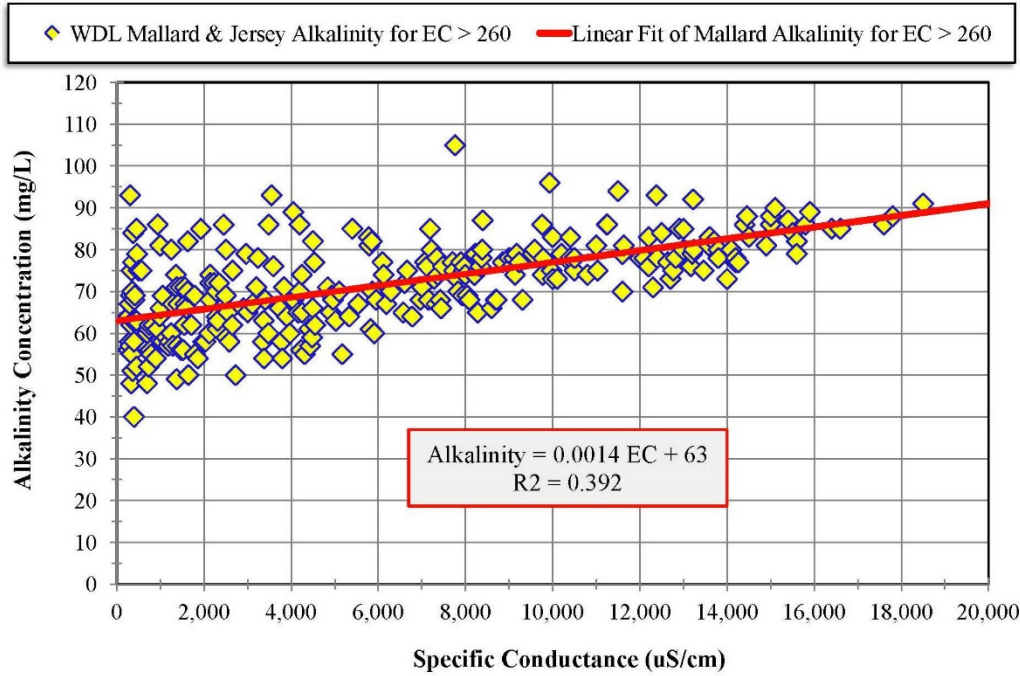


Figure A-20: Variation of alkalinity concentration as a function of specific conductance (EC) at Mallard Island and Jersey Point.

Mallard Island (aka Chipps Island)

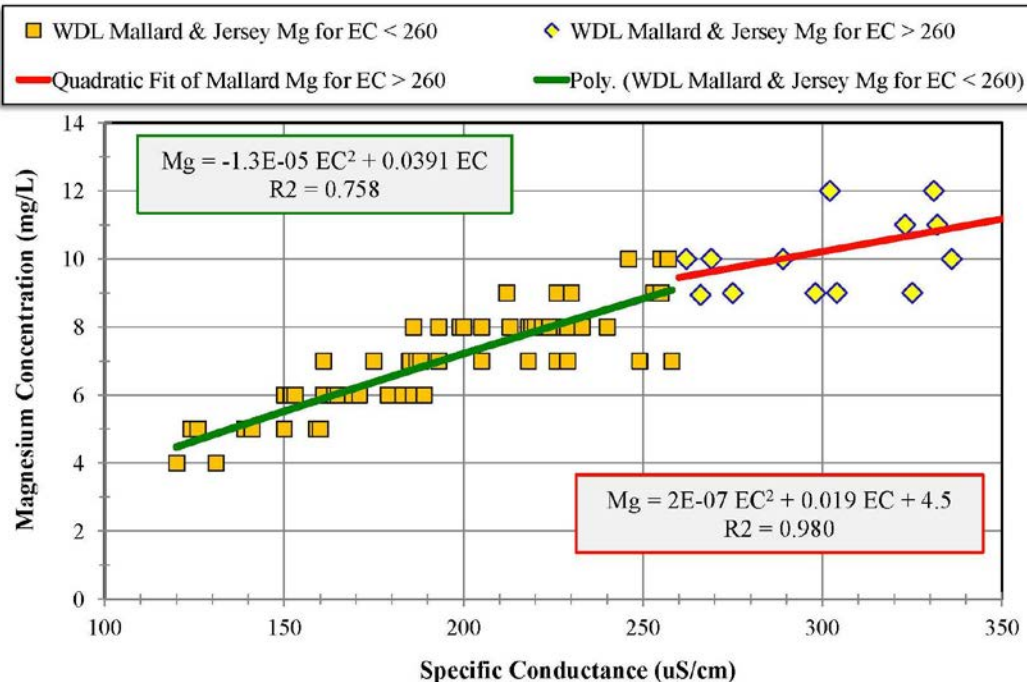


Figure A-21: Variation of alkalinity concentration as a function of specific conductance (EC) at Mallard Island and Jersey Point for EC < 1,100 μ S/cm.

Mallard Island (aka Chipps Island)

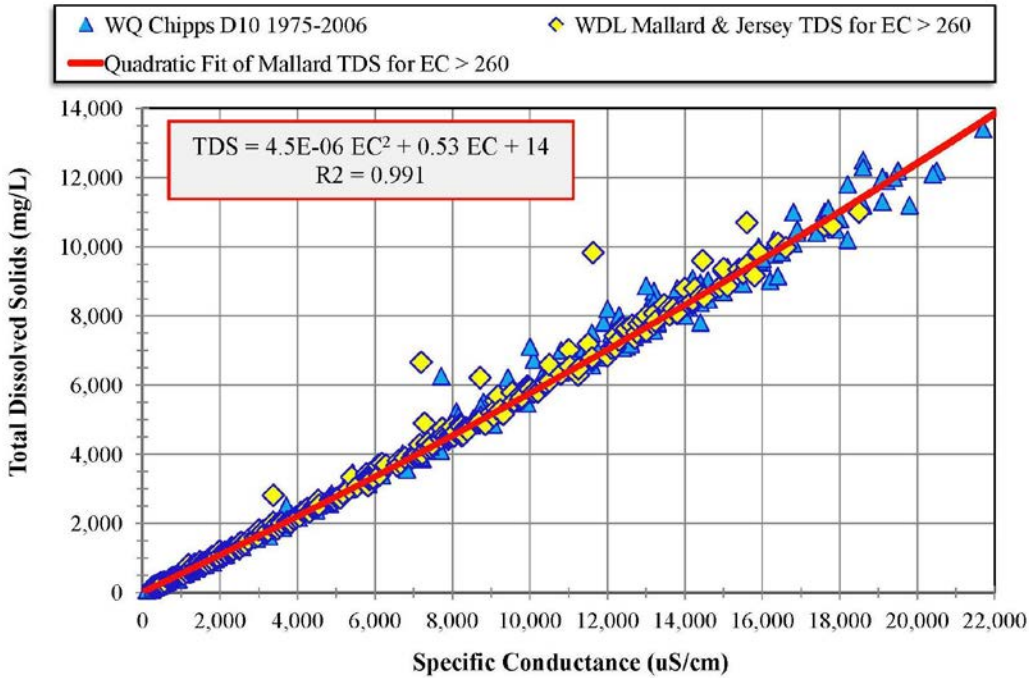


Figure A-22: Variation of total dissolved solids as a function of specific conductance (EC) at Mallard Island and Jersey Point.

Mallard Island (aka Chipps Island)

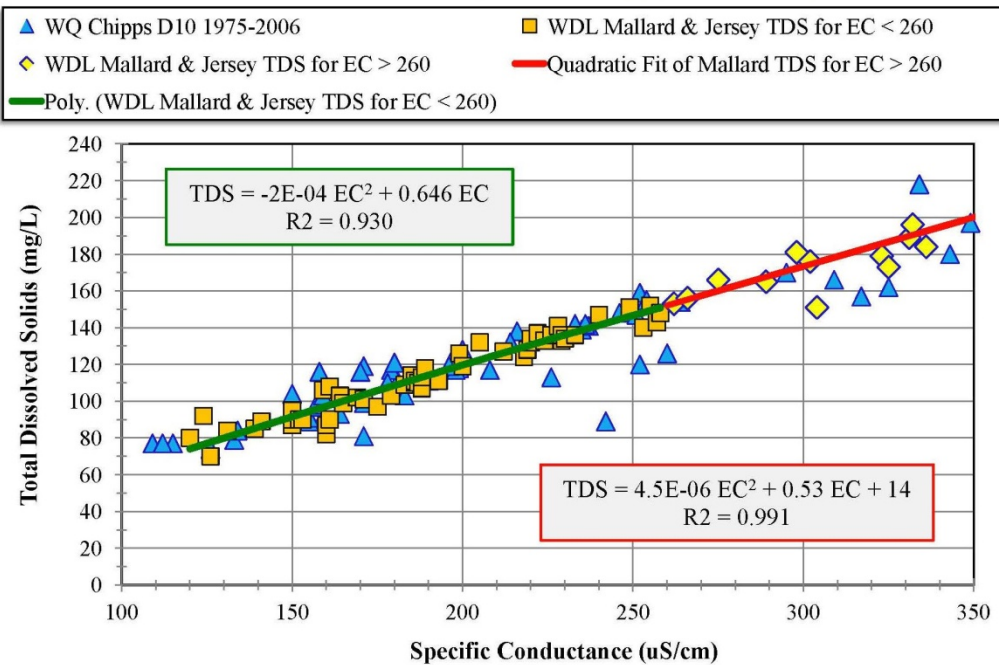


Figure A-23: Variation of total dissolved solids as a function of specific conductance (EC) at Mallard Island and Jersey Point for EC < 350 μ S/cm..

A.2: Variation with Total Dissolved Solids

Figures A-24 and A-25 show the variation of chloride concentration with TDS at Mallard Island and Jersey Point. The variations show the same trends as the variation with EC. Figure A-24 shows the full range of grab sample data (from DWR's Water Data Library), i.e., TDS as high as 14,000 mg/L. Figure A-25 shows the variation over the lower range of EC to illustrate the variation when Delta outflows are very high and a blend of Sacramento and San Joaquin water dominates.

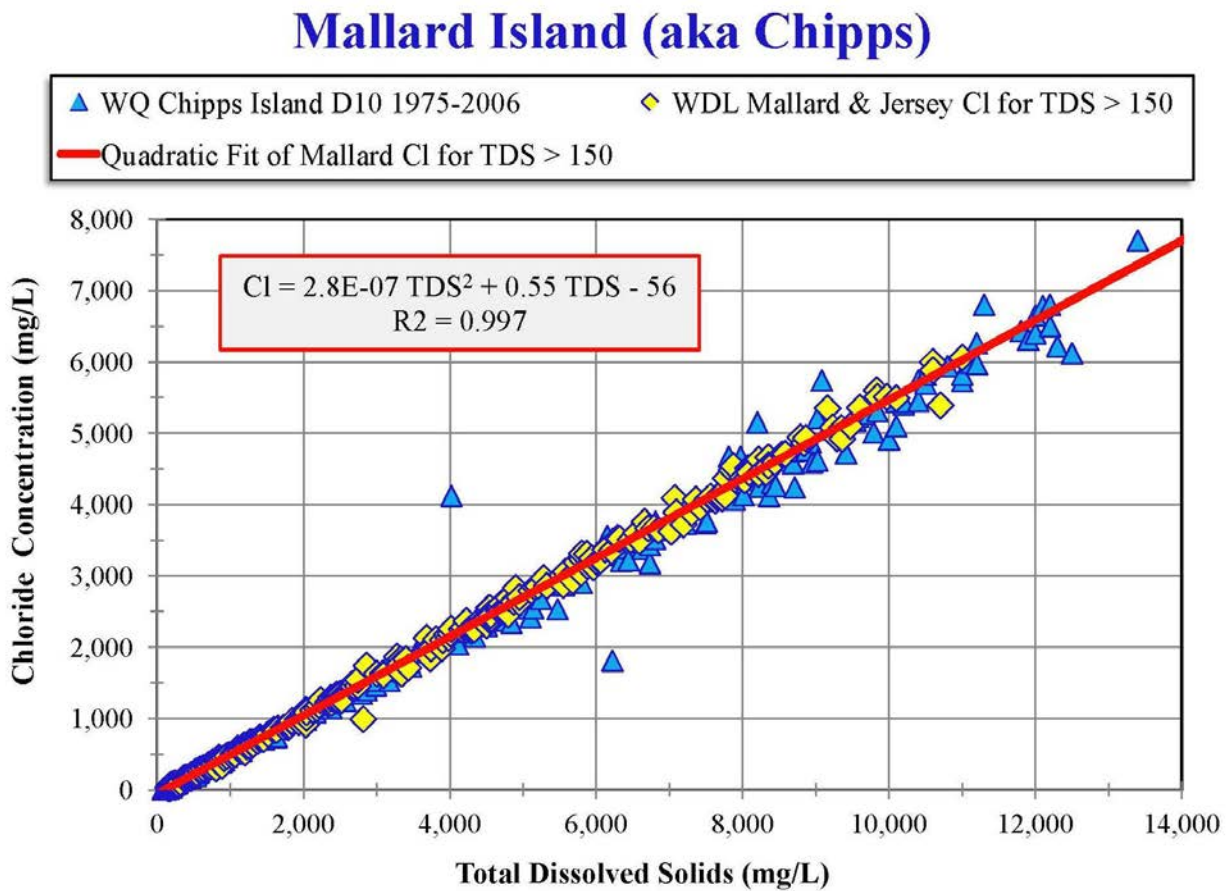


Figure A-24: Variation of chloride concentration as a function of total dissolved solids (TDS) at Mallard Island and Jersey Point.

Mallard Island (aka Chipps)

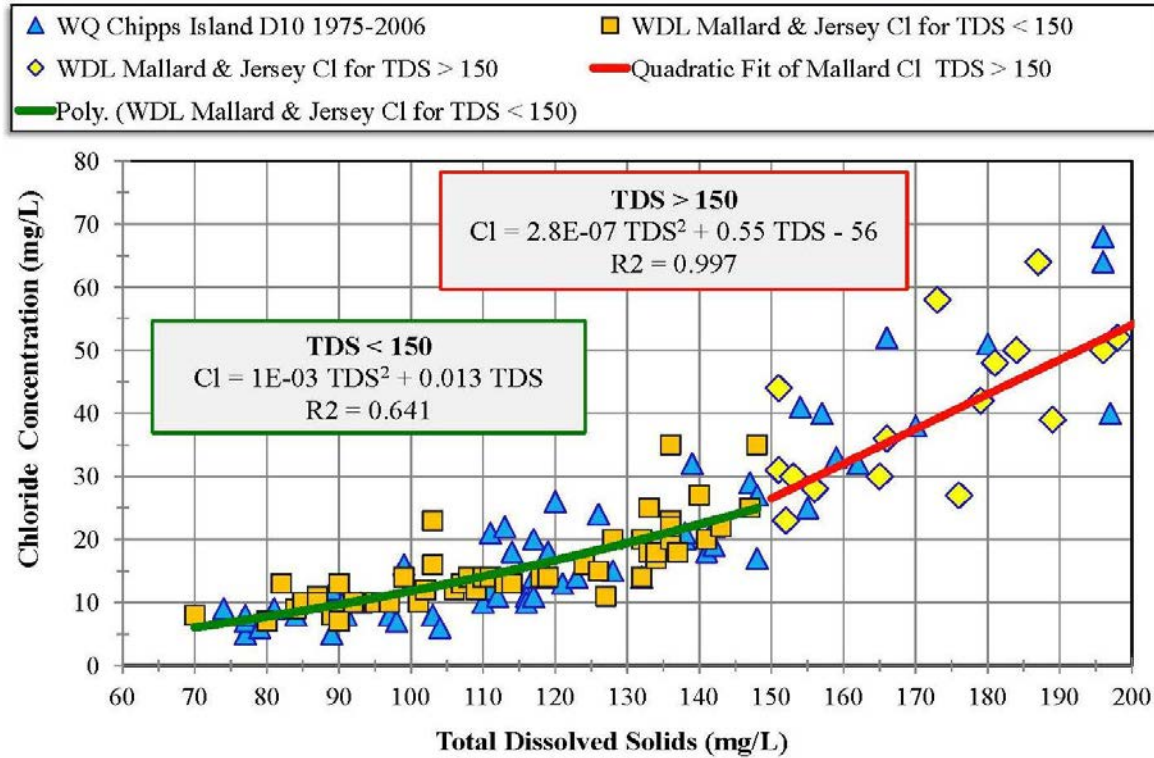


Figure A-25: Variation of chloride concentration as a function of TDS at Mallard Island and Jersey Point for TDS < 200 mg/L. The break between seawater dominated and agricultural drainage dominated water occurs at about a TDS of 150 mg/L.

A.3: Bromide as a function of Chloride Concentration

Bromide grab sample data are sometimes presented as bromide concentration as a function of chloride concentration. Figures A-26 and A-27 show the bromide versus chloride regression equations for grab sample data from Mallard Island and Jersey Point.

Mallard Island (aka Chipps Island)

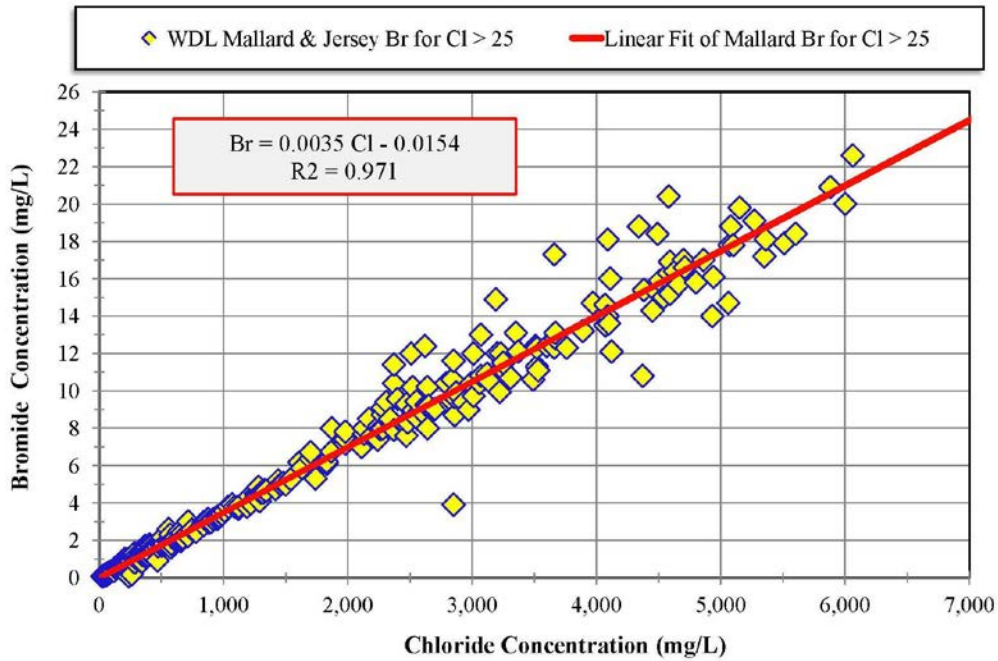


Figure A-26: Variation of bromide (Br) concentration as a function of chloride (Cl) concentration at Mallard Island and Jersey Point.

Mallard Island (aka Chipps Island)

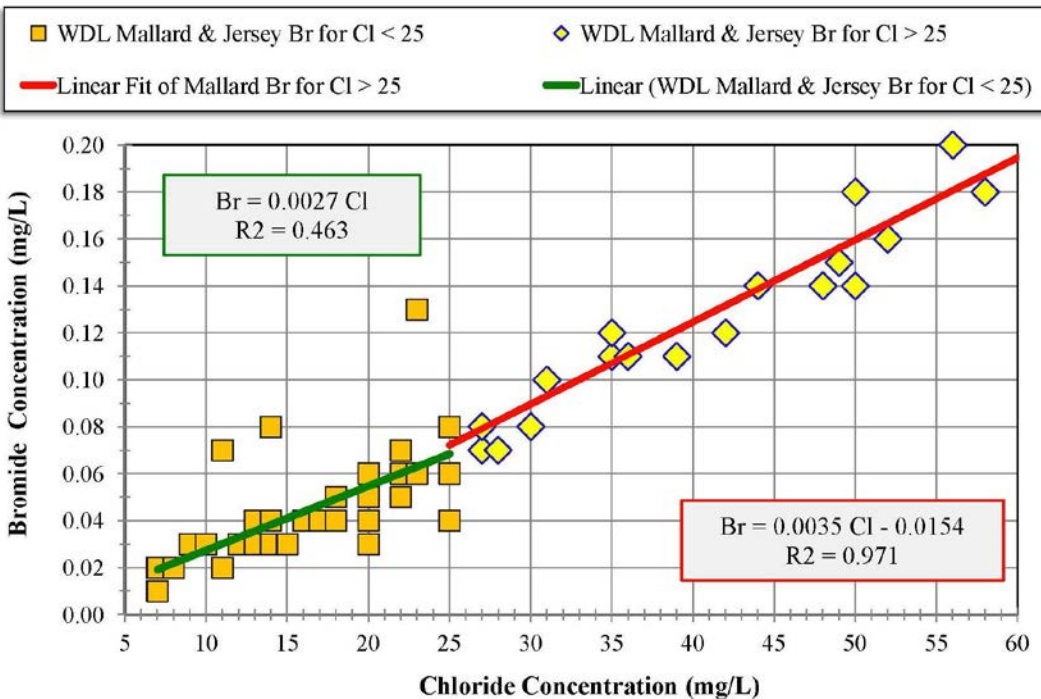


Figure A-27: Variation of bromide concentration as a function of chloride concentration at Mallard Island and Jersey Point for Cl < 60 mg/L.

Appendix B**San Joaquin River Boundary Condition**

A key contribution to the water quality in the south and central Delta in particular is the inflow of San Joaquin River water at Vernalis. Grab sample data are also available for Maze, a station located south of Vernalis at the Maze Road Bridge. The regression equations were developed by fitting the data from both stations combined.

Hutton (2006) analyzed grab sample data from Vernalis and found the following typical distribution of water quality constituents (Table B-1).

Table B-1: San Joaquin River percentages of TDS from Hutton (2006)

Ion	Symbol	Valence	Percentage of TDS
Chloride	Cl	1-	21
Sodium	Na	1+	18
Sulfate	SO ₄	2-	22
Magnesium	Mg	2+	4
Calcium	Ca	2+	8
Potassium	K	1+	1
Bicarbonate	HCO ₃	1-	16
Nitrate	NO ₃	1-	10

As shown in Figures B-1 and B-2, the percentages of TDS are not constant but vary with TDS. Typically, salinity at Vernalis is lowest during high San Joaquin flows (although there may be a “first flush” effect where concentrations of water quality constituents are often high during the first storm runoff event). During high runoff periods, the contribution of fresher water from the eastern Sierra tributaries is higher, diluting the sources of agricultural drainage.

During periods of lower San Joaquin flows, TDS values will be higher and the percentage of agricultural drainage will be greater. The data corresponding to high TDS are therefore more representative of the percentage contributions from agricultural drainage.

The Vernalis and Maze grab sample data presented below suggest that the percentage contributions for agricultural drainage are closer to those shown in Table B-2.

Table B-2: Updated San Joaquin River percentages of TDS

			MWQI Data (high TDS)
Ion	Symbol	Valence	Percent of TDS
Chloride	Cl	1-	25
Sodium	Na	1+	20
Sulfate	SO ₄	2-	28
Magnesium	Mg	2+	4
Calcium	Ca	2+	8
Alkalinity			15

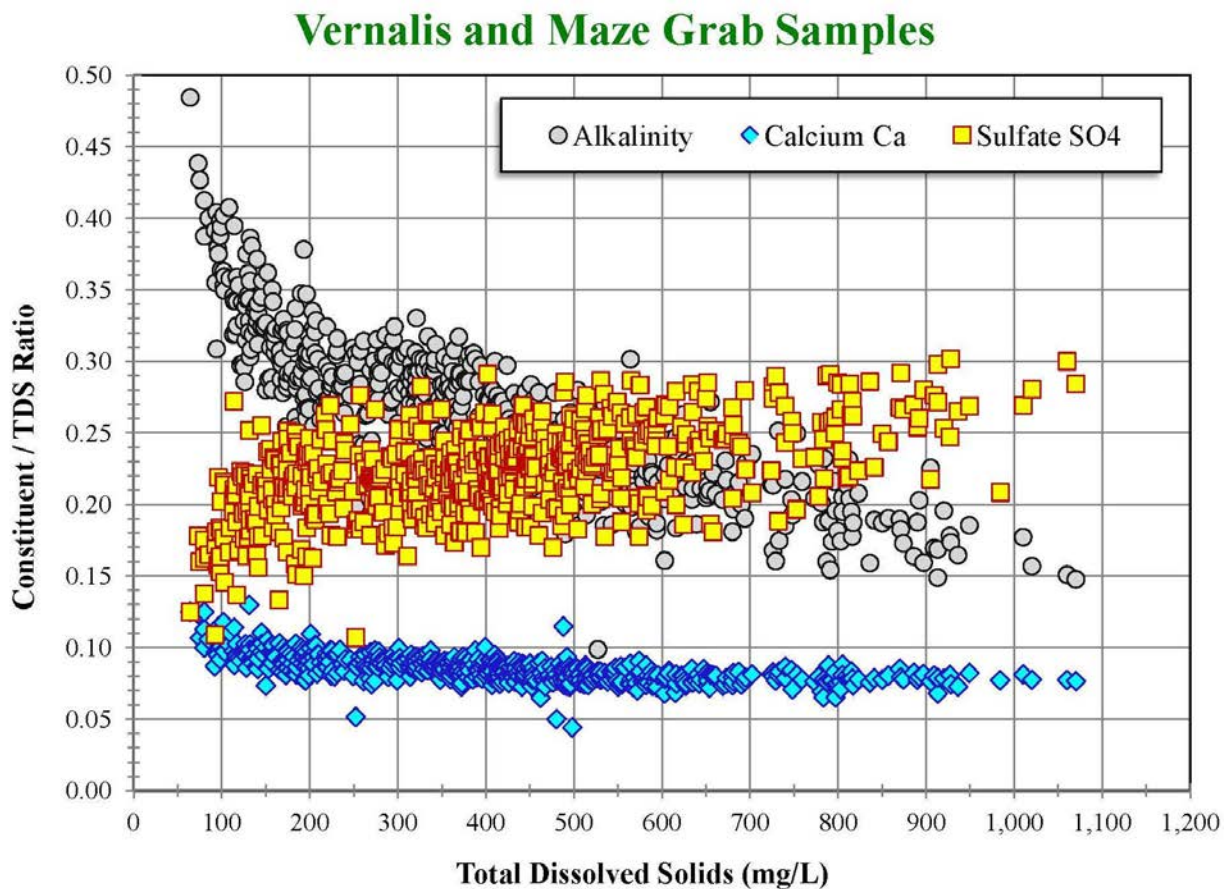


Figure B-1: Variation of alkalinity, calcium and sulfate ratios of total dissolved solids with TDS from the San Joaquin River at Vernalis and at Maze. These stations represent the source of San Joaquin Valley inflow to the Delta.

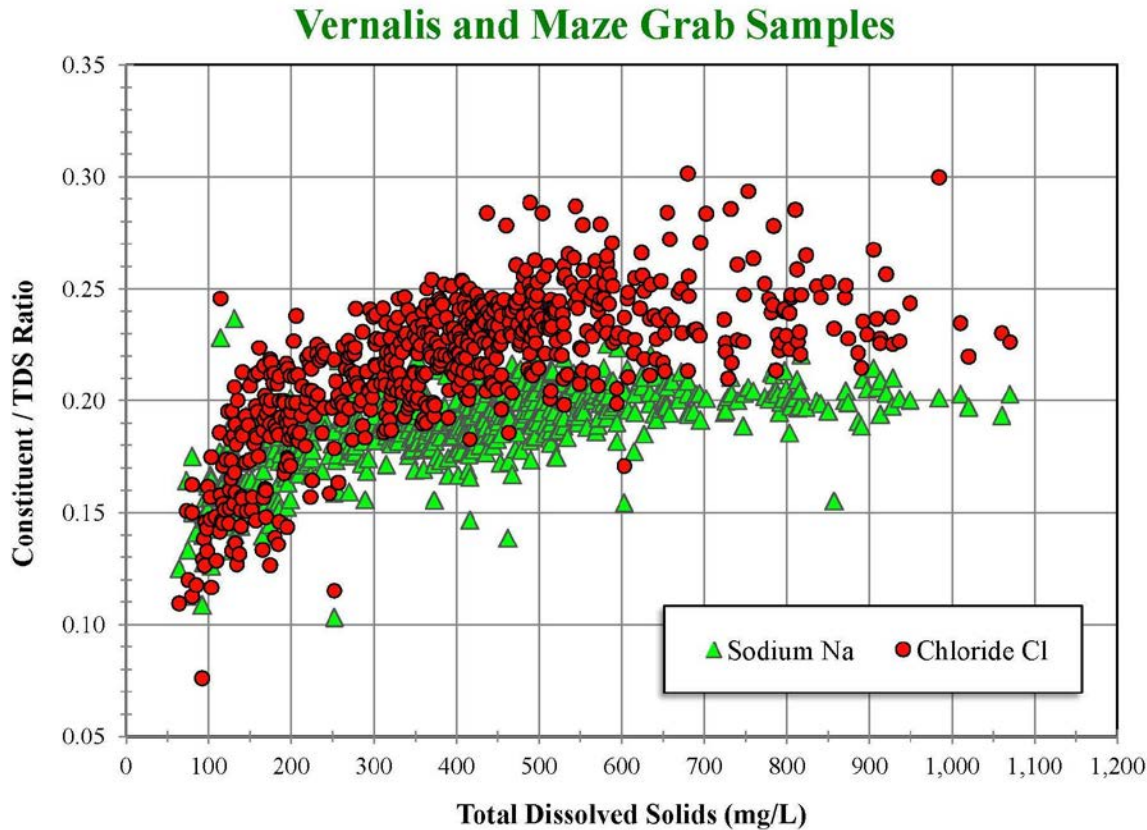


Figure B-2: Variation of sodium and chloride ratios of total dissolved solids with TDS from the San Joaquin River at Vernalis and at Maze.

Because the constituent ratios vary with increasing TDS, a simple linear regression will not be sufficient to represent the regression relationship between TDS (or EC) and the individual water quality constituents.

B.1: Variation of Water Quality Constituents with EC

The following graphs (Figures B-3 to B-12) show the variation of each of the water quality constituents at Vernalis and Maze on the San Joaquin River with specific conductance (EC). The maximum EC for these sets of data was about 1,700 $\mu\text{S}/\text{cm}$.

Some of the hardness data were presented as dissolved hardness and some as total hardness. The data in Figure B-10 are both dissolved and total hardness. No significant difference was detected in the regression equations for the two types of hardness.

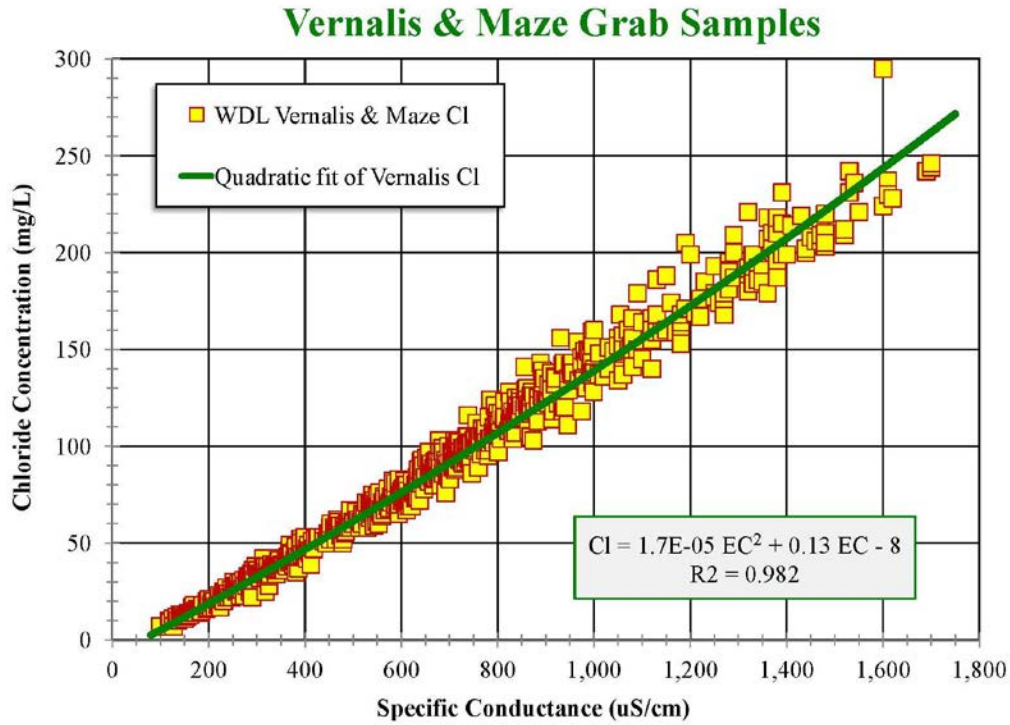


Figure B-3: Variation of chloride concentration with specific conductance (EC) for grab samples from the San Joaquin River at Vernalis and at Maze.

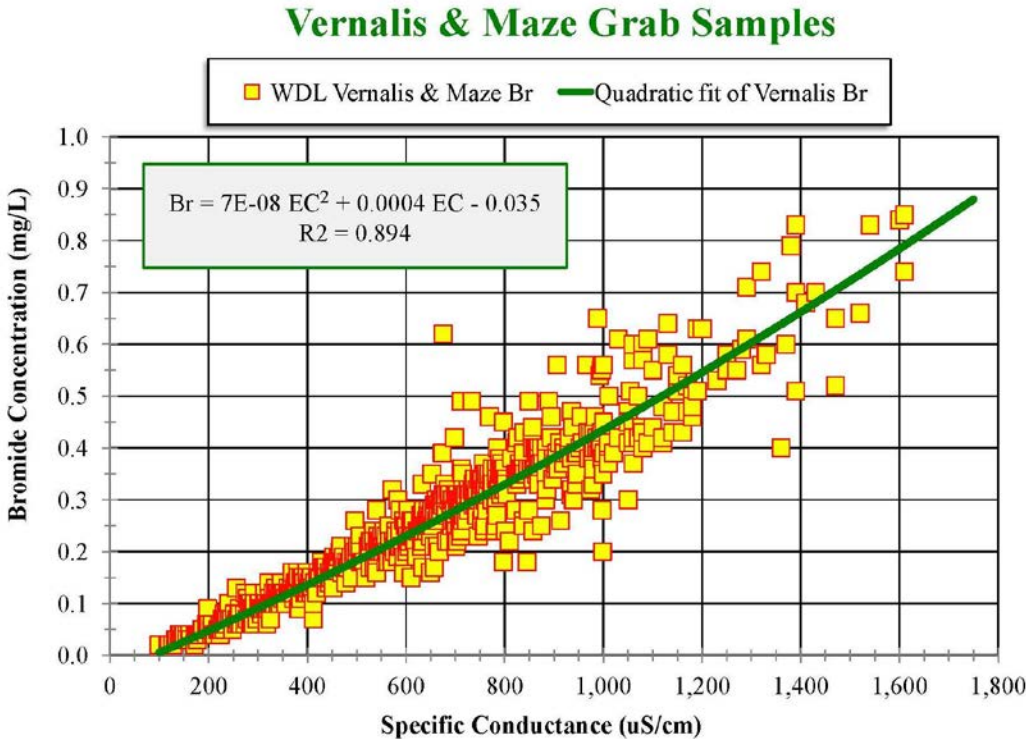


Figure B-4: Variation of bromide concentration with specific conductance (EC) for grab samples from the San Joaquin River at Vernalis and at Maze.

Vernalis & Maze Grab Samples

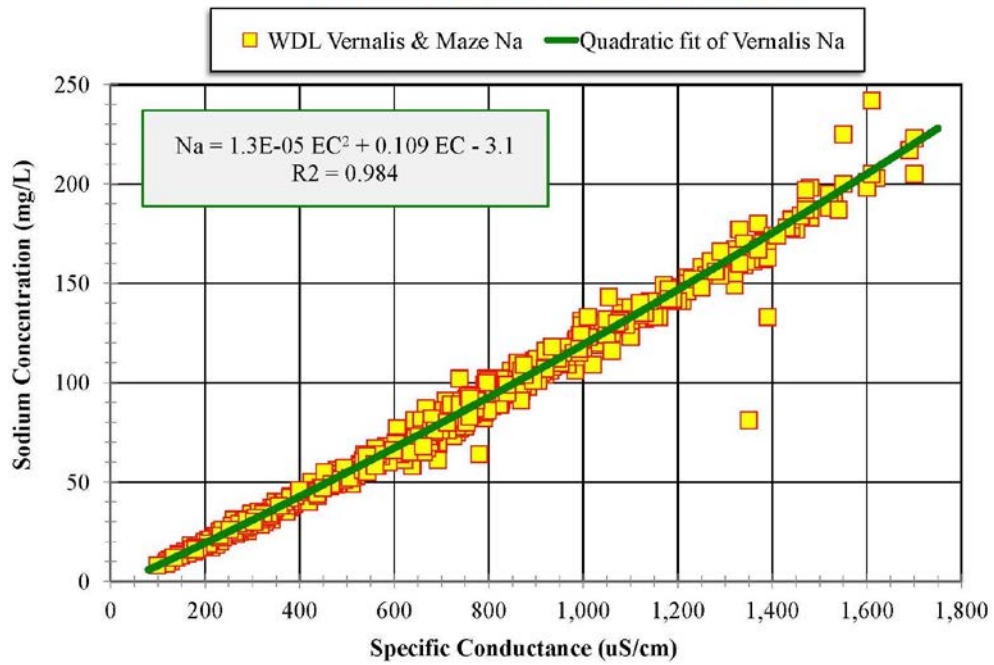


Figure B-5: Variation of sodium concentration with specific conductance (EC) for grab samples from the San Joaquin River at Vernalis and at Maze.

Vernalis & Maze Grab Samples

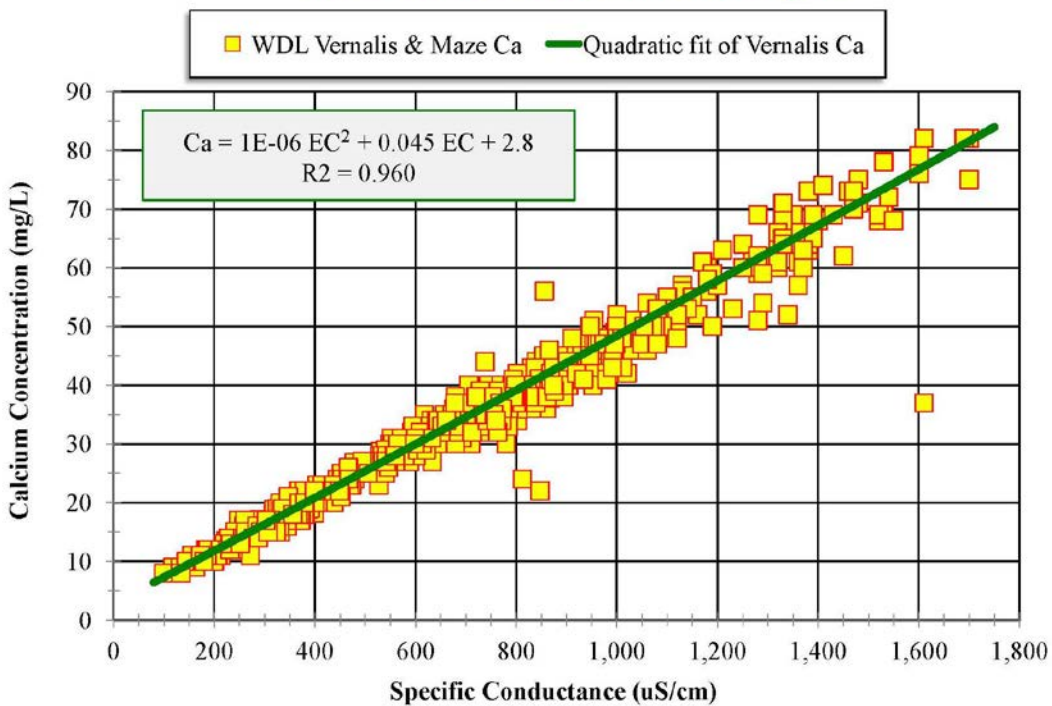


Figure B-6: Variation of calcium concentration with specific conductance (EC) for grab samples from the San Joaquin River at Vernalis and at Maze.

Vernalis & Maze Grab Samples

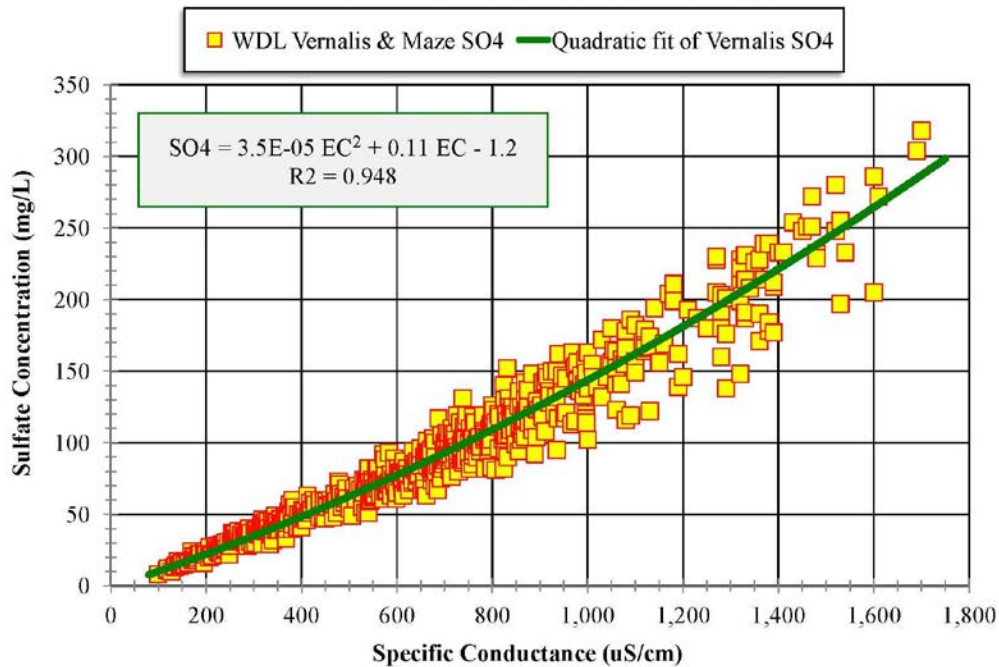


Figure B-7: Variation of sulfate concentration with specific conductance (EC) for grab samples from the San Joaquin River at Vernalis and at Maze.

Vernalis & Maze Grab Samples

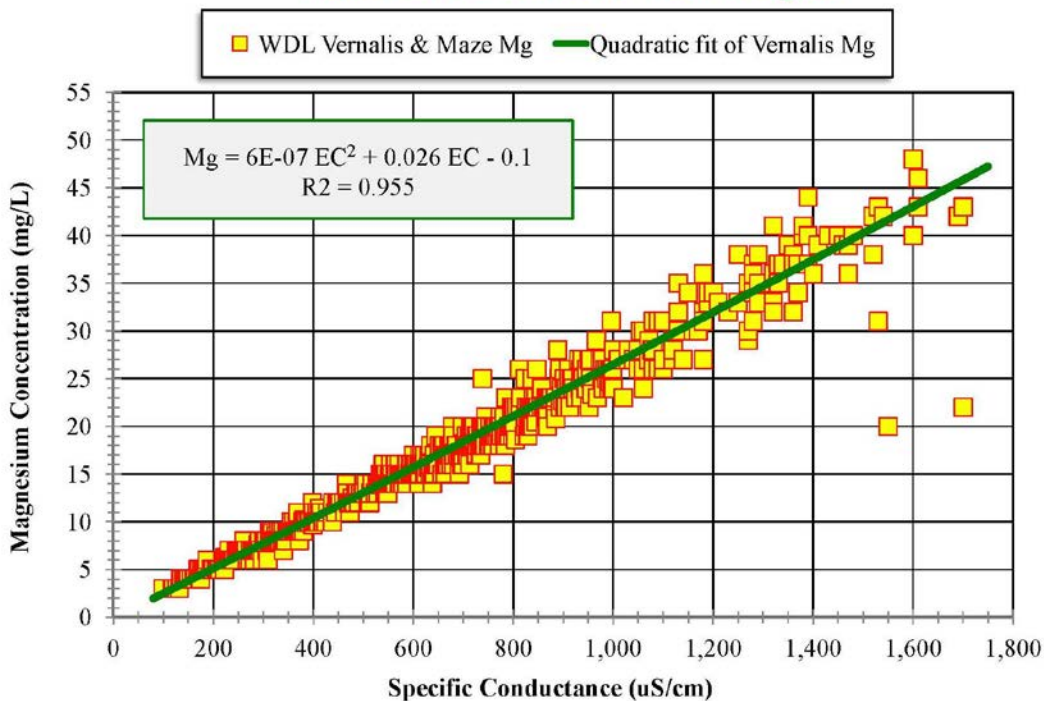


Figure B-8: Variation of magnesium concentration with specific conductance (EC) for grab samples from the San Joaquin River at Vernalis and at Maze.

Vernalis & Maze Grab Samples

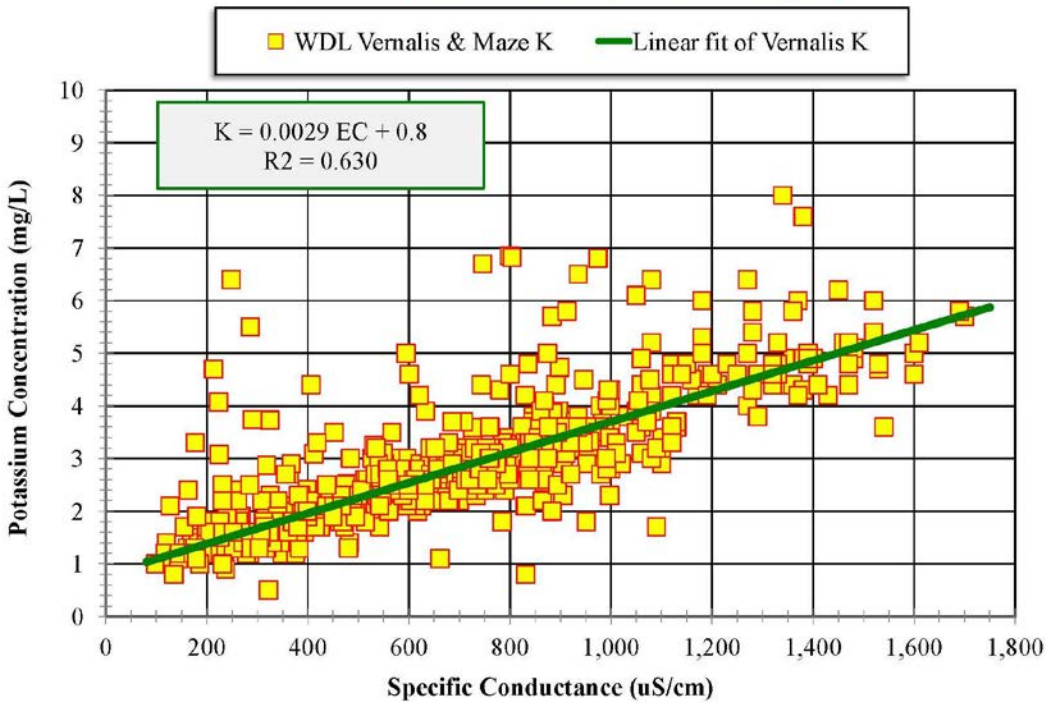


Figure B-9: Variation of potassium concentration with specific conductance (EC) for grab samples from the San Joaquin River at Vernalis and at Maze.

Vernalis & Maze Grab Samples

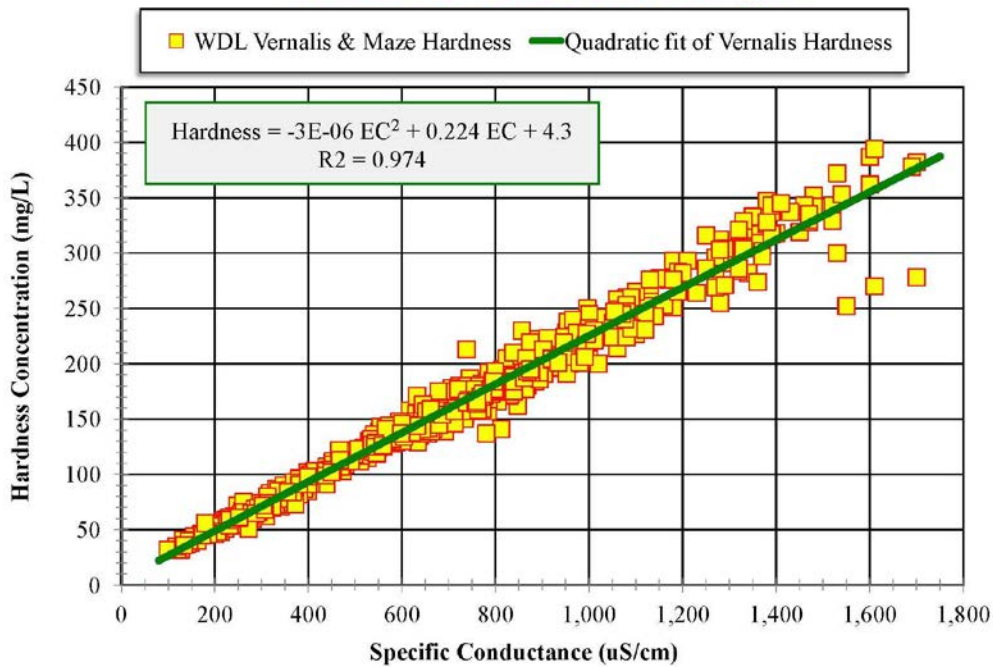


Figure B-10: Variation of hardness concentration with specific conductance (EC) for grab samples from the San Joaquin River at Vernalis and at Maze.

Vernalis & Maze Grab Samples

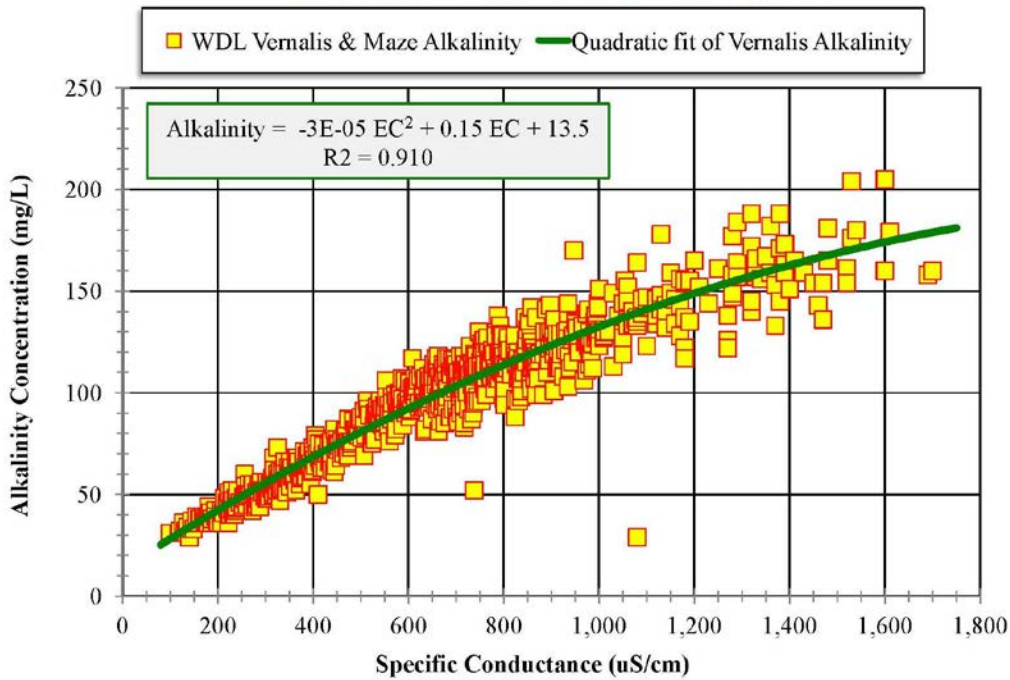


Figure B-11: Variation of alkalinity concentration with specific conductance (EC) for grab samples from the San Joaquin River at Vernalis and at Maze.

Vernalis & Maze Grab Samples

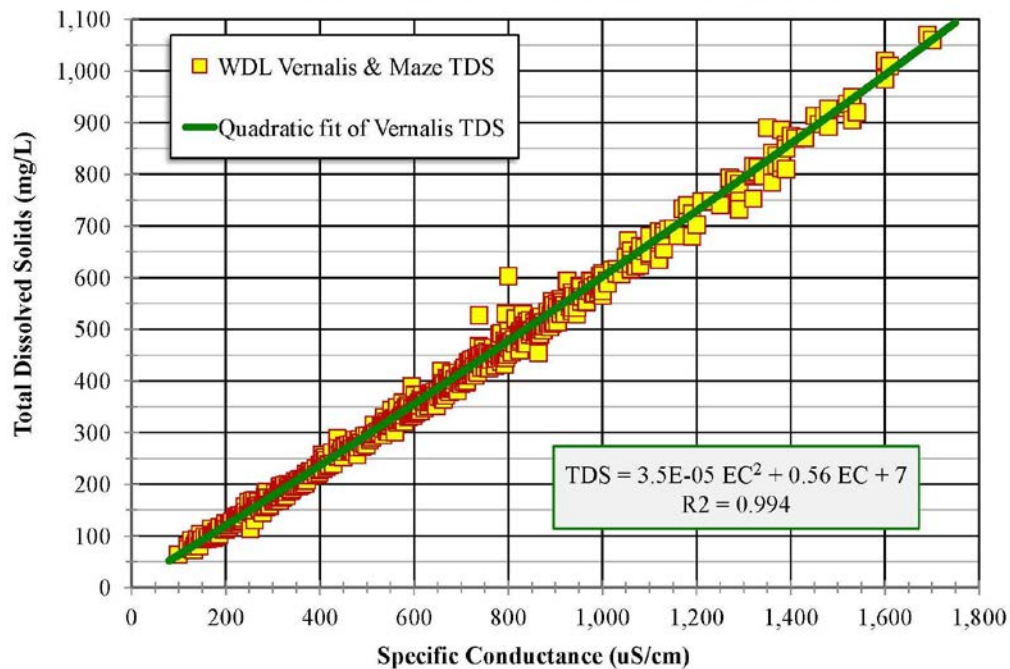


Figure B-12: Variation of total dissolved solids with specific conductance (EC) for grab samples from the San Joaquin River at Vernalis and at Maze.

B.2: Variation of Water Quality Constituents with TDS

The variations of the water quality constituents with total dissolved solids are similar to the equivalent variations with specific conductance. Figure B-13 shows the variation of chloride concentration with TDS.

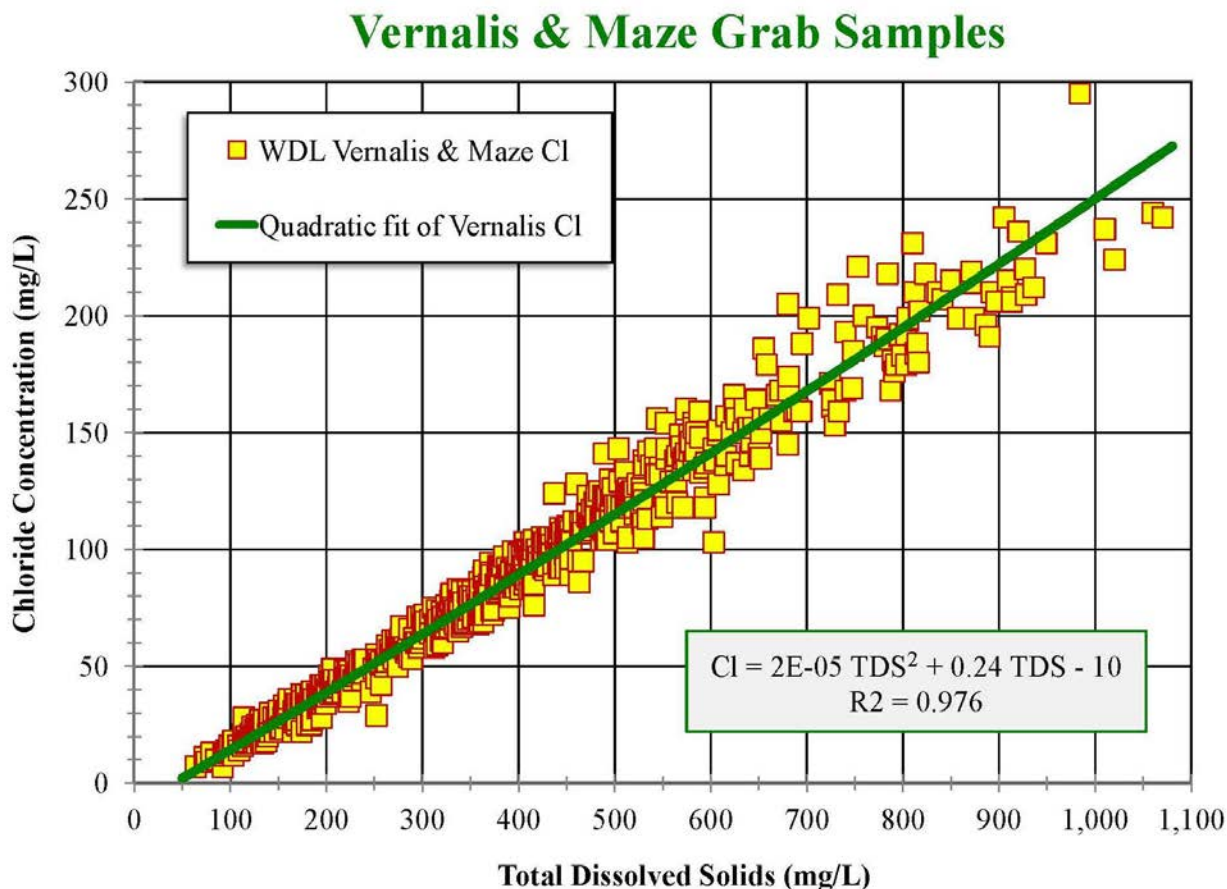


Figure B-13: Variation of chloride concentration with total dissolved solids (TDS) for grab samples from the San Joaquin River at Vernalis and at Maze.

B.3: Bromide as a function of Chloride Concentration

The bromide concentration in urban source water is an important factor affecting the production of drinking water disinfection byproducts. The water quality at urban (municipal and industrial) intakes in the Delta on the other hand is regulated in terms of the chloride concentration (see, e.g., State Water Resources Control Board's Water Rights Decision 1641). The relationship between bromide and chloride is therefore of some interest. The corresponding relationship for grab samples from the San Joaquin River at Vernalis and Maze (representing the San Joaquin boundary condition) is shown in Figure B-14. The Vernalis and Maze data show the characteristics of agricultural drainage. As shown in Figure 3-4, agricultural return flows into Rock Slough show the same chloride versus EC relationship as the Vernalis data.

Vernalis & Maze Grab Samples

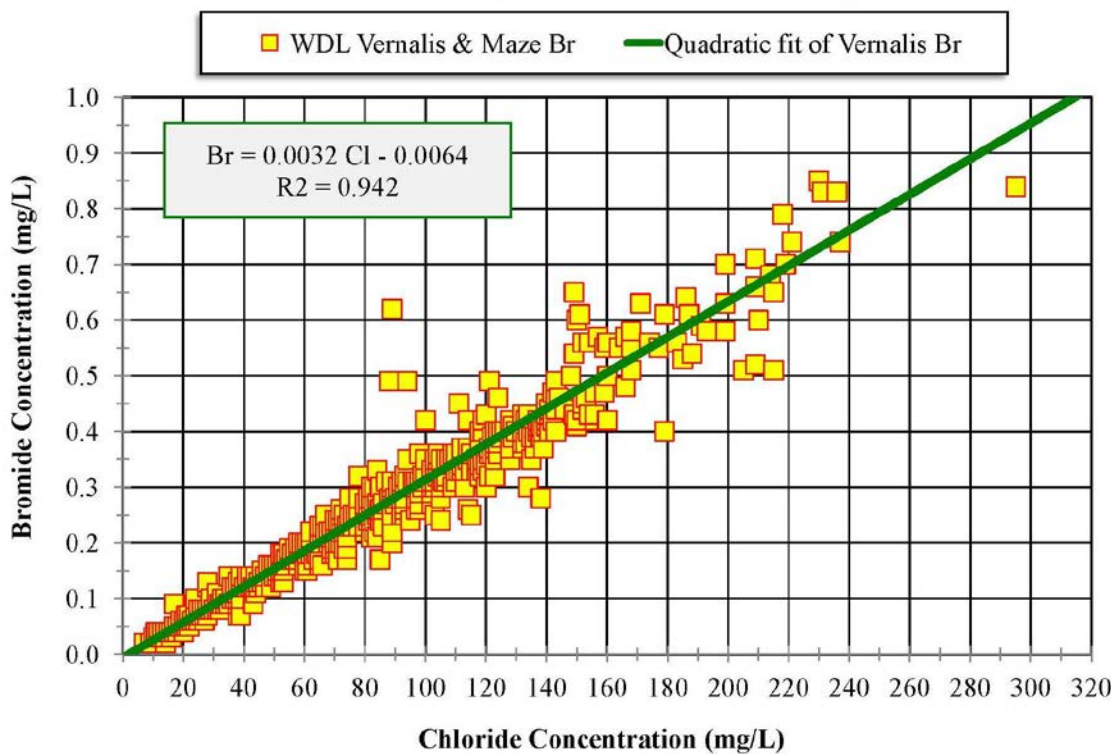


Figure B-14: Variation of bromide concentration as a function of chloride concentration for grab samples from the San Joaquin River at Vernalis and Maze.

B.4: Influence of Export Water Quality on Vernalis Water Quality

A closer inspection of the Vernalis salinity data suggests that during prolonged dry periods when the salinity of Delta water, and therefore export water quality, increases, there is a delayed increase in salinity of the San Joaquin water at Vernalis and Maze.

Water entering the Delta at Vernalis can be thought of as a mixture of water from three sources:

- (a) relatively fresh water from the eastside tributaries;
- (b) agricultural drainage, primarily from the west side of the San Joaquin Valley; and
- (c) irrigation water that has been exported from the Delta, used in the San Joaquin Valley, and has ended up back in the San Joaquin River.

Because the chloride to TDS ratio for seawater is higher (0.55) than for San Joaquin water (0.23-0.25), increased percentage of seawater returning to the Delta via the San Joaquin River during or after a prolonged dry period will increase the chloride/TDS ratio at Vernalis.

The winter of 1993 was wet and the water at Mallard Island was relatively fresh for almost 6 months (Figure B-15). The corresponding chloride/TDS ratio at Vernalis remained below 0.25. Periods of high runoff from the Sacramento Valley are often accompanied by higher runoff from

the San Joaquin Valley at Vernalis. This will cause the chloride to TDS ratio at Vernalis to decrease below 0.25.

Chloride to TDS Ratios

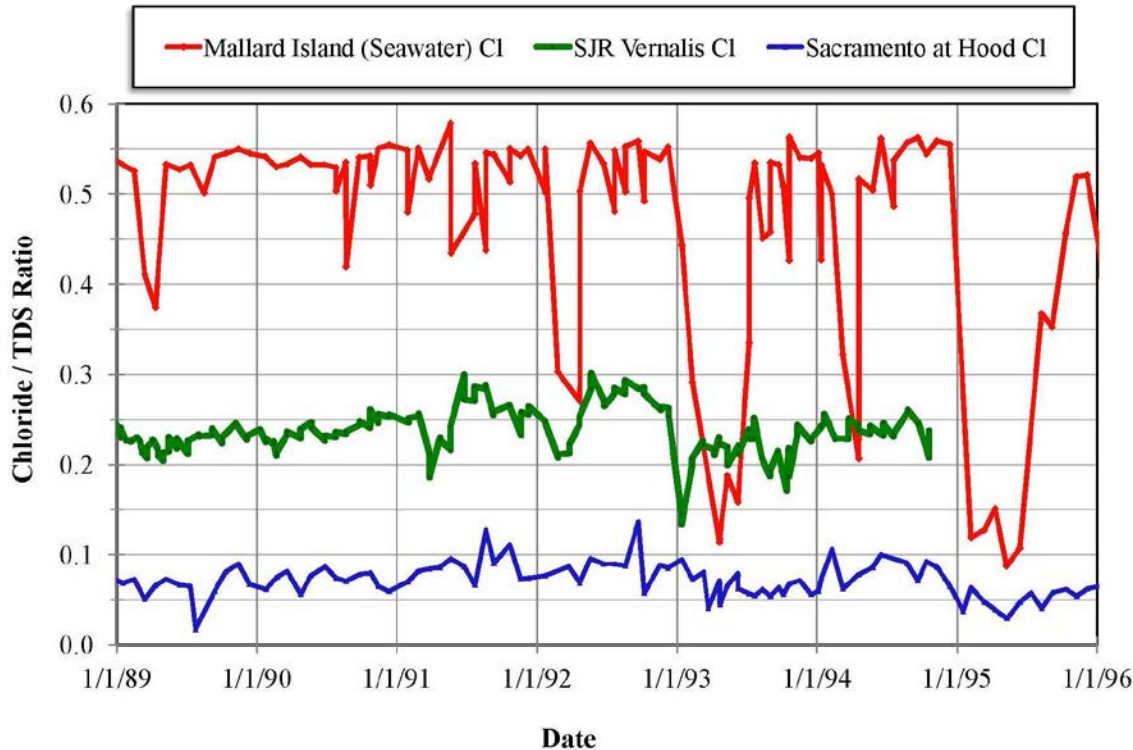


Figure B-15: Variation of chloride to TDS ratios for seawater, San Joaquin and Sacramento boundary conditions from 1989-1995. During periods of high outflow, the chloride/TDS ratio at Mallard Island decrease significantly to a value representing a mixture of Sacramento and San Joaquin water. During prolonged dry periods, export of saltier Delta water, containing a higher proportion of seawater, causes a subsequent increase in the chloride/TDS ratio at Vernalis. No data are available at Vernalis for 1995.

The Sacramento Valley water year types from 1988 through 1995 are shown in Figure B-16. The period from 1988 through 1992 consisted of only critical and dry years and Delta salinities remained high for most of this period (corresponding to chloride/TDS ratios of 0.5 or higher in Figure B-15). Higher salinity water was exported to the San Joaquin Valley during this period and caused the corresponding ratio at Vernalis to increase to as high as 0.30. There will be a built in time delay for these effects on salinity at Vernalis because of the time required for exports from the Delta to reach San Joaquin Valley farms and the subsequent return flows to reach Vernalis. There is also a cumulative effect of salt build up in the soils. This salt can be released later after local rain storms or leaching by the farmer. The Cl/TDS ratio will not necessarily decrease straight away in response to fresher water in the Delta, e.g., the February-March 1992 lower salinity event in Figure B-16.

In the winter and spring of wetter years, e.g., 1993 and 1995, seawater intrusion is greatly reduced, salinities decrease, and the water quality at Mallard Island is dominated by Sacramento River water with some agricultural drainage. The Cl/TDS ratio decreases significantly.

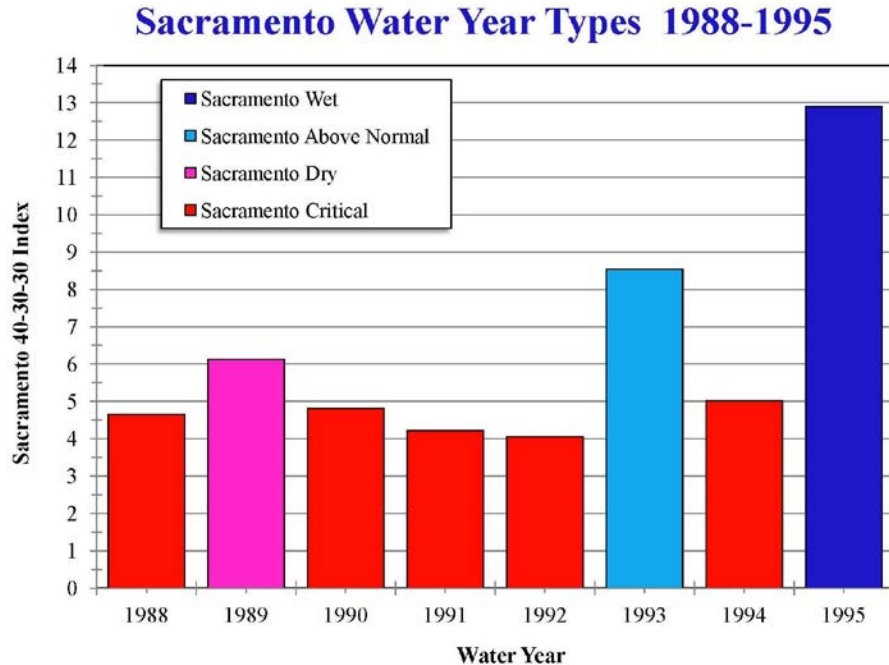


Figure B-16: Sacramento Basin 40-30-30 water year indices for 1988 through 1995.

Figure B-17 shows the corresponding variation in the ratio of calcium to TDS at the same three boundary condition locations. Because the percentage of calcium in fresh Sacramento River water and agricultural drainage are higher than in seawater, the calcium/TDS ratio at Mallard Island increases during periods of higher Delta inflow.

The calcium/TDS ratio for agricultural drainage is about 0.07-0.09 and the ratio for seawater is only 0.02. The effect of higher salinity export water on the calcium/TDS ratio at Vernalis is, therefore, as obvious (Figure B-18).

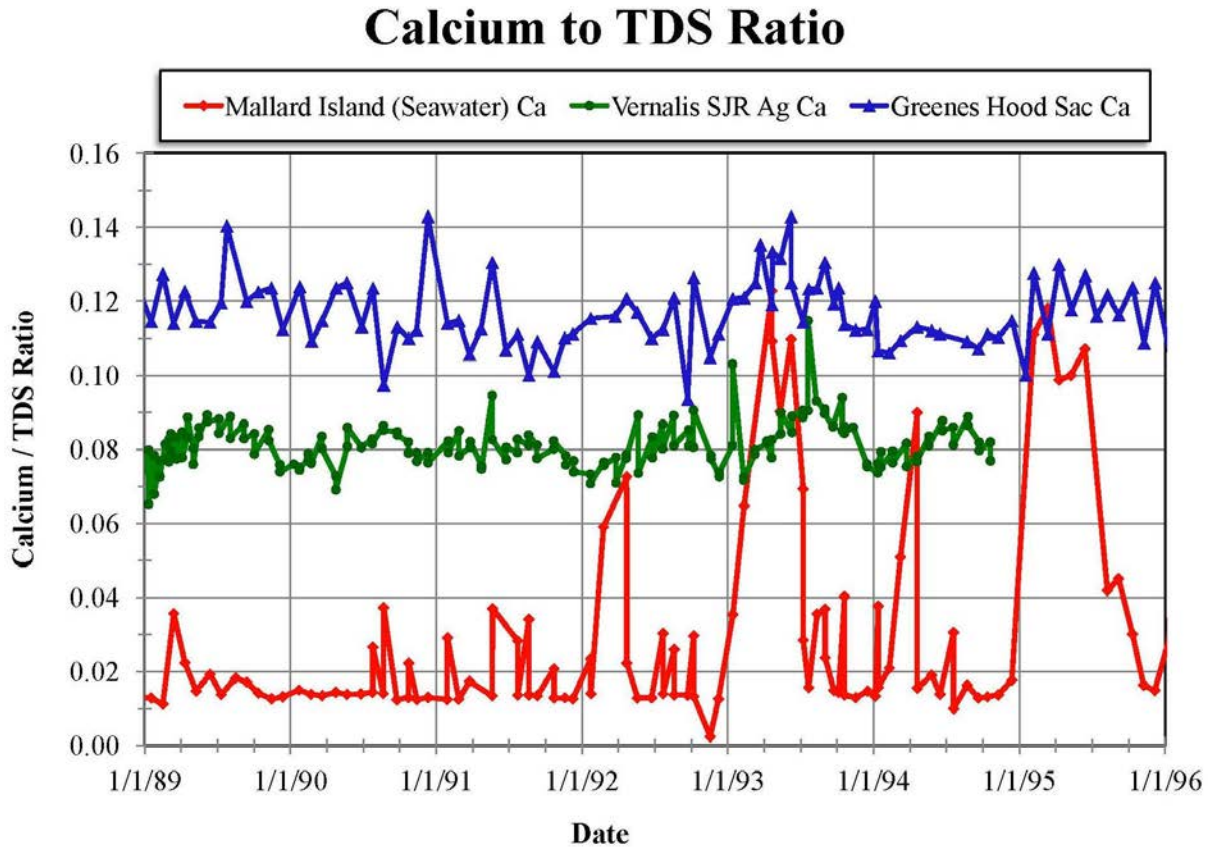


Figure B-17: Variation of calcium to TDS ratios for seawater, San Joaquin and Sacramento boundary conditions from 1989-1995. During periods of high outflow, the calcium/TDS ratio at Mallard Island increases significantly to a value representing a mixture of Sacramento and San Joaquin water. No data are available at Vernalis for 1995.

As shown in Table 4.1, the percentage contribution of chloride to TDS in seawater is high (55%) but the percentage is lower in agricultural drainage (21%). On the other hand, the percentage contribution of sulfate to TDS is high in agricultural drainage (22%) and extremely low in seawater (8%). Plotting chloride concentration as a function of sulfate concentration is a good way to more clearly distinguish between water that is dominated by seawater and water that is dominated by agricultural drainage. A similar approach was used by Suits (2002) who plotted calcium versus chloride.

Figure B-18 shows the relationship between chloride and sulfate concentrations for grab samples from the San Joaquin River at Vernalis and Maze (representing the San Joaquin boundary condition). The seawater-dominated regression equation (the red line labeled Sea Cl) was derived from grab samples from Mallard Island and Jersey Point. The corresponding agricultural drainage-dominated regression equation was derived from Vernalis and Maze grab samples collected since 1982. These equations represent an upper and lower limit on the grab sample data plotted in Figure B-18.

Vernalis & Maze Grab Samples

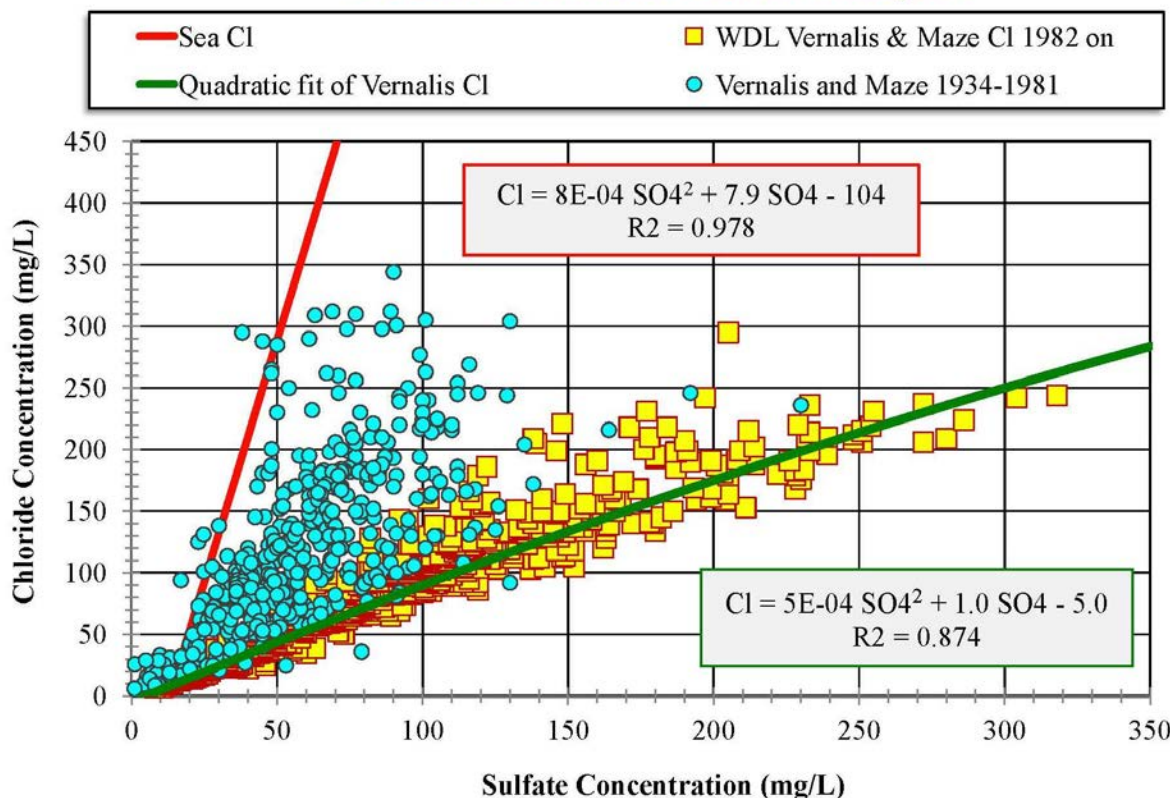


Figure B-18: Variation of chloride concentration as a function of sulfate concentration for grab samples from the San Joaquin River at Vernalis and Maze showing grab sample data collected prior to 1982. The higher chloride concentrations for a given sulfate concentration suggest the water in the San Joaquin River prior to 1982 often had a higher percentage of seawater than after 1982. The regression equation is based on post 1982 data only.

The relationship between chloride and sulfate at Vernalis and Maze appears to have changed over time. DWR recently posted additional grab sample data for Vernalis and Maze on the Water Data Library website that date back to 1934. The San Joaquin River data prior to 1982 appear to indicate a higher proportion of seawater (i.e., higher chloride concentration for a given sulfate concentration) than the post 1982 data.

The higher proportion of water with seawater characteristics prior to the 1980s may be due to high salinity water in the Tuolumne River from gas well operations. The gas wells were capped in 1979 using SWRCB Board cleanup and abatement account funds. Prior to the capping of these wells, the Tuolumne River salinity was about four times that of the Merced and Stanislaus Rivers (Les Grober, 2015, personal communication). The earlier Tuolumne River salinity problem is discussed in more detail in Kratzer and Grober (1991).

The regression equation for Vernalis and Maze data presented in this report is based on the original data set (1982 onwards) only.

Appendix C**Sacramento River Boundary Condition**

The Sacramento River below Sacramento is a key contributor to water quality in the north Delta. Detailed grab sample data from the Sacramento River at Hood (1982-2012) and Greenes Landing (1993-1998) were used to represent the Sacramento River boundary condition. Regression equations were developed by fitting the longer Hood data set. These regression equations are only applicable over the range of the Hood data, i.e., $70 < EC < 240 \mu\text{S}/\text{cm}$ and $45 < TDS < 140 \text{ mg/L}$, respectively.

The specific conductance of distilled water is about $1 \mu\text{S}/\text{cm}$ (Hem, 1985). It was, therefore, assumed that a fit of water quality constituents as a function of either EC or TDS had a zero intercept. Similarly, fits of water quality constituents as a function of TDS for the Sacramento River region were assumed to have a zero intercept. Where there appeared to be some distinct curvature to the data, the data were fitted with a quadratic equation with zero intercept.

At lower Sacramento River locations, such as below the Rio Vista Bridge, the grab sample data are consistent with the Hood and Greene Landing data during periods of high flow. However, as discussed in Chapter 8, seawater intrusion becomes a factor during very low Delta outflow periods, and the Rio Vista data follow the regression relationship for the seawater boundary condition.

As shown in Figure C-1 and C-2, the constituent percentages of TDS for the Sacramento River boundary condition stations are not constant but vary slightly with TDS. For chloride and sulfate the ratio increases with increasing TDS, whereas the calcium ratio decreases. The low range of concentrations (and the fact that much of the data are reported as integers) means that these ratios are not very precise.

Hood and Greenes Landing

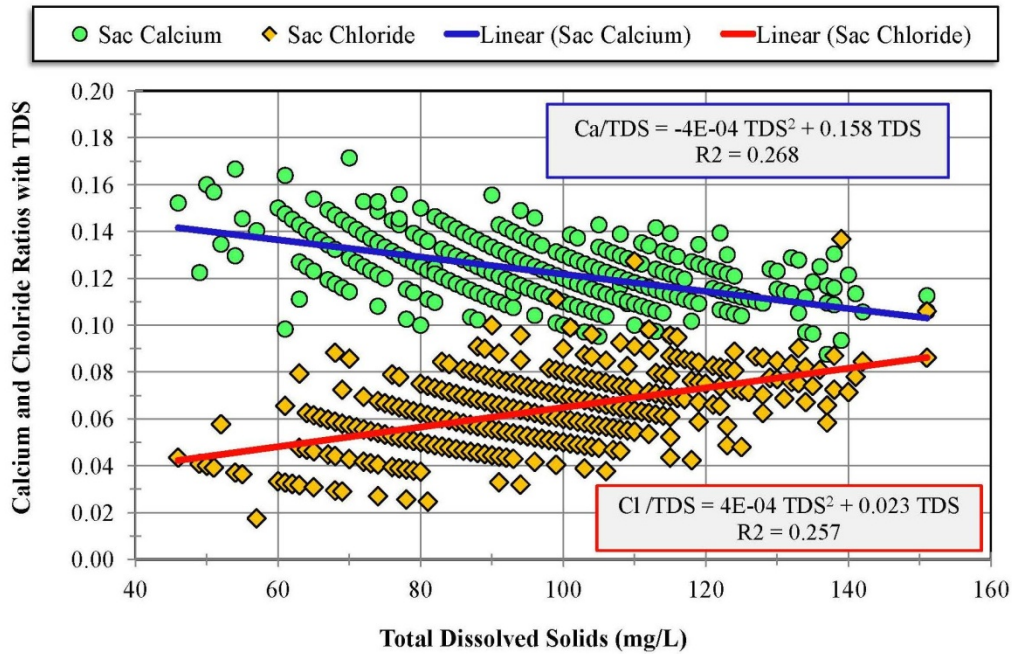


Figure C-1: Variation of the ratios of chloride and calcium concentration to total dissolved solids (TDS) as a function of TDS for the combined grab samples from the Sacramento River at Hood and Greenes Landing.

Hood and Greenes Landing

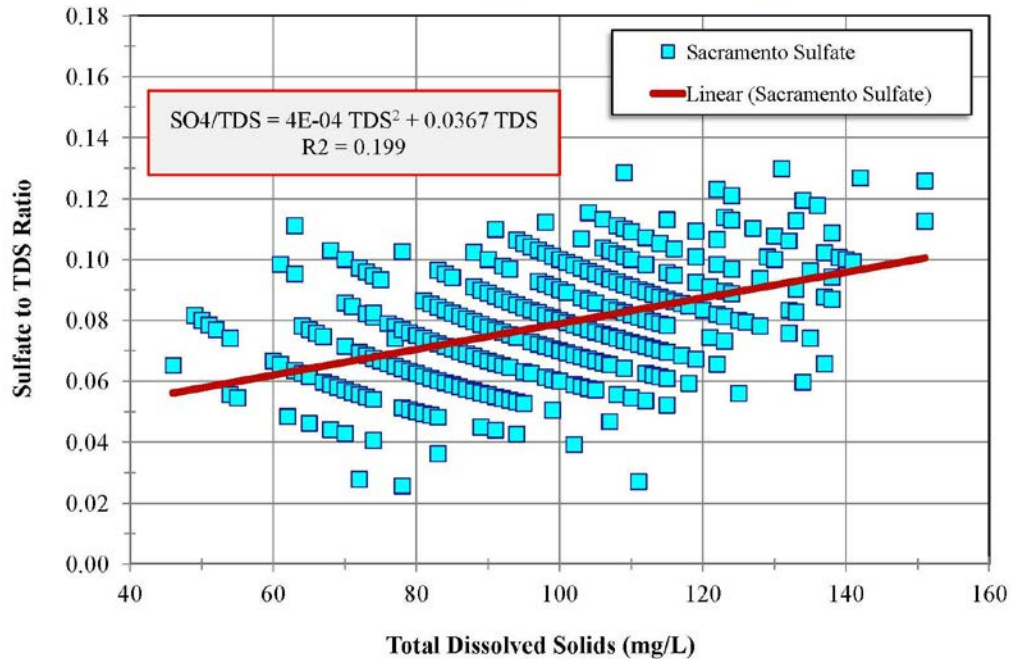


Figure C-2: Variation of the ratio of sulfate concentration to TDS as a function of TDS for the combined grab samples from the Sacramento River at Hood and Greenes Landing.

Figures C-3 through C-11 show the variations of the water quality constituents as a function of specific conductance (EC), i.e., chloride, bromide, sodium, calcium, sulfate, magnesium, potassium, hardness and alkalinity, respectively. Figure C-12 shows the variation of TDS with specific conductance for Hood and Greenes Landing.

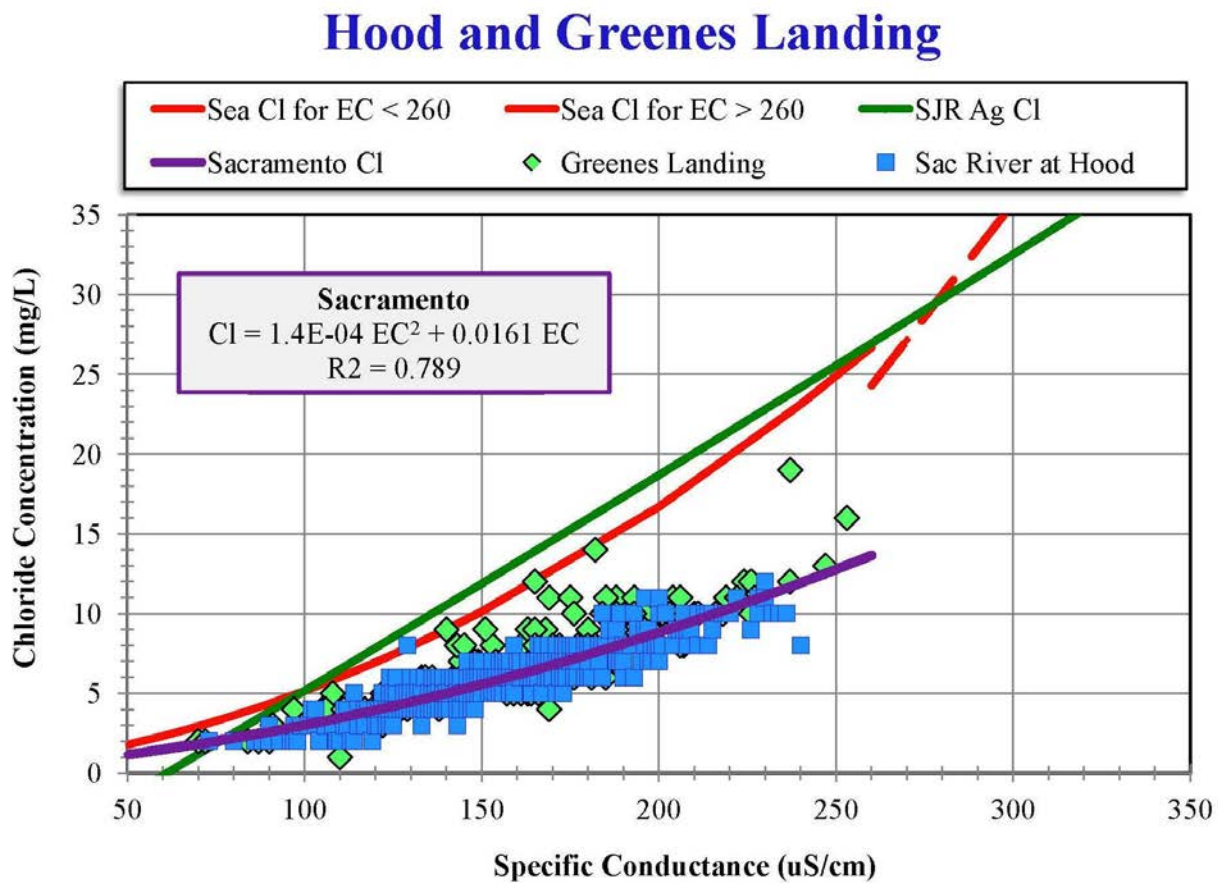


Figure C-3: Variation of chloride concentration as a function of specific conductance on the Sacramento River at Hood and Greenes Landing.

Hood and Greenes Landing

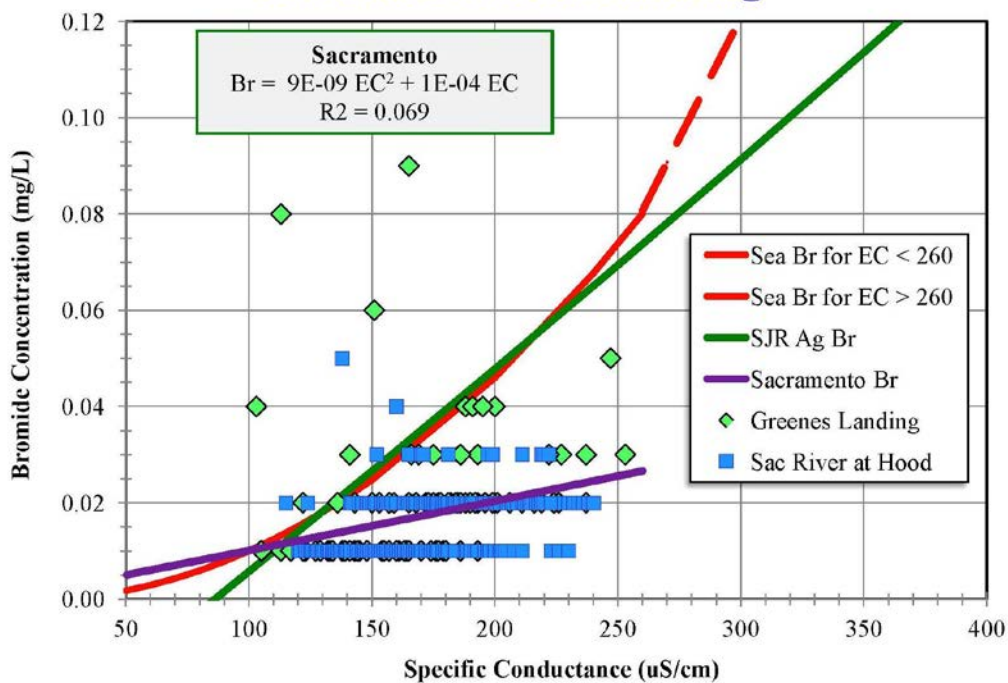


Figure C-4: Variation of bromide concentration as a function of specific conductance on the Sacramento River at Hood and Greenes Landing.

Hood and Greenes Landing

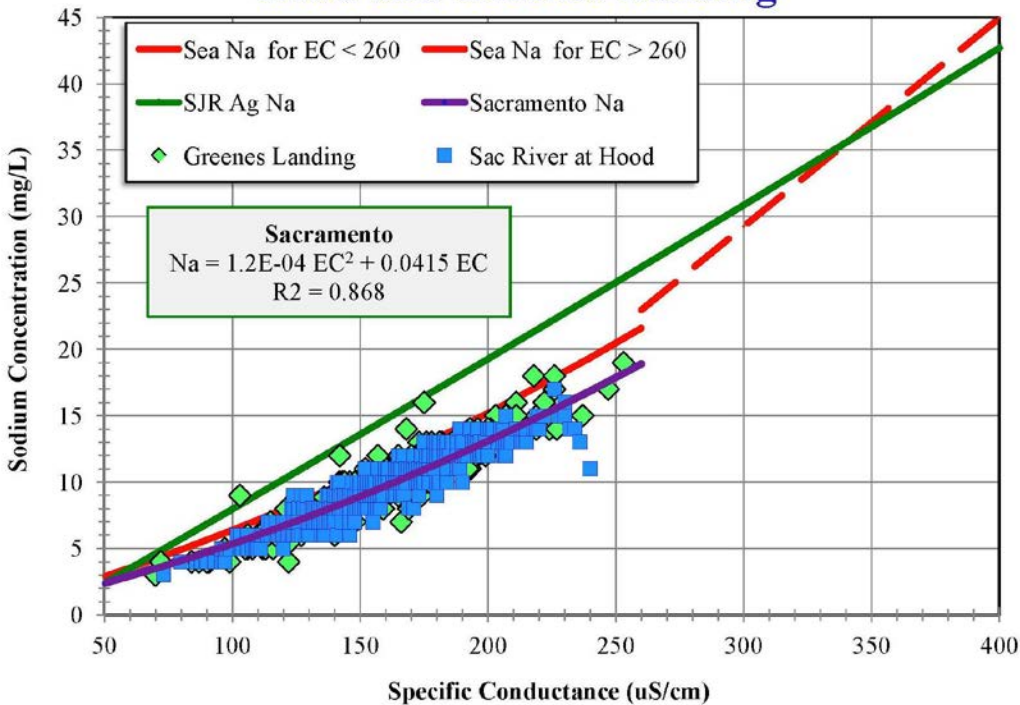


Figure C-5: Variation of sodium concentration as a function of specific conductance on the Sacramento River at Hood and Greenes Landing.

Hood and Greenes Landing

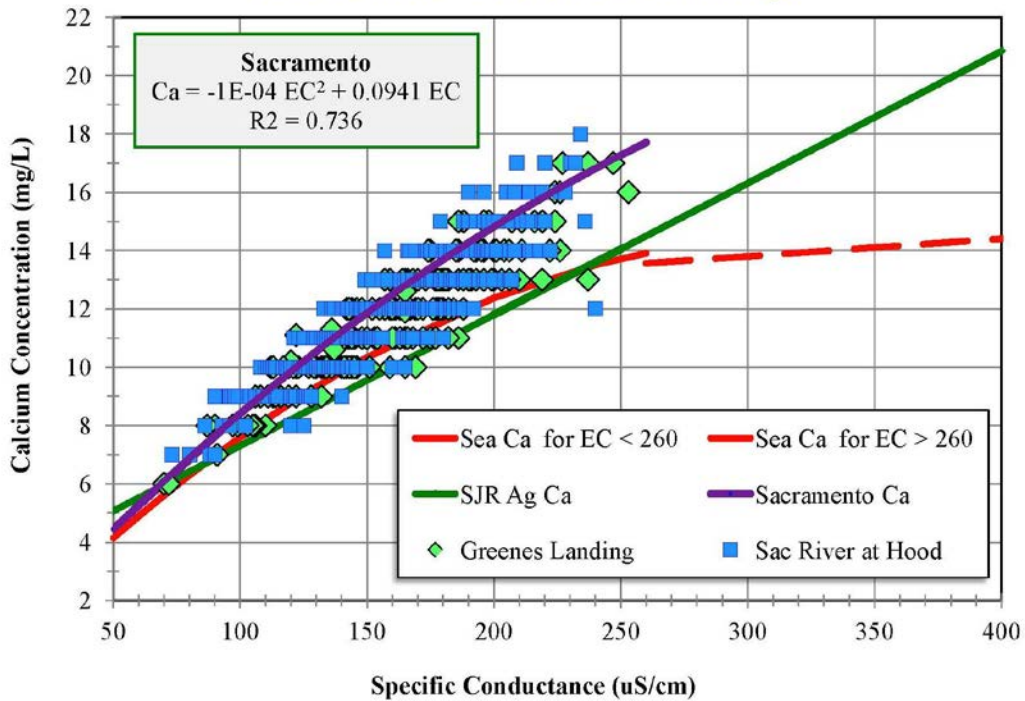


Figure C-6: Variation of calcium concentration as a function of specific conductance on the Sacramento River at Hood and Greenes Landing.

Hood and Greenes Landing

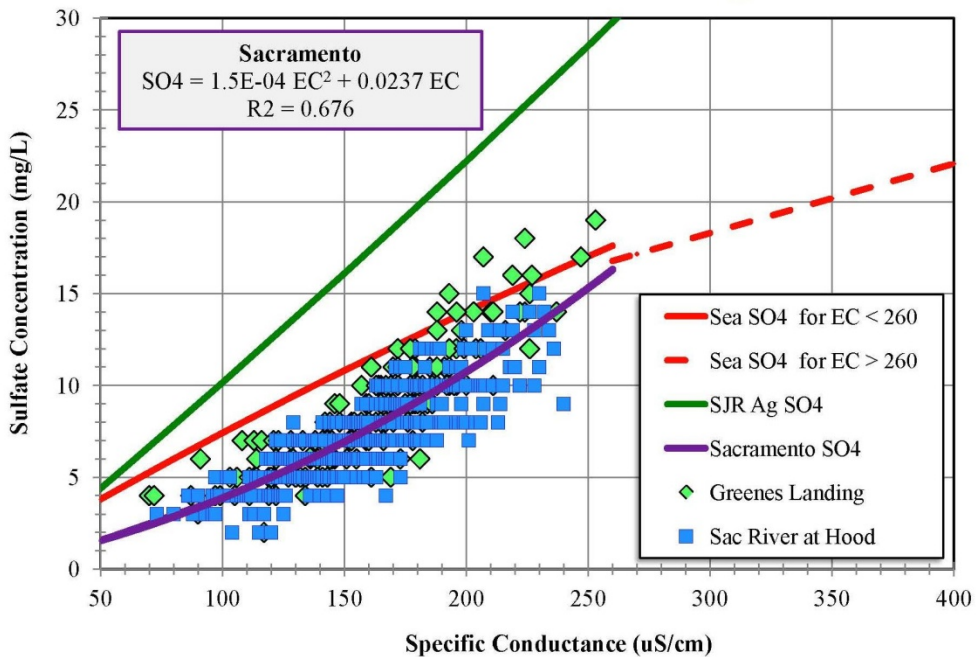


Figure C-7: Variation of sulfate concentration as a function of specific conductance on the Sacramento River at Hood and Greenes Landing.

Hood and Greenes Landing

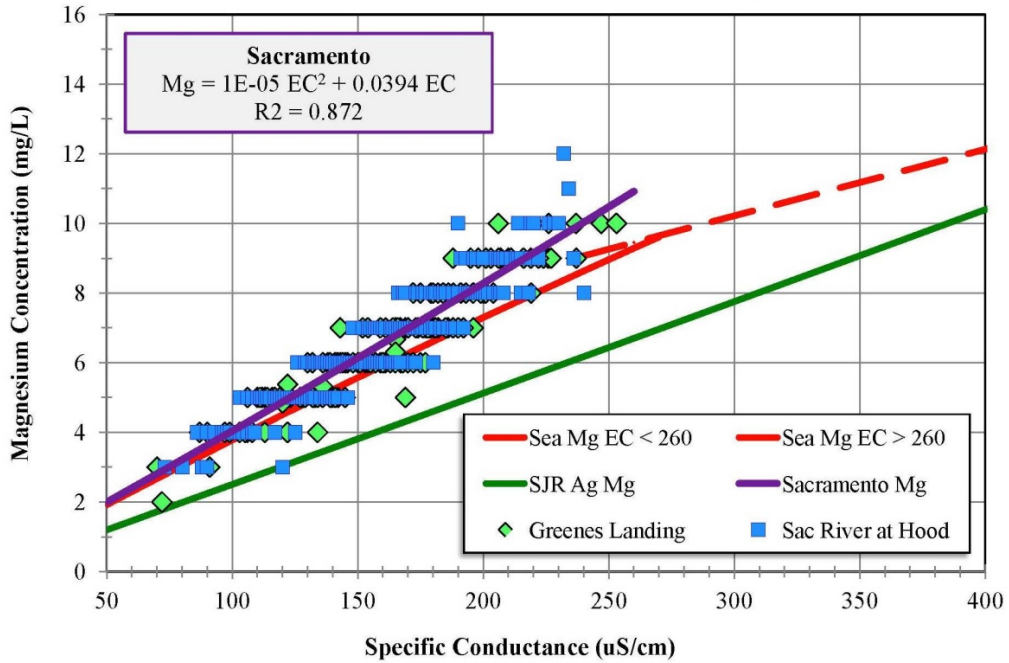


Figure C-8: Variation of magnesium concentration as a function of specific conductance on the Sacramento River at Hood and Greenes Landing.

Hood and Greenes Landing

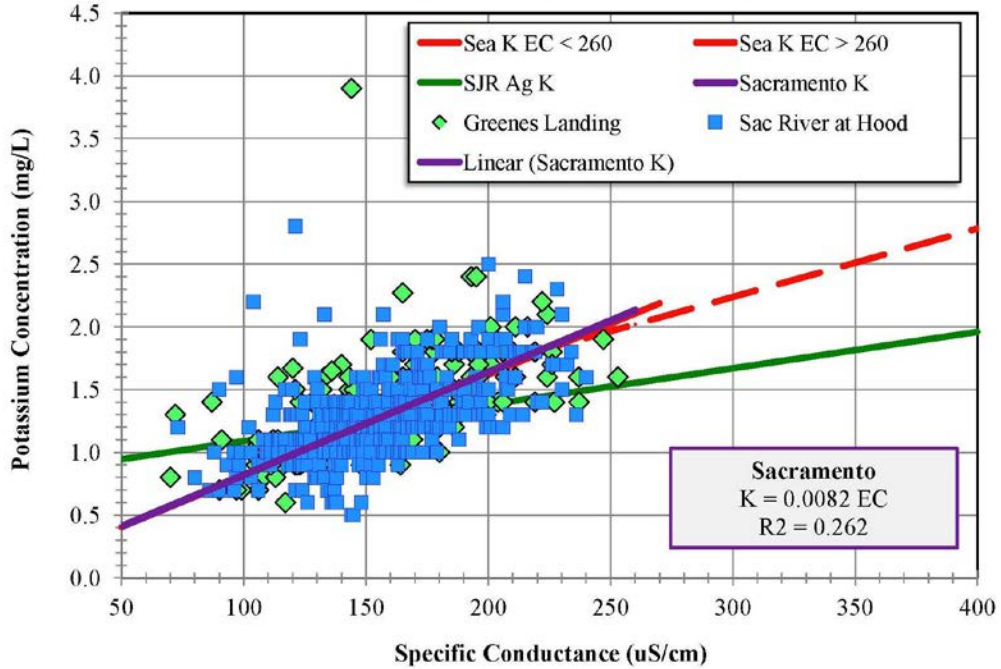


Figure C-9: Variation of potassium concentration as a function of specific conductance on the Sacramento River at Hood and Greenes Landing.

Hood and Greenes Landing

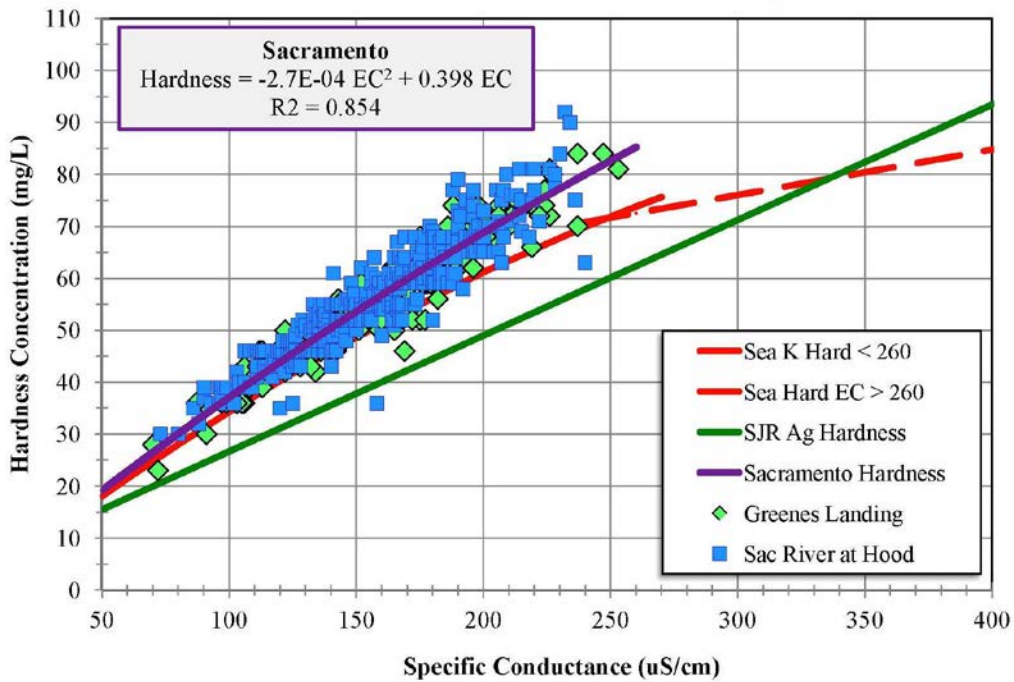


Figure C-10: Variation of hardness as a function of specific conductance on the Sacramento River at Hood and Greenes Landing.

Hood and Greenes Landing

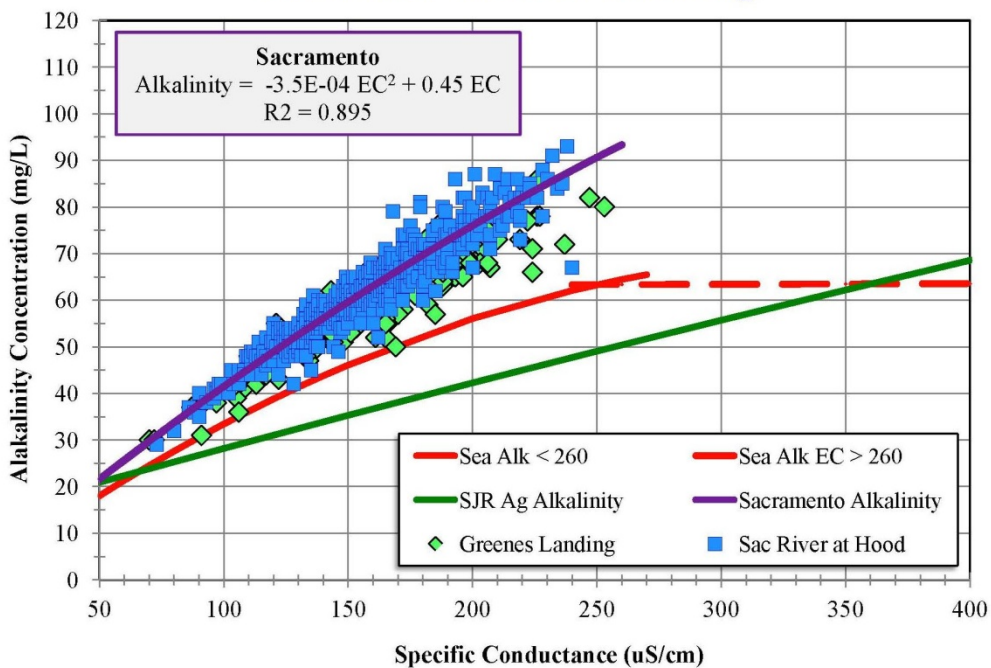


Figure C-11: Variation of alkalinity concentration as a function of specific conductance on the Sacramento River at Hood and Greenes Landing.

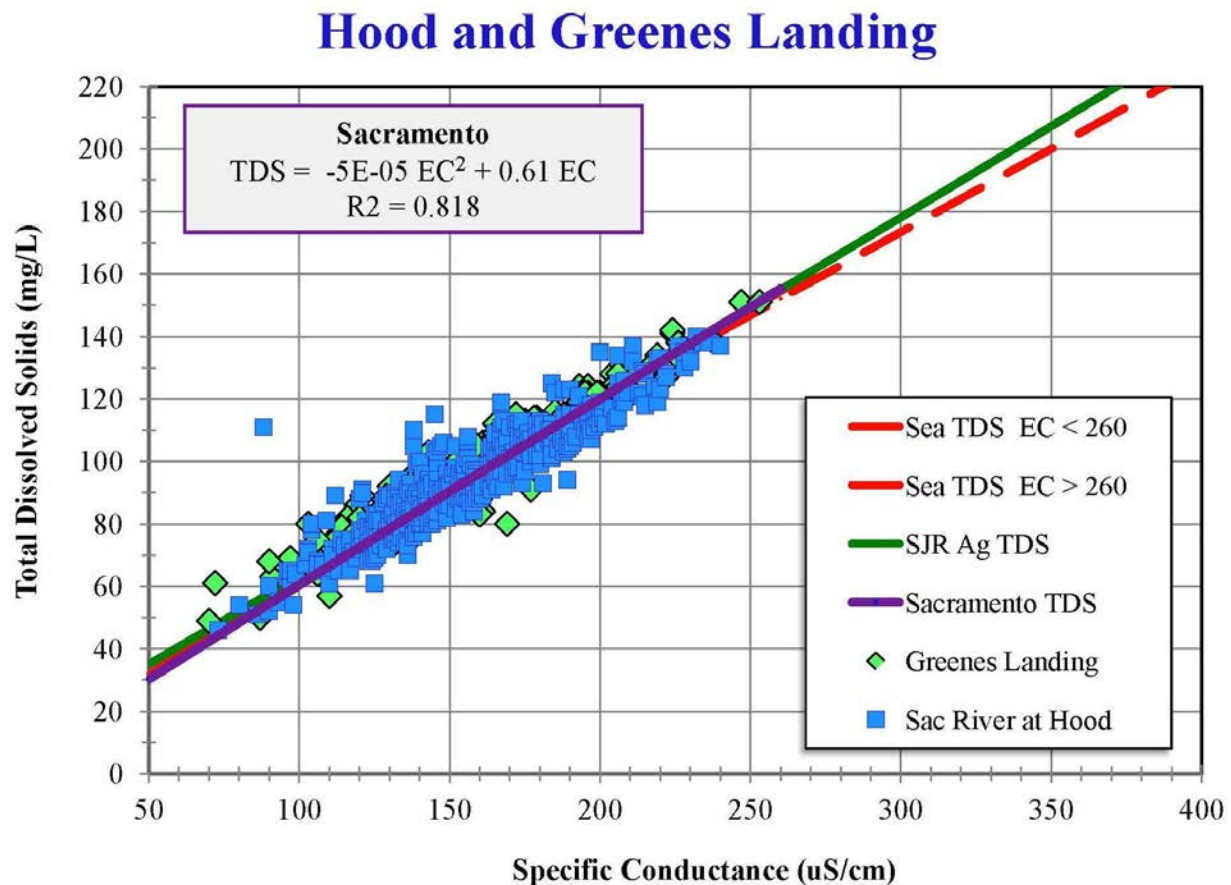


Figure C-12: Variation of total dissolved solids as a function of specific conductance on the Sacramento River at Hood and Greenes Landing.

The variation of the water quality constituents with TDS is similar to those with EC. The variation of chloride concentration with TDS is show in Figure C-13.

Hood and Greenes Landing

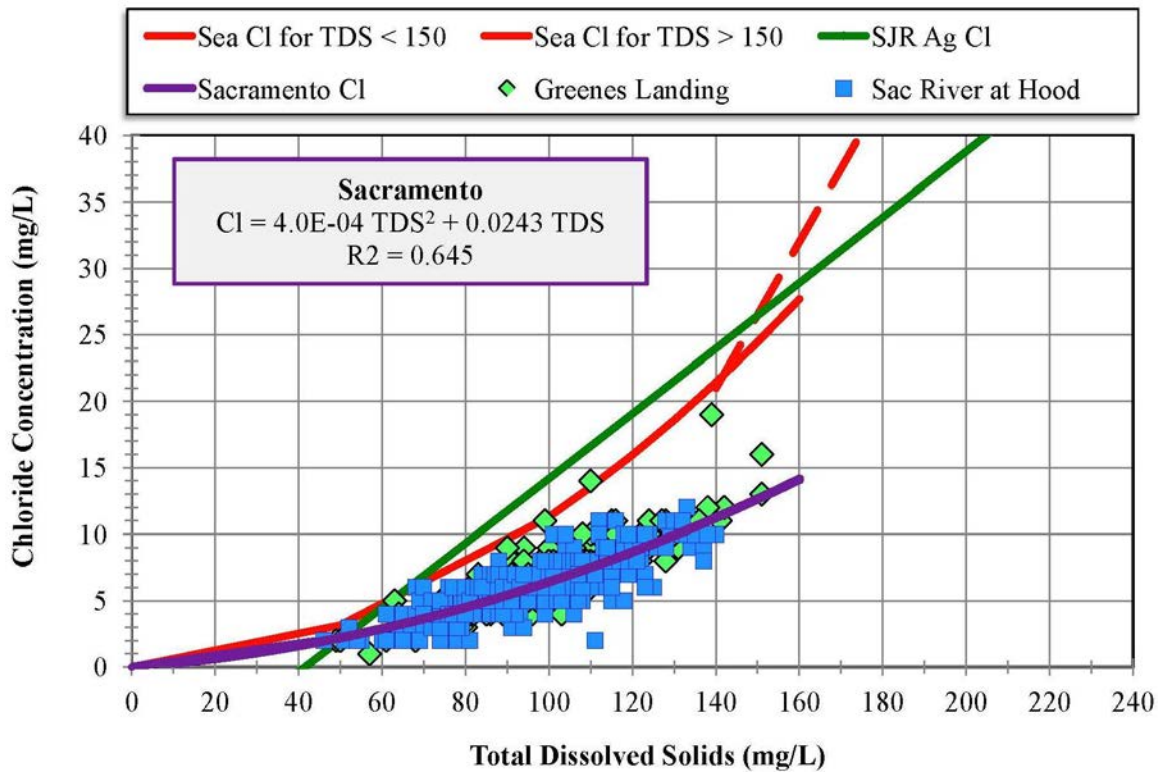


Figure C-13: Variation of chloride concentration as a function of total dissolved solids (TDS) on the Sacramento River at Hood and Greenes Landing.

The variation of bromide with chloride for Sacramento River inflow is shown in Figure C-14.

Hood and Greenes Landing

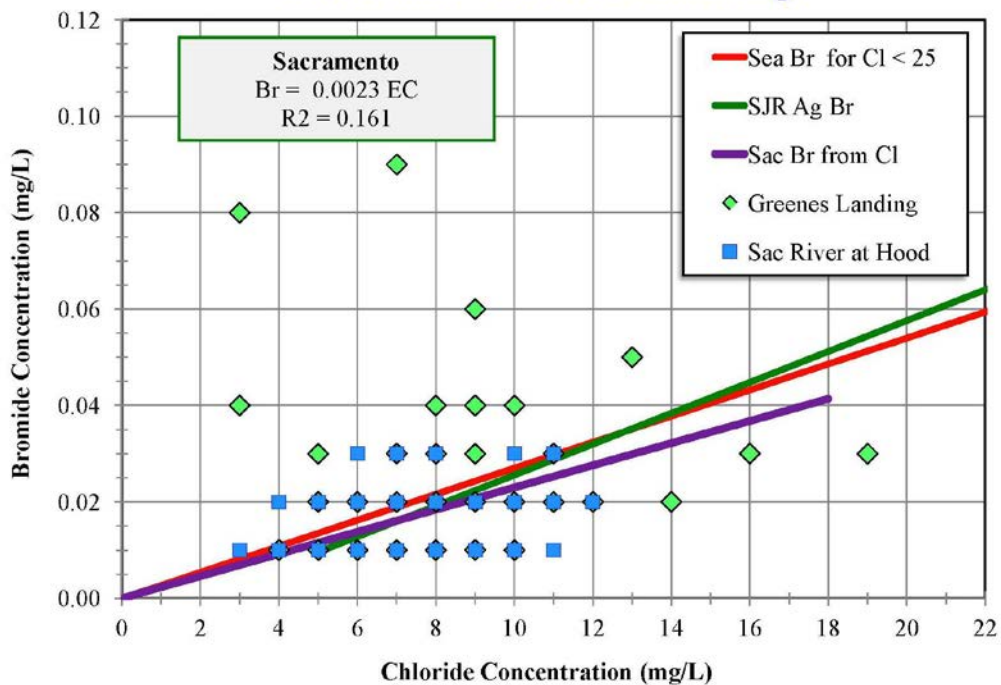


Figure C-14: Variation of bromide concentration as a function of chloride concentration on the Sacramento River at Hood and Greenes Landing.

The regression equations for the Sacramento River inflow boundary stations are best estimates but are not very accurate because of the low values of the grab sample concentrations and reporting of limited numbers of significant values.

Appendix D

Mokelumne River Boundary Condition

The Mokelumne River flows through Lodi and enters the Delta east of the Delta Cross Channel. The smaller Cosumnes River flows into the Mokelumne where it enters the Delta. The Mokelumne then splits into two forks, the North and South Forks, on either side of Staten Island and flows to the San Joaquin River on the west side of Bouldin Island.

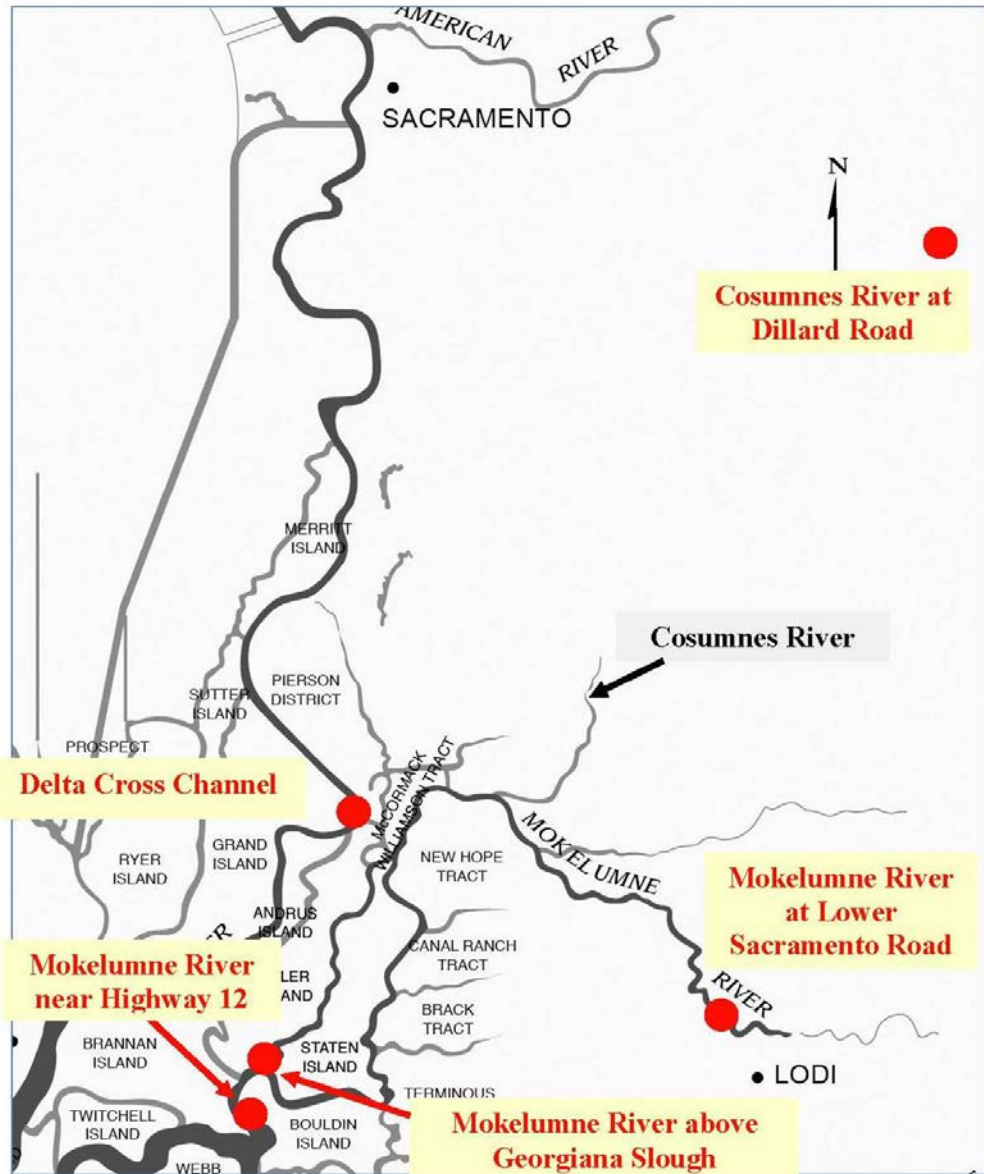


Figure D-1: Map showing key stations on the Mokelumne and Cosumnes River as well as the location of the adjacent Delta Cross Channel.

The relationship between water quality constituents (e.g., chlorine, calcium and sulfate) and specific conductance (EC) for the Mokelumne and Cosumnes Rivers where they enter the Delta appear to be very similar to the Sacramento River. As shown in Figure D-2, the chloride concentrations follow the same relationship as the equation for Sacramento River water (Appendix C).

The regression equations derived from the Sacramento River grab sample data (Hood and Greenes Landing) in Appendix C are for labeled in Figures D-2, D-3 and D-4. The corresponding seawater-dominated and agricultural drainage-dominated regression equations (Appendices A and B, respectively) are also shown for comparison purposes.

Mokelumne and Cosumnes Rivers

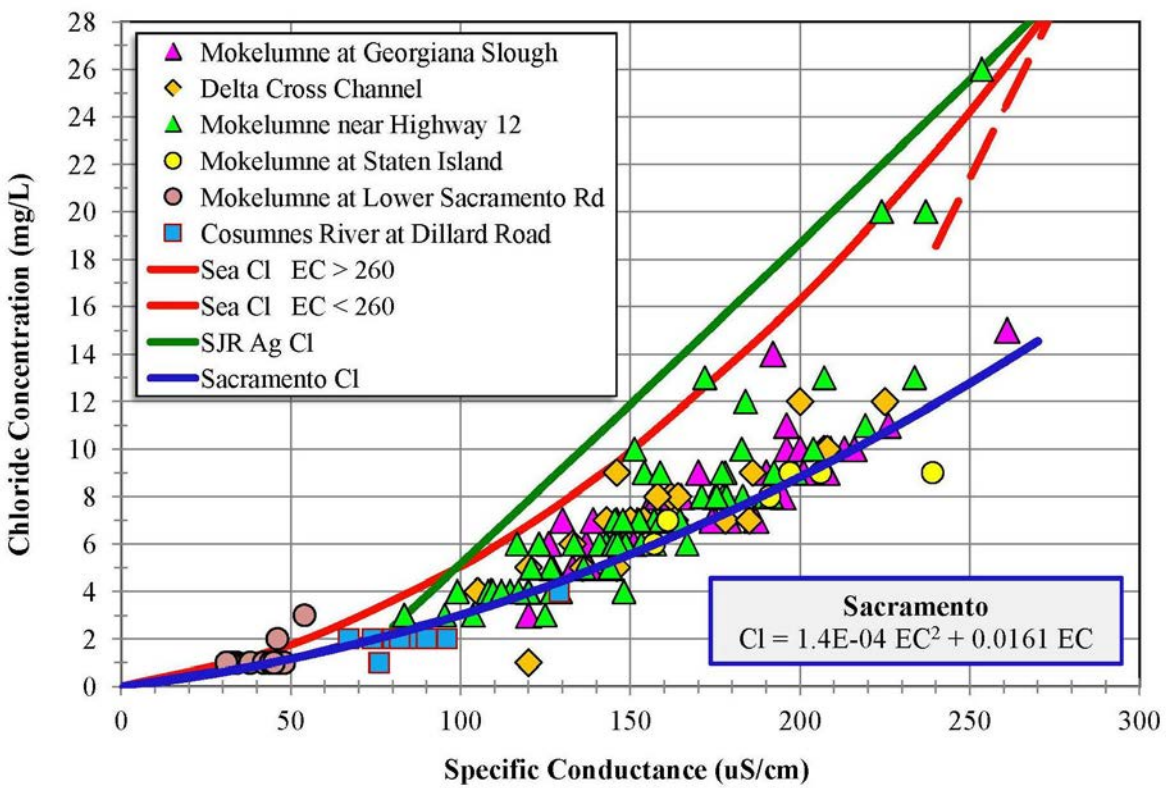


Figure D-2: Variation of Mokelumne and Cosumnes chloride concentrations as a function of specific conductance.

There are very few grab samples data points for the Mokelumne River at Lower Sacramento Road and Cosumnes River at Dillard Road. Additional stations from the Mokelumne River region were included in Figure D-2 and subsequent figures to check the consistency with Sacramento River data.

Seawater intrusion is not expected to influence water quality in this region outside of severe drought conditions. The high chloride concentrations for the Mokelumne River near Highway 4

(up to 26 mg/L) occurred during January-March 2012 which was a below normal water year (Figure 8-44). Only chloride, bromide and EC are available at that station so it is difficult to determine whether these high chlorides during this period were due to seawater intrusion or agricultural drainage.

The relationships for calcium and sulfate concentrations are also similar to the Sacramento River boundary conditions (Figures D-3 and D-4).

Mokelumne and Cosumnes Rivers

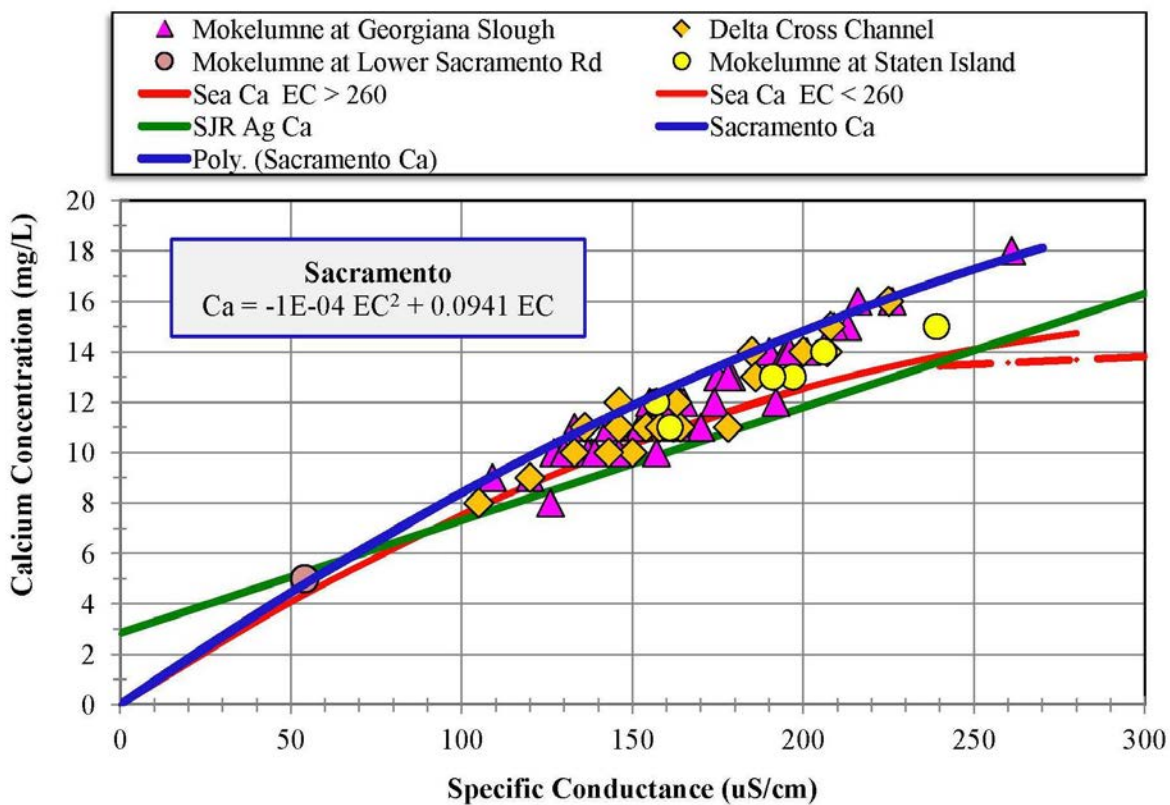


Figure D-3: Variation of Mokelumne and Cosumnes calcium concentrations as a function of specific conductance.

Mokelumne and Cosumnes Rivers

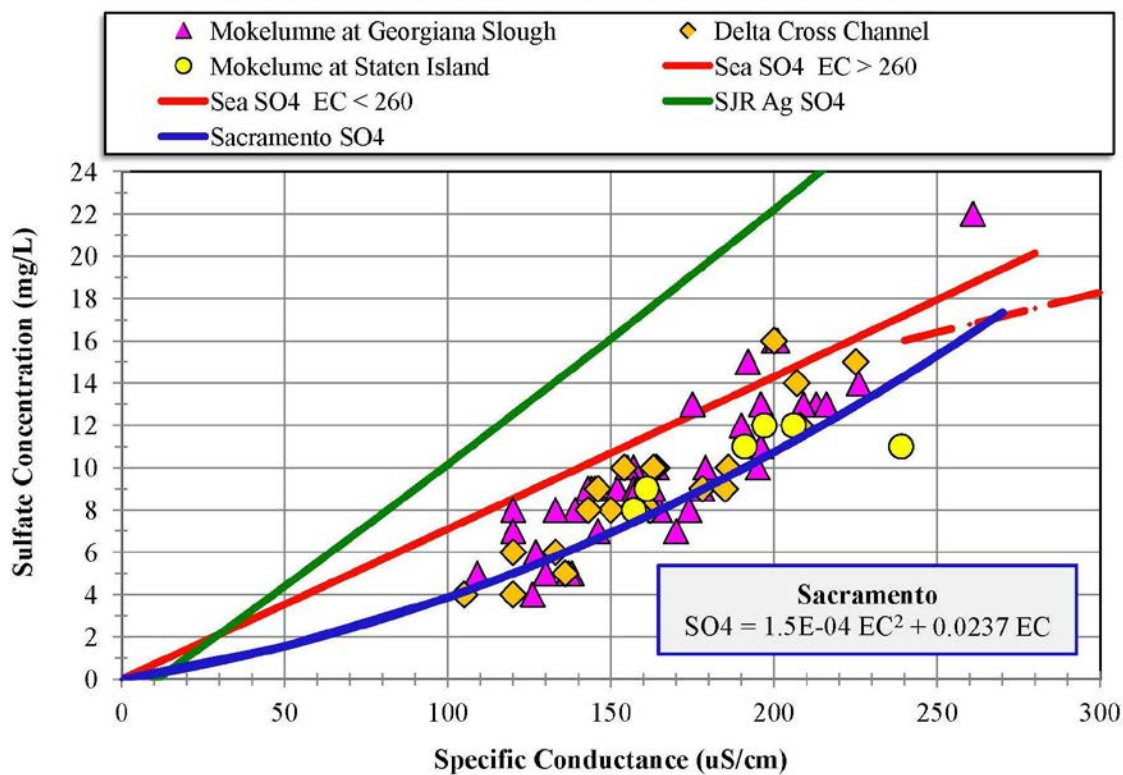


Figure D-4: Variation of Mokelumne and Cosumnes sulfate concentrations as a function of specific conductance.

Appendix E

Water Quality Constituent Ratios

Hutton (2006) reported that the constituent percentages of TDS for seawater, Sacramento River water at Greenes Landing, and San Joaquin River water at Vernalis were as shown in the following table.

Table E-1: Constituent Concentrations as a Percentage of Total Dissolved Solids

Mineral	Symbol	Percentage for Seawater (Mallard Island)	Percentage for Sacramento River water (Greenes Landing)	Percentage for San Joaquin River water (Vernalis)
Chloride	Cl	55	7	21
Sodium	Na	31	11	18
Sulfate	SO ₄	8	9	22
Magnesium	Mg	4	8	4
Calcium	Ca	1	14	8
Potassium	K	1	2	1
Alkalinity (as Bicarbonate)	HCO ₃		44	16
Nitrate	NO ₃		5	10

At Mallard Slough, e.g., the ratio of chloride to TDS would be expected to be about 0.55 under very low Delta outflow conditions (high TDS) when seawater dominates. However the Cl/TDS ratio decreases to less than 0.10 under very high outflow conditions when seawater intrusion is negligible and Sacramento River water dominates.

The variations in the Cl/TDS ratio with TDS for the three main sources of Delta water follow well-defined relationships, as shown in Figure E-1. In the (typically) seawater dominated region, represented by grab sample data from Mallard Island and Jersey Point, the Cl/TDS ratio increases as seawater intrusion increases (higher TDS and lower Delta outflows) eventually reaching the seawater-dominated ratio of 0.55. Under high Delta outflow conditions, the western Delta and Suisun Bay stations are swamped with Sacramento River water and highly diluted San Joaquin River water.

The Cl/TDS ratio at Vernalis shows a similar trend, reaching a maximum range of 0.21 to 0.30 under high TDS (low San Joaquin flow) conditions. It should be noted that San Joaquin River water at Vernalis is a mixture of relatively fresh water from the eastside tributaries, and agricultural drainage. Any agricultural drainage reaching the San Joaquin River from the westside of the San Joaquin Valley includes irrigation water pumped from the Delta at the SWP Banks and CVP Jones intakes. After long periods of low Delta outflow, the salinity of the water pumped from the Delta increases. The Cl/TDS ratio at Vernalis increases above 0.21 when the salinity of the applied irrigation water is highest.

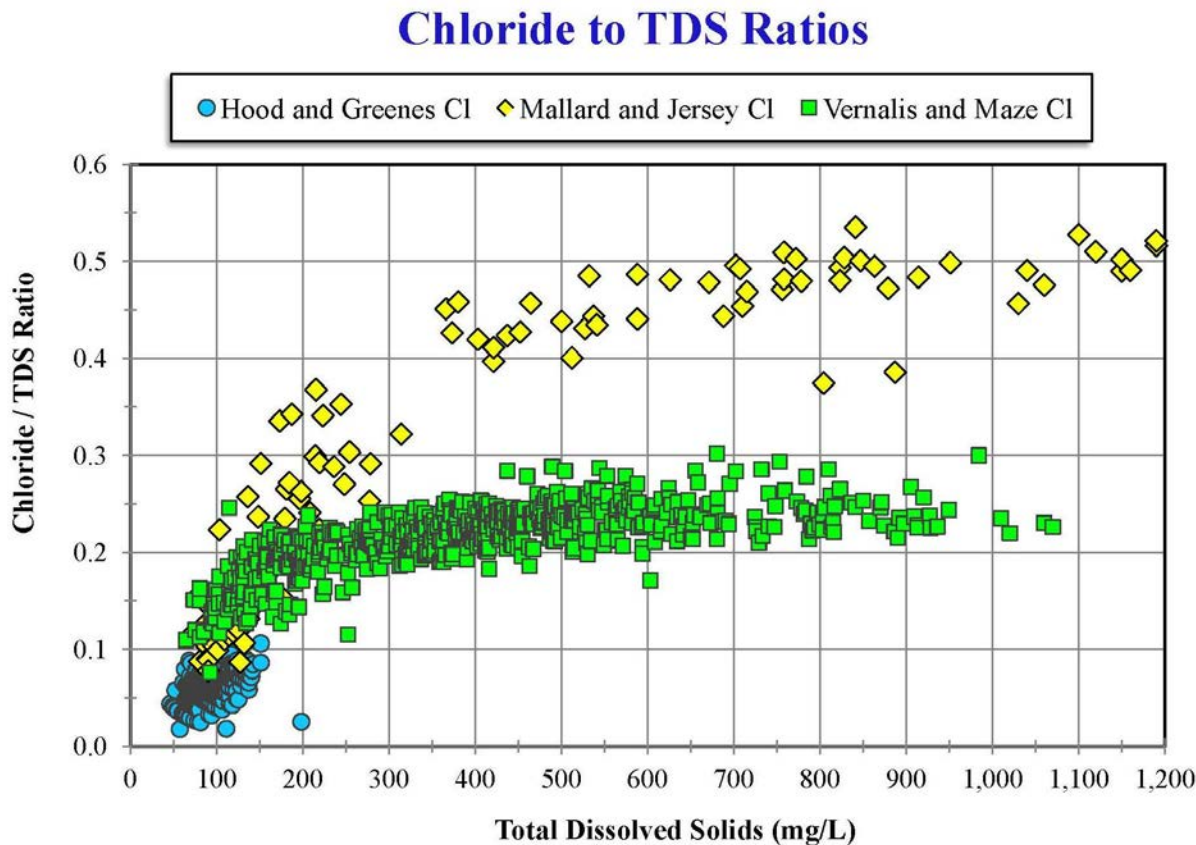


Figure E-1: Ratio of chloride concentration to total dissolved solids as a function of TDS for three different sources of Delta water: seawater intruding through Suisun Bay (represented by grab samples from Mallard Island and Jersey Point), San Joaquin inflow and Sacramento inflow.

Figures E-2 through Figure E-9 show the corresponding variations in the constituent to TDS ratios for the three sources of Delta water for bromide, sodium, calcium, sulfate, magnesium, potassium, hardness and alkalinity, respectively. Figure E-10 shows the variation of the ratio of specific conductance to TDS as a function of TDS.

The variations of the different ratios as a function of TDS can be categorized into four groups. The ratios of chloride, bromide and sodium show similar patterns as a function of TDS (and EC). The seawater ratio tends to a higher value than the agricultural drainage value at high TDS. At low TDS, all the curves tend to a low ratio, corresponding to Sacramento-dominated water.

The variations of calcium, magnesium, hardness (which is calculated from Ca and Mg), and alkalinity have the same pattern. The variations of the different ratios as a function of TDS can be categorized into four groups. The seawater ratio tends to a lower value than the agricultural drainage value at high TDS. At low TDS, all the curves tend to a high ratio, corresponding to Sacramento-dominated water.

The ratio of sulfate to TDS is different in that agricultural drainage data tends to a high ratio (0.28) at high TDS whereas the seawater-dominated tends to a low ratio asymptote (0.07). Both trend toward a low ratio at low TDS.

The ratio of potassium to TDS is different than the other three categories in that both agricultural drainage and seawater-dominated data tend to low ratio asymptotes. Unlike for calcium and magnesium, the agricultural-dominated asymptote is lower than the seawater asymptote.

Bromide to TDS Ratios

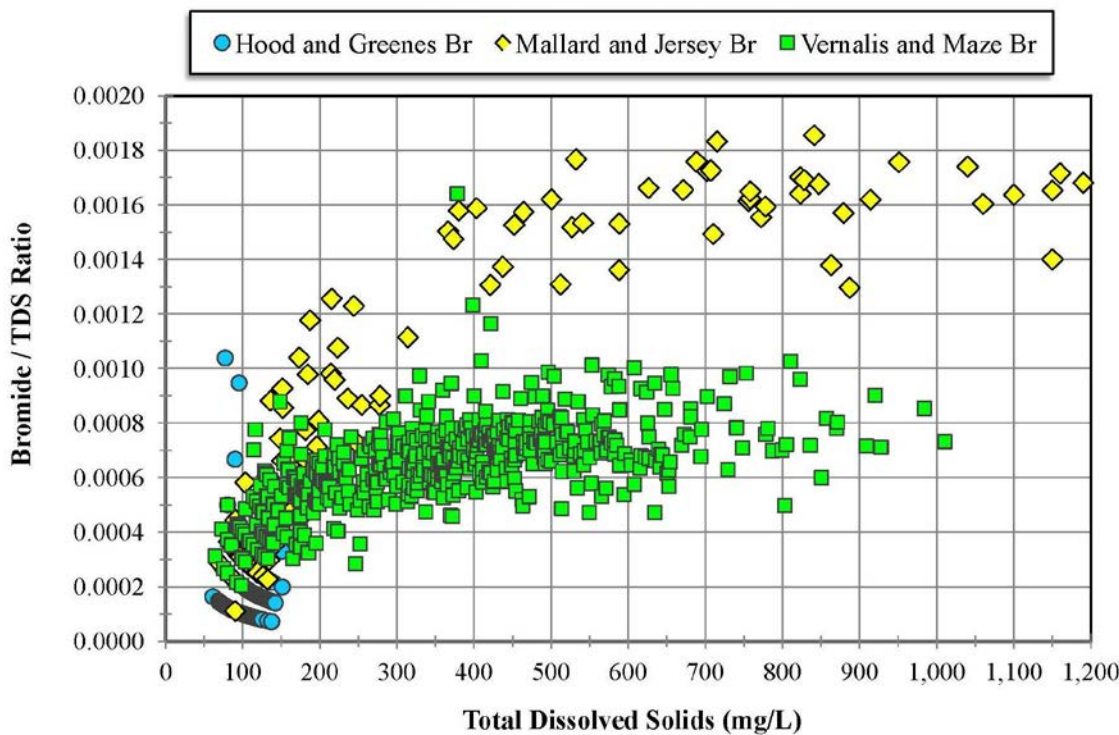


Figure E-2: Ratio of bromide (Br) concentration to total dissolved solids as a function of TDS for three different sources of Delta water: seawater intruding through Suisun Bay (represented by grab samples from Mallard Island and Jersey Point), San Joaquin inflow and Sacramento inflow. The trend is similar to that for chloride concentration.

Sodium to TDS Ratios

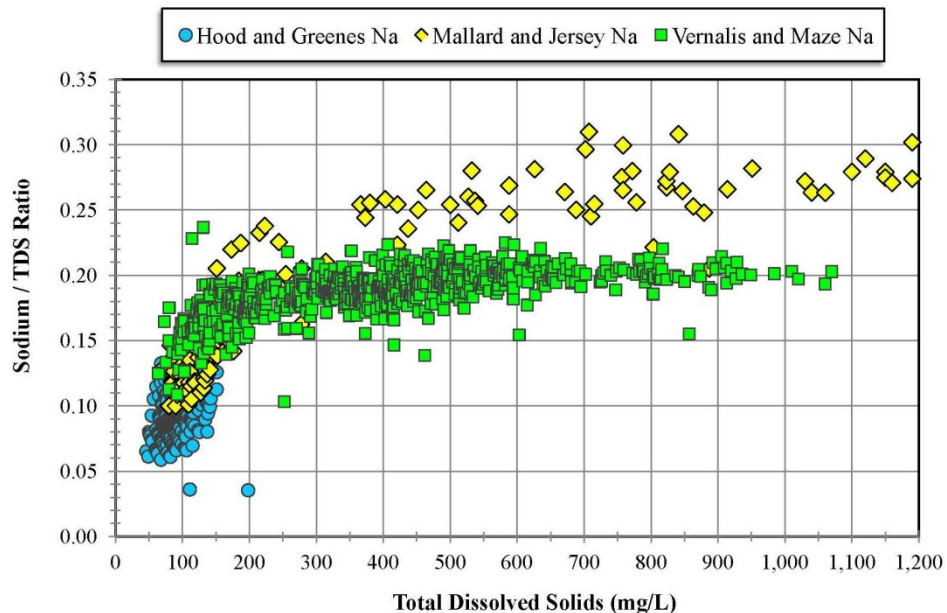


Figure E-3: Ratio of sodium (Na) concentration to total dissolved solids as a function of TDS for three different sources of Delta water: seawater intruding through Suisun Bay, San Joaquin inflow and Sacramento inflow. The trend is similar to that for chloride and bromide concentrations.

Calcium to TDS Ratios

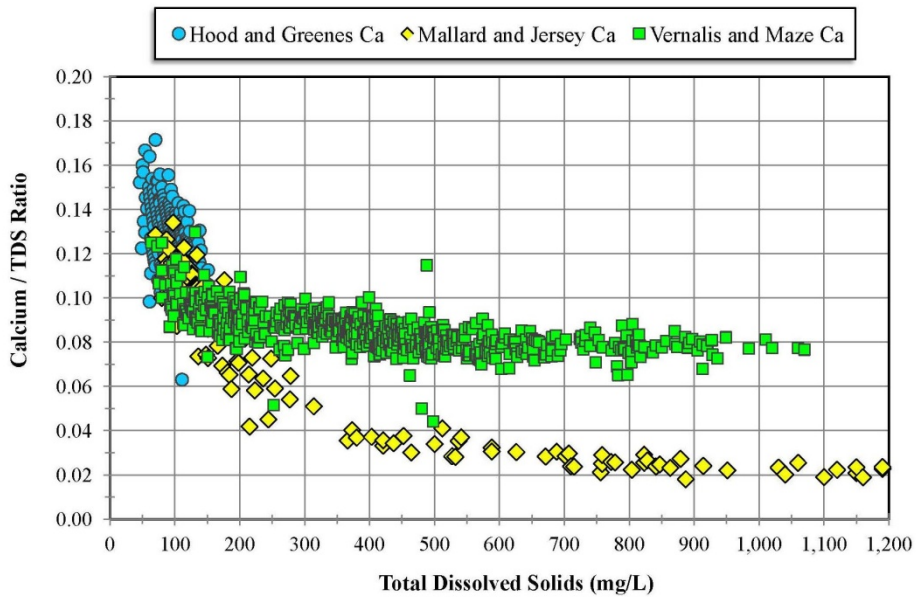


Figure E-4: Ratio of calcium (Ca) concentration to total dissolved solids as a function of TDS for three different sources of Delta water: seawater intruding through Suisun Bay, San Joaquin inflow and Sacramento inflow. In this case, the Ca/TDS ratio for seawater is much lower than for San Joaquin River water, i.e., the opposite of the chloride concentration ratios.

Sulfate to TDS Ratios

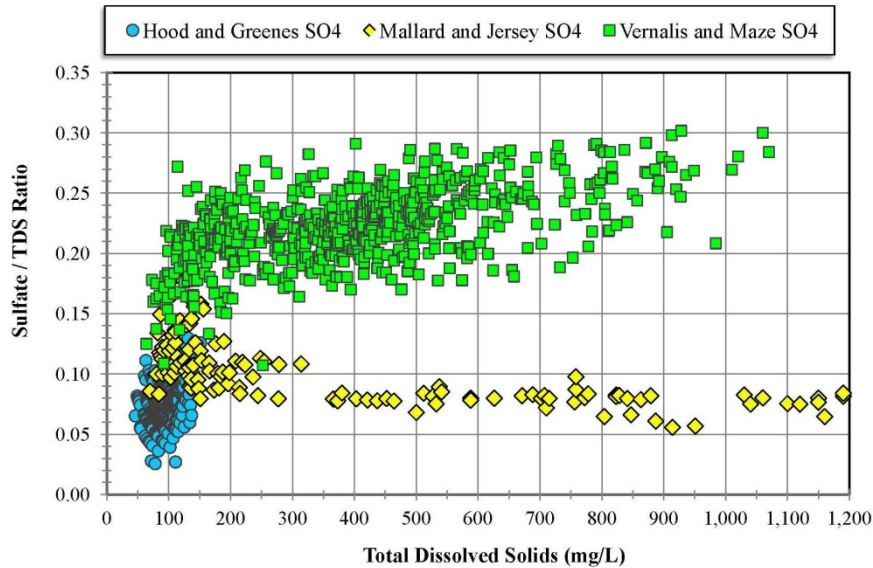


Figure E-5: Ratio of sulfate (SO_4) concentration to total dissolved solids as a function of TDS for three different sources of Delta water: seawater intruding through Suisun Bay, San Joaquin inflow and Sacramento inflow. As was the case for calcium, the SO_4/TDS ratio for seawater is much lower than for San Joaquin River water. However, unlike for calcium, the SO_4/TDS ratio for San Joaquin River water decreases at low TDS rather than increasing.

Magnesium to TDS Ratios

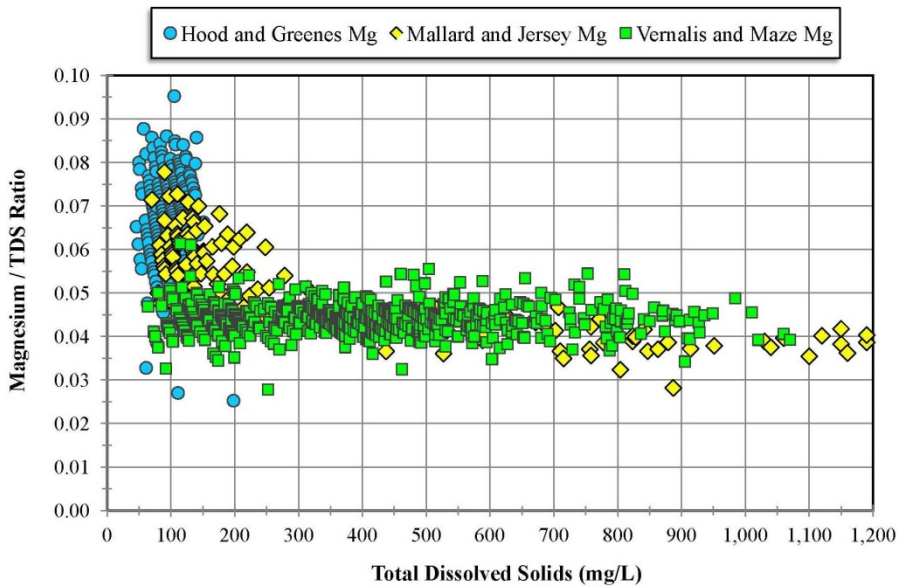


Figure E-6: Ratio of magnesium (Mg) concentration to total dissolved solids as a function of TDS for three different sources of Delta water: seawater intruding through Suisun Bay, San Joaquin inflow and Sacramento inflow. The Mg/TDS ratio for seawater increases as TDS decreases. The San Joaquin River water ratio remains relatively constant with TDS and is only slightly larger than the seawater ratio at high TDS.

Potassium to TDS Ratios

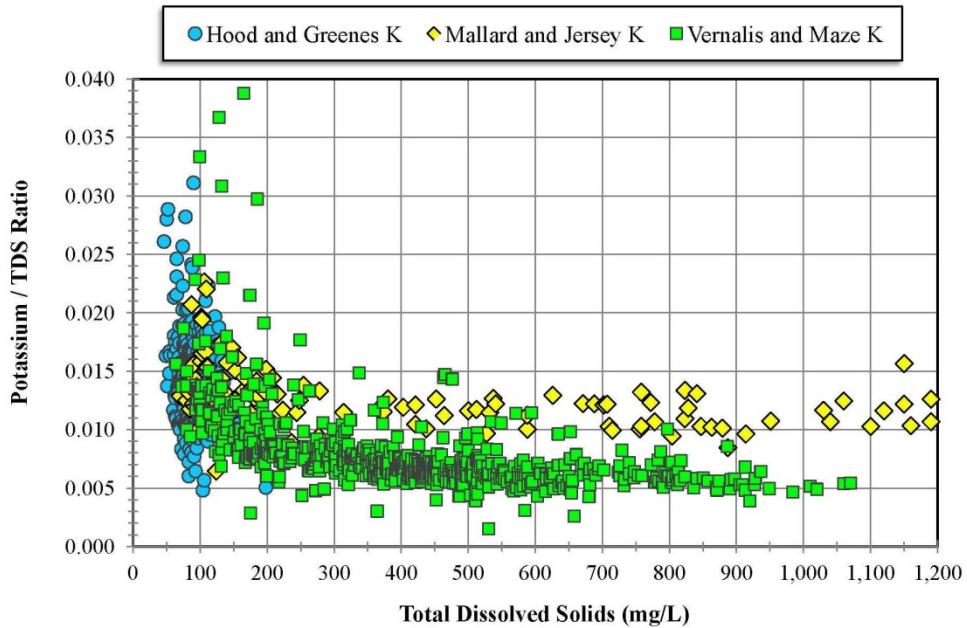


Figure E-7: Ratio of potassium (K) concentration to total dissolved solids as a function of TDS for three different sources of Delta water: seawater intruding through Suisun Bay, San Joaquin inflow and Sacramento inflow. The K/TDS ratios for seawater and San Joaquin River water both increase as TDS decreases.

Hardness to TDS Ratios

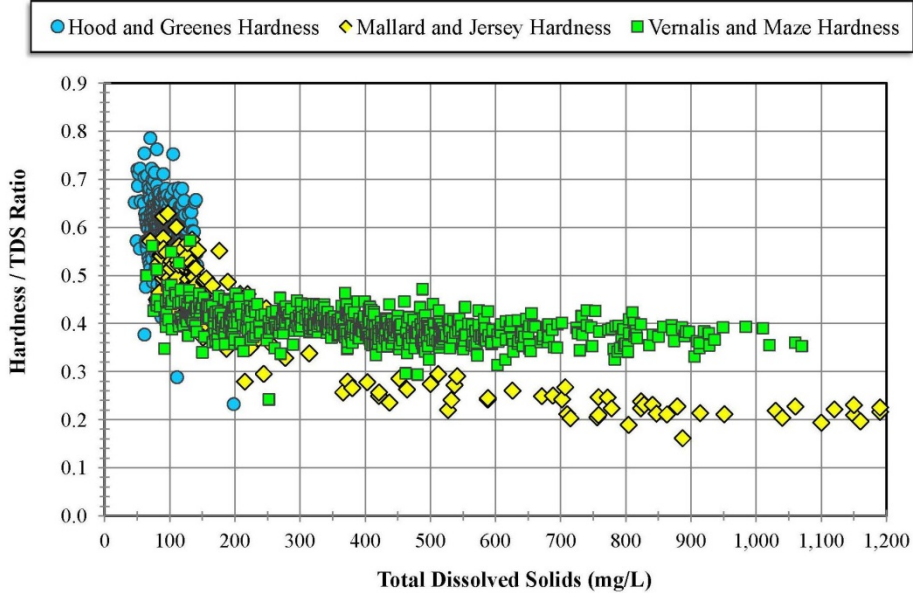


Figure E-8: Ratio of hardness to total dissolved solids as a function of TDS for three different sources of Delta water: seawater intruding through Suisun Bay, San Joaquin inflow and Sacramento inflow. The hardness ratios for seawater and San Joaquin River water both increase as TDS decreases.

Alkalinity to TDS Ratios

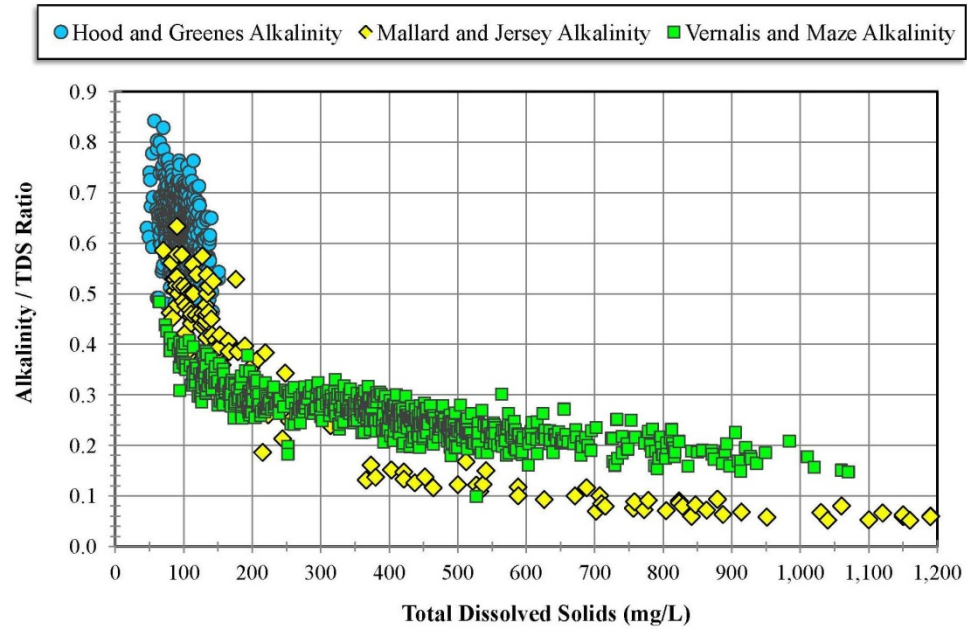


Figure E-9: Ratio of alkalinity to total dissolved solids as a function of TDS for three different sources of Delta water: seawater intruding through Suisun Bay, San Joaquin inflow and Sacramento inflow.

Specific Conductance to TDS Ratios

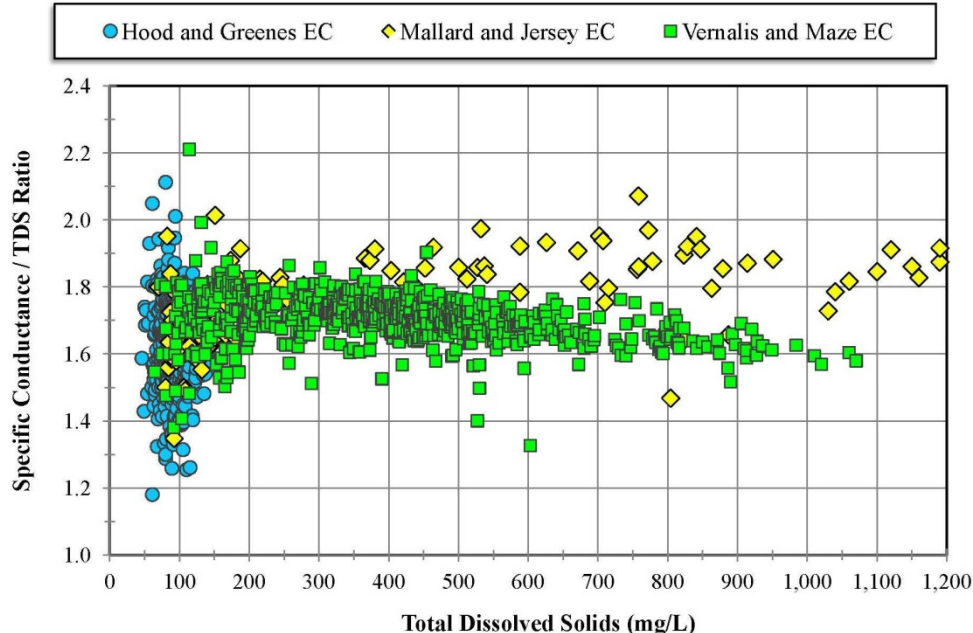


Figure E-10: Ratio of specific conductance to total dissolved solids as a function of TDS for three different sources of Delta water: seawater intruding through Suisun Bay, San Joaquin inflow and Sacramento inflow.

Appendix F

Tracking Sources of Delta Water Using DSM2 Fingerprint Data

The California Department of Water Resources's Delta Simulation Model (DSM2) can be used to compute the transport of salinity from multiple sources throughout the Delta. The salinities resulting from five different sources are tracked independently. The five sources are the downstream seawater boundary condition (Suisun Bay at Martinez), the Sacramento inflow at Freeport, the San Joaquin inflow at Vernalis, the inflow from the eastside streams (Mokelumne, Cosumnes, Calaveras and other miscellaneous streams), as well as local agricultural discharges within the Delta. This technique for tracing the EC and volumes of water from different sources is commonly referred to as "fingerprinting."

DWR's fingerprint modeling is discussed in more detail in the following reports:

- Methodology for Flow and Salinity Estimates in the Sacramento-San Joaquin Delta and Suisun Marsh, 23rd Annual Progress Report, June 2002. Chapter 14: DSM2 Fingerprinting Methodology, by Jamie Anderson
<http://modeling.water.ca.gov/delta/reports/annrpt/2002/2002Ch14.pdf>
- Methodology for Flow and Salinity Estimates in the Sacramento-San Joaquin Delta and Suisun Marsh, 26th Annual Progress Report, October 2005. Chapter 6: Fingerprinting: Clarifications and Recent Applications, by Jamie Anderson and Jim Wilde
<http://modeling.water.ca.gov/delta/reports/annrpt/2005/2005Ch6.pdf>

Bob Suits (DWR) provided fingerprint data from a DSM2 historical simulation for 1975-2010. This historical study preserved all the operational details of the actual historical Delta and upstream operations.

The DSM2 fingerprint data were used to determine the periods, e.g., when seawater dominated in given locations in the Delta, and when agricultural return flows from the San Joaquin Valley and local discharges dominated. As shown later in this appendix, the specific conductance (EC) at interior Delta locations due to seawater intrusion was highly correlated with the EC at Jersey Point. This was consistent with the results of the analysis of grab sample data and historical continuous EC records in the Delta.

Figure F-1 shows the DSM2 fingerprint data for the San Joaquin River at Jersey Point in the western Delta. As expected, the periods of high EC (during lower outflow periods) are dominated by seawater intrusion. Figure F-2 shows the same data in more detail during a prolonged period of high Delta outflow, in particular 1983, when the EC at Jersey Point was very low and primarily from San Joaquin River mixed with Sacramento River water. Because the San Joaquin salinities are much higher than the Sacramento River salinities, the San Joaquin EC dominates. Note that during periods of lower Delta outflow, the salinity contribution from the San Joaquin River is minimal, and the Sacramento River is the main secondary source of salinity at Jersey Point.

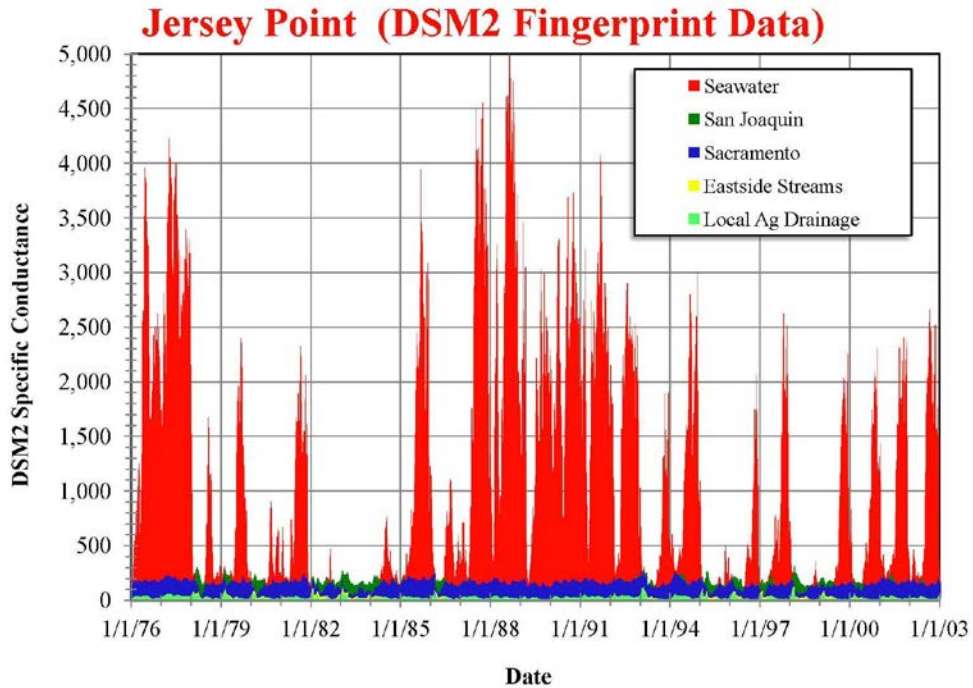


Figure F-1: DSM2 salinity fingerprint data for the San Joaquin River at Jersey Point in the western Delta for the period 1976 through 2002. This period includes the 1976-1977 and 1987-1992 droughts as well as the very wet year 1983.

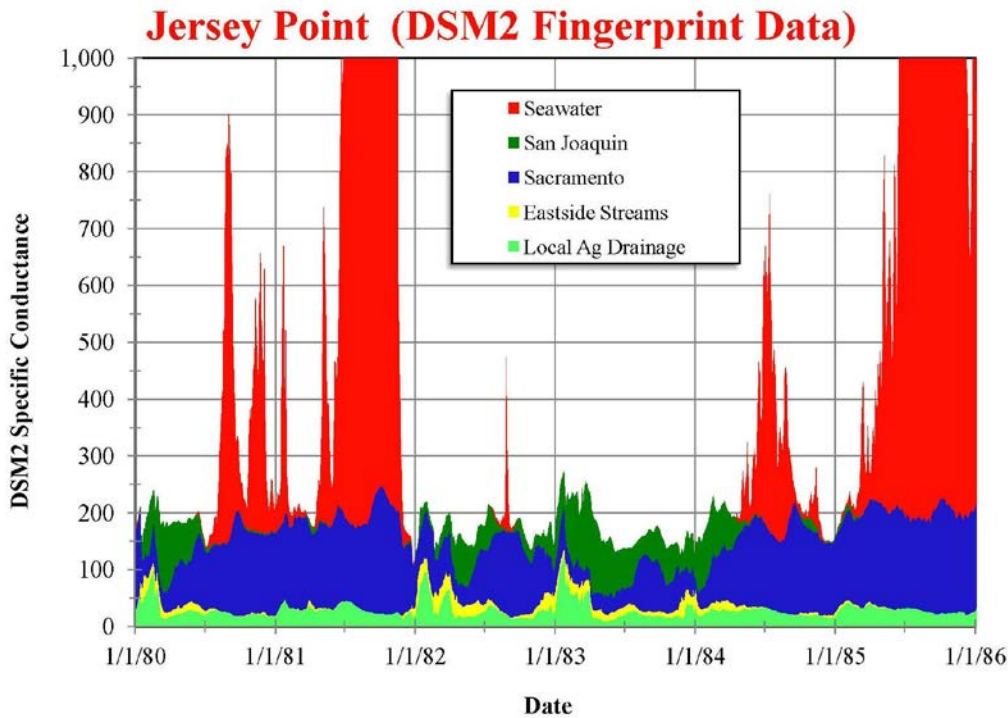


Figure F-2: DSM2 salinity fingerprint data for the San Joaquin River at Jersey Point in the western Delta for the period 1980 through 1985. During the wet years 1982 and 1983 there is almost no seawater intrusion at Jersey Point.

Figures F-3 and F-4 show the contributions to salinity at the State Water Project's Clifton Court Forebay and the intake to the Central Valley Project's Delta Mendota Canal in the south Delta. During periods of lower Delta outflow at least half of the salinity is due to seawater intrusion (red bars). During periods of higher Delta outflow, which often corresponds to periods of higher San Joaquin flow at Vernalis, the water quality at Clifton Court and the Delta Mendota Canal intake is dominated by San Joaquin River water. When San Joaquin flows are high, there is no seawater intrusion and Sacramento River water is displaced from the southern Delta by the San Joaquin River inflow.

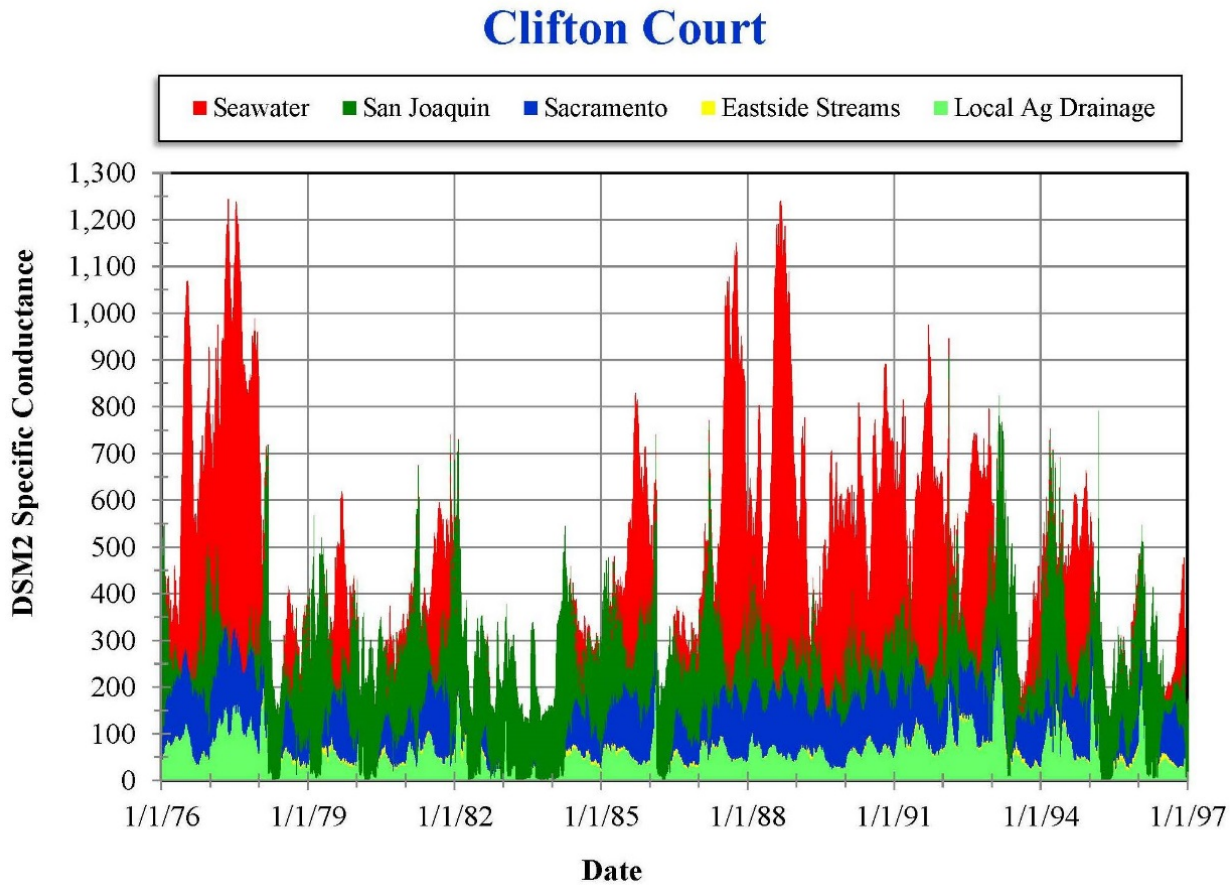


Figure F-3: DSM2 salinity fingerprint data for the Clifton Court Forebay in the southern Delta for the period 1976 through 1996.

Delta Mendota Canal

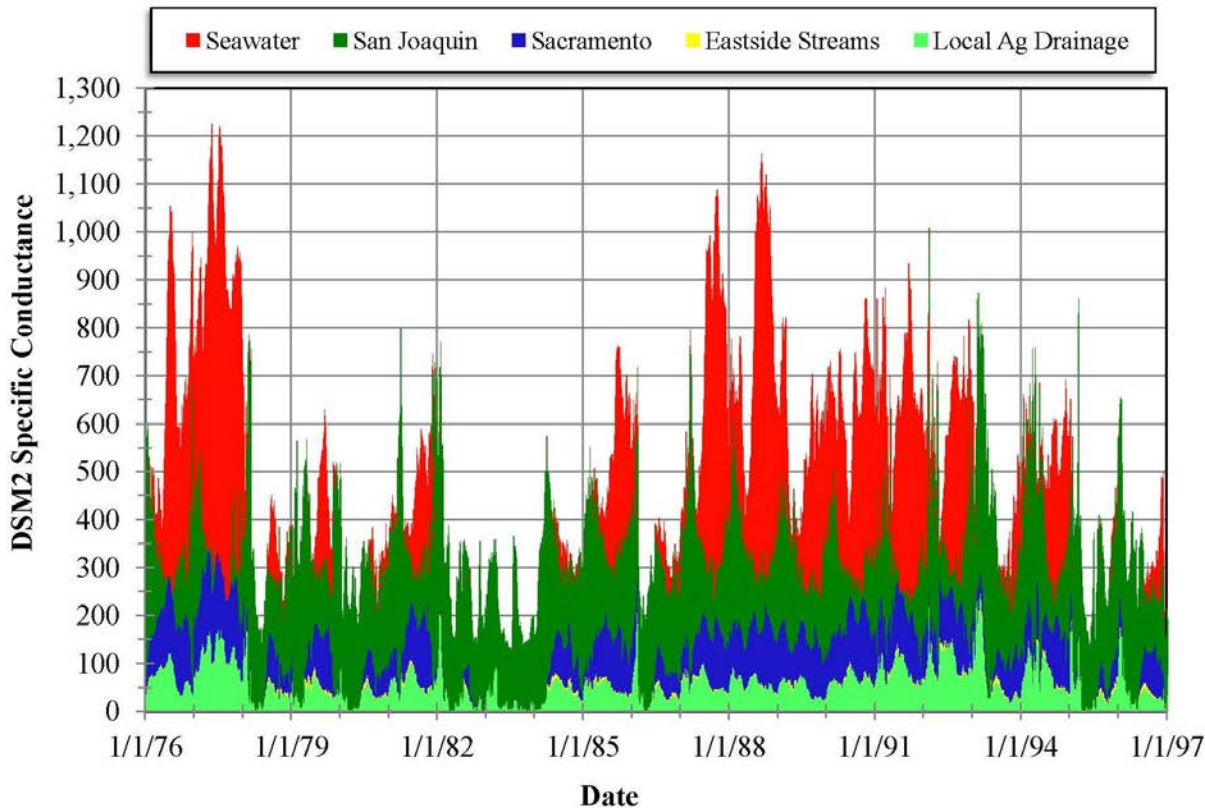


Figure F-4: DSM2 salinity fingerprint data for the Jones Pumping Plant and intake to the Delta Mendota Canal in the southern Delta for the period 1976 through 1996.

Figure F-5 shows the corresponding contributions to salinity at Middle River at Union Point. The relative contributions to total salinity at this location are very similar to those at the Delta Mendota Canal intake (Figure F-4), but with slightly less seawater intrusion. Figure F-6 shows the variation in salinity at Prisoners Point. Because Prisoners Point is located further north on the San Joaquin River at Venice Island, Sacramento River water makes a greater contribution than in the south Delta. Seawater makes a significant contribution during low flow periods. During higher flow periods (wetter periods), both the seawater and Sacramento River water tend to be displaced by San Joaquin River water.

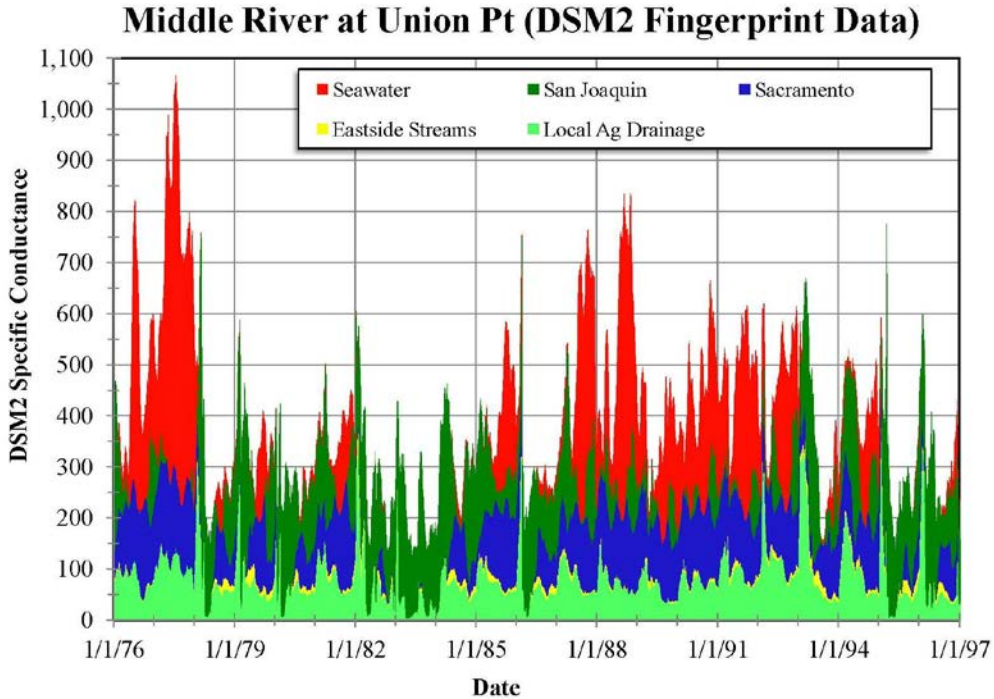


Figure F-5: DSM2 salinity fingerprint data for Middle River at Union Point (near the Highway 4 crossing) in the southern Delta for the period 1976 through 1996.

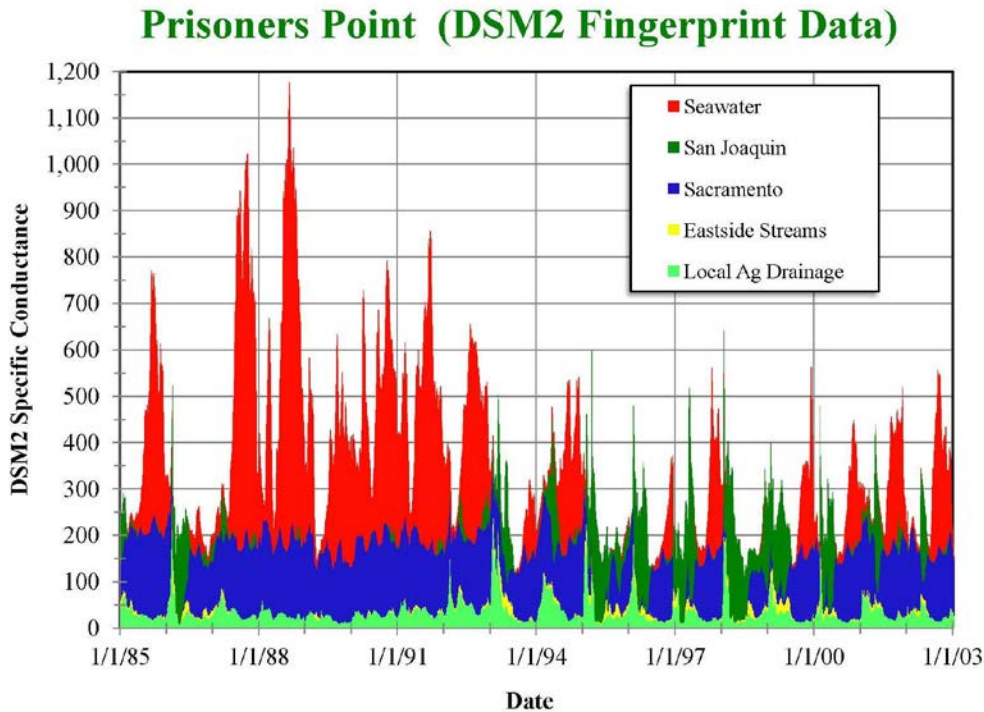


Figure F-6: DSM2 salinity fingerprint data for the San Joaquin River at Prisoners Point (on Venice Island) in the central Delta for the period 1985 through 2002.

Figure F-7 shows the DSM2 fingerprint data for the North Bay Aqueduct intake at Barker Slough. Because of its location in the north Delta, Barker Slough is unaffected by San Joaquin water, and the DSM2 simulation shows only traces of water from the eastside streams. Seawater intrusion is also minimal this far north. The DSM2 simulation indicates local agricultural drainage makes a continuous contribution and tends to dominate during the wetter February-April periods.

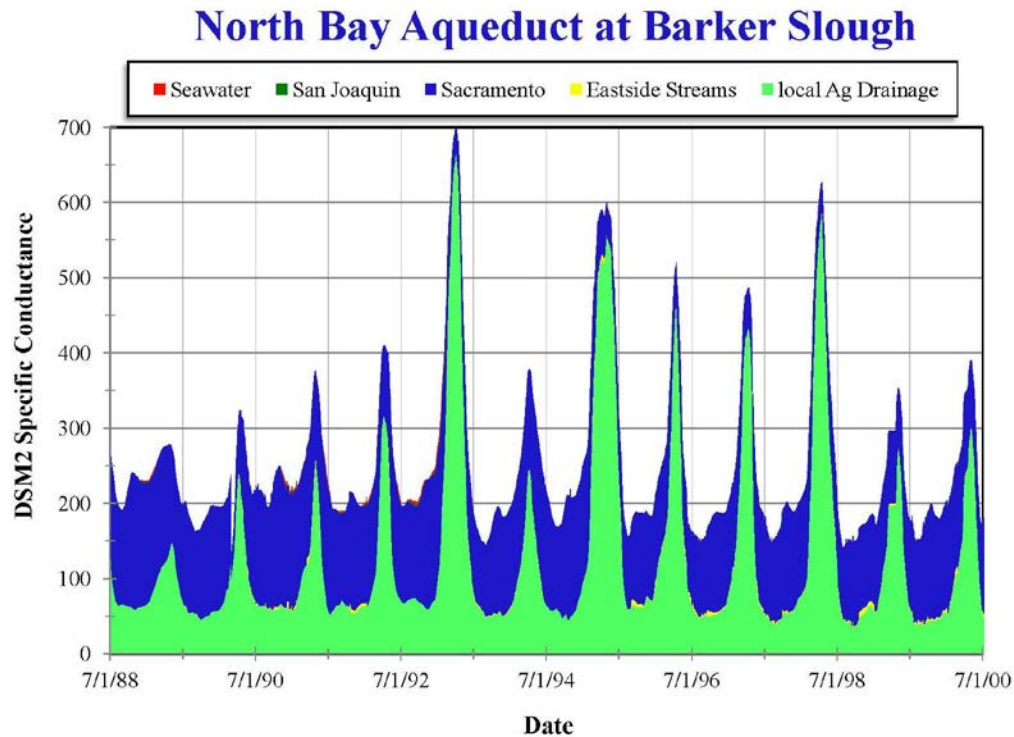


Figure F-7: DSM2 salinity fingerprint data for the intake to the North Bay Aqueduct at Barker Slough in the northern Delta for the period 1988 through 2000.

In order to estimate chloride concentrations, or other water quality constituents, from EC (or TDS) it is necessary to separate the contributions from seawater from the contributions from San Joaquin and agricultural drainage sources. The DSM2 fingerprint data provide information regarding the seawater contributions and can be used to check the feasibility of using Jersey Point salinity to estimate the seawater intrusion contribution at interior Delta stations.

Figure F-8 shows the seasonal variation in daily seawater EC at Bacon Island on Old River in the central Delta, at Clifton Court intake in the south Delta (southwestern corner), and at Middle River at Union Point (south Delta on the eastern side near the San Joaquin River). The Bacon Island is closest to Suisun Bay and the ocean so receives the most seawater. The Middle River station is furthest from the ocean so receives the least amount of seawater intrusion.

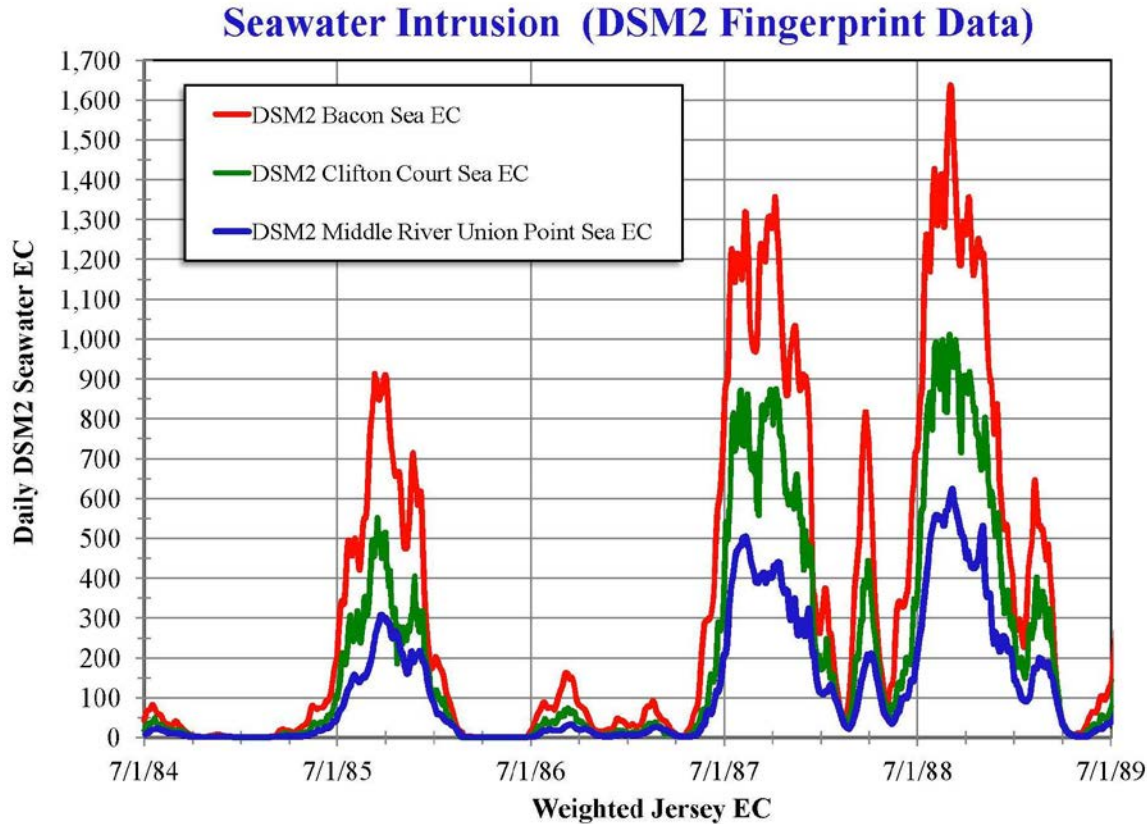


Figure F-8: Variation in daily EC due to seawater intrusion (DSM2 salinity fingerprint data) for Old River at Bacon Island, Clifton Court Forebay intake, and Middle River at Union Point in the central and south Delta for the period 1984 through 1989.

Figure F-9 shows how the contributions from seawater at Clifton Court Forebay intake is highest when Jersey Point EC is high (corresponding to low Delta outflows) and lowest when Jersey Point EC is low. Increases in seawater contribution at the interior Delta stations occur 10-20 days after increases at Jersey Point. This delayed response is taken into account using a “weighted” Jersey Point EC. In Figure F-9, the weighting factors used were:

$$\text{Weighted Jersey Point EC (t)} = 0.0 * \text{Average Jersey EC (t-6 through t)} + 0.5 * \text{Average Jersey EC (t-13 through t-7)} + 0.4 * \text{Average Jersey EC (t-20 through t-14)} + 0.1 * \text{Average Jersey EC (t-27 through t-21)}$$

where t represents the current day and $t-n$ represents the conditions n days earlier.

The relationship between Clifton Court seawater EC and weighted Jersey Point EC for this example (i.e., derived from the Clifton Court DSM2 EC data) is:

$$\text{Clifton Court seawater EC (t)} = 2.7\text{E-}05 * (\text{Weighted Jersey EC (t)})^2 + 0.111 * \text{Weighted Jersey EC (t)} - 22.3.$$

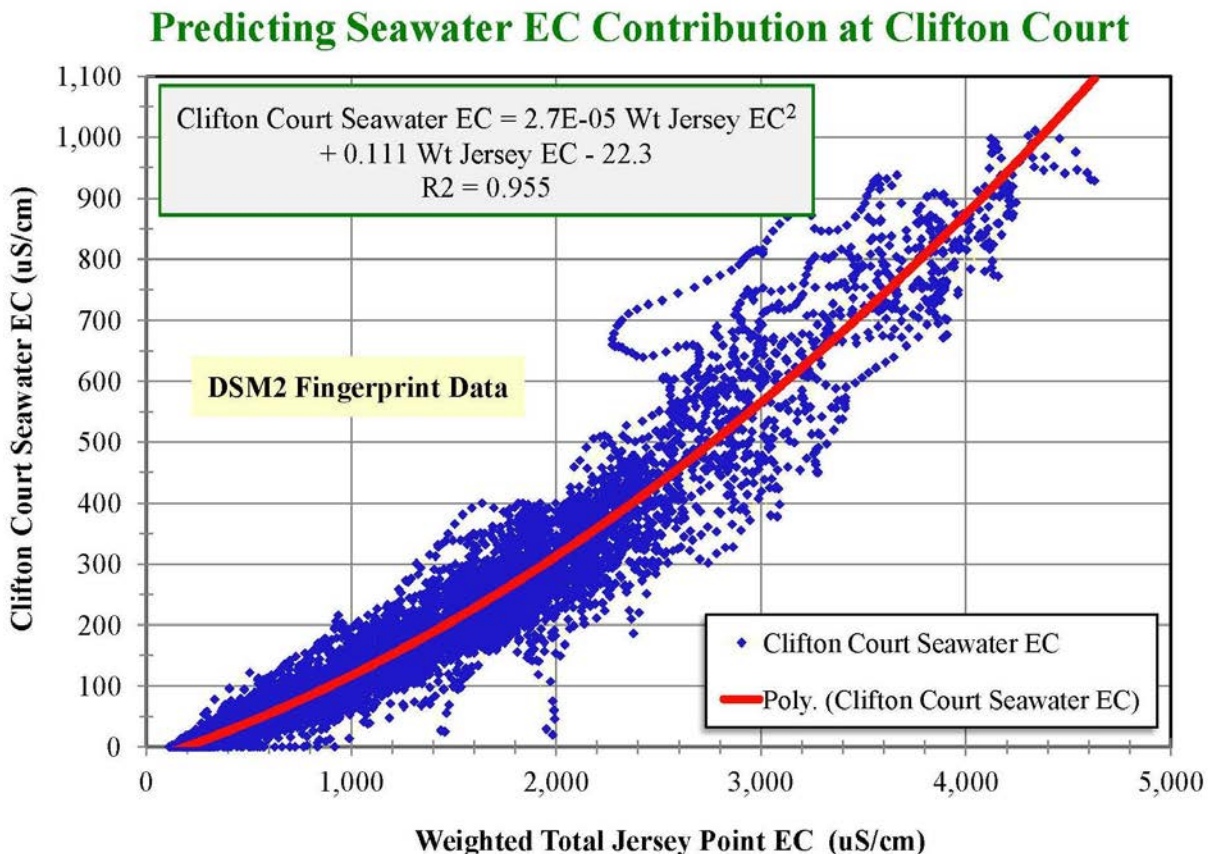


Figure F-9: Relationship between EC due to seawater at Clifton Court Forebay intake and total EC at Jersey Point (taking into account an approximate 14 day time lag in response).

The ability of this method to predict the seawater contribution at Clifton Court (for DSM2 output data) is shown in Figures F-10 and F-11. Note that the relationships for predicting the seawater contributions for grab samples in the field at interior Delta stations from historical Jersey Point EC measurements will be similar to those for DSM2 modeling output, but will need to be calibrated using field rather than model data.

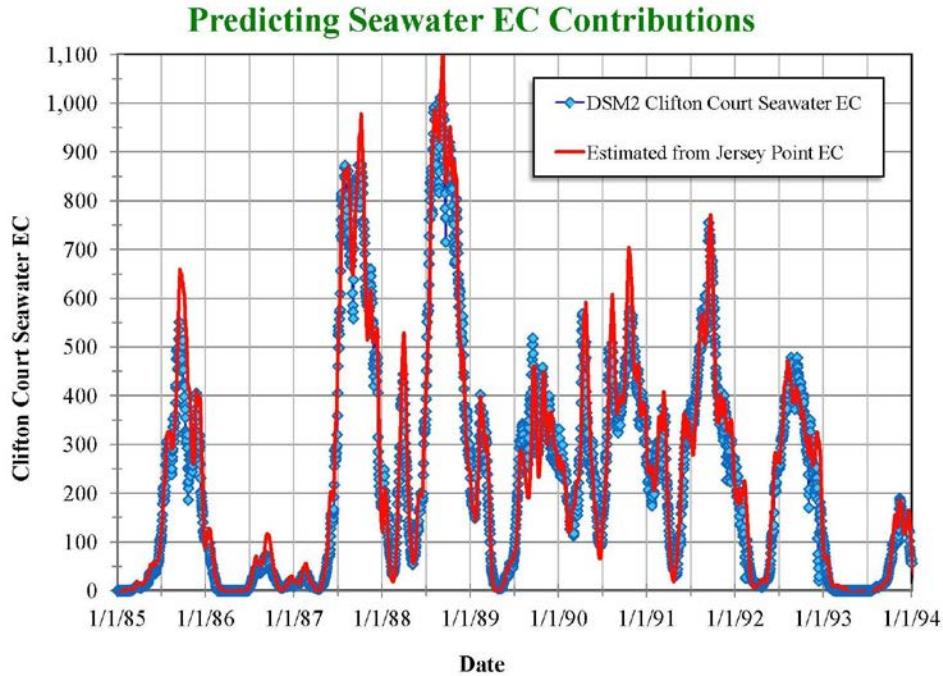


Figure F-10: Comparison of the DSM2 EC at Clifton Court due to seawater intrusion alone and the prediction based on total EC at Jersey Point for the period 1985 through 1993.

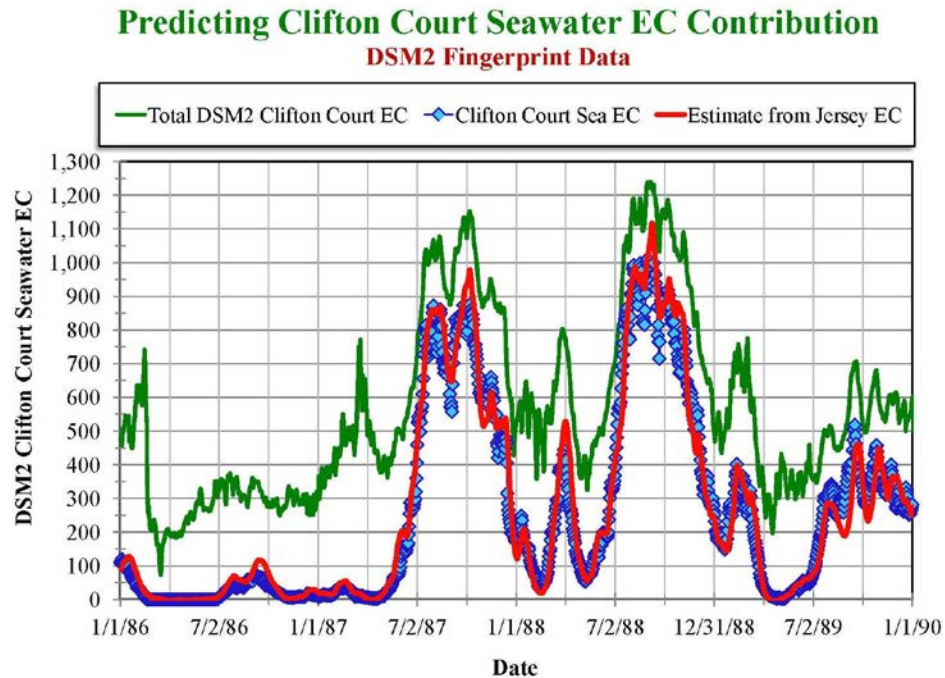


Figure F-11: A more detailed comparison of the DSM2 EC at Clifton Court due to seawater intrusion alone and the prediction based on total EC at Jersey Point for the period 1986 through 1989. The total EC at Clifton Court is also shown to indicate the relative contributions from other sources of salinity.

General Mixing Equations for Three Sources of Water

At western Delta locations, the water quality is the result of the mixing of three general sources of water:

- (a) Seawater from San Francisco Bay and the ocean;
 - (b) Freshwater from the Sacramento River and the Delta eastside streams; and,
 - (c) Agricultural return flows from the San Joaquin Valley and local sources within the Delta.

These three general sources also affect the water quality at other locations in the Delta.

Note that even the water quality in the San Joaquin River at Vernalis can be considered in terms of three general sources of water:

- (a) Agricultural return flows
 - (b) Freshwater, primarily from the Stanislaus, Tuolumne and Merced Rivers; and,
 - (c) Saline water exported to the San Joaquin Valley from the Delta via the CVP Delta Mendota Canal and SWP California Aqueduct.

Montoya (2004) diluted both seawater from San Francisco Bay and San Joaquin River water with Sacramento River water and analyzed the resulting changes in sulfate concentration and other water quality constituents with EC (see, e.g., his Figure 4). A simple set of mixing equations can be derived to quantify the relationship between, say, chloride concentration and total dissolved solids for these three sources.

The equation for TDS at a given Delta location is

where

Sea = Ocean seawater conditions

Ag = San Joaquin River plus local Delta Island drainage

Sac = Sacramento River and Delta eastside streams

The coefficients a and b are the percentages by volume of seawater and agricultural drainage at a given location.

Similarly, the equation for, say, chloride concentration at a given location is:

or

where the coefficients A, B and C are the chloride to TDS ratios for the three sources of water.

As discussed in Appendix E, these ratios are approximately $A = 0.55$, $B = 0.25$ and $C = 0.03$, respectively. Note the seawater value of 0.55 represents the asymptote at very high TDS. The San Joaquin value of 0.25 represents the lower range of the Cl/TDS ratio at high TDS. After prolonged dry periods, the water quality at Vernalis can be affected by seawater exported to the San Joaquin Valley via the south Delta export pumps. This can increase the Vernalis ratio relative to the value that applies when the export water and irrigation water remains relatively fresh. The Sacramento value of 0.03 represents the average value at low TDS when agricultural drainage is not contributing to the water quality at Hood and Greenes Landing.

The Cl / TDS ratio observed at a given Delta location can be calculated from equations G.1 and G.2 where the TDS values for the three sources are “known” (i.e., 35,000, 1,500 and 70, for seawater, agricultural drainage and Sacramento water, respectively), the coefficients A, B and C are known, and only the volumetric percentages a and b are unknown.

For a constant value of the San Joaquin source proportion b, equation G.3 becomes

$$\text{Total Cl} = a [A \text{ TDS}_{\text{Sea}} - C \text{ TDS}_{\text{Sac}}] + [b B \text{ TDS}_{\text{Ag}} + (1 - b) C \text{ TDS}_{\text{Sac}}] \quad \dots\dots\dots (G.4)$$

where all the quantities on the right hand side of equation G.4 are known except the coefficient a.

The corresponding relationship between Total Cl and Total TDS for constant b is a linear equation of slope A, and from equation 1, the only unknown coefficient a is

$$a = \{ \text{Total TDS} - [b \text{ TDS}_{\text{Ag}} + (1 - b) \text{ TDS}_{\text{Sac}}] \} / [\text{TDS}_{\text{Sea}} - \text{TDS}_{\text{Sac}}] \quad \dots\dots\dots (5)$$

i.e., another linear relationship.

Figure G-1 shows the calculated chloride concentration as a function of TDS. The theoretical curves are compared with grab sample data representing the Delta’s seawater boundary condition (Mallard Island, Chippis Island and Jersey Point). Four different cases are plotted: no agricultural drainage source water ($b = 0$), 5% agricultural drainage by volume ($b = 0.05$), $b = 0.20$, and a scenario where the seawater contribution is zero ($a = 0$). This latter case represents the high Delta outflow case where seawater intrusion is insignificant and the water at Mallard Island consists primarily of Sacramento and San Joaquin water.

The theoretical relationships (for a given value of b) are linear relationships that shift in the decreasing chloride direction as the percentage of San Joaquin water increases. The slope of the lines is the ratio of Cl/TDS for seawater. Note that the data scatter is greater than the variation over the range $0 < b < 0.1$. As suggested by the DSM2 fingerprint data (Appendix F), the contribution at Mallard Slough from the San Joaquin River source varies as Delta outflow (and San Joaquin River inflow) increases.

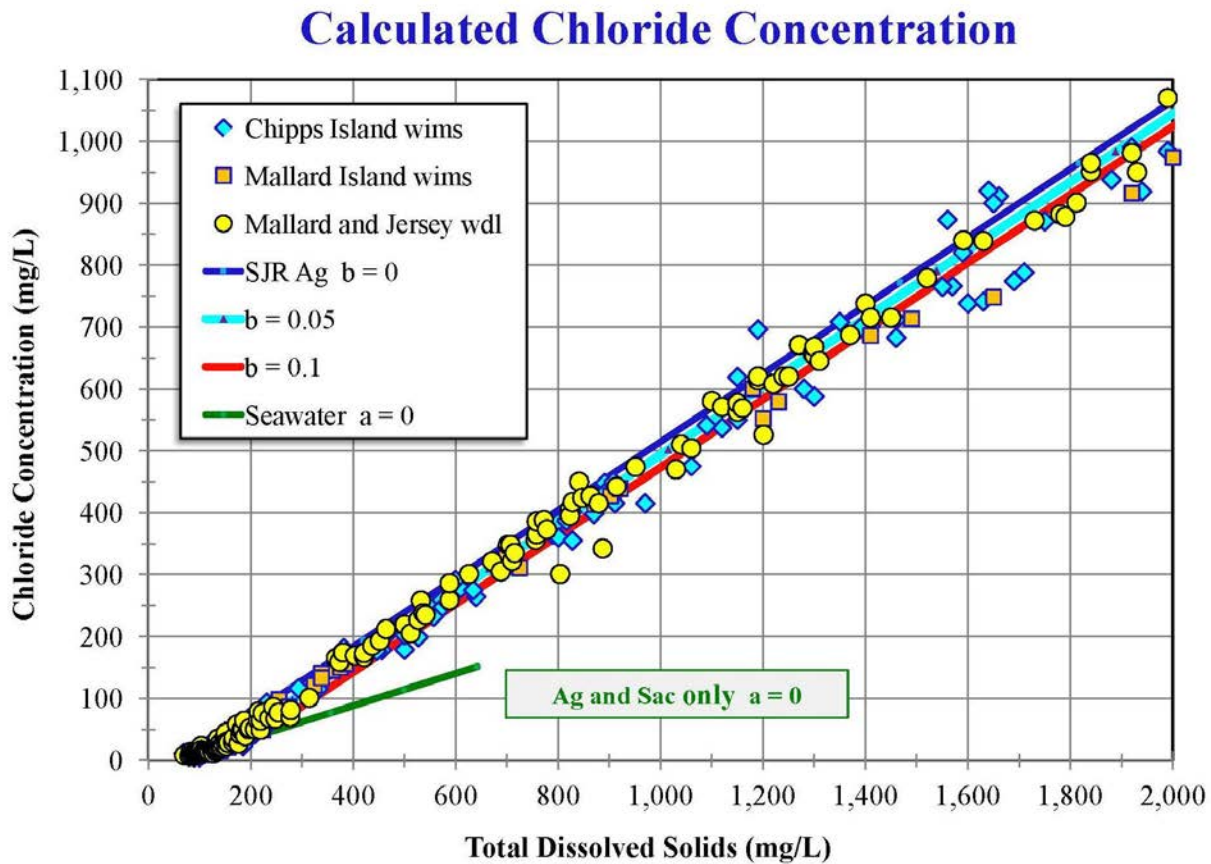


Figure G-1: Theoretical relationship between the chloride concentration and total dissolved solids derived from the mixing equations for three sources. The theoretical equations are compared with grab sample data from Mallard Island, Chipps Island, and Jersey Point. Seawater typically dominates at this location but not when Delta outflows are very high (low TDS).

Figure G-2 shows the same theoretical relationships in more detail over the lower TDS range (< 400 mg/L) representing periods of high Delta outflow when the influence of dilution by Sacramento and San Joaquin is important. As TDS decreases the percentage of seawater (represented by the coefficient a) decreases until eventually a = 0 and the data conform to a theoretical curve representing mixture of Sacramento and San Joaquin water only.

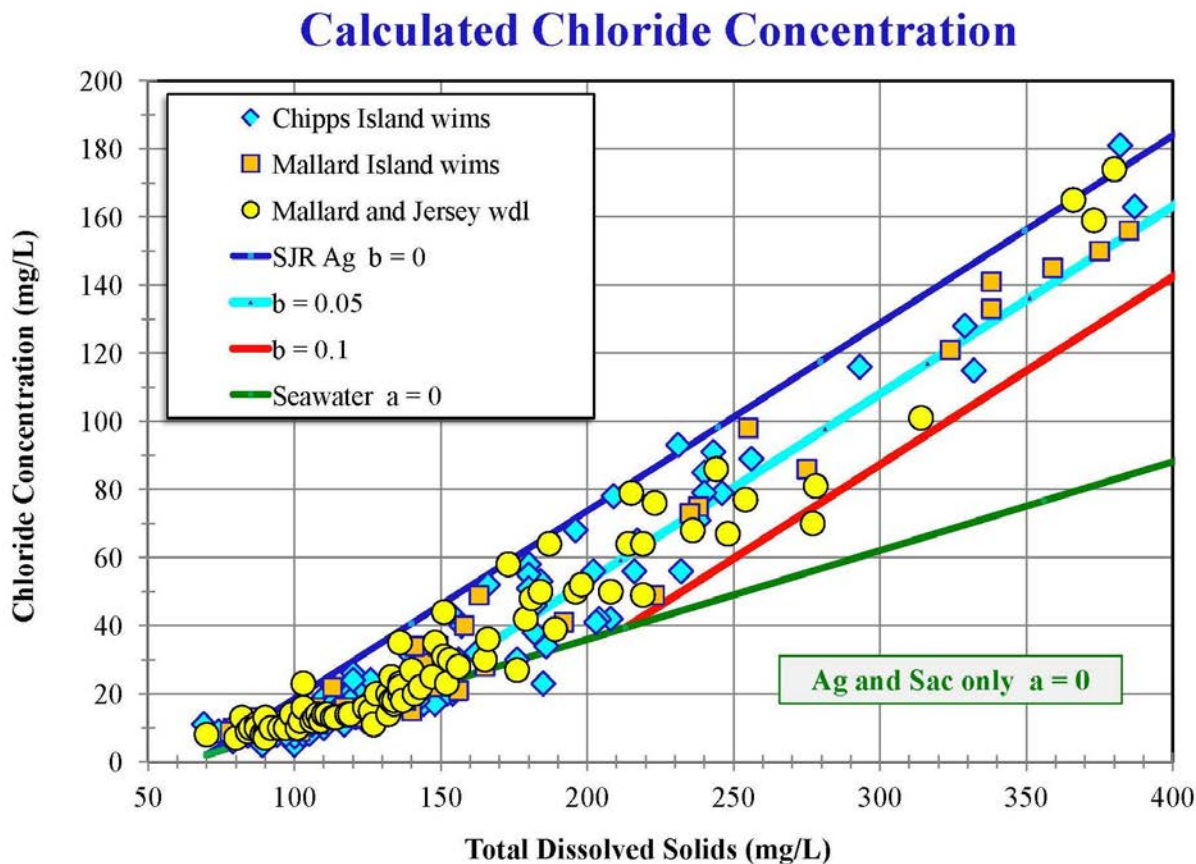


Figure G-2: Theoretical mixing relationship between chloride concentration and total dissolved solids for TDS < 400 mg/L (high Delta outflows). At very high outflows, seawater intrusion is negligible ($a = 0$) and the Mallard Island and Jersey Point data follow the mixing equation for Sacramento and San Joaquin sources only.

Figure G-3 shows the corresponding variation of the chloride/TDS ratio with TDS for TDS < 400 mg/L. These theoretical mixing curves are consistent with the grab sample data and the DSM2 fingerprint data (Appendix E) and reflect domination of seawater intrusion when Delta outflows are low (high TDS and EC) and Sacramento and San Joaquin water dominating during high outflow events (low TDS and EC).

Calculated Chloride Ratio

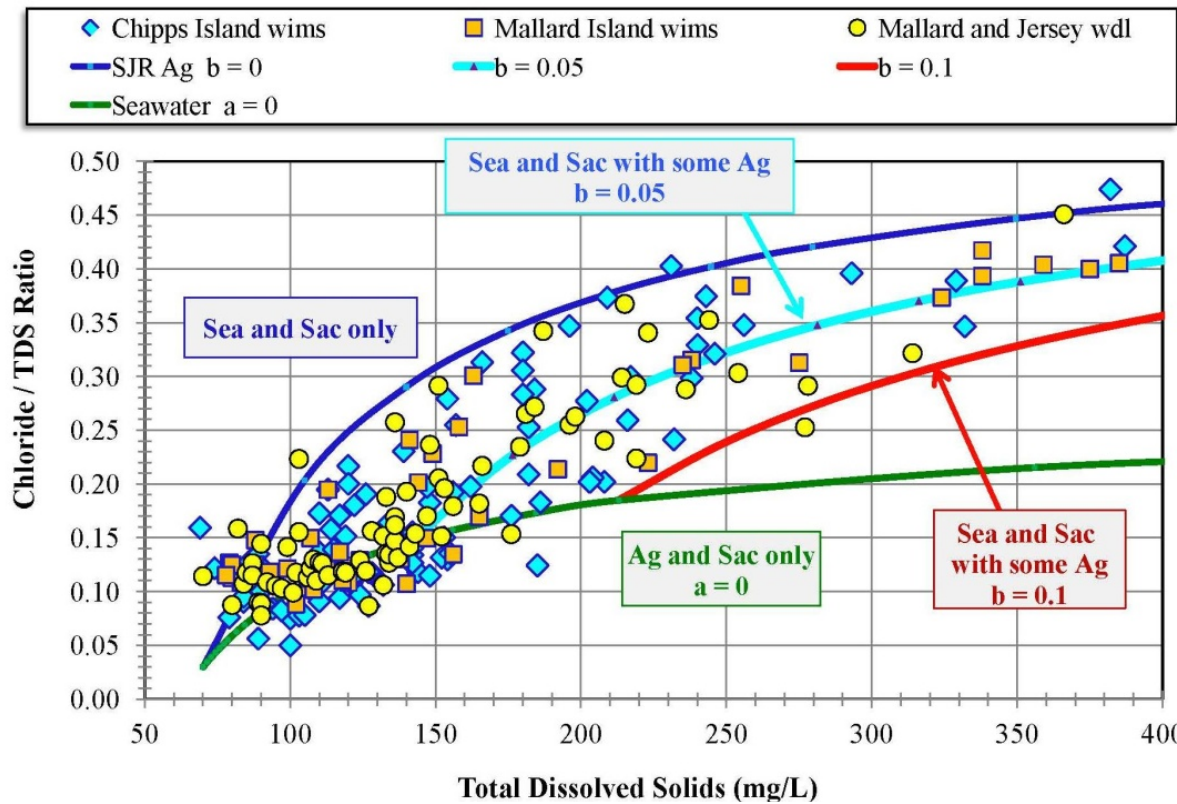


Figure G-3: Theoretical mixing relationship between the chloride/TDS ratio and total TDS for TDS < 400 mg/L (higher Delta outflows). At very high outflows (very low TDS), seawater intrusion is negligible ($a = 0$) and even the Mallard Island and Jersey Point data tend to follow the mixing equation for Sacramento and San Joaquin sources only.

Figure G-4 shows a comparison between the three-source mixing equations and the corresponding chloride/TDS ratios calculated from the quadratic equation fits to the chloride grab sample data. The seawater boundary condition equation for TDS > 150 mg/L closely follows the mixing equation for $b = 0.05$. At very low TDS, the mixing curves are very sensitive to the coefficients chosen to represent the TDS of “pure” Sacramento River and the corresponding (minimum) chloride to TDS ratio. The error bars on the chloride/TDS ratio for the grab samples are also large because the chloride and TDS data values are small and only reported as integers.

Calculated Chloride Ratio

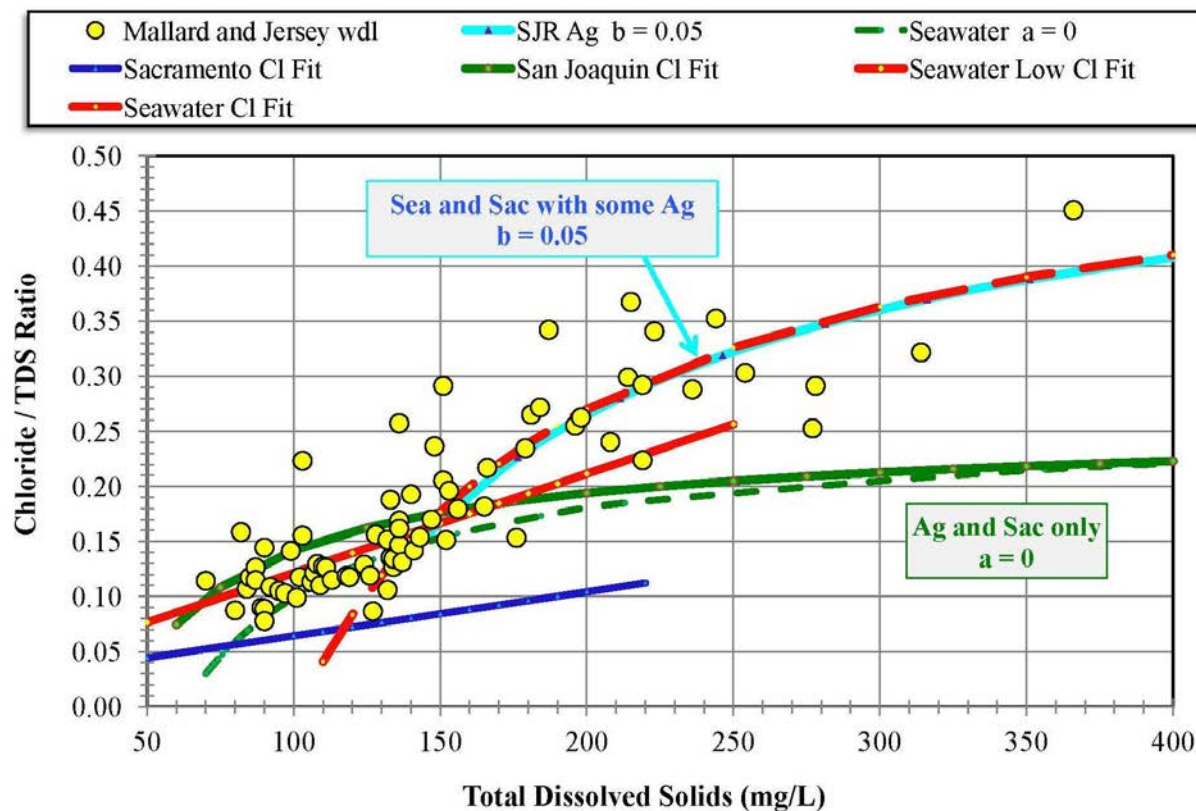


Figure G-4: Comparing the theoretical three-source mixing equations for $b = 0.05$ and $a = 0$ with the fitted quadratic equations for chloride concentration as a function of TDS (for seawater, San Joaquin and Sacramento River boundary conditions).

These theoretical relationships also apply to other water quality constituents, such as calcium and sulfate. In the case of calcium, for example, the value of the coefficients in equation G.3 above, A, B and C, are the ratios of calcium to TDS for seawater, San Joaquin and Sacramento water, respectively. The theoretical variation of calcium concentration with TDS is shown in Figure G-5. In this case, A = 0.013, B = 0.080 and C = 0.140.

Calculated Calcium Ratio

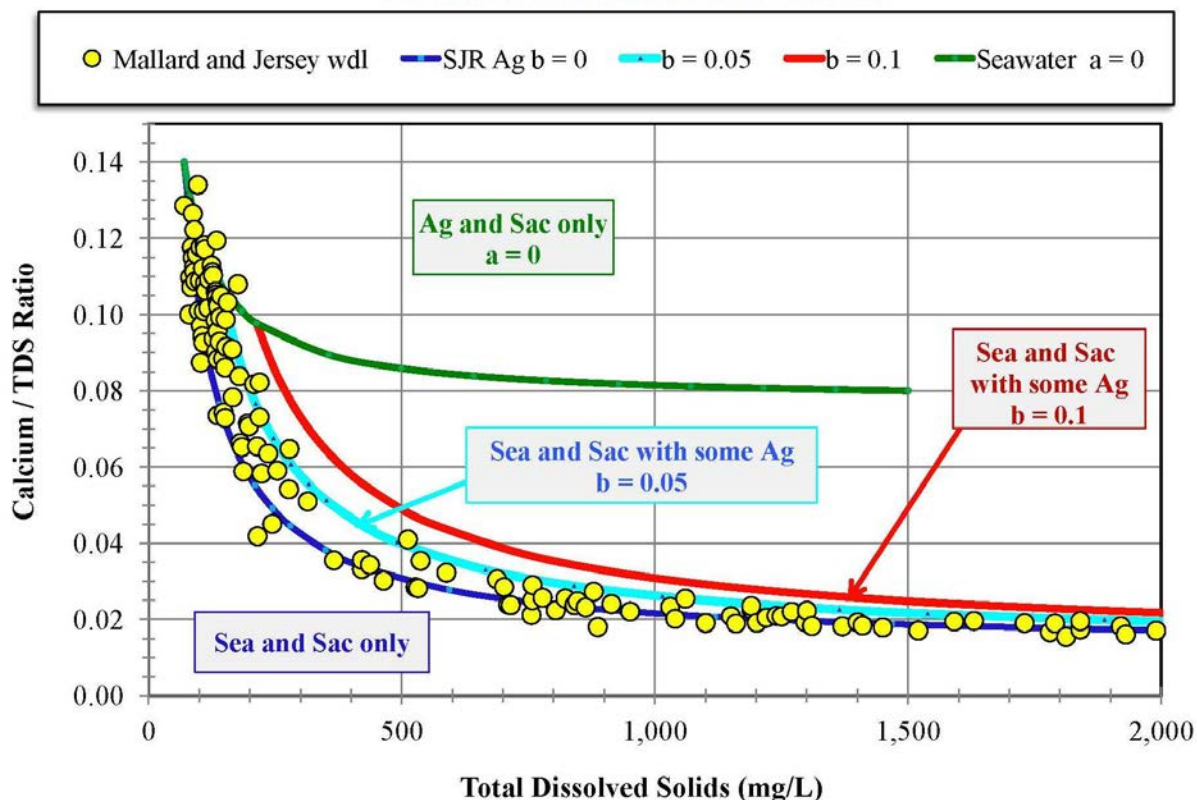


Figure G-5: Corresponding three-source mixing equations for the calcium/TDS ratio as a function of TDS. These theoretical curves are compared with data from Mallard Island and Jersey Point.

The theoretical curves apply not only to data in the western Delta but also to other locations within the Delta, such as Clifton Court in the south Delta. The Clifton Court grab sample data will typically be bounded by the seawater-Sacramento water curve ($b=0$) and the San Joaquin-Sacramento River water curve ($a = 0$), depending on the time of year and Delta outflow conditions.

Because the relative percentages of San Joaquin and Sacramento water, by volume (coefficients a and b) vary with TDS and are hard to quantify, these mixing equation relationships were not used to prescribe relationships for the water quality constituents as a function of EC and TDS in this report. Simpler quadratic and linear relations were sufficient to prescribe the variation in concentration of the water quality constituents with EC and TDS over the range of the grab sample data.

Appendix H

Checking the Quality of the Grab Sample Data

The quality of the Bay-Delta water quality grab sample data is generally very good. DWR's Bryte Laboratory employs extensive methods to ensure the quality assurance and quality control of the data¹. However, there are a number of methods that can be used to check the quality of data, both in the current DWR Water Data Library, and in the earlier data bases extending back to the 1950s. Errors can occur due to contamination of a sample or errors in the analytical equipment. Errors can also be produced during data entry.

Because the correlation between the various water quality constituents, EC and TDS is generally very good at many locations throughout the Delta, outliers and errors can be easily identified. An outlier on a plot of chloride concentration versus sulfate may be due to an error in either constituent, or both. However, a check against other constituents will typically reveal which was in error.

Plotting one constituent against another from the same grab sample allows outlier data that may have been recorded or analyzed incorrectly to be identified. These methods were also used to check the integrity of regression equations produced as part of this project.

The accuracy and consistency of the data can be checked using the following techniques (Hem 1985):

- (a) Mass Balances: The sum of anions and cations should approximately equal TDS (in mg/l)
- (b) Charge balances: The sum of anions approximately equals sum of cations (in meq/l)
- (c) Sum of cations (in meq/l) times 100 approximately equals EC (in $\mu\text{S}/\text{cm}$)

Note, for an anion-cation balance, everything is converted to an "electrical charge per volume," expressed in milliequivalents per litre (meq/L). The conversion is based on the relationship between the mass and the charge for each ion species. Some examples are shown in Table H-1.

Hem (1985) also suggested that the TDS value in mg/L should generally be from 0.55 to 0.75 times the specific conductance in micromhos per centimeter (for TDS < 2,000 mg/L). These relationships between EC and TDS break down for high TDS (> 50,000 mg/L) and very low TDS. As shown in Chapter 3 and Appendix E (Figure E-12), the TDS/EC ratio in the Delta varies depending upon the particular mixture of sources of water. During very high TDS conditions in Suisun Bay, TDS/EC tends to 0.60-0.65 (Figure 3-1). During high TDS periods at Vernalis, EC/TDS tends to a similar value (Figure 3-2).

As also discussed in this appendix, another check of the report EC values can be obtained by summing the ion conductances of each of the ions. This works well over the typical range of EC in the interior Delta (EC < 1,500 $\mu\text{S}/\text{cm}$) but the ion conductance factors decrease at very large EC.

¹ http://www.water.ca.gov/waterquality/drinkingwater/docs/brytelab_qa_manual_2013.pdf

Table H.1: Valences and atomic weights for key water quality constituents

Constituent	Symbol	Valence	Atomic Weight (g)	Units
Sodium	Na+	1	22.99	mg/L
Calcium	Ca+2	2	40.08	mg/L
Magnesium	Mg+2	2	24.31	mg/L
Potassium	K+	1	39.10	mg/L
Manganese	Mn+2	2	54.94	mg/L
Iron	Fe+2	2	55.85	mg/L
Phosphorus	P 3+	3	30.97	mg/L
Chloride	Cl-	1	35.45	mg/L
Sulfate	SO4--	2	96.06	mg/L
Alkalinity (as CaCO ₃)	HCO3-	1	61.02	mg/L CaCO ₃
Bromide	Br-	1	79.90	mg/L

These QA/QC methods will be illustrated using a few examples obtained from the grab sample data from DWR's Water Data Library. The following cation-anion balance calculation table (Table H-2) is based in part upon a worksheet at the following link: <http://coalgeology.com>

Table H.2 shows the ion concentrations for a grab sample taken from the Sacramento River at Mallard Island (B0702000) on April 7, 2009 at 9:34 am. No manganese or iron concentrations are reported for that grab sample, but both concentrations are typically very small. The sum of the anions and cations in mg/L is 675.3 mg/L which agrees well with the reported TDS of 688 mg/L (1.8% error).

The sum of the cations in meq/L is 11.13 and the sum of the anions is 11.14 meq/L. The Charge Balance Error is -0.1%. The Charge Balance Error (%) is calculated as ((Total Cation meq/L - Total Anion meq/L) / (Total Cation meq/L + Total Anion meq/L))*100.

Table H.2: Concentration Data and Charge Balance Calculations for a Mallard Island Grab Sample (B0702000) from 4/7/2009 at 9:34 am

Constituents	Atomic Weight (g)	Measured Concentration (mg/L)	Molality (mmol/L)	Valence	Charge (meq/L)
Na+	22.99	172	7.48	1	7.48
Ca+2	40.08	21	0.52	2	1.05
Mg+2	24.31	29	1.19	2	2.39
K+	39.10	8.4	0.21	1	0.21
Mn+2	54.94			2	
Fe+2	55.85			2	
Cl-	35.45	305	8.60	1	8.60
Br-	79.90	1.21	0.02	1	0.02
SO4--	96.06	57	0.59	2	1.19
HCO3-	61.02	79.4	1.30	1	1.30
CO3-	60.01	0.6	0.01	1	0.01
NO3-	62.00	1.7	0.03	1	0.03

Total Cation (mg/L)	230.4
Total Anion (mg/L)	444.9
Total Cation + Anion (mg/L)	675.3

Measured TDS (mg/L)	688
TDS Error	-12.7
Percentage TDS error	-1.84 %

Total Cation (meq/L)	11.13
Total Anion (meq/L)	11.14
Charge Balance Error	-0.1 %

A third check of the quality of the grab sample data is whether the sum of cations (in meq/l) times 100 approximately equals EC (in $\mu\text{S}/\text{cm}$). In this case, the specific conductance was 1,250 $\mu\text{S}/\text{cm}$ and the field EC was 1,345 $\mu\text{S}/\text{cm}$. The estimate of EC from the sum of the cations is 1,113 $\mu\text{S}/\text{cm}$.

Another check is to calculate total EC from the conductance of individual ions. The ion conductances for the key constituents are given at the following link:

<http://www.cwc.nic.in/main/HP/download/08%20Understanding%20EC.pdf>

For this example, the sum of the conductances of the individual ions is 1,346 $\mu\text{S}/\text{cm}$, compared to the laboratory EC measurement of 1,250 $\mu\text{S}/\text{cm}$ and field EC of 1,345 $\mu\text{S}/\text{cm}$ (Table H.3).

Note that the ion conductivity factors are not constant but decrease with increasing concentration at high concentrations. They are reasonably constant over the range of salinities in the interior Delta, i.e., EC < 1,500 $\mu\text{S}/\text{cm}$.

Table H.3: Calculation of Specific Conductance from Individual Ion Conductances

Constituents	Measured Concentration (mg/L)	Ion Conductivity Factor ($\mu\text{S}/\text{cm}$ per mg/L)	EC ($\mu\text{S}/\text{cm}$)
Na+	172	2.13	366
Ca+2	21	2.60	55
Mg+2	29	3.82	111
K+	8.4	1.84	15
Mn+2			
Fe+2			
Cl-	305	2.14	653
Br-	1.21		
SO4--	57	1.54	88
HCO3-	79.4	0.72	57
CO3-	0.6		
NO3-	1.7	1.15	2
Total			1,346

For this Mallard Island grab sample the TDS/EC ratio is **0.55**.

The grab sample concentrations include alkalinity reported in mg/L. To determine the corresponding concentrations of bicarbonate (HCO_3^-) and carbonate (CO_3^{2-}), Bryte Laboratories use the following equations that represent the effect of different acidity (pH)²

$$\text{Bicarbonate} = ([\text{Alkalinity}] - 5 * \text{Exp}(([\text{pH}] - 10) * 2.302585093)) / (1 + 0.94 * \text{Exp}(([\text{pH}] - 10) * 2.302585093))$$

$$\text{Carbonate} = [\text{Alkalinity}] * \text{Exp}(([\text{pH}] - 10) * 2.302585093) / (1 + 0.94 * \text{Exp}(([\text{pH}] - 10) * 2.302585093) * 0.94 * \text{Exp}(([\text{pH}] - 10) * 2.302585093))$$

For this grab sample the laboratory pH was 7.9, and the alkalinity was 80 mg/L. At this pH, the bicarbonate ion dominates.

If one or more of the ion concentrations are incorrect this will result in disagreement between the sum of the cations and anions (in mg/L) and the measured total dissolved solids, as well as the

² Private communication from Kelley Pepper of Bryte Labs (2014)

cation-anion balance. Table H.4 shows measured concentrations for this Mallard Island grab sample, as well as the estimated values using the regression equations based on measured EC and measured TDS as well as the estimate of bromide from chloride (Chapter 7). The agreement is not exact, but there aren't any obvious outliers among the reported data.

Table H.4: Comparison of measured ion concentrations with estimates from different regression equations

Constituent	Grab Sample (mg/L)	From EC	From TDS	Br from Cl
EC	1,250		1244	
TDS	688	684		
Cl	305	311	323	
Br	1.21	1.09	1.11	1.03
Na	172	180	179	
Ca	21	20	20	
SO₄	57	55	56	
Mg	29	29	28	
K	8.4	7.5	8.0	
Alkalinity	80	65	65	

Table H.5 shows another example using the grab sample data from the Sacramento River at Mallard Island (B0702000) from January 6, 2009 at 10:25 am. At this time, Delta outflow had been low and the salinity was very high, i.e., laboratory EC = 13,220 µS/cm and field EC = 14,080 µS/cm.

Table H.5: Concentration Data and Charge Balance Calculations for a Mallard Island Grab Sample (B0702000) from 1/6/2009 at 10:25 am

Constituents	Atomic Weight (g)	Measured Concentration (mg/L)	Molality (mmol/L)	Valence	Charge (meq/L)
Na+	22.99	2,310	100.48	1	100.5
Ca+2	40.08	108	2.69	2	5.39
Mg+2	24.31	307	12.63	2	25.3
K+	39.10	98.3	2.51	1	2.51
Mn+2	54.94			2	
Fe+2	55.85			2	
Cl-	35.45	4,490	126.66	1	126.7
Br-	79.90	18.4	0.23	1	0.23
SO4--	96.06	636	6.62	2	13.24
HCO3-	61.02	91.4	1.50	1	1.50
CO3-	60.01	0.6	0.01	1	0.01
NO3-	62.00	3.4	0.05	1	0.05

Total Cation (mg/L)	2,823
Total Anion (mg/L)	5,240
Total Cation + Anion (mg/L)	8,063

Measured TDS (mg/L)	8,080
TDS Error	-16.9
Percentage TDS error	-0.21 %

Total Cation (meq/L)	133.6
Total Anion (meq/L)	141.7
Charge Balance Error	-2.9 %

For this grab sample, the sum of the cations and anions in mg/L is 8,063 mg/L which agrees well with the measured TDS of 8,080 mg/L. The corresponding Charge Balance Error is -2.9%. The rough EC estimate from the sum of the cations (in meq/L) is 13,364 µS/cm compared to the laboratory EC of 13,220 µS/cm and field EC of 14,080 µS/cm.

For this example, the laboratory TDS/EC ratio is **0.61**.

Appendix I**Summary of Grab Sample Data Used in this Analysis**

The grab sample data used to develop the regression equations in this report were primarily downloaded from DWR's Water Data Library <http://www.water.ca.gov/waterdatalibrary/>. At the time the data were downloaded, the data typically only extended back to the early 1980s.

As discussed in Chapter 4, the data were collected by DWR as part of the Municipal Water Quality Investigations (dating back to 1983), and its predecessor the Interagency Delta Health Monitoring Program (IDHAMP). Earlier grab sample data from DWR's Water Information Management System (1948-1991) were also used to check the regression equations. DWR and U.S. Bureau of Reclamation grab sample data dating back at least to 1964 are also available from the U.S. Environmental Protection Agency's STORET website.

DWR has recently updated the Water Data Library to include pre-1983 grab sample data, such as the data from WIMS. The sample dates listed in this appendix reflect the data periods used to develop the regression equations and not the longer data periods that are now available from DWR's WDL website.

- **Boundary Condition Stations**

Station Name	Station Number	First Sample Date	Last Sample Date
Sacramento River @ Mallard Island	E0B80261551	05/08/1985	03/04/2013
San Joaquin River at Jersey Point	B9D80311413	07/10/1990	06/14/1995
San Joaquin River near Vernalis	B0702000	03/30/1982	03/15/2013
San Joaquin River @ Maze Rd. Bridge	B0704000	05/03/1988	10/20/1994
Sacramento River at Greene's Ldg.	B9D82071327	07/21/1983	05/26/1998
Sacramento River @ Hood	B9D82211312	03/30/1982	03/12/2013
Mokelumne River @ Lower Sacramento Road	B0210520	07/21/1983	10/02/1990

- **Suisun Bay – Sea Water Stations**

There were only limited data sets in DWR's Water Data Library for the northern San Francisco Bay region when the data for this report were downloaded. The data plotted in Chapter 8 are from the WIMS data set.

- Sacramento River Stations

Station Name	Station Number	First Sample Date	Last Sample Date
Sacramento River @ Rio Vista Bridge	B9D80961411	09/15/1988	10/13/1994

- Old River (Lower)

Station Name	Station Number	First Sample Date	Last Sample Date
Holland Cut near Bethel Island	B9D80101349	04/04/2008	08/21/2012
Holland Cut at Holland Marina	B9D75841349	03/11/2008	03/05/2013
Old River north of Rock Slough (Station 4B)	B9D75891348	06/28/1988	07/20/1994
Old River near Bacon Island @ USGS Pile	B9D75821343A	04/23/2008	02/28/2013
Old River south of Rock Slough (Station 5A)	B9D75811343	06/28/1988	06/28/1988
Rock Slough @ Old River	B9D75841348	07/26/1983	10/20/1994
Contra Costa Pumping Plant Number 1	B9591000	10/02/1990	02/28/2013
Rock Slough at Delta Road Bridge	B9D75861372	03/11/2008	03/05/2013
Santa Fe-Bacon Island Cut near Old River	B9D75651333	07/25/1989	07/20/1994
Woodward / North Victoria Canal near Old River	B9D75481334	07/25/1989	07/20/1994
Old River near Byron (Station 9) (Near Highway 4 Bridge)	B9D75351342	03/02/1989	03/04/2013
West Canal at Clifton Court Forebay Intake	B9D74971331	07/25/1989	07/20/1994
Clifton Court Intake	KA000000	07/26/1983	02/19/2013
Delta Pumping Plant Headworks at	KA000331	03/30/1982	03/13/2013

Harvey O. Banks Pumping Plant			
-------------------------------	--	--	--

- **Middle River (Lower)**

Station Name	Station Number	First Sample Date	Last Sample Date
Connection Slough at Mandeville Island Bridge	B9D80031294	07/25/1989	01/23/1992
Middle River near Latham Slough (Ferry Site)	B9D80011307	07/25/1989	01/23/1992
Middle River near Holt	B9D80021306	04/10/2008	08/21/2012
Middle River at Bacon Island Bridge	B9D75741317	07/25/1989	10/20/1994
Middle River at Woodward Canal	B9D75481310	08/10/1988	07/27/1989
Middle River at Union Point	B9D75351292	07/05/2006	03/04/2013
Middle River at Borden Highway	B9D75351293	02/06/1985	09/03/1997
North Canal near Old River	B9D75171329	07/25/1989	07/20/1994

- **San Joaquin River**

Station Name	Station Number	First Sample Date	Last Sample Date
Three Mile Slough near San Joaquin River	B9203300	05/30/2008	05/21/2009
Old River near Frank's Tract	B9D80431347	04/10/2008	08/21/2012
San Joaquin River at Prisoner's Point	B9D80361334	04/10/2008	02/16/2010
Little Connection Slough at Empire Tract	B9D80371300	02/06/1985	07/20/1994
San Joaquin River at Holt Road	B9D75971227	06/18/1997	01/19/2011
San Joaquin River at Highway 4	B9D75571196	07/19/1988	08/07/2001

San Joaquin River at Brandt Bridge	B9D75191193	12/12/2009	02/26/2010
San Joaquin River at Mossdale Bridge	B9D74711184	03/02/1989	02/26/2010

- **South Delta Stations**

Station Name	Station Number	First Sample Date	Last Sample Date
Middle River at Mowry Bridge (Undine Road)	B9D75011229	07/25/1989	07/20/1994
Old River at Middle River	B9D84931224	07/19/1988	07/19/1988
Grant Line Canal at Tracy Road Bridge	B9D74921269	03/02/1989	03/07/2013
Old River near Tracy	B9D74731285	03/02/1989	07/20/1994
Middle River at Howard Road	B9D75261230	09/12/2007	03/01/2013
Mokelumne River near Highway 12	B9204500	06/12/2008	08/28/2012

- **Barker Slough Stations**

Station Name	Station Number	First Sample Date	Last Sample Date
Barker Slough at Hay Road	B9D81901543	10/22/1997	02/02/1998
Barker Slough at Dally Road	B9D81811521	10/22/1997	01/29/1998
Barker Slough at Cook Road	A0922000	07/01/1996	07/06/2011
Barker Slough Near Pumping Plant	B9D81651476	09/03/1987	12/23/1998
North Bay Aqueduct at Barker Slough Pumping Plant	KG000000	09/15/1988	02/20/2013
Barker Slough at North Bay Pumping Plant	B9D81661478	09/15/1988	02/20/2013
Lindsey Slough at Hastings Cut	B9D81581462	07/11/1984	07/01/1996
Calhoun Cut at Highway 113	B9D81561483	07/01/1996	07/06/2011

Appendix I**Summary of Grab Sample Data Used in this Analysis**

Cache Slough at Vallejo Pumping Plant	B9D81781448	01/31/1984	01/22/1992
Cosumnes River at Dillard Road	B0117501	07/21/1983	12/05/1984
Mokelumne River near Highway 12	B9204500	06/12/2008	08/28/2012
Little Potato Slough at Terminous	B9D80691298	07/20/1988	07/20/1994

Data from DWR's Water Information Management System (1948-1991) were also used to analyze the relationship between the water quality constituents in the Delta and San Francisco Bay. These data were collected as early as the 1950s. Key stations in the WIMS database are tabulated below. Many of these stations and data have since been uploaded by DWR to the Water Data Library database.

Station Name	Station Number	First Sample Date	Last Sample Date	Number of Grab Samples
MOKELUMNE R A LOWER SACTO RD	B0210520	7/21/1983	12/5/1984	20
SAN JOAQUIN R NR VERNALIS	B0702000	4/11/1951	3/27/1985	942
DELTA-MENDOTA CA NR TRACY	B9592500	7/11/1952	9/17/1969	211
DELTA MENDOTA CA A LINDEMAN RD	B9C74901336	7/26/1983	3/27/1985	24
SAN JOAQUIN R A MOSSDALE BR	B9D74721184	9/24/1952	8/2/1984	625
OLD R NR TRACY	B9D74731285	10/27/1952	9/14/1966	173
DELTA MENDOTA CA - TRACY PUMP-STA	B9D74781351	11/2/1956	8/19/1964	10
OLD R A TRACY RD BR	B9D74831269	5/2/1966	7/2/1991	380
DELTA-MENDOTA IT CA A BYRON RD	B9D74871347	7/11/1952	4/3/1968	448
GRANT LINE CA A TRACY RD BR	B9D74921269	6/16/1954	12/13/1973	132
OLD R A CLIFTON COURT FERRY	B9D74951331	9/24/1952	5/14/1971	184
WEST CA A MO OF IT CLIFTON COURT	B9D74981332	3/6/1973	8/3/1984	217
SAN JOAQUIN R A BRANDT BR	B9D75191193	9/6/1950	7/2/1991	195
MIDDLE R A TRACY RD BR	B9D75291273	6/18/1977	9/25/1991	123
MIDDLE RIVER A UNION POINT	B9D75351292	10/5/1982	9/25/1991	125
MIDDLE R A BORDEN HWY	B9D75351293	11/10/1961	7/2/1991	249
OLD R NR BYRON	B9D75351342	1/31/1957	2/1/1973	39
SAN JOAQUIN R A HWY 4	B9D75571196	9/24/1952	12/13/1973	193

Appendix I**Summary of Grab Sample Data Used in this Analysis**

Station Name	Station Number	First Sample Date	Last Sample Date	Number of Grab Samples
WHISKY SLU A HOLT	B9D75611258	10/9/1968	12/18/1972	50
MIDDLE R A MOKELOMNE AQU	B9D75621317	4/12/1977	9/9/1986	160
OLD R A ORWOOD RR BR	B9D75641335	9/25/1952	9/13/1966	169
MIDDLE R A BACON ISLAND BR	B9D75741317	6/19/1959	2/3/1975	37
OLD R NR ROCK SLU AB RANCHO DEL R	B9D75811343	5/4/1972	3/1/1991	273
OLD R OPPOSITE RANCHO DEL RIO	B9D75821343	7/6/1973	8/2/1984	219
ROCK SL A OLD RIVER	B9D75841348	7/26/1983	3/27/1985	21
ROCK SLU A CONTRA COSTA CA IT	B9D75861383	9/24/1952	2/4/1975	218
CONTRA COSTA CA A ROCK SLU	B9D75861384	10/16/1975	7/1/1991	212
SAN JOAQUIN R A BUCKLEY COVE	B9D75871229	2/2/1968	8/2/1984	302
TURNER CUT A MCDONALD ISL FY	B9D75881285	3/25/1974	2/3/1975	20
OLD R A HOLLAND TRACT	B9D80051348	5/24/1955	1/14/1974	182
SAN JOAQUIN R A ANTIOCH	B9D80111481	4/20/1951	8/23/1976	228
SAN JOAQUIN R BY ANTIOCH	B9D80111488	1/10/1962	10/14/1968	65
SAN JOAQUIN R A ANTIOCH-SHIP CH	B9D80121485	3/28/1968	8/7/1984	420
SAN JOAQUIN R A ANTIOCH BR CO-LIN	B9D80151450	8/23/1960	7/11/1972	23
SAN JOAQUIN R A ANTIOCH BR (L-12)	B9D80161452	6/19/1959	2/13/1974	128
SAN JOAQUIN R A ANTIOCH BR	B9D80171450	5/24/1955	5/29/1967	65
OLD R (STA-12)	B9D80191348	6/24/1972	7/16/1973	19
SAN JOAQUIN R A BLIND POINT	B9D80191432	9/12/1963	3/2/1991	410
DISAPPOINTMENT SLU A BISHOP CUT	B9D80261251	3/25/1974	8/2/1984	196
SAN JOAQUIN R A JERSEY PT	B9D80311413	2/28/1957	8/7/1984	474
FALSE R A WEBB PUMP	B9D80371361	5/24/1955	11/15/1973	135
SACRAMENTO R AB PT SACRAMENTO	B9D80381492	3/4/1971	8/6/1984	342
OLD R A MANDEVILLE ISL	B9D80391345	12/14/1954	9/1/1966	146
SACRAMENTO R A COLLINSVILLE	B9D80441510	8/5/1965	1/9/1970	77
SAN JOAQUIN R A POTATO PT	B9D80471340	3/3/1971	8/6/1984	264
SACRAMENTO R A EMMATON	B9D80511443	3/28/1968	7/1/1991	349

Appendix I**Summary of Grab Sample Data Used in this Analysis**

Station Name	Station Number	First Sample Date	Last Sample Date	Number of Grab Samples
SAN JOAQUIN R A TWITCHELL ISL	B9D80581401	2/8/1968	8/6/1984	270
SAN JOAQUIN R NR SAN ANDREAS LDG	B9D80591352	1/28/1957	2/5/1975	133
SAN JOAQUIN R A SAN ANDREAS LDG	B9D80621354	6/15/1954	4/26/1965	21
LITTLE POTATO SLU A TERMINOUS	B9D80691298	9/24/1952	9/15/1967	215
MOKELOMNE R SF BL SYCAMORE SLU	B9D80761297	3/26/1974	9/27/1983	176
MOKELOMNE R A HWY 12	B9D80761347	2/27/1957	5/29/1967	106
SACRAMENTO R A RIO VISTA A BM-30	B9D80891415	4/20/1951	4/11/1960	122
GEORGIANA SLU ISLETON	B9D80901358	3/26/1974	2/4/1975	18
SACRAMENTO R BL RIO VISTA BR	B9D80941410	4/6/1966	8/6/1984	324
SACRAMENTO R A RIO VISTA BR	B9D80961411	5/2/1960	9/14/1973	130
MOKELOMNE R,NORTH BL SNODGRASS SL	B9D81341303	6/21/1982	3/2/1991	45
SACRAMENTO R A WALNUT GROVE	B9D81441310	6/21/1982	3/2/1991	48
DELTA CROSS CH NR WALNUT GROVE	B9D81481305	9/25/1952	9/11/1967	210
LINDSEY SLU A HASTINGS TRACT FY	B9D81481417	6/14/1954	11/1/1955	10
LINDSEY SLU NR RIO VISTA	B9D81481424	10/28/1952	8/19/1982	255
MOKELOMNE R NR THORNTON	B9D81531263	3/25/1949	3/15/1978	240
LINDSAY SLU A HASTINGS CUT	B9D81581462	11/7/1980	10/26/1987	65
BARKER SLU AT PUMP HOUSE	B9D81651476	5/28/1986	10/26/1987	13
CACHE SLU A VALLEJO PUPL	B9D81781448	11/16/1984	4/25/1986	88
SACRAMENTO R A GREENS LDG	B9D82071327	9/14/1962	3/6/1985	608
SAN PABLO BAY A POINT SAN PABLO	E0B75772256	11/30/1962	6/2/1986	100
CARQUINEZ STR A MARTINS FRY LDG	E0B80172083	1/28/1957	8/19/1969	106
SAN PABLO BAY NR PINOLE PT	E0B80182223	3/24/1971	8/7/1984	110
SUISUN BAY OFF BULLS HD PT	E0B80232071	3/29/1968	3/20/1974	72
SUISUN BAY A BENICIA (END-PIER)	E0B80242082	12/4/1962	2/6/1969	93

Appendix I**Summary of Grab Sample Data Used in this Analysis**

Station Name	Station Number	First Sample Date	Last Sample Date	Number of Grab Samples
SUISUN BAY A PGE DOCK A PITTSBURG	E0B80251537	1/3/1958	10/21/1964	84
SUISUN BAY A BENICIA (M OF PIER)	E0B80252081	3/11/1969	6/3/1971	21
SACRAMENTO R A MALLARD ISL	E0B80261551	8/10/1961	10/5/1984	93
SUISUN BAY OFF BULLS HD PT MARTNZ	E0B80272070	10/4/1972	8/7/1984	324
SACRAMENTO R A CHIPPS ISL	E0B80281550	1/26/1968	8/7/1984	432
SACRAMENTO R A CHIPPS ISL	E0B80301550	4/23/1976	11/9/1981	146
SUISUN BAY A PORT CHICAGO	E0B80342023	1/3/1966	1/8/1970	21
SAN PABLO BAY A PT DAVIS	E0B80342156	12/4/1962	1/8/1970	76
SUISUN BAY NR PORT CHICAGO	E0B80352014	10/4/1971	11/13/1973	45
SAN PABLO BAY NR RODEO	E0B80352170	3/24/1971	12/12/1979	172
SUISUN BAY OFF MIDDLE PT	E0B80361593	1/26/1968	8/7/1984	351
CLIFTON COURT	KA000000	11/8/1983	2/27/1985	16
DELTA PUMPING PLANT HEADWORKS	KA000331	11/8/1983	2/27/1985	16